

# **For Reference**

---

**NOT TO BE TAKEN FROM THIS ROOM**



Ex LIBRIS  
UNIVERSITATIS  
ALBERTAENSIS





Digitized by the Internet Archive  
in 2020 with funding from  
University of Alberta Libraries

<https://archive.org/details/Lutley1981>





THE UNIVERSITY OF ALBERTA

RELEASE FORM

NAME OF AUTHOR        H.J.Lutley

TITLE OF THESIS        Stability    Analysis    in        Underground  
   Hydraulic Mining

DEGREE FOR WHICH THESIS WAS PRESENTED    Master of Science

YEAR THIS DEGREE GRANTED        Spring 1981

Permission is hereby granted to THE UNIVERSITY OF ALBERTA LIBRARY to reproduce single copies of this thesis and to lend or sell such copies for private, scholarly or scientific research purposes only.

The author reserves other publication rights, and neither the thesis nor extensive extracts from it may be printed or otherwise reproduced without the author's written permission.







THE UNIVERSITY OF ALBERTA

Stability Analysis in Underground Hydraulic Mining

by



H.J.Lutley

A THESIS

SUBMITTED TO THE FACULTY OF GRADUATE STUDIES AND RESEARCH  
IN PARTIAL FULFILMENT OF THE REQUIREMENTS FOR THE DEGREE  
OF Master of Science

Mining Engineering

EDMONTON, ALBERTA

Spring 1981







THE UNIVERSITY OF ALBERTA  
FACULTY OF GRADUATE STUDIES AND RESEARCH

The undersigned certify that they have read, and recommend to the Faculty of Graduate Studies and Research, for acceptance, a thesis entitled Stability Analysis in Underground Hydraulic Mining submitted by H.J.Lutley in partial fulfilment of the requirements for the degree of Master of Science.





## Abstract

The current rapid expansion of the Western Canadian coal mining industry will include the extraction of steeply dipping seams in the foothills and mountain region.

A computer model has been developed to investigate induced stresses in various sub-level mining configurations. It utilizes a linear elastic finite element analysis and provides graphical output to identify stress concentrations and possible areas of instability. The results from the numerical analysis were compared with a physical model analysis and observations in operating mines, and were found to be compatible. Zones of high stress concentration and areas suitable for future development were located.



## ACKNOWLEDGEMENTS

I wish to thank my family and friends, and staff and colleagues at the University of Alberta for their support and encouragement during the completion of this project. Particular thanks are due to Dr.M.Jeremic who supervised my studies.

I would also like to acknowledge the financial support provided by Gulf Canada Resources'Inc. and the permission granted by them, and Denison Mines Ltd., to use property data gathered on one of their mining leases.





## Table of Contents

Chapter	Page
1. Introduction .....	1
1.1 Coal Reserves .....	1
1.2 Available Technology for Extraction from Tectonically Disturbed Seams .....	2
1.3 Research Methods .....	4
2. Factors Influencing Mine Model Design .....	6
2.1 Geological .....	6
2.2 Mining .....	8
2.3 Geotechnical .....	11
2.3.1 Uniaxial Tests .....	12
2.3.2 Triaxial Tests .....	13
2.3.3 Test Results .....	13
2.4 Pre-Mining Stress Distribution .....	15
3. Method of Numerical Analysis .....	17
3.1 Introduction .....	17
3.2 The Finite Element Program .....	18
3.3 The Element Mesh and Element Properties .....	19
3.4 Initial Stress Distribution and Boundary Conditions .....	20
4. Stress Analysis of Sublevel Mining Configurations .....	22
4.1 Introduction .....	22
4.2 Loading Conditions .....	22
4.3 Configuration 1 .....	23
4.3.1 Extraction Method .....	23
4.3.2 Final Stress Distribution Throughout the Structure .....	23





4.3.3	Final Stress Distribution Around the Excavations .....	24
4.3.4	Significance of Observed Stress Distribution .....	27
4.4	Configuration 2 .....	28
4.4.1	Extraction Method .....	28
4.4.2	Loading Conditions .....	29
4.4.3	Final Stress Distribution Throughout the Structure .....	29
4.4.4	Final Stress Distribution Around the Excavations .....	30
4.4.5	Significance of Observed Stress Distribution .....	32
4.5	Configuration 3 .....	33
4.5.1	Extraction Method .....	33
4.5.2	Loading Conditions .....	33
4.5.3	Final Stress Distribution Throughout the Structure .....	34
4.5.4	Final Stress Distribution Around the Excavations .....	35
4.5.5	Significance of Observed Stress Distribution .....	36
4.6	Configuration 4 .....	37
4.6.1	Extraction Method .....	37
4.6.2	Loading Conditions .....	37
4.6.3	Final Stress Distribution Throughout the Structure .....	37
4.6.4	Stress Distribution Around the Excavations ..	38
4.6.5	Significance of Observed Stress Distribution .....	39
5.	Comparison of Theoretical Results with Mine Observations .....	40



5.1 Introduction .....	40
5.2 Observations in Chinese Hydraulic Mines .....	40
5.3 Observations at the Kaiser Resources Hydraulic Mine .....	43
5.4 Observations at the Mindola Mine .....	45
6. Physical Model Studies in Steep Seam Mining .....	47
6.1 Introduction .....	47
6.2 Model Materials .....	47
6.2.1 Coal .....	48
6.2.2 Sandstone .....	48
6.3 Model Frame and Loading Conditions .....	49
6.4 Operating the Model .....	50
6.5 Physical Model Results .....	51
6.5.1 Deformation Throughout the Structure .....	52
6.5.2 Deformation Around the Sublevels .....	53
7. Conclusions and Recommendations .....	55
Appendix 1 .....	134
Appendix 2 .....	156
Appendix 3 .....	158





## List of Figures

FIGURE		PAGE
1	Coal Reserves of Western Canada by Rank	61
2	Hydraulic Mine Sublevel Layout	62
3	Illustration of Angle of Break	63
4	Angle of Break Chart	63
5	Idealised Section for Mathematical Model Analysis	64
6	Location Map of Sample Sites	65
7	Finite Element Mesh	66
8	Calculation of Vertical Stress	67
9	Initial Horizontal Stress	68
10	Initial Vertical Stress	69
11	Plan and Section of Configuration 1	70
12	Loading Conditions for Configuration 1	71



13	Horizontal Stress Distribution Throughout the Mesh	72
14	Vertical Stress Distribution Throughout the Mesh	73
15	Principal Stresses Throughout the Mesh	74
16	Horizontal Stress Distribution Around the Excavations	75
17	Vertical Stress Distribution Around the Excavations	76
18	Principal Stresses Around Excavations	77
19	Horizontal Stress Sections	78
20	Horizontal Stress Sections	79
21	Vertical Stress Sections	80
22	Vertical Stress Sections	81
23	Plan and Section of Configuration 2	82





24	Loading Conditions for Configuration 2	83
25	Horizontal Stress Distribution Throughout the Mesh	84
26	Vertical Stress Distribution Throughout the Mesh	85
27	Principal Stresses Throughout the Mesh	86
28	Horizontal Stress Distribution Around the Excavations	87
29	Vertical Stress Distribution Around the Excavations	88
30	Principal Stresses Around Excavations	89
31	Horizontal Stress Sections	90
32	Horizontal Stress Sections	91
33	Vertical Stress Sections	92
34	Vertical Stress Sections	93



35	Plan and Section of Configuration 3	94
36	Loading Conditions for Configuration 3	95
37	Horizontal Stress Distribution Throughout the Mesh	96
38	Vertical Stress Distribution Throughout the Mesh	97
39	Principal Stresses Throughout the Mesh	98
40	Horizontal Stress Distribution Around the Excavations	99
41	Vertical Stress Distribution Around the Excavations	100
42	Principal Stresses Around Excavations	101
43	Horizontal Stress Sections	102
44	Horizontal Stress Sections	103
45	Vertical Stress Sections	104





46	Vertical Stress Sections	105
47	Plan and Section for Configuration 4	106
48	Loading Conditions for Configuration 4	107
49	Horizontal Stress Distribution Throughout the Mesh	108
50	Vertical Stress Distribution Throughout the Mesh	109
51	Principal Stresses Throughout the Mesh	110
52	Horizontal Stress Distribution Around the Excavations	111
53	Vertical Stress Distribution Around the Excavations	112
54	Principal Stresses Around Excavations	113
55	Horizontal Stress Sections	114
56	Horizontal Stress Sections	115



57	Vertical Stress Sections	116
78	Vertical Stress Sections	115
59	Stress/Strain Properties of Coal and Model Material	118
60	Stress/Strain Properties of Sandstone and Model Material	119
61	Plan and Section of Physical Model	120
62	Physical Model Loading Conditions	121
63	Initial Configuration of Model	122
64	Modelled Hanging Wall Caving	122
65	Hanging Wall Fully Caved	123
66	Deformation Around Sublevels (1)	123
67	Deformation Around Sublevels (2)	124
68	Deformation Around Sublevels (3)	124









## List of Tables

TABLE		PAGE
1	Coal Resources of Western Canada by Rank and Province	126
2	Petrographic Description of a Typical Western Canadian Coal Seam	127
3	Uniaxial Test Results Summary	128
4	Triaxial Test Results Summary	129
5	Coal Test Data	130



## List of Plates

PLATE		PAGE
1	Initial Configuration of Model	131
2	Modelled Hanging Wall Caving	131
3	Hanging Wall Fully Caved	132
4	Deformation Around Sublevels (1)	132
5	Deformation Around Sublevels (2)	133
6	Deformation Around Sublevels (3)	133





## 1. Introduction

### 1.1 Coal Reserves

Western Canada produces approximately ninety percent of total Canadian coal output but of this less than ten percent is by underground methods.<sup>1</sup> Table 1 indicates the present estimated reserves and Figure 1 shows their distribution.<sup>2</sup> Approximately eighty-five percent of the high grade, low sulphur coking reserves of the mountain region of Alberta are mineable by underground methods and the remainder by open-pit. Since reserves in the mountain region accessible by surface methods are rapidly being depleted, underground reserves and consequently underground methods will become more important. Up to seventy percent of the valuable coking coal reserves of western Alberta and northeastern British Columbia are contained in the steeply dipping seams of the foothills and mountain region. This region is characterized by a high degree of tectonic disturbance leading to shear zones in the coal, slickensided surfaces in the adjacent strata and thrust faults at low angles to bedding throughout the coal series. The seams tend to be unstable and consist of bands of hard and soft coal; this banding is due in part to the petrographic composition and also to the tectonic history of the seam.



## 1.2 Available Technology for Extraction from Tectonically Disturbed Seams

Current production by the underground mining of tectonically disturbed seams in western Canada is limited because until recently the relatively easy access to supplies of high quality coking coals in other countries restricted the development of the mountain region. However with depletion of other reserves the western Canadian seams become economically more favourable. The room and pillar mining method is the most common and is practiced at the McIntyre Mines Ltd. Grande Cache operation and was practiced at Coleman Collieries operations in southern Alberta until their recent closure. Continuous miners are used for development and production<sup>3</sup> and belt conveyors for underground transportation of the coal. The room and pillar technique is suited only to gently dipping seams and if there is considerable tectonic disturbance in the coal and adjacent strata, large pillars and a thick coal floor have to be left which decrease overall recovery rates.

Mechanised longwall mining has not been operated in western Canada although McIntyre Mines experimented with this technique. Longwall mining in inclined thick seams is practiced successfully in the Blanzky coalfield in France.<sup>4</sup> Combinations of shield supports, artificial roofs and coal caving are utilised. Longwall methods are used in the United States and have been investigated for application to thick seams.<sup>5</sup>



The third technique currently used underground is sub-level caving. This is practiced in the Loire and Auvergues coal fields in France and at the Michel colliery in the Crow's Nest Basin in southeastern British Columbia.<sup>6</sup> The French practice a horizontal slicing method with sub-level caving of an intermediate slice of coal. This method allows the mining of very irregular steep seams with good results and proceeds down dip with caving occurring above the worked slice. Other techniques working up dip include hydraulic stowing of the mined out area to improve stability and reduce the risk of spontaneous combustion.. At the Michel colliery operated by Kaiser Resources Ltd. sub-level hydraulic mining is used. This replaced a more conventional drilling and blasting sub-level mining technique. Sub-level blocks or panels are developed with continuous miners and these are subsequently extracted by hydraulic monitors. Coal transportation is also by water through pipes and flumes on the roadway floors. This method has proved to be safe and productive increasing the overall recovery rate from fifteen to fifty-five percent. Because of the success of this technique in western Canadian conditions, and the growing interest in sub level hydraulic mining, it was decided to concentrate the research on this mining method.





### 1.3 Research Methods

The design concepts used in this research project utilise accepted mine analysis and planning techniques. Because of the temporary nature of many mine excavations (e.g. production sub-levels) design and planning is aimed to obtain the most cost effective solution for the excavation's projected life. Thus an excavation's cost will not only include the ground breakage and support costs but also maintenance to keep it in such a condition that operations can continue. This requires an optimisation of initial support costs against maintenance costs and often leads to a minimum of support and an allowance for maintenance during the life of the excavation. In contrast Civil Engineering structures, for example, which are normally of a more permanent nature, (e.g. road tunnels) are designed with long term stability as an objective, and as a result may require greater detail in design and analysis. This level of detail is rarely required in mine design because of the flexibility in choice of geometry and the possibility of solving local instability problems by additional support which maybe of a temporary nature. In consequence the research and design techniques utilised in mining and civil engineering are often similar (e.g. mathematical modelling) but the depth and detail of a pre-mining engineering study may be of a lesser degree.

A further problem encountered in deep, underground mining is the variation in rock properties with depth and



from to place to place. Exploration drilling cannot provide enough detail to define all geological structures underground. Also sampling and physical property testing procedures cannot completely define the behaviour of the rock materials. Therefore any research must recognize and work within the limits of the data. In the research program, which is the subject of this thesis, little initial data was available, so the analytical techniques utilise simplifying assumptions which will be described as they are encountered.



## 2. Factors Influencing Mine Model Design

### 2.1 Geological

The main geological factors influencing mineability and choice of mining method are related to the geometry of the deposit, the nature of the surrounding strata and the petrographic composition of the coal. For this study which is concerned with steeply dipping seams it has been assumed that seam inclination is greater than 25° and that therefore conventional room and pillar or longwall mining is not possible. Also it can be assumed that seam thickness is sufficient to permit economic extraction by sub-level hydraulic mining.

The lithology of the mountain formations is generally comprised of thin- to thick-bedded sandstones, siltstones, mudstones and shales with interbedded coal seams.<sup>7</sup> The fine to coarse grained clastics vary in colour from light grey to black. The coal seams of the Kootenay Formation of southern B.C. are remarkable for their thickness and continuity. Thicknesses vary up to fifty feet of coal and more than thirteen seams greater than four feet in thickness have been identified. In other formations in the foothills region (Luscar, Commotion, Gething) seams tend to be less continuous due to the lensing nature of the coal bearing beds, and because of the complexly folded and faulted structure of the foothills strata. As is to be expected in an area of such structural disturbance the seams are





normally steeply inclined and in some instances severely contorted, thickened or thinned, cut off by faults, and the coal so severely crushed as to make it extremely friable. In other instances, however, these structures have so oriented the seam with respect to the surface, or so thickened the seam that excellent recovery can be made by strip mining.<sup>8</sup>

At the Michel colliery, Sparwood, a fifty foot thick seam known locally as the Balmer seam is currently being extracted by sub-level methods. Its average dip is 35° and the adjacent strata consists of shales and sandstones which provide a competent roof. Since mining has proved feasible under these conditions the choice of mining configurations for the theoretical modelling of this thesis was influenced by the geological structures observed in this mine which have been described in the literature.<sup>10</sup>

The strength and deformational behaviour of coal is briefly described in section 2.3 but since it is related to the petrography of the seam a short description is included here. Using the Stopes-Heerlen classification a particular coal can be described on a macroscopic level in terms of the lithotypes vitrain, clarain, durain and fusain. These macroscopic forms correspond to the bright, dull, hard and soft bands seen in a seam section. Structurally fusain is the softest coal type, vitrain is stronger but brittle, clarain is mechanically strong and durain is the strongest. Table 2 shows the petrography of a western Canadian seam in the Kootenay Formation.<sup>9</sup> The predominant lithotype of this





section is clarain with vitrain and durain present as interbands. Apart from the roof and floor coal, the seam, if undisturbed, would appear to be structurally strong because of the presence of firm clarain and durainous clarain bands. This type of information may be relevant to mine design when considering strength of coal pillars and their modes of failure provided that the seam has not been severely disturbed by tectonic action. The investigation into strength and deformational properties of coal and other strata and the values used for modelling is described in section 2.3.

## 2.2 Mining

Within a particular method chosen for extraction of a coal deposit modifications can be made to increase recovery, mineability and stability. Four different configurations were analysed using the mathematical model but the overall layout, dimensions and depth were similar for each of these sub-level caving methods.

The sub-level hydraulic mining method used at the Michel colliery is outlined here because the basic layout of this mine would be similar to other sub-level coal operations. Development is by continuous miners feeding directly into a flume line with the coal being washed down by water chute. Two main entries are driven to the rise at  $7^{\circ}$  at an acute angle to strike.<sup>10</sup> Crosscuts at 800 foot intervals connect the main entries to establish a



ventilation circuit and simplify access. Sub-levels inclined at about  $9^{\circ}$  are turned off the main entries at an angle of approximately  $155^{\circ}$ . These sub-levels are on 80 foot centres and are kept as close to parallel as conditions will allow, (Fig.2). Support is by 16 x 10 foot timber lagged steel arches at five foot intervals. The three sub-levels furthest in-by are equipped with a feeder-breaker and monitor and the necessary pipes and flumes. Since belt conveyors are not used in the mine straight line drivages are not essential but careful control of gradient is necessary.

Bulk production is achieved using high pressure water fed through the monitor which is mounted on the feeder-breaker. The monitor is remotely controlled by the operator from a small cabin which is at least thirty-five feet behind the monitor site. Immediately prior to extraction the arch supports in the extraction zone are removed and then the high pressure jet is directed to the up dip side of the sub-level. Cutting continues until connection is made with the previous extraction area and then the whole of the 70 x 40 foot block is extracted. This allows a completion of the ventilation circuit from the main entry, up the sub-level and out through the gob. Usually a degree of roof caving occurs before extraction is complete, but rock dilution due to this is rarely more than ten percent. After extraction is completed, the equipment is retreated forty feet down the sub-level. The pipe range is recoupled, the flume line reassembled to the feeder-breaker,



eight arches are withdrawn and the process of extraction is repeated. Three sub-levels are equipped at any one time. One is mined, one is pulling back and the third is standing by in case of any unforeseen stoppages in the production sublevels.

When a sub-level is retreated to a point not less than sixty feet from the main road, the equipment is withdrawn for re-installation in another sub-level. A temporary stopping is erected to prevent ventilation leakage. This sixty foot pillar is extracted by a monitor retreating down the main road. The temporary stoppings are destroyed as the pillar is mined but ventilation leakage is prevented as an extraction area is completed by erecting a permanent stopping in the main entry and leaving a barrier pillar.

The caving characteristics of the roof rock at the Michel colliery have not been published so an estimate of the cave line of the hanging wall for the model was obtained from analytically established criteria.<sup>11</sup> This analysis provided an angle of break chart which can be used to estimate the angle of break,  $\psi_b$ , given the depth of the excavation, depth of caved material, the density of the hanging wall rock, the cohesive strength of the hanging wall rock and its internal friction angle, (Figs.3 and 4). Using this chart  $\psi_b$  was determined to be  $68^\circ$  and this value was used in the mathematical model.

Having assumed the likely geological conditions and the general mining method that will be present in extraction of





a hypothetical foothills or mountain pitching seam it was possible to create an idealised section for model analysis. This cross section is illustrated in Figure 5. It assumed that mining has progressed to a depth of 150 metres and that the resulting void has been filled by caved material from the hanging wall. The coal seam was assumed to be fourteen metres in thickness and to have an inclination of  $45^\circ$ . The ground surface was assumed to be level. The hanging wall was assumed to consist of competent sandstone which caves at the break angle described above. The footwall was also idealised as massive sandstone with the same properties as the hanging wall. The idealisation of the country rock as sandstone was considered to be reasonable since sandstones, and high strength siltstones, are common rock types in the foothills coal bearing formations. A description of the deformational properties of several samples of the rocks follows in section 2.3.

### 2.3 Geotechnical

The strength and deformational characteristics of coal and adjacent strata were based on tests on samples obtained from the Belcourt property in the northeast coal block of British Columbia, and the Grande Cache Mine in the Alberta Foothills. The former is a joint venture managed by Denison Mines Limited's Coal Division and Gulf Canada Resources Inc. and the results are published with their permission. The locations of the two sample sites are illustrated in Figure



6. The samples consisted of 60 millimetre diameter diamond drill cores between 30 and 50 centimetres in length. Each sample was wrapped in plastic film and then coated with wax. This treatment was designed to retain the natural moisture and protect the sample. Uniaxial and triaxial compression tests were then performed on a number of samples in the Department of Mineral Engineering's Rock Mechanics Laboratory.

### 2.3.1 Uniaxial Tests

Uniaxial tests were performed to determine unconfined compressive strength, Young's Modulus and Poisson's ratio. Five core samples were taken and cut so that their length to diameter ratio was approximately two to one. The ends of these samples were then lapped on a lapping table so that their surface smoothness varied by no more than 0.050 millimetres. Four electrical resistance strain gauges were attached to the sample, two axially and two laterally, using epoxy resin adhesive, in the standard manner. A slow curing adhesive was used without heating to accelerate the hardening process, because it was feared that heat may have caused clay-bearing samples to disintegrate. Each pair of strain gauges was connected to provide a full bridge circuit in a strain meter so that the strain under loading could be determined in microstrain units. The sample was placed in a servo controlled, 600,000 lb. MTS compression frame and loading commenced at a rate of 0.10 millimetres per minute



for stronger materials and half that rate for weaker materials. Strain and load measurements were taken at regular intervals until the sample failed.

### 2.3.2 Triaxial Tests

Triaxial tests were performed to determine the cohesion and internal friction of the samples. Samples 32 millimetres in diameter were cored from the 60 millimetre diameter diamond drill cores so that their length to diameter ratio was approximately two to one. The ends were lapped in the same way as the uniaxial samples. Each sample was tested in a Hoek-Franklin triaxial cell. It consists of a thick walled cylinder and two end caps. The rock core is enclosed in a tough rubber sleeve which is so designed that when hydraulic fluid is pumped into the cell, the sleeve self-seals and no fluid escapes. The axial load is provided by the MTS compression frame. Each sample type was tested at various confining pressures and the axial failure load for each confining pressure recorded.

### 2.3.3 Test Results

The uniaxial and triaxial test results are contained in Appendix 1. Values of Young's Modulus were obtained from graphs of axial load against axial strain. Straight line plots were obtained in each case suggesting linear elastic behaviour along the axis. Values varied from  $2.55 \times 10^4$  MPa for claystones and siltstones to  $6.18 \times 10^4$  MPa for





sandstones. The results are summarised in Table 3.

Poisson's ratio for each uniaxial sample was obtained from a plot of lateral strain against axial strain. In the higher strength sandstones a straight line was obtained and only one value of Poisson's ratio recorded. In the softer rock materials non-linear behaviour was encountered at high stress levels as failure approached. The value of Poisson's ratio selected was that occurring in the linear portion of the plot. These results are also summarised in Table 3.

The triaxial results were examined using Mohr circle diagrams to obtain values of internal angle of friction and cohesion. The coarse sandstones gave the highest internal friction angle and the silty claystones the lowest. The cohesive strength was low in all cases. The results are contained in Appendix 1 and are summarised in Table 4.

The coal physical property data was obtained from tests on samples from the No. 4 and the No. 11 seam at Grande Cache, Alberta. Uniaxial and triaxial tests were performed and the data is summarised in Table 5. Preparation of coal samples for testing is usually difficult due to its low inherent strength and the presence of many fractures. Therefore the samples which survive the preparation process are usually representative of higher strength and more brittle coal types. For this reason it was possible to obtain elastic constants for coal although the mechanical behaviour across the whole seam may be other than linear elastic.





The mechanical properties of the rock materials obtained from these tests were used in the finite element model. The program employs linear elastic analysis and the predominant rock type, sandstone, exhibits this behaviour. However it has been seen that coal and soft rock materials exhibit behaviour other than linear elastic at higher stress levels.<sup>24</sup> The aim of the analysis is not to predict precise stress levels or deformations around excavations but to identify regions in which stress concentrations will occur and support problems may be encountered. Therefore approximating all the rock behaviour as linear elastic is considered justified because the errors introduced by this assumption will be small.

## 2.4 Pre-Mining Stress Distribution

The factors influencing mine design that have been considered so far are the materials present, their properties, and methods of obtaining coal production. The fourth factor that must be considered when designing excavations is the pre-mining stress distribution, including the effect of tectonic forces. Many investigators throughout the world have measured in-situ lateral and vertical stresses and calculated  $K_0$ , the ratio between lateral and vertical stress.<sup>12</sup> Values vary from 0.4 to over 5.0 and depend on the mechanical properties of the rock and the tectonic history. In the Rocky Mountain Foothills region no in-situ stress measurements have been published to date so



assumption of a value of  $K_0$  should be based on what is known of the tectonic history. The tectonic disturbance seen in the Foothills region is a result of lateral thrusting along a NE-SW axis. This is responsible for the numerous southwest dipping thrust faults found to the east of the Rocky Mountain Trench. This would indicate that lateral tectonic stresses may be significantly high. However Heim's Rule suggests that in weak strata, such as coal bearing strata, the rock is unable to support large stress differences and that in conjunction with time dependent deformation of the rock mass over geological time lateral and vertical stress may equalise. Furthermore erosional effects may enhance this lateral stress release. Therefore some criterion has to be adopted for evaluating a horizontal to vertical stress ratio and it was decided to use the approach of Terzaghi and Richart.<sup>13</sup> This leads to a value for  $K_0$  of 0.33 which is the value widely adopted for theoretical calculations of pre-mining stress fields. This may appear to be on the low side considering the tectonic history of the region but since no data was available to indicate otherwise the above approach was adopted.



### 3. Method of Numerical Analysis

#### 3.1 Introduction

The aim of the proposed numerical analysis was to provide a semi-quantitative assessment of the stress distribution around various excavation configurations. To obtain this a two dimensional linear elastic finite element analysis was performed and the results are displayed in two forms. The first consists of contour plots of horizontal and vertical stress distributions. These were produced from the stress values calculated at the nodal points and contoured using the program SURFACE II available in the University of Alberta, Computing Library files. The second form of display consists of major and minor principal stresses represented in magnitude and direction by arrows. The length of the arrow is proportional to the magnitude of the principal stress and its inclination indicates the direction in which it acts. The arrowheads indicate whether the point is in compression or tension; pointing towards each other represents compression and the reverse represents tension. The principal stress plotting program, PLOTGRID, was made available by its author Mr. P. Weerenburg of the University of Alberta, Department of Civil Engineering.



### 3.2 The Finite Element Program

The main computational program that was employed for the model is a two dimensional finite element program developed in the University of Alberta, Department of Civil Engineering. It performs a two dimensional, linear elastic analysis for plane strain problems using a constant strain triangle and outputs displacements, element stresses, maximum principal stresses and average nodal stresses. For use in this problem it was necessary to increase the program limitations. The maximum number of nodes was increased from 200 to 450, the number of elements from 200 to 900 and the half-bandwidth from 40 to 200. The limitations therefore read as:

Number of Nodes 450

Number of Elements 900

Half Band Width 200

Materials 8

Total Storage Required 720k

The program can be run under the Michigan Terminal System on the AMDAHL 470 V/7 computer at the University of Alberta. The required Central Processing Unit (CPU) time is approximately 45 seconds.







### 3.3 The Element Mesh and Element Properties

The finite element mesh is illustrated in Figure 7. It has 432 nodal points and 812 elements with a high concentration in the seam and in the immediate hangingwall and footwall. The elements in the seam are so arranged that different mining configurations can be modelled with this mesh by assigning different element material properties and loading conditions without having to change nodal coordinates or element nodal points. Also a high number of elements are placed on the coal/sandstone interface in the region of the excavations. This is to prevent displacements in the coal being overly restrained by the relatively stiff sandstone since the ratio of elastic moduli, coal to sandstone, is 1 to 20.

The elastic properties used for elements representing coal and sandstone were those established in the materials testing program (Chapter 2). For excavated zones such as the working-places and the sublevels the elements were assigned near zero stiffness i.e. the value used for Young's Modulus was 10.0 MPa and that for Poisson's ratio 0.25. These values are selected to allow deformation into these regions to occur readily. The caved sandstone was assigned a Young's Modulus of 1200.0 MPa and Poisson's ratio of 0.25. No specific values were available for this material so the moduli ratio of coal to caved sandstone was chosen as 2 to 1. For solid rock the Young's Modulus value used was 50,000 MPa and the Poisson's ratio 0.2. This was an average



obtained from the testing program summarised in Table 3. The values for coal were 2400 and 0.35 respectively. These values were gained from the coal physical property tests summarised in Table 5.

The use of linear elastic analysis for this problem may be considered an over simplification especially since more complex analyses can be performed. The most advanced method currently available for calculating stresses in a problem of this nature is by means of a finite element method using incremental loading to simulate the mining history and non-linear, stress path dependent stress-strain relations for the materials involved. With proper use this procedure has been shown to lead to reliable estimates of the stress distribution as well as the deformations resulting from a given loading sequence. However, it has been shown<sup>23</sup> that if deformations are not required, then for many cases a simple linear elastic, single step analysis may give satisfactory results with less expenditure of time and money.

### 3.4 Initial Stress Distribution and Boundary Conditions

The initial vertical stress was assumed to be due to the weight of overlying material. Therefore the vertical stress at a point  $z$  metres below the surface is given by

$$\sigma_v = \gamma \cdot z$$

where  $\gamma$  is the unit weight of the material.

If a point occurred below more than one material the vertical stress value was calculated as  $\sigma_v = \gamma_1 \cdot z_1 + \gamma_2 \cdot z_2 + \dots$



The unit weights for coal, sandstone and caved sandstone were 1300, 2700 and 1890 kg/m<sup>3</sup> respectively.

The initial horizontal stress distribution was calculated from

$$\sigma_h = K_0 \cdot \sigma_v$$

where  $K_0$  is the value of the horizontal to vertical stress ratio established in Chapter 2. The initial horizontal and vertical stress distributions are illustrated in Figures 9 and 10. The axes indicate distances in metres and the contour values represent stresses in Mega-Pascals.

The initial stress distribution could have been calculated using the "switch on gravity" method. This is achieved by running the finite element program with the self weight of each element being applied. The advantage of this approach is that shear stresses developed along boundaries where materials possess different stiffnesses are simulated. However away from the boundaries the horizontal to vertical stress ratio will be that arising due to the elastic properties of the materials and will give a similar initial stress distribution to that obtained by the calculation described in the preceeding paragraph.

The element mesh boundary conditions were defined such that the nodes on the boundary were fixed in both the horizontal and vertical directions. The mesh is sufficiently large that boundary conditions do not influence behaviour around the excavations.





## 4. Stress Analysis of Sublevel Mining Configurations

### 4.1 Introduction

The particular panel layout in a sublevel mine may change from panel to panel to allow for geological variations or to improve strata control. For this reason it was decided to analyse four alternative panel layouts by the method previously described. For each layout a section and plan describe the extraction method and another section describes the loading conditions in the region of the excavations. Stress contours and principal stress diagrams illustrate the results.

### 4.2 Loading Conditions

The method of calculating the excavation loading conditions was the same for each configuration. The stress at each nodal point on the boundary of the excavation was obtained from the listing of initial stress distribution. These values were used to calculate loads which are applied at each node along the excavation boundary to create a stress free boundary around the excavation (Figure 12). A sample calculation of loading conditions is given in Appendix III. The induced stress distribution caused by this loading and calculated by the finite element program is summed with the initial stress distribution to give the final stress distribution around the excavation.





## 4.3 Configuration 1

### 4.3.1 Extraction Method

Coal blocks due for extraction were assumed to be bounded by development sublevels turned off the main entry almost parallel to strike. They are retreated back towards the main entry by hydraulic extraction and all roads are sufficiently inclined to allow hydraulic transportation of the broken coal. Coal on the down dip side of the extraction sublevel is trimmed off so that the coal wall is perpendicular to the roof. The layout and dimensions are illustrated in Figure 11.

### 4.3.2 Final Stress Distribution Throughout the Structure

The horizontal and vertical stress distributions resulting from this configuration are illustrated in Figures 13 and 14. In comparison with the initial stress distribution diagram (Figure 9) it can be seen that there is a certain reduction in horizontal stress in the footwall and a slight increase in the hanging wall. Also a zone of horizontal tensile stress is induced near the surface which coincides with what would be the location of the new cave line. A high horizontal stress gradient is seen in the hanging wall sandstone as it approaches the sandstone/coal interface in the region of the excavations.

The vertical stress distribution is characterised by a slight lowering of stress magnitude in the footwall and a slight increase in the hanging wall. As would be expected



variations from the initial stress levels increase closer to the excavation. The vertical stress along the boundary between the intact and the caved sandstone is low because displacement of the intact rock into the stope allows stress release.

The principal stress distribution diagram (Figure 15) adds more to the detail provided by the horizontal and vertical stress diagrams. The development of the new cave line is illustrated by the major principal stress near the surface being horizontal and tensile. Also it can be seen that in the hanging wall the major principal stress is oriented parallel to the seam and is large and compressive. Its significance will be discussed in the next section.

#### 4.3.3 Final Stress Distribution Around the Excavations

The stress distributions are illustrated in Figures 16, 17 and 18 and stress sections through regions of particular interest are contained in Figures 19 to 22. It should be noted that the stress levels indicated by these sections are those occurring along each straight section line. Figure 19 shows that the horizontal stress in the immediate hanging wall is almost constant parallel to the seam from the uncaved stope to below the next working drift. This is contrary to the initial stress distribution where the horizontal component increases linearly with depth and, for a given depth, is lower. A similar section in the footwall shows that stresses increase with depth except immediately



below the uncaved stope. Stress sections perpendicular to the seam (Figure 20) show high horizontal stress in the hanging wall dropping abruptly in the coal, reaching a minimum in the excavation wall on the footwall side and rising slowly in the sandstone footwall. This distribution is partly a result of the initial condition where footwall stresses are low because the loading provided by the less-dense caved material is lower than that of the intact rock which loads a large part of the hanging wall. Another factor causing this particular stress redistribution is stress transfer around the openings. The horizontal component is transferred below the lower excavation and through the pillar between the two excavations. Also the vertical component is forced around the excavation in the sandstone hanging wall and the major principal stress becomes oriented parallel to the seam (Figure 18) This adds a further component to the already increased horizontal component.

In the footwall the horizontal stresses are considerably lower than in the hanging wall. Destressing occurs in the immediate floor of the stope and in the walls of the development drift. The orientations of the major principal stresses are much nearer to their original orientations (i.e. vertical) except for immediately below the stope where they tend to the horizontal. This results in a local horizontal stress concentration which is, however, relatively small.





The vertical stress distribution is characterised by high hanging wall stress, moderately high pillar stress, high stresses in the walls of the development drifts, and localised zones of stress concentration and relaxation. Low stress in the footwall is partly a result of the reduced overburden load caused by the caved material but also due to relaxation immediately below the stope.

As has already been noted the major principal stresses in the region of the stope become aligned parallel to the roof and floor. Figure 18 illustrates the manner in which stress is transferred around the end of the stope and this causes a vertical stress concentration in the sandstone hanging wall in the region of the top corner of the stope. In the footwall there is a destressed zone in the sandstone below the stope. This appears to be caused by relaxation in that bottom corner and also because there is no transfer of stress through the region. This gives a high differential stress across the end of the stope which is well illustrated in the upper section in Figure 22.

In the pillar section between the two excavations stress transfer gives rise to a moderate increase in stress level with a subsequent drop in stresses in the footwall. The footwall stresses in this zone tend to be similar in magnitude and orientation to the initial stresses. Around the lower excavation vertical stress is predictably transferred around the drift leading to high stress in the walls and destressing in the roof and floor. The area



influenced by the excavation continues for at least 75 metres below the lower excavation giving higher stresses in the hanging wall but not significantly affecting stress distribution in the footwall. This suggests that overburden load from the overlying rock is transferred around the excavation as a whole and will always lead to a zone of increased stress in the hanging wall at depths in which further development workings will have been initiated.

#### 4.3.4 Significance of Observed Stress Distribution

The analysis of this configuration can give some initial insight into possible ground behaviour around an uncaved stope. The major principal stress in the stope roof is compressive and aligned parallel to the seam so this will have the effect of closing any joints in the roof and preventing failure by sliding of unsupported blocks. The localised tensile zone where the stope roof joins the previously caved material suggests where roof failure will be initiated and its continuation through to the surface locates the new cave line.

The horizontal and vertical stress concentrations located in the hanging wall may cause stability problems on the corner at the junction between the sandstone roof and the coal wall. High compressive stresses are created in the coal wall and may cause its failure which would remove support from the roof. This could in turn induce the failure of the hanging wall. The eventual caving of the hanging wall



is of course desired but not at the expense of depletion of recoverable coal from the adjacent coal block.

The overall destressing of the footwall will be significant in the location of permanent excavations such as major haulages, slurry pumping stations and shafts. As the workings go to greater depths shafts will have to be deepened or subshafts added and these will all be located in the footwall to take advantage of the destressed and more stable ground.

## 4.4 Configuration 2

### 4.4.1 Extraction Method

The extraction method for this configuration is similar to the previous one but a number of changes are embodied which will affect the resulting stress distributions. As before extraction blocks are defined by continuous miners and production is achieved by retreat hydraulic mining back towards the main entry. No trimming is performed on the down-dip side so the resulting stope retains the original profile of the extraction sublevel. Furthermore the pillar between the stope and the lower sublevel is of lesser volume in this configuration which should also affect the final stress distribution. The mining layout is illustrated in plan and section in Figure 23.





#### 4.4.2 Loading Conditions

The loading conditions for this configuration are calculated as before and are illustrated in Figure 24.

#### 4.4.3 Final Stress Distribution Throughout the Structure

The overall stress distribution is illustrated in Figures 25, 26 and 27. The horizontal stress distribution is similar to that of Configuration 1 but the change in geometry does create some differences. The tensile zone near the surface is still present but is not so extensive. This suggests that the new cave line will be propagated in the same location but may not occur so readily. The release of horizontal stress in the footwall is as in the previous mining layout with a slightly lower level of horizontal stress below the pillar. As before the initial stress distribution is significant in determining the footwall stress condition.

Predictably, the vertical stress distribution across the mesh varies little from that of the previous configuration. The destressing along the boundary between intact and caved sandstone is still observed as is the considerable relaxation in the footwall below the stope. The principal stress diagram (Figure 27) shows the orientation of the major principal stress in the stope roof parallel to the seam and shows a transfer of stress around the excavation as a whole.





#### 4.4.4 Final Stress Distribution Around the Excavations

The small variation in geometry and pillar size in this configuration results in a change in horizontal stress distribution around the excavations. The stress section in the hanging wall parallel to the seam (Figure 31) shows an almost linear increase in stress with depth, a sharp drop as the lower excavation is encountered, and then a resumption of the linear increase with depth. The drop in stress coincides with the location of the destressed vertical wall of the lower sublevel. The equivalent stress section in the footwall shows stress decreasing to a minimum below the stope, rising as the pillar is encountered but remaining constant through the footwall of the pillar, increasing rapidly below the lower sublevel, and then showing a gentle linear increase with depth below the excavation zone. Stress sections perpendicular to the seam show horizontal stress levels rising in the hanging wall to a peak on the interface between coal and sandstone, dropping sharply and remaining constant or increasing slowly in the footwall.

The most significant horizontal stress concentration induced by the excavations is in the hanging wall sandstone adjacent to the coal pillar (Figure 28). As before this is a result of horizontal stress transfer around the openings and the reorientation of the major principal stress. The major principal stress becomes oriented parallel to the seam and thus adds to the horizontal component. Stress relaxation in the footwall is slightly more extensive and more uniform



than in the previous configuration.

Vertical stress in the hanging wall rises rapidly from almost zero to peak in the sandstone adjacent to the vertical wall of the stope. It then falls to an intermediate minimum above the roof of the lower sublevel, rises to the original peak in the wall of the sublevel and stays at this value until it is well below (60 metres) the lower excavation. In the footwall vertical stress decreases almost linearly until it reaches a minimum below the bottom corner of the stope. From there it rises sharply through the pillar region to a peak which coincides with the wall of the sublevel. Below the sublevel considerable destressing is observed and then a sharp increase in stress in the vertical wall on the down-dip side. From that point on stress increases linearly with depth to achieve levels similar to those present in the initial stress distribution. Across the seam (Figure 34) stress rises to a peak in the hanging wall, falls sharply around the excavation and recovers slowly in the footwall. In the pillar region stress increases to a maximum in the centre of the pillar, decreases in the footwall then assumes initial values and increases linearly with depth.

The most significant vertical stress concentrations occur in the lower sublevel walls and in the single vertical wall of the stope. Relaxation is seen above and below both excavations. The stress gradient across the seam and the magnitude of the peak stresses are slightly lower in this



configuration than the previous one. The variation in stope geometry has only had a minor effect on vertical stress distribution. The principal stress diagram illustrates stress transfer through the pillar and around the excavations as a whole. The tensile zone in the roof of the stope where bed separation may occur and roof caving will be initiated. Below the excavation zone initial stress conditions are soon regained as can be seen from the way in which the principal stresses return to being vertical and horizontal.

#### 4.4.5 Significance of Observed Stress Distribution

As in the previous configuration the compressive major principal stress aligned parallel to the stope roof will add to its stability by closing joints perpendicular to bedding. Similarly further development in terms of access should be located in the footwall sandstone to take advantage of the destressed and more stable conditions. Since no trimming is performed on the down-dip side of the sublevel the bottom of the stope retains the sublevel profile. On comparison of the principal stress diagrams of these first two configurations (Figures 18 and 30) it appears that Configuration 2 is more desirable because of the way in which stress is distributed around the lower end. In Configuration 1 the magnitude of the major principal stress at several points is higher than in Configuration 2. Also in Configuration 2 the highest stresses are in the sandstone and located further from the





coal than in Configuration 1 thus reducing the risk of premature caving and coal loss. The differences pointed out here are, however, marginal and the stability could be affected by other factors such as the presence of soft coal or poor roof conditions. As a result a choice between these two mining configurations would be based on factors such as productivity and ease of mining rather than the optimisation of stability by consideration of stress distribution.

## 4.5 Configuration 3

### 4.5.1 Extraction Method

The third layout to be considered embodies the broad sub-panel layout as practiced in some Chinese hydraulic mines (Chapter 5). Extraction blocks are smaller and are subdivided by crosscuts (Figure 35) to improve access and ventilation. Development work is carried out with continuous miners and bulk production is achieved by hydraulic retreating towards the main entry. With this layout more than one block is extracted simultaneously to offset the lower production rate caused by mining smaller blocks. Flumes for coal slurry transportation are located in the production sublevels and the main entry.

### 4.5.2 Loading Conditions

The loading conditions for the chosen section through the workings (Figure 35) are illustrated in Figure 36. These are calculated as described earlier and as can be seen from



the diagram result in a fairly simple configuration to be analysed.

#### 4.5.3 Final Stress Distribution Throughout the Structure

The selected section through the mine workings is such that stresses around three sublevels are analysed so in relation to the rest of the structure, the actual volume of unexcavated rock is small. This is seen in Figures 37, 38 and 39 where away from the excavations the alteration from the initial stress distribution is minimal. There is a slight rise in horizontal stress in the hanging wall in the region of the excavations and this is due to transfer of stress through the solid coal pillars. In the footwall, where away from the excavation the stress level rises linearly with depth, the stress distribution becomes almost identical to that of the initial stress. The tensile zone at the surface is very low in magnitude and small in extent and would be unlikely to promote any caving.

The overall vertical stress distribution diagram emphasises that away from the excavation there is little variation from initial conditions. Above the uppermost sublevel there is a certain relaxation of stress along the boundary between the caved and the intact sandstone but not as significant as that observed above the stope in the two previous configurations. There is also a slight destressing in the hanging wall above the excavations and a stress increase in the hanging wall below the excavation. Vertical



stress has been transferred around the excavation zone as can be seen from the major principal stress trajectories in Figure 39.

#### 4.5.4 Final Stress Distribution Around the Excavations

Stress sections parallel to the seam show a steady increase in horizontal stress with depth in the hanging wall, with a small peak adjacent to each pillar caused by local transfer of stress around each sublevel (Figure 43). In the footwall the stress level is more or less constant until below the bottom sublevel. A sharp increase here is due to the overall stress transfer around the excavation zone. Sections perpendicular to the seam illustrate the destressing in the sublevel walls and the subsequent concentration in the floor.

Vertical stress sections illustrate a similar pattern of relaxation and concentration in the hanging wall and footwall. The general trend is for stress magnitude to increase with depth and there are local peaks where vertical stress is channelled through a pillar. The peaks actually occur in the sublevel walls but the stress levels in the pillars are still higher than those occurring prior to extraction. The principal stress diagram illustrates the stress trajectories around the excavations. It also illustrates an anomaly in the roof and floor of the excavations caused by the way in which stresses are calculated at nodes. Stresses at nodes (which are contoured





here) are calculated by averaging of the stresses in the elements surrounding the node. On the boundary of the excavations stresses are therefore averaged between the elements at zero in the excavation and the stressed elements in the surrounding rock. Above and below the excavations, vertical destressing has occurred but the magnitude of the average vertical stress is still greater than the horizontal stress. This results in the inaccurate representation of the major principal stress on the excavation boundary.

#### 4.5.5 Significance of Observed Stress Distribution

Since the section analysed passes through consecutive pillars and sublevels and does not include any large unsupported excavations, the structure appears fairly stable. This will be misleading as each block is retreated because as the excavation front approaches the section line, stress variations will arise in the third dimension. Such an effect is, however, beyond the scope of this investigation. There appear to be no real problem areas created by this excavation configuration but two points should be noted. The concentration of vertical stress in the sublevel walls may result in their failure especially as operations proceed to greater working depths. This will require increasingly stronger support to be set immediately after excavation as is the practice in some hydraulic mines (Chapter 5). The second point is that as the pillars are stressed they may become more liable to violent failure or outbursts of





powdered coal and gas.

## 4.6 Configuration 4

### 4.6.1 Extraction Method

The layout illustrated in Figure 47 and analysed as Configuration 4 is typical of the method of long pillar mining or narrow sub-panel mining (Chapter 5). Unlike the three previous methods the direction of excavation is almost down-dip as opposed to being just off strike. As before the extraction blocks are defined by continuous miners and are then retreated towards a cut-off drift. In this method the coal slurry runs down the production sublevels, along the cut-off drift and into the main entry.

### 4.6.2 Loading Conditions

Nodal loadings to simulate the desired excavations are calculated as before and illustrated in Figure 48.

### 4.6.3 Final Stress Distribution Throughout the Structure

Figure 49 illustrates the general horizontal stress distribution and it can be seen that apart from local alterations around the excavations and a slight destressing in the footwall, there is little alteration from the initial stress distribution. At the surface there is a small tensile zone but its magnitude and extent are not sufficient to give rise to instability. The same is true with regard to vertical stress distribution. Localised effects are seen around the



excavations and some vertical stress is released in the footwall, but generally the stress distribution is the same as that prior to excavation.

#### 4.6.4 Stress Distribution Around the Excavations

In the hangingwall the magnitude of horizontal stress rises with depth and attains a peak above the lower sublevel. It then falls above the sublevel wall but recovers its peak value and continues to rise linearly with depth. In the footwall a similar situation occurs with minimum levels below the sublevel walls and magnitude increasing with depth. Stress sections across the seam reiterate this pattern and the section through the coal pillar shows only a marginal concentration in this region.

The vertical stress sections show almost constant stress between the two excavations parallel to the seam, with destressing above each sublevel and stress concentration in the sublevel walls. In the footwall the relaxation and concentration occurs as in the hanging wall, but between the sublevels stress magnitude increases with depth as it would prior to mining. Sections across the seam show a slight increase of stress level in the central pillar and the predictable concentration in the excavation walls. The principal stress diagram shows the principal stress trajectories and the stress transfer around the sublevels.



#### 4.6.5 Significance of Observed Stress Distribution

As was observed in the previous configuration there are no severe problems created by the stress redistribution around the sublevels. Concentration in the walls can be alleviated by suitable support and there should be little danger of outbursting in the pillar zone because the magnitude of the induced stresses rarely exceeds the initial stress levels. The pillar adjacent to that between the sublevels (the pillar being extracted, Figure 47) will no longer support overburden load and will transfer stress to the caved material and the pillar which has been considered here. This will increase the stress level in this pillar but an assessment of the influence of this stress transfer would have to be performed by three dimensional analysis which lies beyond the scope of this project.





## 5. Comparison of Theoretical Results with Mine Observations

### 5.1 Introduction

In order to validate the results from the mathematical model analysis it was decided to compare them with reports of observations made at three mines operating with similar configurations. In China, hydraulic mines have been operated for approximately thirty years and some of their strata control problems have been described.<sup>14</sup> In the Michel colliery of Kaiser Resources (Chapter 2) deformation and convergence measurements were performed and their significance evaluated.<sup>15</sup> Finally in Zambia, at the Mindola Mine, a steeply dipping, low strength copper orebody is extracted by sublevel methods and its similarity in mine structure allows useful comparisons to be made.<sup>16</sup> Unfortunately, none of these descriptions quantify stress magnitudes and they provide only qualitative observations. Since so few studies have been made in steep seam operations these observations can only be used in general comparison.

### 5.2 Observations in Chinese Hydraulic Mines

Since the inception of observations in 1956 the Chinese have been investigating roof stability in the workings, deformation in the extraction blocks under pressure, and roadway maintenance. They conclude that the behaviour of the immediate hanging wall strata (main roof) plays a predominant role in deformation in coal blocks and the



damage incurred in roadways. If the hanging wall fails to cave stress is transferred to the coal causing crushing of coal pillars, increasing the unsupported roof span, and extending the area affected. Problems are more acute in areas of high productivity and high methane content.

At the Hsiechiachi No.3 Colliery in working a 5.6 metre thick seam, dipping at 23° and at a depth of 250 to 500 metres, it was found that loading on roadways caused severe deformation and maintenance problems. It was decided therefore to locate main entries in the footwall strata and plan production so that required roadway life was minimised. Development of a panel adjacent to the panel under extraction is only commenced when extraction of the first panel is near completion. By fast drivage techniques the sublevel is completed in five days and the resulting panel extracted in ten days. An average production rate of 200 tonnes per hour yields a daily production, from each panel, of 2000 tonnes. This is equivalent to a doubled output per man shift (OMS) and is accompanied by a 60 percent drop in timber consumption compared with former methods. The success of this method is due to the reduction of roadway life and the fact that roof caving has been initiated before the next roadway is started. By the time the roadway is completed and the new panel commences extraction, the roof has caved and the broken rock can support overlying strata thus relieving the coal pillars of some of their load.

A second technique to improve working conditions



adopted by the Chinese was to change the panel layout from broad sub-panel to narrow sub-panel. The former is equivalent to Configuration 3 and the latter to Configuration 4 in the model analysis (Chapter 4). It was found that by using this technique stress was transferred to adjacent undeveloped panels which were capable of bearing stress without crushing, until the hanging wall caved. When development was due in these panels it was found that the roadways remained in proper shape and a significant improvement was obtained in production.

Other experiments performed at several other collieries related to increasing support in roadways to prevent closure. Timber sets comprising a cross-bar and three props were employed as were yielding steel arches. Also the spacing between supports was reduced to obtain maximum stability. Drivage by drilling and blasting was replaced by continuous miners to keep roadway wall damage to a minimum and wooden bolting was used to stabilise the sides. Better production planning reduced roadway service time and the overall benefits of these measures made the increase in support costs acceptable.

Many of the conclusions reached by the Chinese engineers by mine observations and "trial and error" can be reliably inferred from the mathematical model analysis. The various studies suggested that high stresses will be found in coal pillars and roadway walls and that their distribution and magnitude is related to the span of





unsupported stopes and roadway spacing. By locating main entries in the footwall strata (Hsiechiachi Colliery) they took advantage of the distressed zones observed in all the mathematically analysed configurations. In changing from broad sub-panel layout to narrow sub-panel layout induced stresses in the pillars were reduced and this is seen by comparison of Configurations 3 and 4. These observation suggest that on a comparative basis the mathematical model is fairly reliable for predicting the location of problem zones and show how the layout can be altered to achieve maximum stability.

### 5.3 Observations at the Kaiser Resources Hydraulic Mine

Operations at the Michel Colliery have been described in Chapter 2 and are similar to the Chinese operations in layout and method of working. Strata control studies were initiated at this mine to assist in planning for production at deeper levels and in the layout of a new mine.<sup>15</sup> The research program was designed to establish support loads in sublevels, the magnitude of pillar deformations, the amount of strata movement above and below the sublevel and the amount of convergence in the sublevel.

The support loads measured on arches located in a production sublevel gave maximum loads of 11 tonnes. This figure is difficult to relate to local stress conditions since the size and spacing of the steel arch supports is not specified. However, it was noted that arches rarely reached





yield load which indicates that either loading in the sublevel is not severe or the sublevel is over supported. Roof convergence was measured along the sublevel as the block was retreated and the maximum value of 60 millimetres was achieved at the measuring point closest to the monitor. Further back down the sublevel convergence was found to be smaller. Strata movements measured by multi-wire extensometers indicated a roof lowering of 17.3 millimetres at a point 36 metres above the sublevel and an uplift of 21.5 millimetres at a depth 6 metres below the sublevel. These measurements corresponded well with the total roadway closure which at the same point was 45 millimetres. Pillar deformation measurements showed maxima occurring at some distance back from the extraction face. In the sublevel the maximum deformation of 18.5 millimetres occurred when the monitor was 76 metres away from the station. This suggests a stress transfer mechanism that induces a maximum loading some distance back from the extraction face.

Relating these results to the mathematical model analysis is difficult because the two types of data obtained cannot be readily compared. The researchers expressed surprise that the convergences and deformations were so small and also that the area of influence tended to be very much greater than would be expected from a conventional mining area within relatively thin seams. The principal stress diagrams generated by the mathematical model (Chapter 4) show that the area of influence of the excavation on the



stress distribution is considerable (in excess of 50 metres from the excavation). However no other conclusions can be readily drawn as to similarities between the two analyses.

#### 5.4 Observations at the Mindola Mine

The sublevel mining system at the Mindola Mine is very different from the two mines previously described because it is a hard rock operation operating at depths of 650 to 1000 metres. However the sublevel layout and the dip of the orebody are similar and the relatively weak ore bounded by hard quartzite country rock can be likened to the coal seams contained in the strong sandstones of the Foothills formations.

A number of observations were made in this mine to discover highly stressed zones, and modifications to the mining system were adopted to alleviate severe problems. It was noted that above the extracted stope the hanging wall roof beam would sag but fail to cave. Eventual failure of this layer produces a violent air blast that effects the safety of working places. This observation concurs with the mathematical model analysis where in Configurations 1 and 2 the alignment of major principal stress trajectories parallel to the stope roof may be responsible for its reluctance to fail. It was further observed at the Mindola Mine that stresses peaked in the hanging wall and footwall of the pillar immediately below the uncaved stope. This is also seen in the mathematical model where stress transfer



mechanisms seem to be similar.

A major problem noted at the Mindola Mine related to blast holes drilled from a sublevel into the extraction block above. All production was achieved by drill and blast techniques as opposed to hydraulic breakage and this required long blastholes to be drilled in rings around a production sublevel. As depths increased it was noted that long holes deviated or closed soon after drilling. To make the long holes functional they had to be charged immediately after drilling although they would not necessarily be blasted for two or three weeks. The high pressures and the ground movements in these blocks promoted premature detonation of some holes and this occurred more frequently at greater depths.

This problem is demonstrated in the mathematical analysis where, especially in Configurations 1 and 2, high pillar stresses occurred. The significance to a sub-level operation is not of course premature blast hole detonation but crushing of valuable coal in the pillar and perhaps the increased likelihood of coal and gas outbursts. Also greater roadway maintenance may be required.





## 6. Physical Model Studies in Steep Seam Mining

### 6.1 Introduction

As an integral part of research into the mining of steeply dipping thick seams physical model studies have been performed by other researchers within the Department of Mineral Engineering.<sup>17</sup> It was considered useful to compare the results of the physical model studies with those of the mathematical analysis. Physical models can provide a qualitative assessment of how an excavation may behave under gravity loading and suggest the location and nature of deformations. The base friction technique employed in these studies has been available for approximately ten years and has been modified and improved upon by various investigators in that period.<sup>18 19</sup> In this chapter the modified base friction technique is described and the results are compared with those obtained from the mathematical analysis performed by the author.

### 6.2 Model Materials

For effective physical modelling model materials must be chosen such that their properties relate to those of the in-situ strata. This is achieved by selecting materials whose compressive strength is at a constant factor lower than the compressive strength of the rock material but has similar stress-strain relationships. Two model materials were selected for simulation of coal and sandstone and their



properties are briefly described below.

### 6.2.1 Coal

Coal is modelled by a mixture of plaster, sand and vermiculite. It is compacted in layers to simulate bedding and the mixed vermiculite grains give a cleat texture to the model material. It is a low density material (1114 - 1282 kg/cu.m) and has a low uniaxial compressive strength between 0.05 and 0.1 MPa. The strength scaling factor of the model material to coal is 1:160 for coal samples taken from the No. 4 seam at Grande Cache. The uniaxial strength of this moderately hard coal is between 10.0 and 17.2 MPa. The stress-strain diagrams (Figure 59) of both coal and the model material were found to be sufficiently similar to make this a valid modelling material.

### 6.2.2 Sandstone

For modelling sandstone a material composed of fine sand and plaster was used. As before it was compacted in layers to simulate bedding. The material has a fine grained texture and a density of 1560 - 1672 kg/cu.m. The model material has a uniaxial compressive strength of 0.58 - 1.03 MPa which when multiplied by the scaling factor of 1:160 falls within the values of sandstone uniaxial strength which are in the range 96 - 200 MPa. The stress-strain behaviour to failure of the model material is similar to sandstone in that they are both linear and exhibit brittle failure



(Figure 60). The axial strain at failure of both the sandstone and its model material is about one quarter of the axial strain at failure of the coal and its model material. Since the strength and strain properties have been scaled uniformly the two materials were considered suitable for modelling.

### 6.3 Model Frame and Loading Conditions

The base friction frame used was built in the Department of Mineral Engineering and has been described in detail elsewhere.<sup>20</sup> It consists of a wooden frame approximately 1.5 metres by 2.5 metres containing a continuous friction belt which is driven by a small electric motor. There is a facility to incline the frame and belt as required (Figure 61). The particular model described here used only the lower portion of the frame since relatively small scale tests were being performed. Another modification adopted by the researchers was similar to that developed by Egger.<sup>21</sup> He describes a model in which the material is confined in the third dimension (out of the plane of the model) by a sheet of plexiglass which is subsequently loaded by compressed air rams. This has the effect of increasing the normal reaction of the model material on the friction belt which in turn increases the shear stress acting on the model material. In the tests described here the compressed air rams were replaced by lead weights spread evenly across the surface of the plexiglass. Additional loading of the





model material was achieved by two other measures. Firstly the belt was inclined at an angle of 25 degrees so that a gravitational component is added to the shear stress induced by the belt. Secondly lead weights were placed along the top edge of the model material to add a further load component (Figure 61). These measures are taken so that higher strength materials can be used with failure still occurring. When dealing with very low strength modelling materials it has proved difficult to obtain constant material physical properties.

The loading conditions and the structural configuration of the model are illustrated in Figure 62. The model material is confined horizontally and along the bottom edge by rigid barriers to prevent displacement in these directions. The model represents a 45 metre thick coal seam dipping at 30 degrees between two beds of sandstone. Mining is simulated to a depth of 150 metres and three sublevels are excavated in the seam by removing coal material (Figure 63). This layout is therefore similar to that analysed in Configuration 3.

#### 6.4 Operating the Model

On completion of construction of the model, with removal of the appropriate coal material, the confining barriers and plexiglass sheet can be positioned. The lead weights are then placed on the plexiglass and along the top edge, and the frame inclined at 25 degrees. The belt is set





in motion by the motor for a few seconds and then stopped. The effect on the model is examined and the result photographed. A problem was reported at this stage because pphotography of the model required removal of the lead weights and the plexiglass. This allowed some minor deformation in the direction supposedly confined by the plexiglass. The deformation in this plane was considered to be so small, however, as to be insignificant. The model is reloaded and the cycle repeated until no further deformation is recorded. The deformation stages are photographed and reproduced in photographic plates 1 to 6. However since definition is rather poor the plates have been represented as line drawings in Figures 63 to 68 and these are used in the following section to assess the physical model results.

## 6.5 Physical Model Results

The nature of the deformations obtained from the physical model tests illustrated in Figures 63 - 68 show reasonable agreement with the observations made in the operating mines and those generated by the mathematical modelling. The results can only be used qualitatively to identify areas of potential instability and modes of failure but the method does provide one of the best visual representations of deformation induced by mining.



### 6.5.1 Deformation Throughout the Structure

In the extracted zone the initial deformation is considerable and predictable. The immediate roof layers separate along a simulated bedding plane to create a roof beam. This starts to sag and then fails in tension perpendicular to bedding (Figure 64). This failure process is repeated throughout the hanging wall zone to the surface until the void is filled with caved material (Figure 65). The failure of the roof layers with progressive sagging and final failure is similar to that observed in the Chinese hydraulic mines (Chapter 5). Figure 65 illustrates the angle of break generated by the caving of the hanging wall. In this case it is found to be 65 degrees which agrees very closely with the angle used in the mathematical model, 68 degrees, which was derived from Hoek's criteria (Chapter 2). Along this boundary two modes of failure are active. The weight of the unsupported overhang results in a tendency for the hanging wall to try and rotate. This generates tensile forces near the surface which are seen in the mathematical model analysis. This may lead to the development and propagation of tension cracks along the boundary (Figure 69). Shear forces due to the weight of the overhanging wedge may also be active along this boundary and their presence will be more noticeable because of the reduction in normal force caused by the rotational effect.

A second major deformational feature seen in the model occurs approximately 50 metres (scaled) above the pillar



between the first and second sublevels. This feature is bed separation and is the result of closing of sublevels and deformation of pillars in the coal seam. Bed separation was recorded in the Kaiser hydraulic mine (Chapter 5) by multi-wire borehole extensometers at a point 36 metres above the sublevel so a similar occurrence in the physical model is encouraging.

### 6.5.2 Deformation Around the Sublevels

The deformations around the sublevels and in the pillars photographed in Plates 4, 5 and 6 and illustrated in Figures 66 - 68 are also observable in the operating mines and the mathematical model. High pillar stresses noted in Configurations 1, 2 and 3 have resulted in partial failure of the pillar between the first and second sublevel especially in the footwall. This is evidenced by the cracking and generation of powdered material. This effect was also observed by the Chinese who described pillars of crushed coal which had very low bearing capacity. The displacements in the pillar would also agree with the deviations and deformations of the blast holes noted in the Mindola Mine (Chapter 5).

Instability in the sublevels is also noticeable with the uppermost sublevel experiencing total closure and the middle sublevel showing deformation in the floor and cracking in the roof. This confirms the need for sublevel support as is utilised in all the hydraulic mines studied.





The uppermost sublevel experienced roof closure and floor uplift. Floor uplift or heave is experienced in many coal mines of varying configurations and is a result of stress redistribution below the excavation. Due to stress relief in the floor vertical stresses at the excavation boundary go to zero so that the immediate floor is effectively in uniaxial compression. This leads to compressive failure in the unconfined direction, vertically upwards, and gives rise to floor heave. In many deep coal mines floor heave of up to one metre in two or three days is not uncommon.

Severe disturbance in the sublevels adjacent to the workings was recorded in the Chinese hydraulic mines with lesser effects noted in the lower sublevels. This is also seen in the physical model and in conjunction with the other observations demonstrates its validity for general prediction of unstable zones.



## 7. Conclusions and Recommendations

This thesis represents a preliminary analysis of some aspects of a mining technique that may be utilised in the extraction of steep seams in the Foothills and Mountain region of Western Canada. It proceeds with little knowledge of the properties of the rocks and coal of the region, and their behaviour under extraction. It indicates that there is a contribution to be made to mine design and planning by modelling techniques. Mining of coal has been practiced around the world for centuries and to a large degree design methods have relied on "rules of thumb" and trial and error techniques. The capital intensive mining developments in the remote areas of the mountain region will require research and planning to reduce the risks and unknowns involved in adopting new mining techniques. The conclusions in this chapter and the resulting recommendations therefore represent the author's opinion of how research should develop so that sublevel hydraulic coal mining can be practiced more efficiently in the future. Although published material on this method of mining is scarce it would appear from experience in China, Russia and the single mine in Western Canada that the sublevel method will see wider utilisation. Certain features increase its safety over conventional methods namely the elimination of explosives, the dust suppression provided by the cutting and transport media, and the removal of the requirement for men to enter the actual working area. Accepting, therefore, that this



method will be employed the following areas must be more closely researched:

Rock samples for testing purposes were obtained from drill core and were suitable for a limited study such as this. However in an operating mine, where shafts and development roads will encounter a greater variety of formations and greater accuracy and certainty will be required, a more wide ranging test program will have to be initiated. Not only will this require many more samples but testing will have to be performed under conditions of natural moisture and saturation to take into account the effects of large quantities of water if hydraulic breakage is used. Investigations will also have to look at time dependant behaviour of both coal and adjacent strata since permanent pillars will probably be used between mine panels to increase mine stability. A field testing program will have to be designed that is related to the mining method so that the maximum possible information can be gained in the sensitive areas of the excavation.

The finite element analysis provides an approximate appraisal of how stresses will be redistributed around the excavations and identifies potential problem areas. The findings show some agreement with reported observations in operating mines. This method of analysis can be made considerably more realistic with more sophisticated computer programs if the initial property data is available. Non-linear, elasto-plastic and plastic analysis and the





simulation of joints and faults are just some of the options available with the finite element method. Reliability with this kind of analysis will only be achieved when an underground district, such as at Kaiser Resources' mine, can be fully instrumented and the resulting data used to verify and improve the accuracy of theoretical techniques.

The physical model studies illustrate the types of failure that are active and where they may occur. Although scaling of strength and deformational properties is incorporated only a qualitative assessment of behaviour can be obtained. Three dimensional physical modelling has been employed for analysis around openings in longwall mines with realistic results.<sup>22</sup> If physical modelling is to be developed for sublevel mine analysis, three dimensional techniques must be used to determine the interaction between extracted stopes and adjacent pillars, and the developing sublevels below.

Any technique that provides greater understanding of excavation behaviour in underground mining situations is useful. Both the mathematical and physical model analyses have been shown to be useful in identifying probable locations in which problems will occur. In the future there will be an increasing adoption of this kind of technique which will do its part in trying to reduce the risks inherent in any new mining venture.





## REFERENCES

- (1) JEREMIC, M.L., Coal Mining in Western Canada  
University of Nottingham Mining Magazine, England  
Volume XVIII, 1978.
- (2) DAMES and MOORE. (Consulting Engineers).  
A Report on the Current Status of the Canadian Coal  
Mining Industry. (pp 49-50) May, 1978.
- (3) WRIGHT, P.L., Layout of the Continuous Miner  
Operations at the Smokey River Mines.  
C.I.M. Bulletin, March 1973.
- (4) ADAM, R., French Thick Seam Mining Practice.  
The Aus. IMM Central Queensland Branch, Symposium  
on Thick Seam Mining by Underground Methods.  
September, 1976.
- (5) U.S.B.M., Research Contract J0265008.  
Longwall Caving Mining Method for Thick Coal.
- (6) PARKES, D. and GRIMLEY, A.W.T.,  
Hydraulic Mining of Coal,  
Mining Congress Journal, May, 1975.
- (7) IRVINE, J.A., Exploration Techniques, Upper Elk  
Coalfield, British Columbia.  
First Geological Conference on Western Canadian Coal,  
1971.
- (8) LATOUR, A., Coal Deposits of Western and Northern  
Canada. First Geological Conference on Western  
Canadian Coal, 1971.
- (9) NORTON, D., and SYMONDS, D.F.,  
Petrography in Coal Processing. First Geological  
Conference on Western Canadian Coal.
- (10) SHAW, J.D., The Kaiser Resources Ltd. Hydraulic  
Coal Mine. The 19th U.S. Symposium on Rock  
Mechanics, 1978.
- (11) HOEK, E., Progressive Caving Induced by Mining  
an Inclined Ore Body. Trans. Inst. Min. and Met.,  
London, October, 1974.



- (12) HOEK, E., and BROWN, E.T.,  
Underground Excavation Engineering.  
In Print, I.M.M. London, England.
- (13) TERZHAGI, K., and RICHART, F.E.,  
Stresses in Rock About Cavities.,  
Geotechnique Vol. 3., 1952. (pp 57-90)
- (14) LIN, Y.L., and PANG, Y.,  
Laws Governing the Manifestations of Rock Pressure  
in Connection with the Hydraulicking of Thick Seams.  
Technical Exchange Division, China Coal Society,  
Peking, People's Republic of China., 1978.  
Sixth International Strata Control Conference,  
Banff, 1977.
- (15) FISECKI, M., and GRIMLEY, A.W.T.,  
Strata Control Studies at the Hydraulic Mine.,  
Sixth International Strata Control Conference,  
Banff, 1977.
- (16) JEREMIC, M.L., Stress Mechanism at the Mindola  
Mine, Zambia., Canadian Mining and Metallurgical  
Bulletin, November, 1978.
- (17) JEREMIC, M.L., Notes on Physical Model Studies in  
Steep Seam Mining., (Unpublished), Dept. of Mineral  
Engineering, University of Alberta, September 1978.
- (18) HOEK, E., Rock Engineering.  
Inaugural Lecture. Imperial College, London 1971.
- (19) GOODMAN, R.E., Methods of Geological Engineering,  
(Chapter 5). West Publishing Co. San Francisco 1976.
- (20) BAUMGARTNER, P., The Effect of Joint Fabric on Rock  
Mass Caving., MSc. Thesis, Dept. of Mineral  
Engineering, University of Alberta, Fall 1979.
- (21) EGGER, P., A New Development in the Base Friction  
Technique. Laboratoire Geotechnique, EPF,  
Lausanne, 1979.
- (22) HOBBS, D.W., Scale Model Studies of Strata Movement  
Around Mine Roadways. Int. Journal of Rock Mec.  
and Min. Sci., 5, (pp 219-235) 1968.



- (23) LEE, K.L., and IDRIS, I.M.,  
Static Stresses by Linear and Nonlinear Methods  
Journal of the Geotechnical Division,  
A.S.C.E. Proceedings, Vol.101, 1975, pp 871-887.
- (24) JEREMIC, M.L.,  
Coal Behaviour in the Rocky Mountain Belt  
of Canada . International Congress on Rock  
Mechanics, Montreux, 1979. pp 189-195





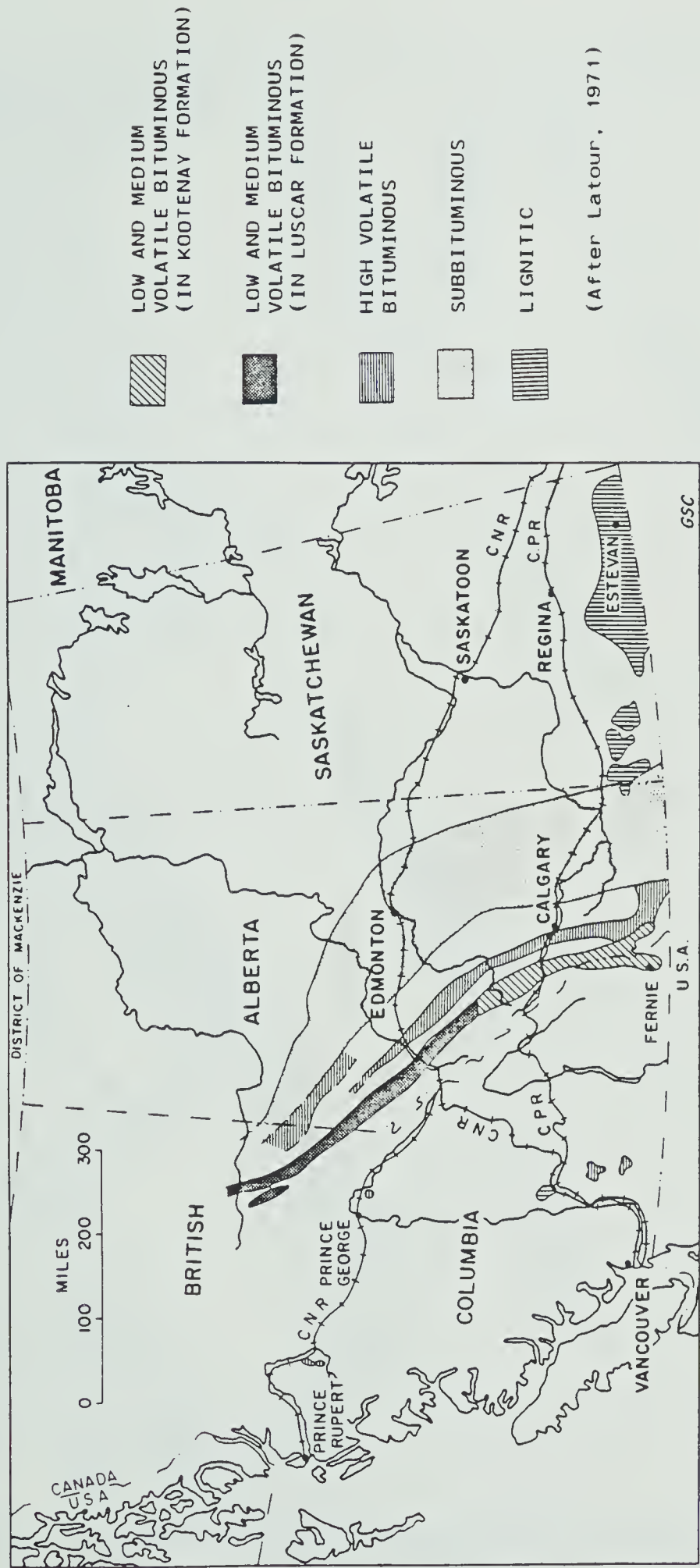


FIGURE 1 COAL DEPOSITS OF WESTERN CANADA BY RANK



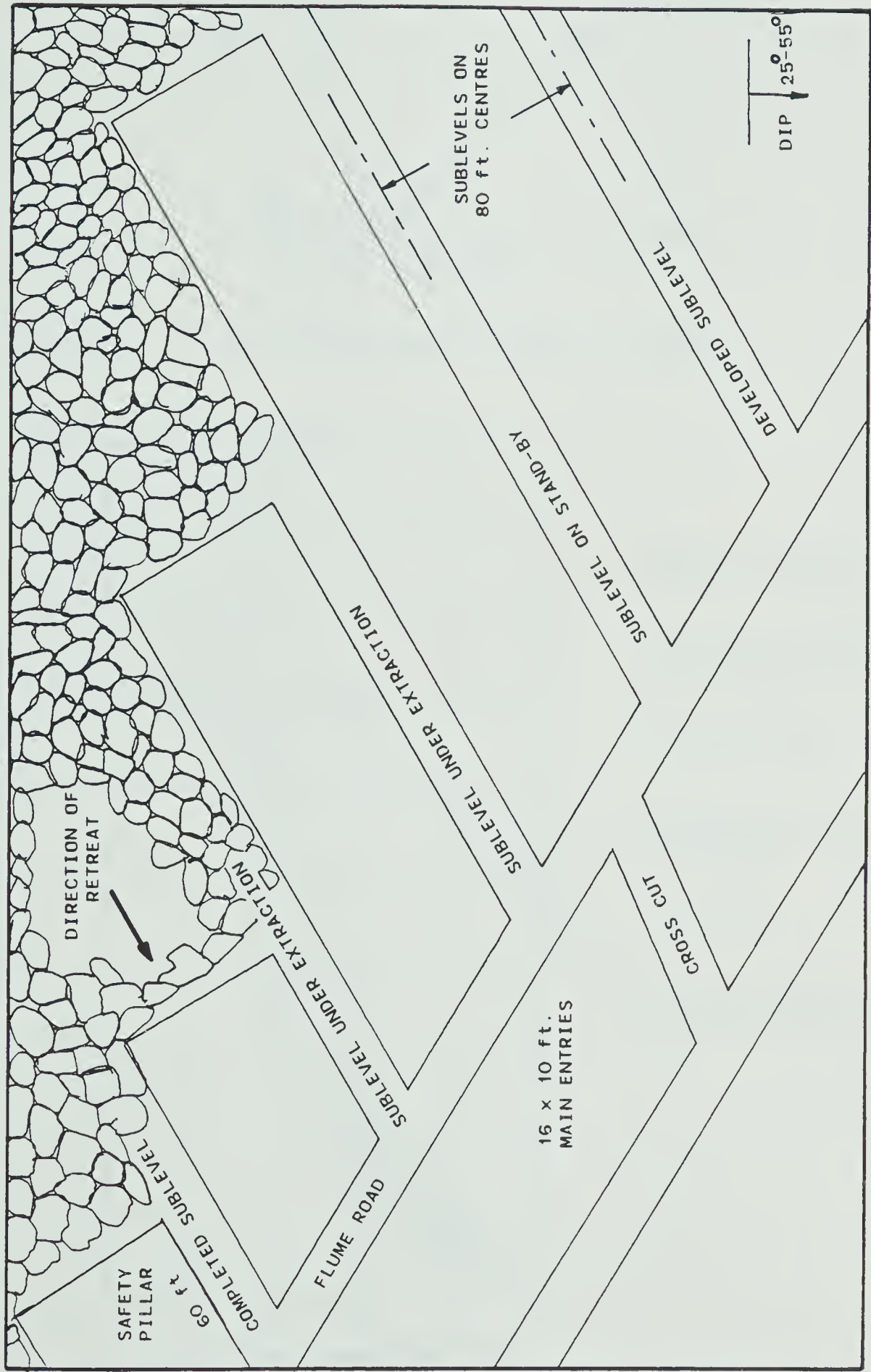


FIGURE 2. HYDRAULIC MINE SUBLEVEL LAYOUT



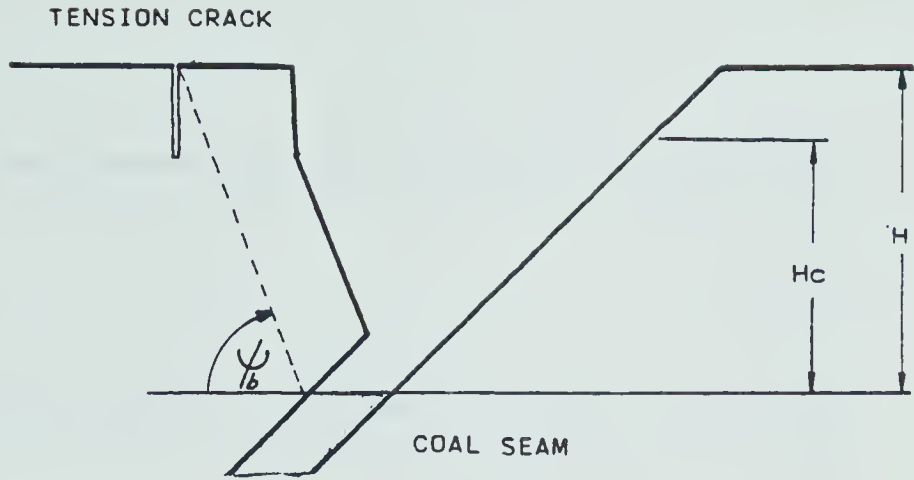


FIGURE 3. ILLUSTRATION OF ANGLE OF BREAK

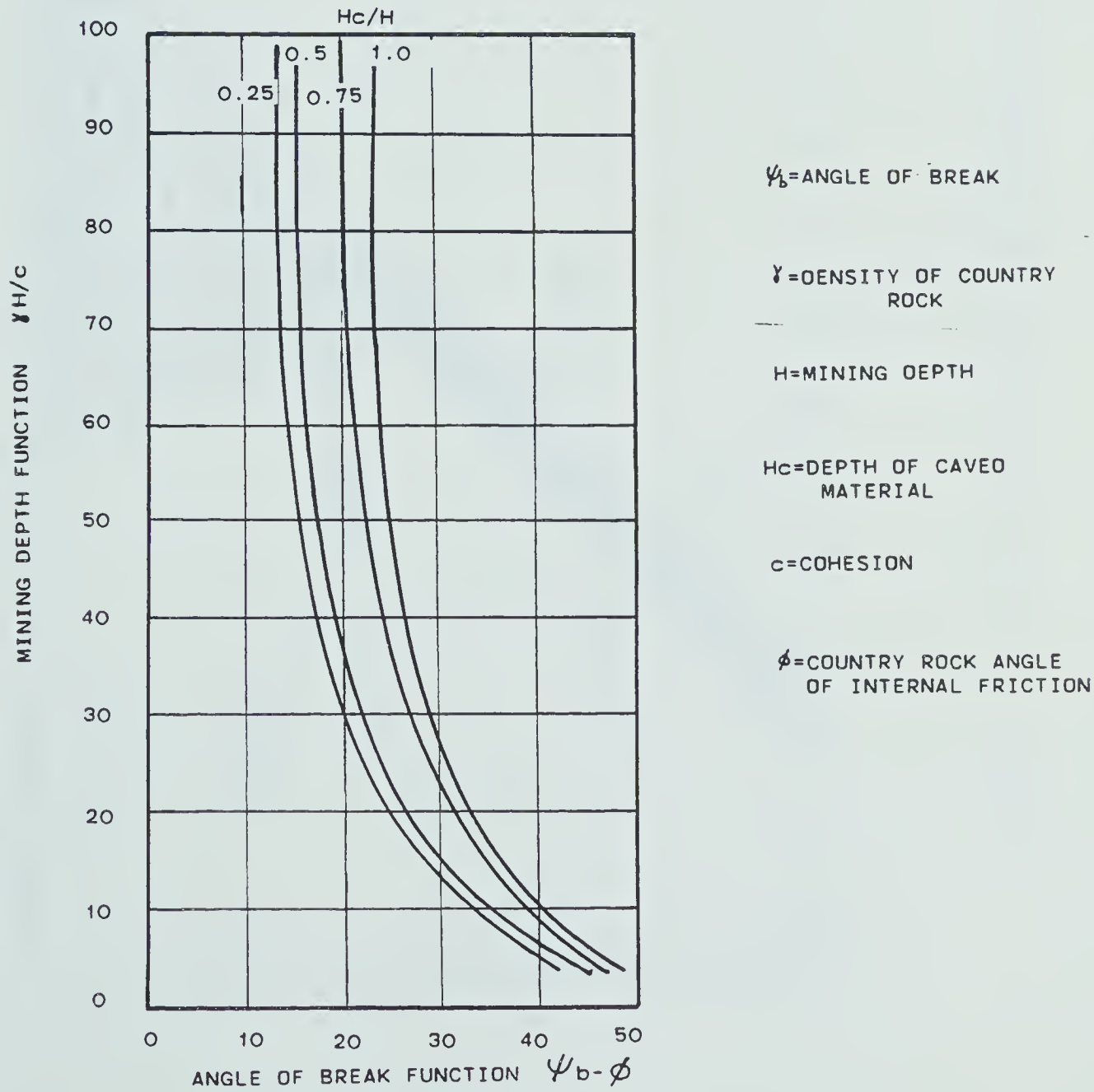


FIGURE 4. ANGLE OF BREAK CHART



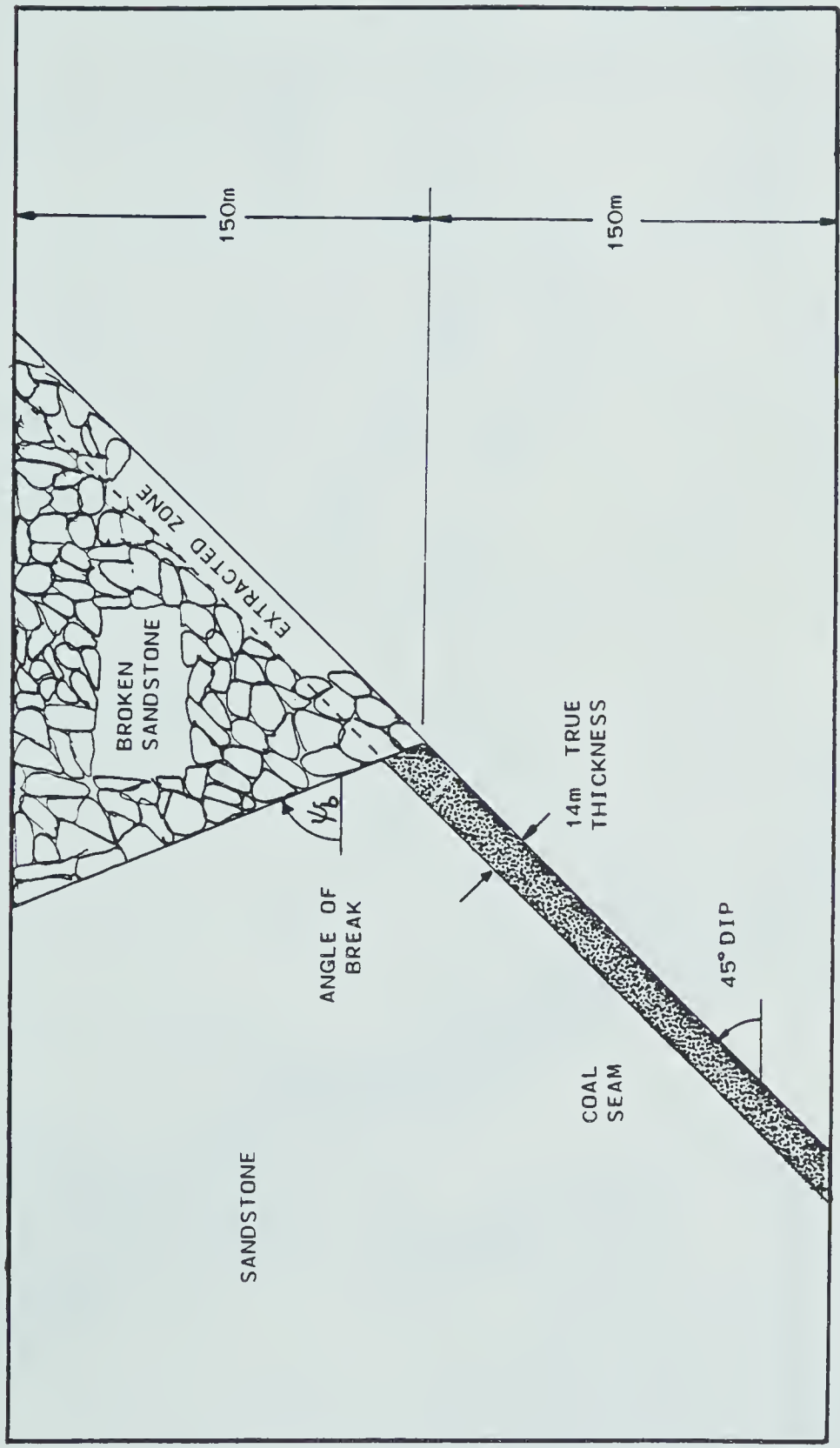
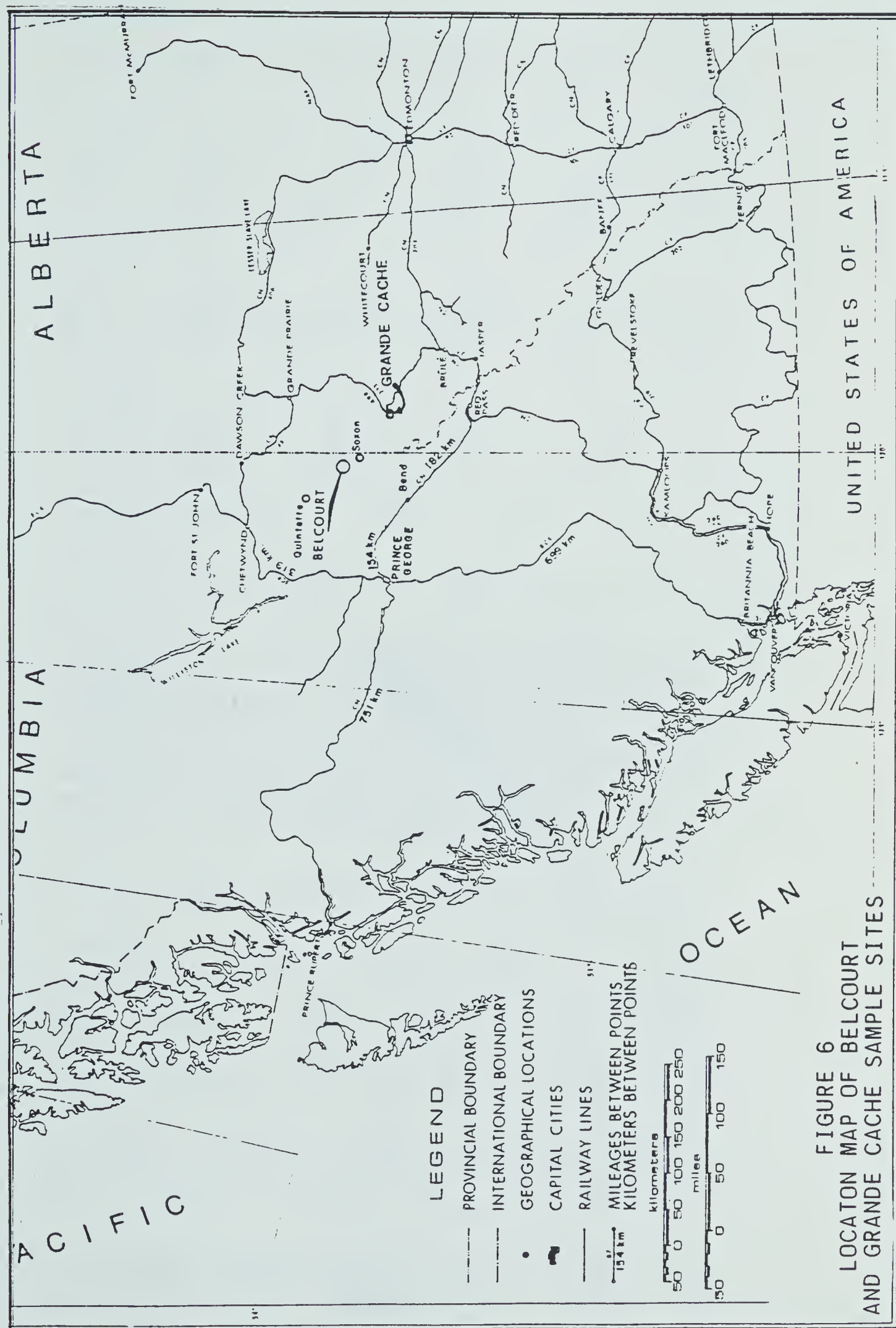


FIGURE 5 IDEALIZED SECTION FOR MATHEMATICAL MODEL ANALYSIS









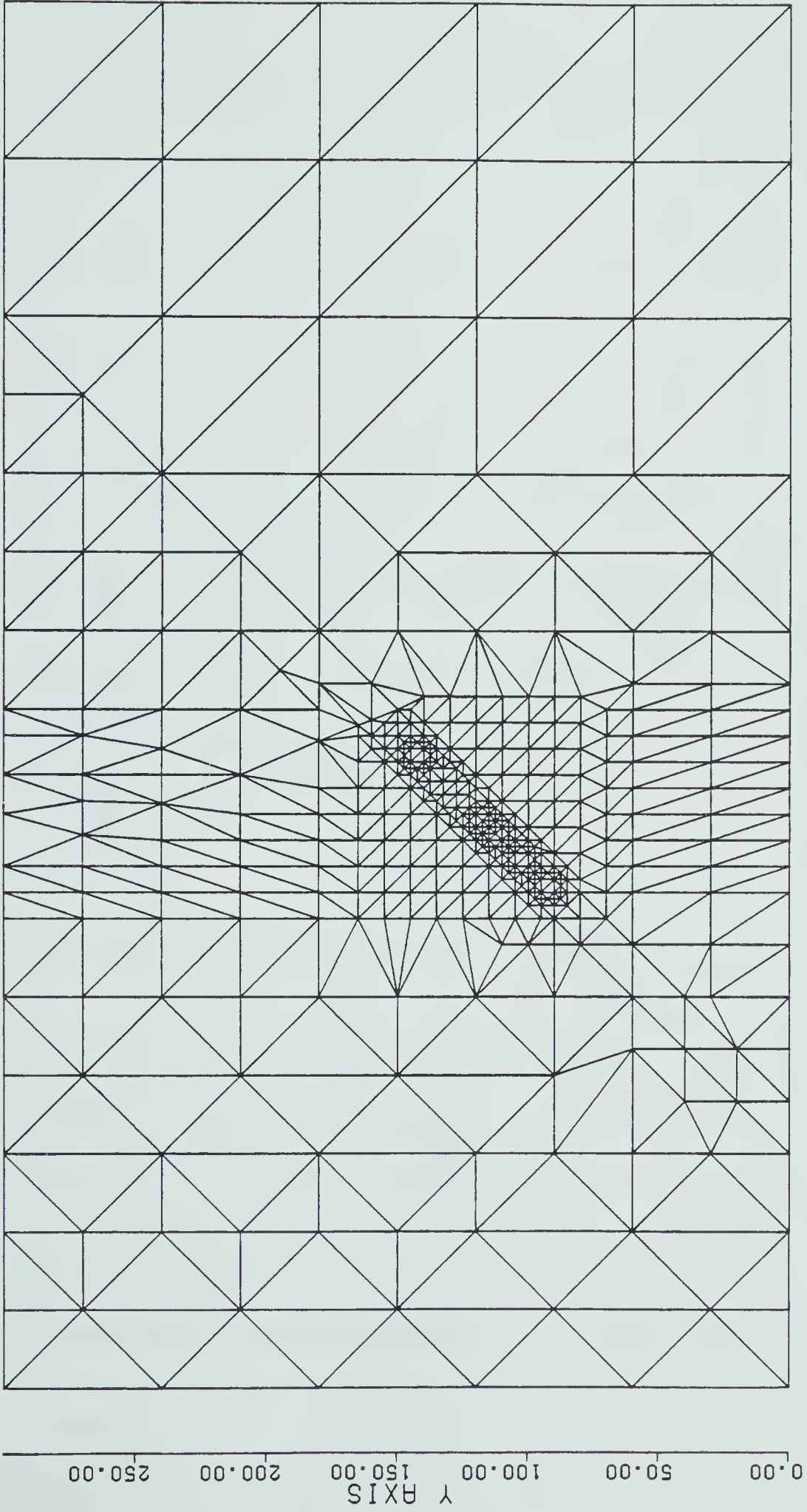


Figure 7. Finite Element Mesh



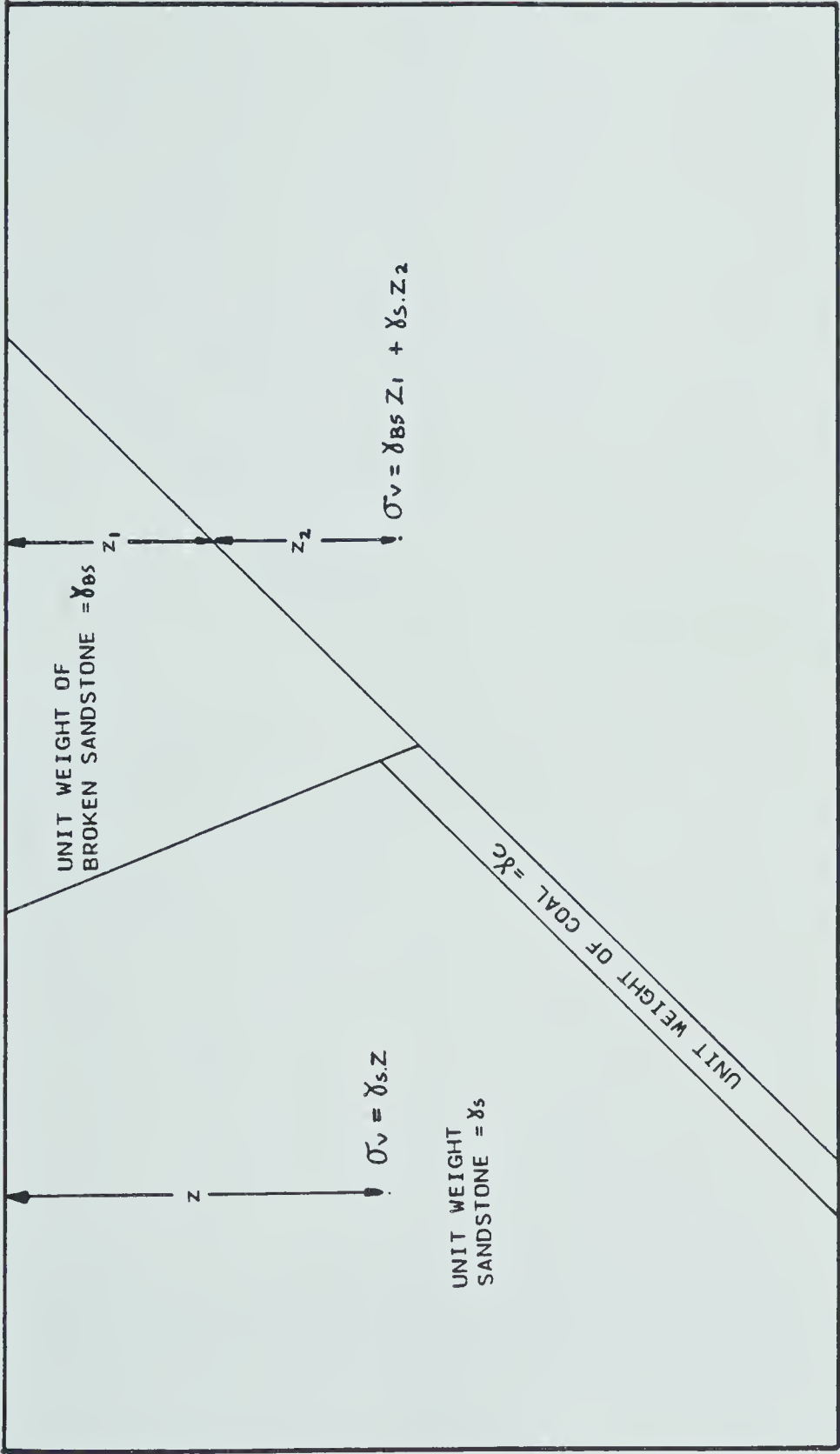


FIGURE 8      CALCULATION OF VERTICAL STRESS AT A POINT





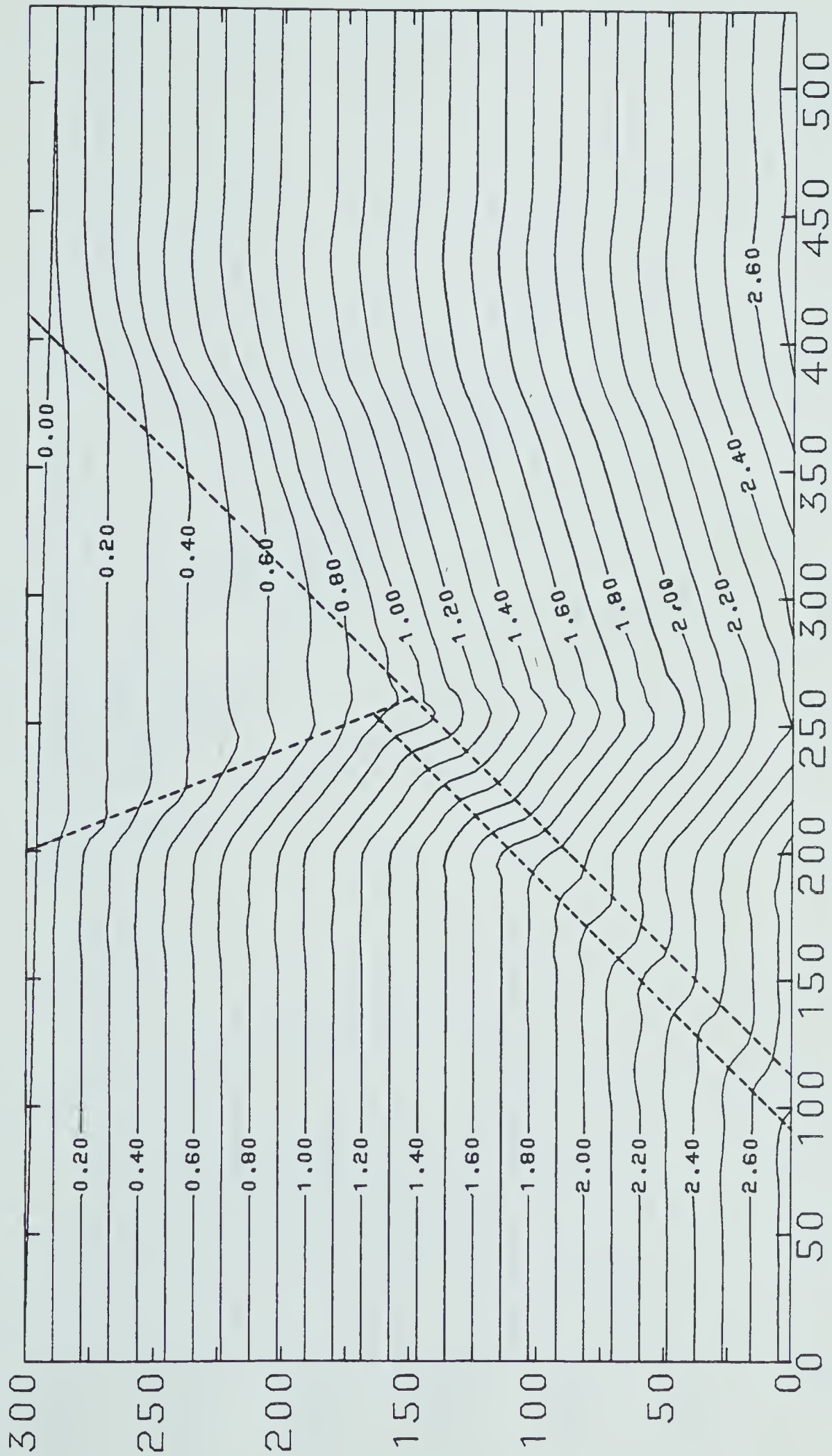


FIGURE 9 Initial Horizontal Stress



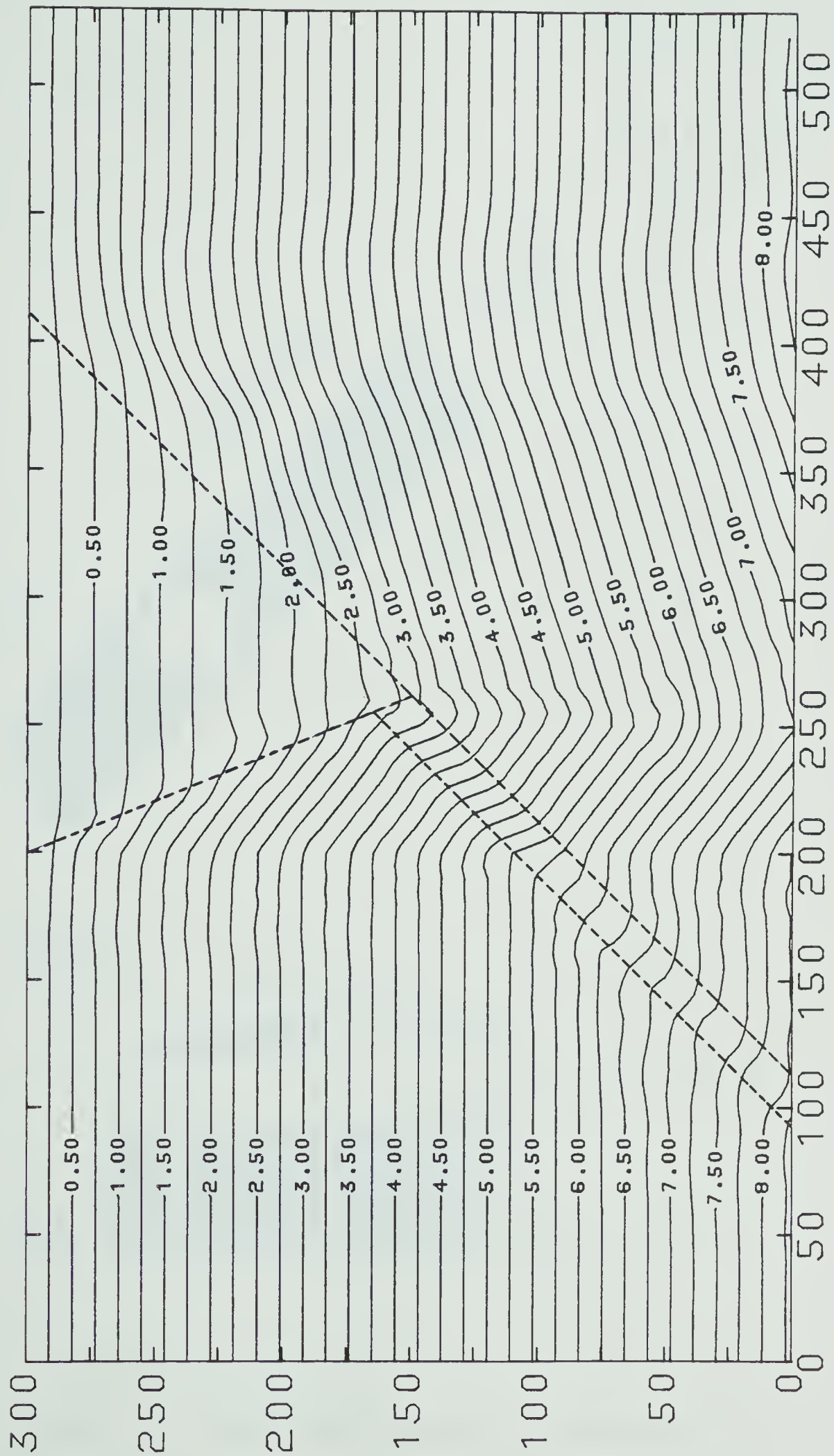


FIGURE 10 Initial Vertical Stress



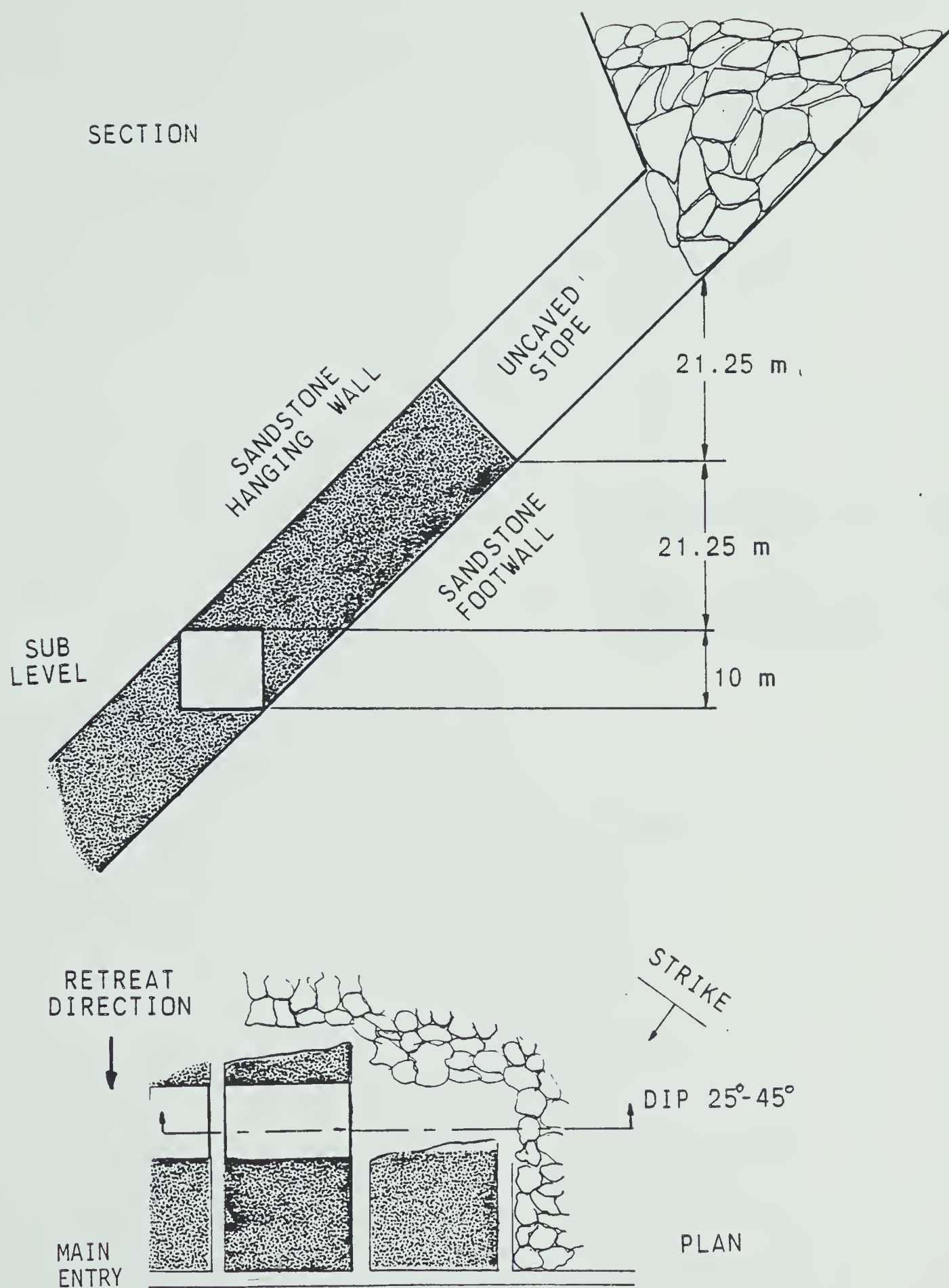


FIGURE 11 PLAN AND SECTION OF CONFIGURATION 1



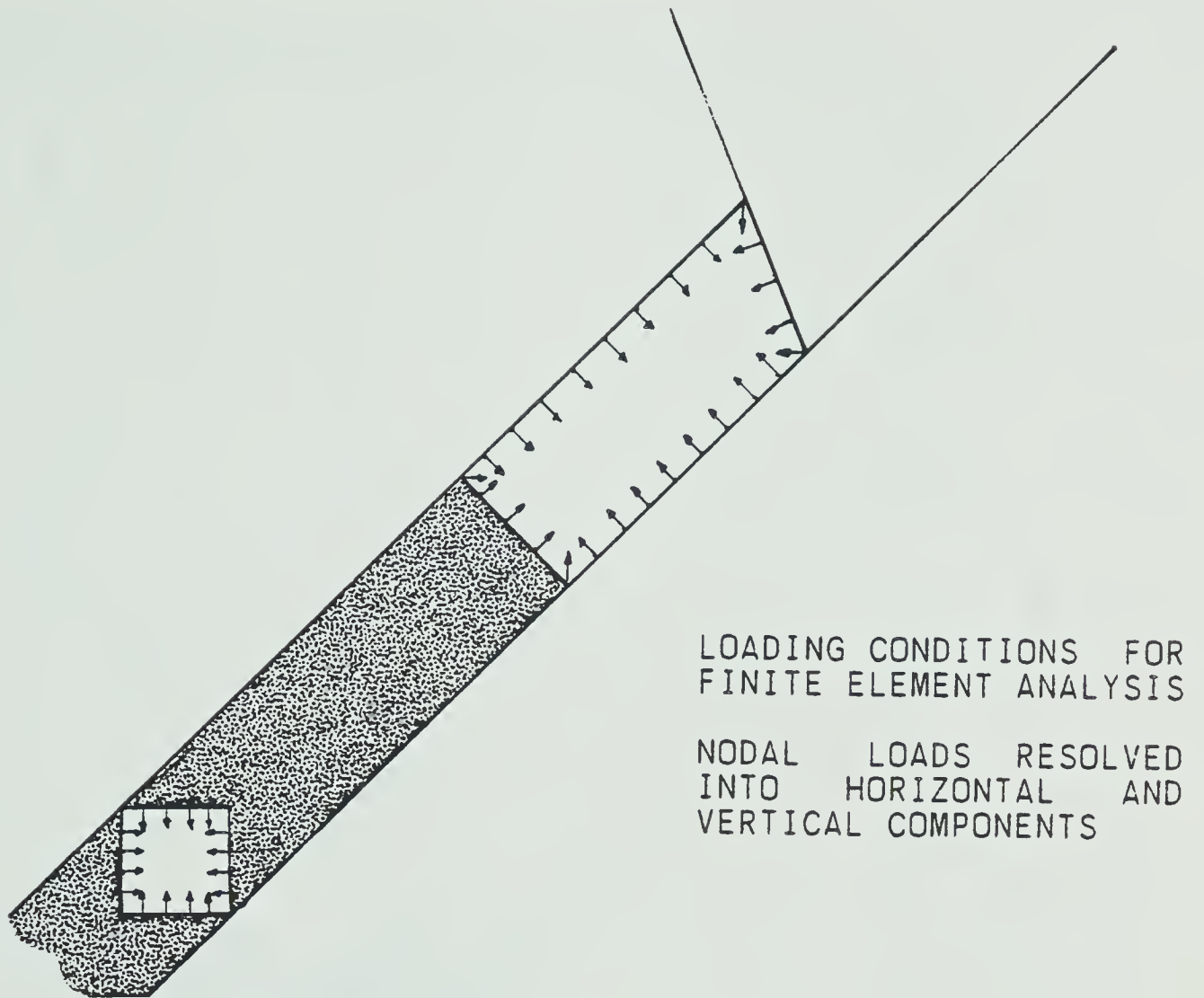


FIGURE 12      LOADING CONDITIONS FOR CONFIGURATION 1





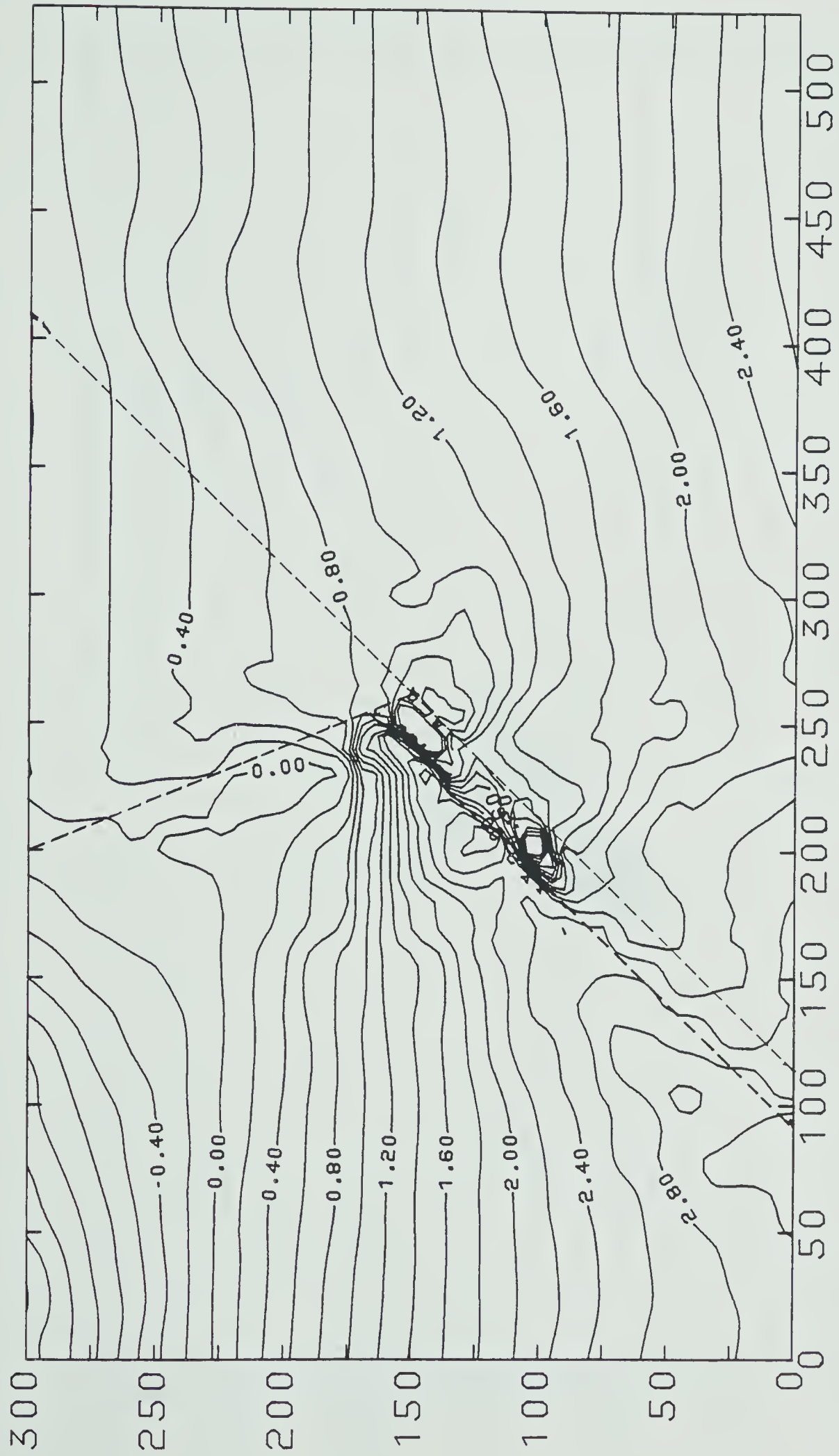


FIGURE 13  
HORIZONTAL STRESS DISTRIBUTION THROUGHOUT THE MESH



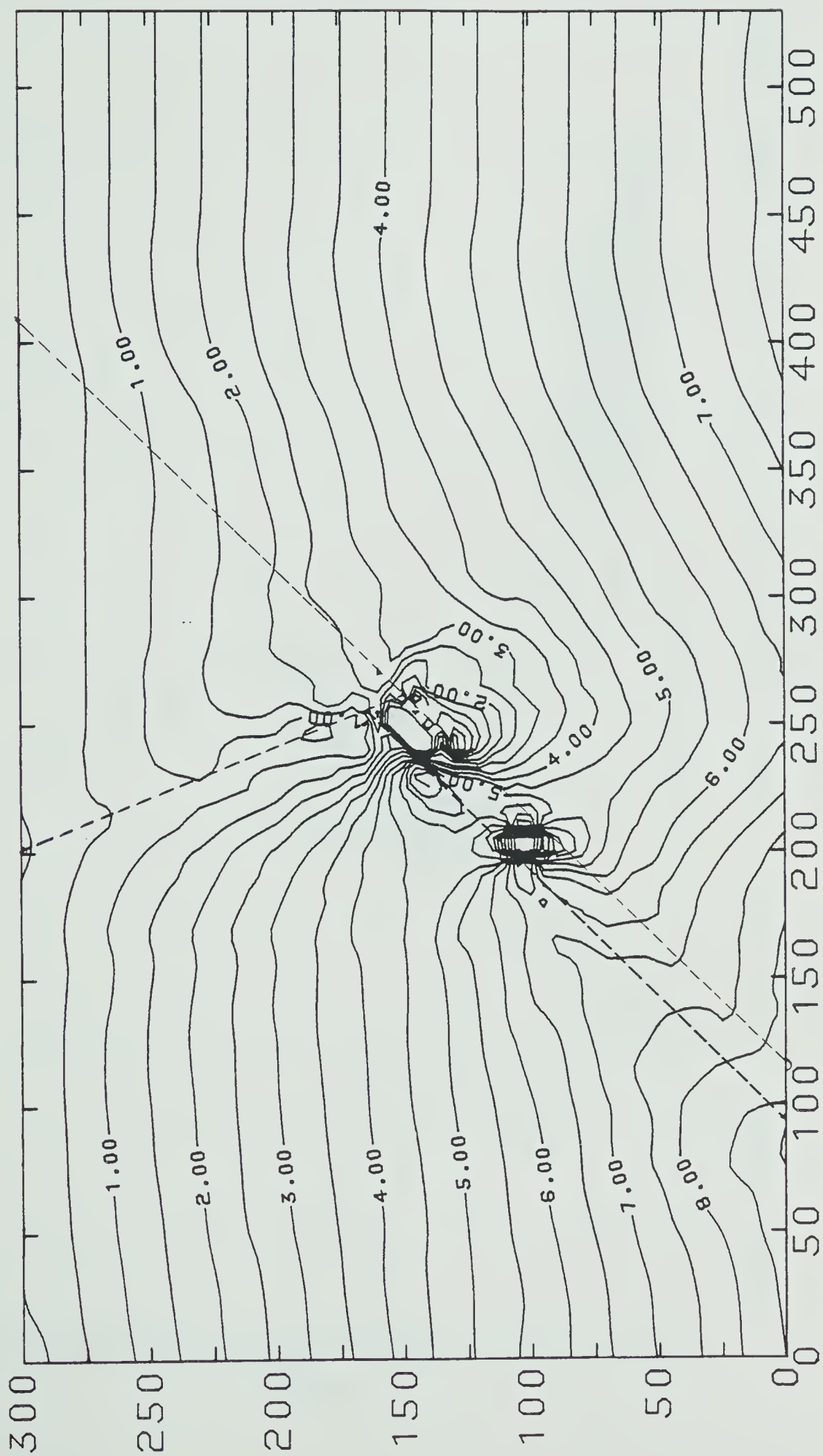


FIGURE 14  
VERTICAL STRESS DISTRIBUTION THROUGHOUT THE MESH



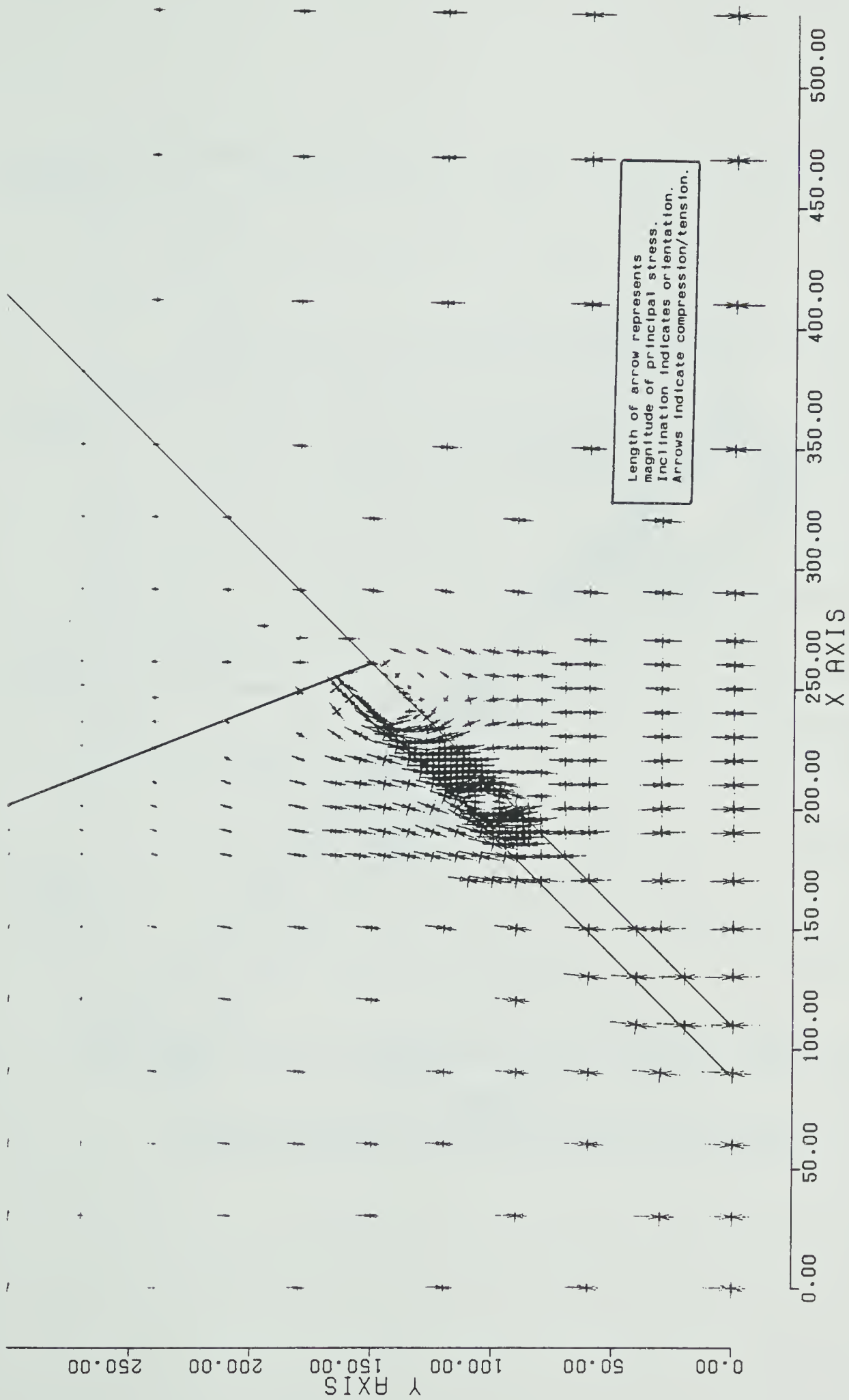


FIGURE 15 PRINCIPAL STRESSES THROUGHOUT THE MESH





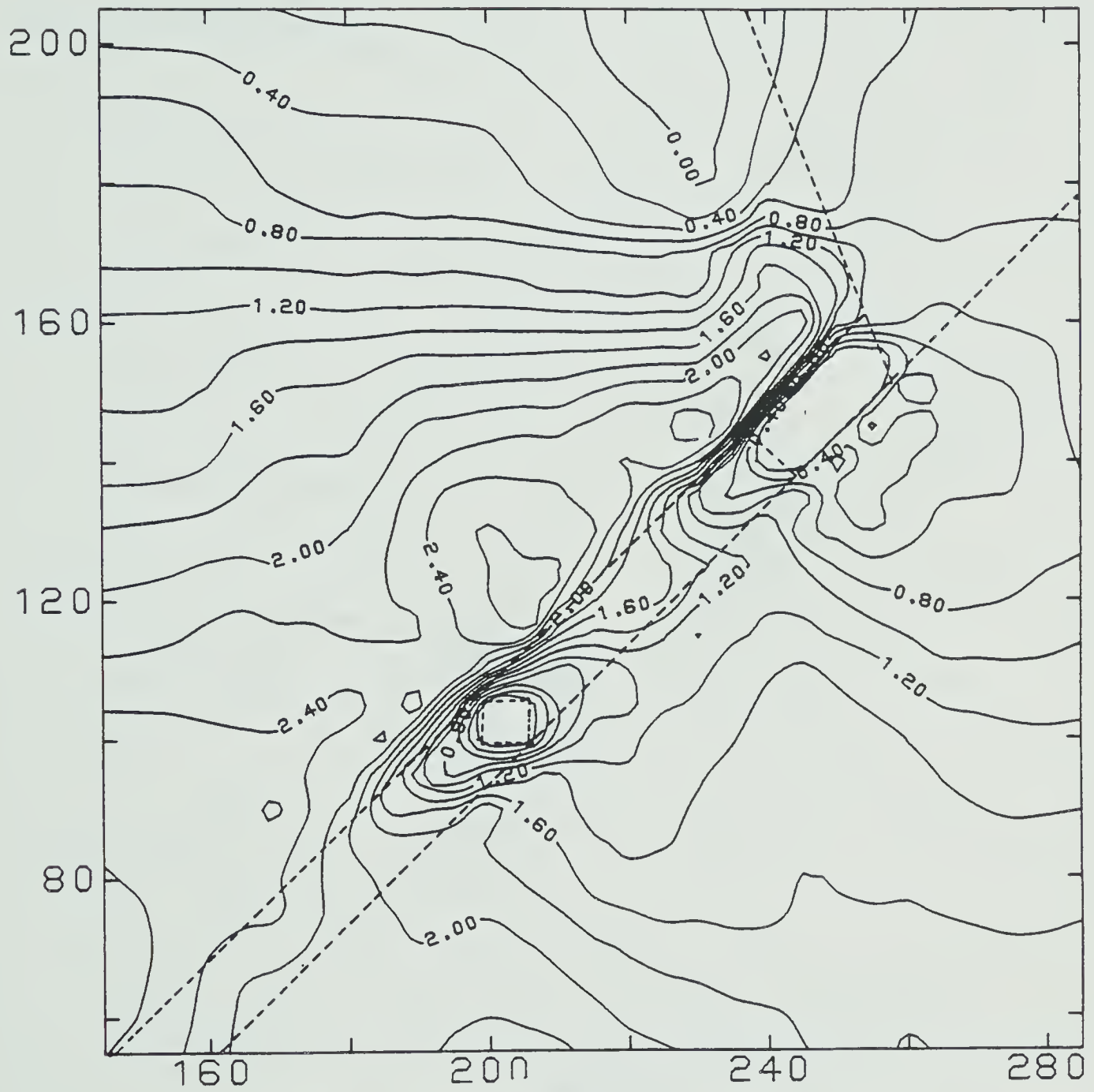


FIGURE 16  
HORIZONTAL STRESS DISTRIBUTION AROUND THE EXCAVATIONS



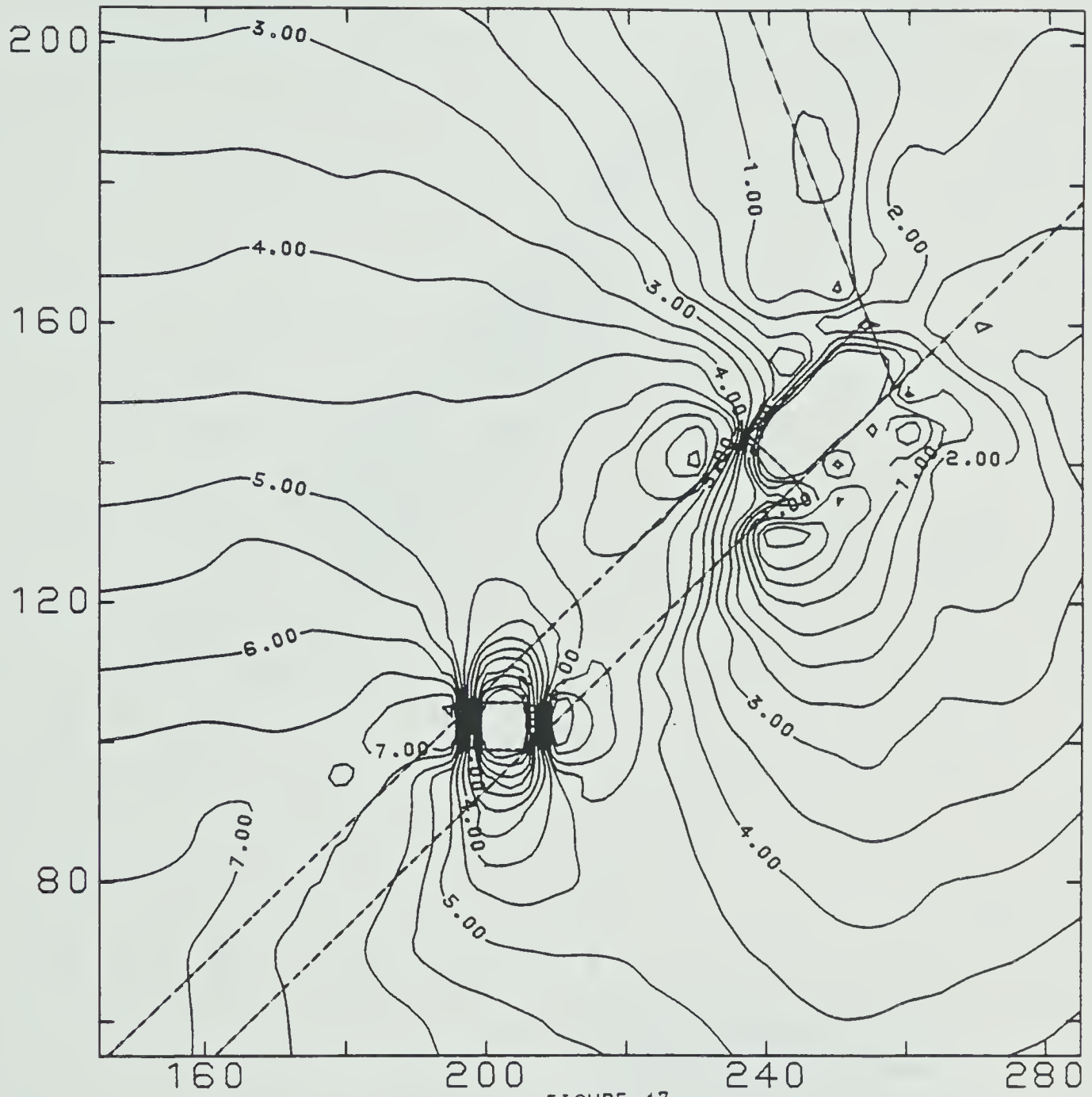


FIGURE 17

VERTICAL STRESS DISTRIBUTION AROUND THE EXCAVATIONS



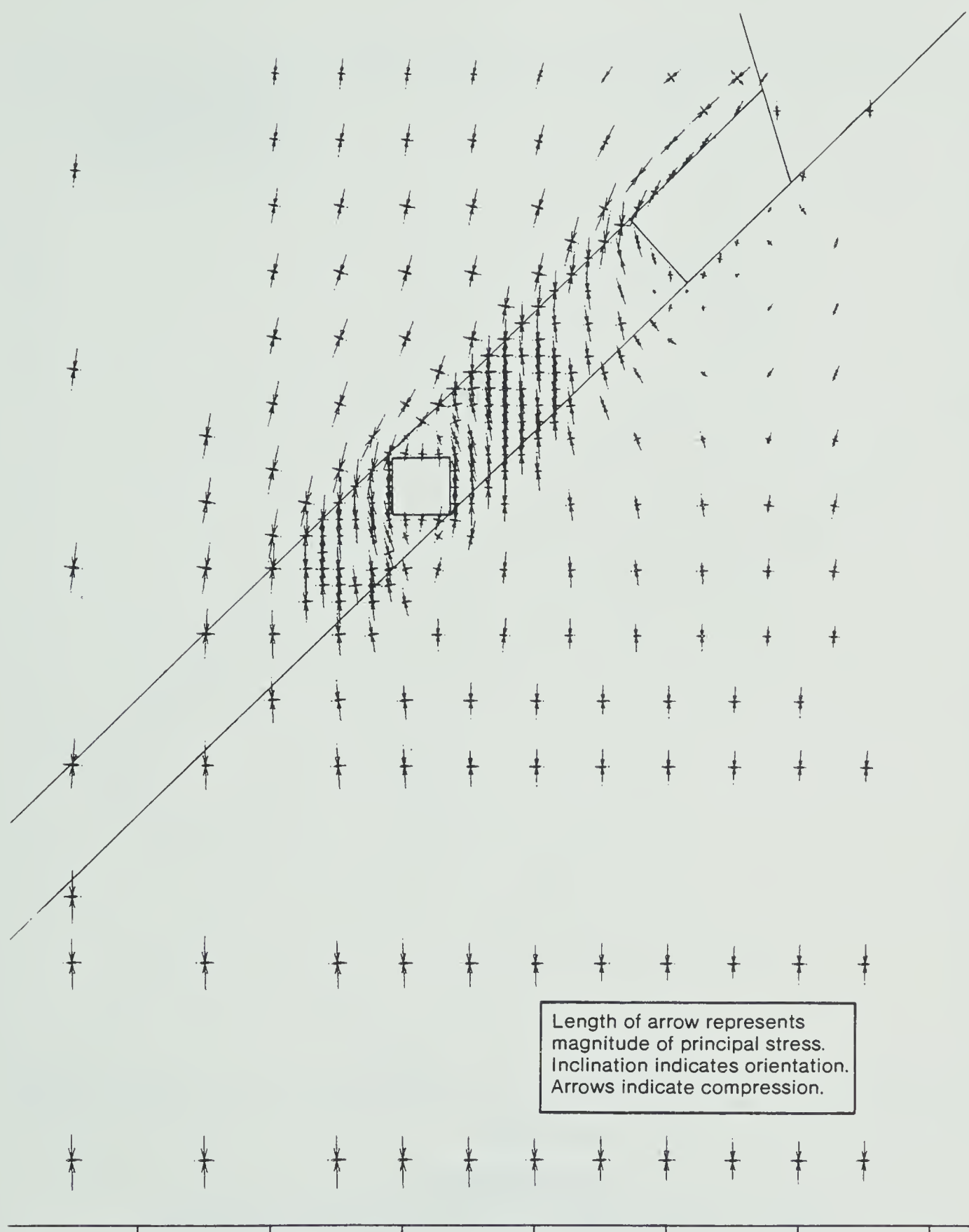


FIGURE 18 PRINCIPAL STRESSES AROUND THE EXCAVATIONS



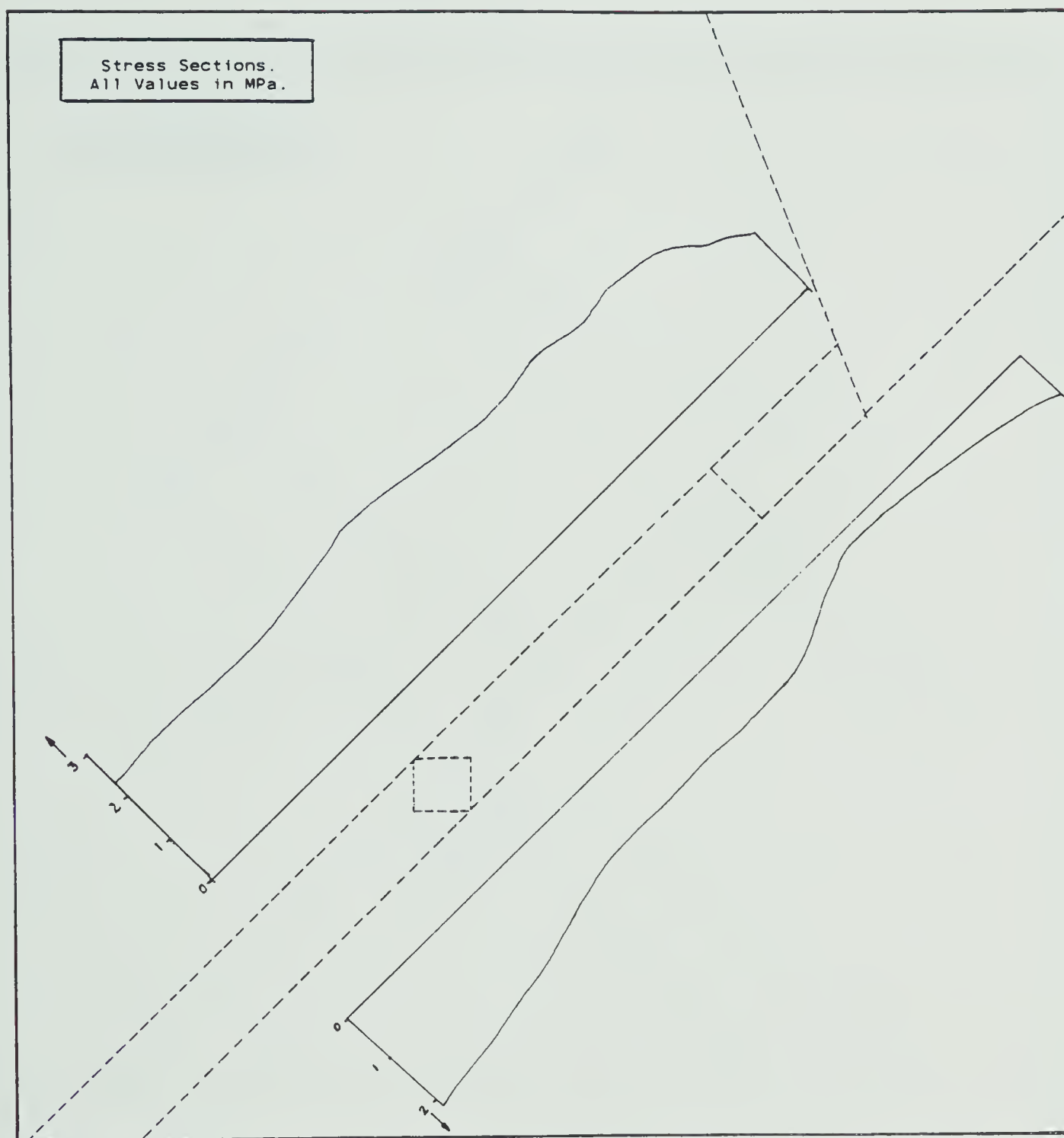


FIGURE 19

CONFIGURATION 1  
HORIZONTAL STRESS VARIATION ALONG GIVEN SECTIONS





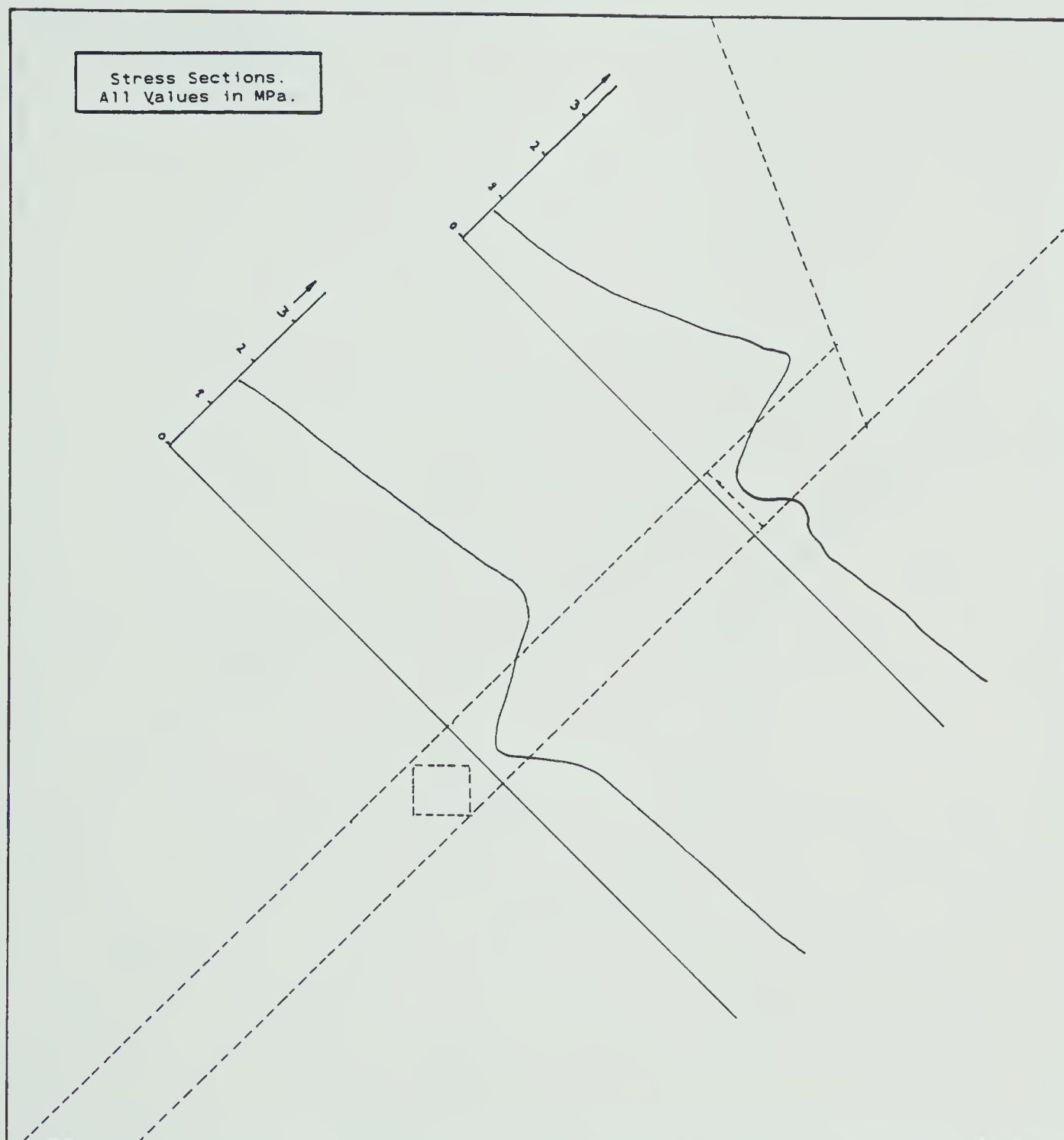


FIGURE 20  
CONFIGURATION 1  
HORIZONTAL STRESS VARIATION ALONG GIVEN SECTIONS



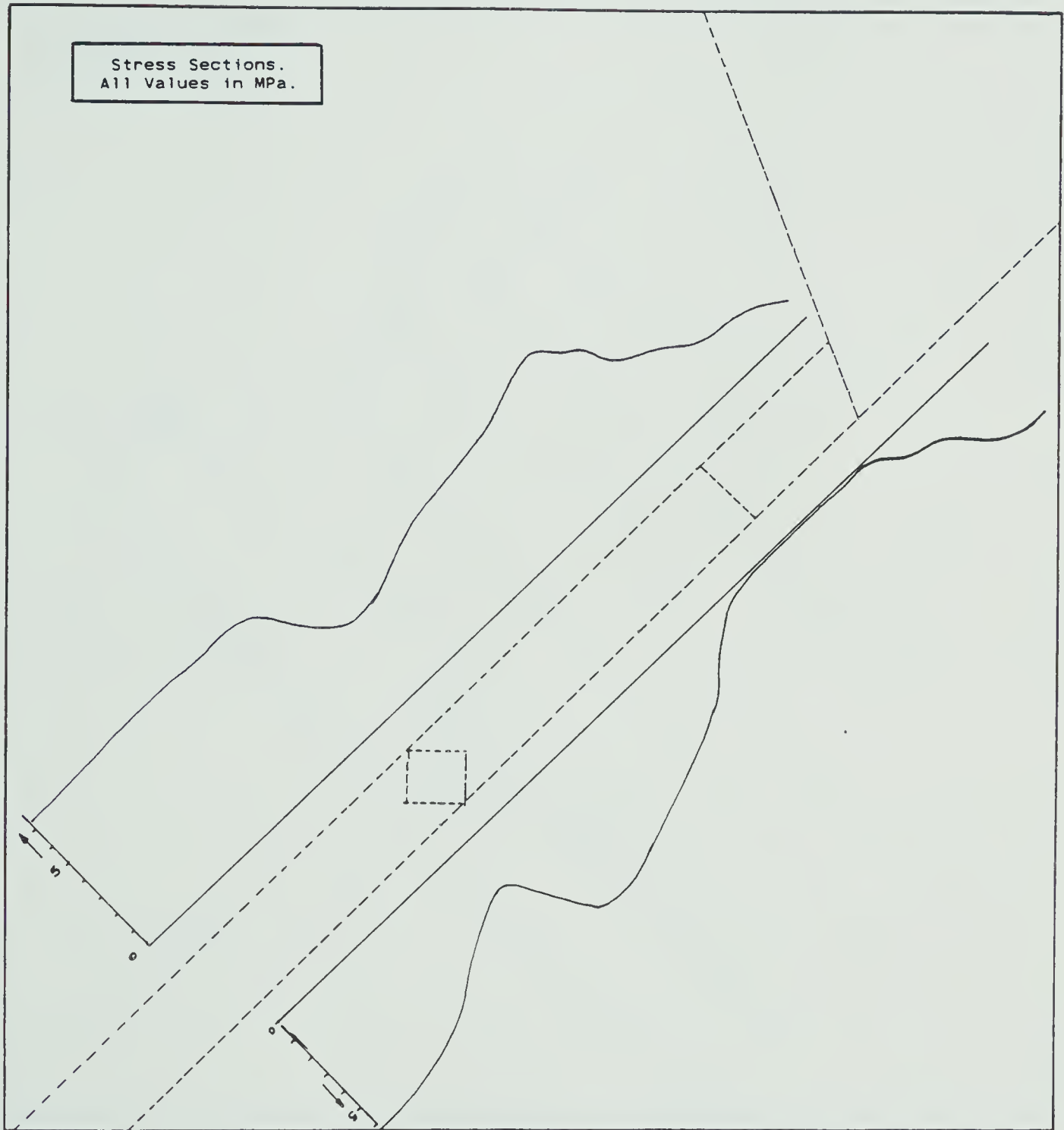


FIGURE 21  
CONFIGURATION 1  
VERTICAL STRESS VARIATION ALONG GIVEN SECTIONS



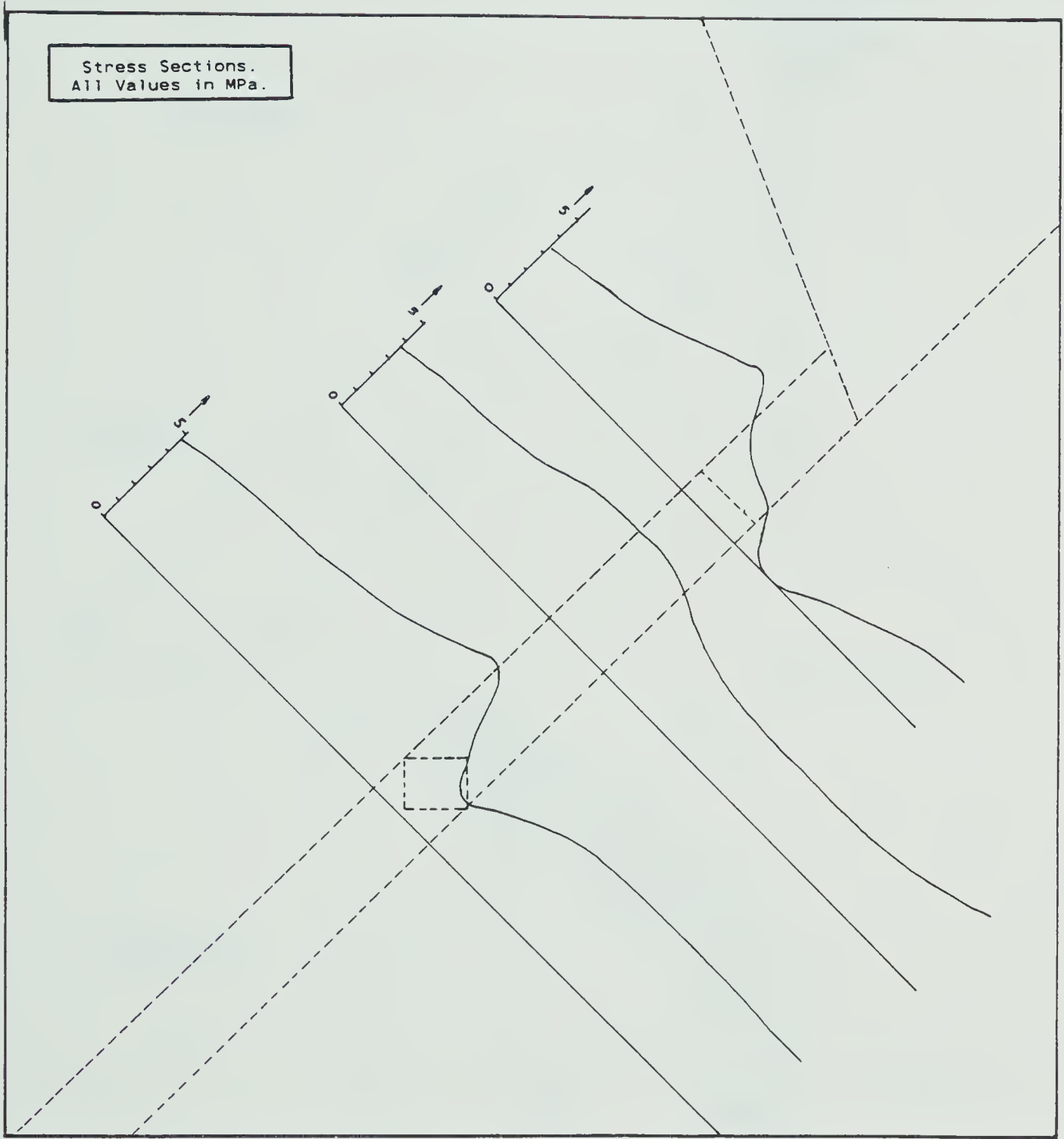


FIGURE 22  
CONFIGURATION 1  
VERTICAL STRESS VARIATION ALONG GIVEN SECTIONS





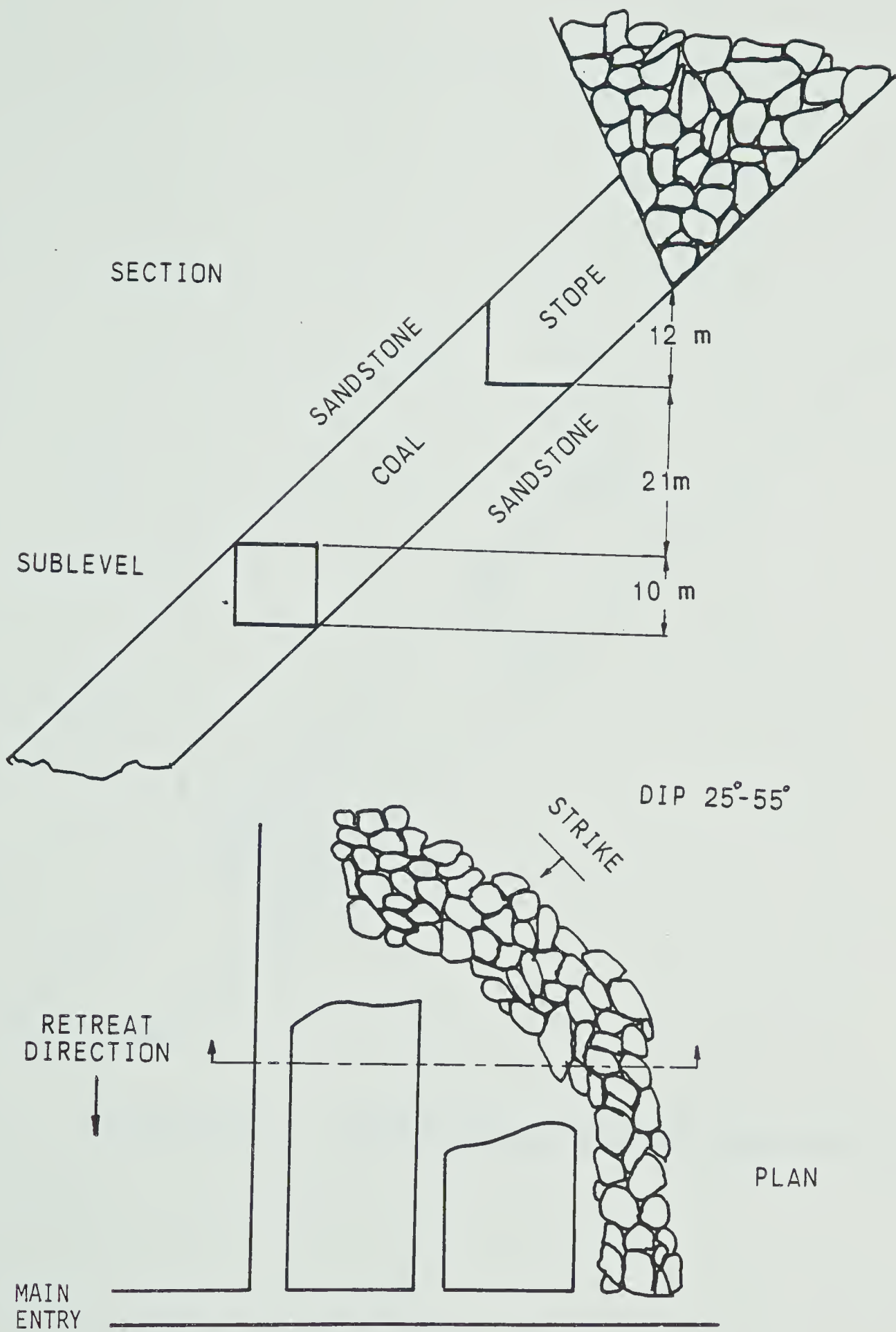


FIGURE 23 PLAN AND SECTION OF CONFIGURATION 2



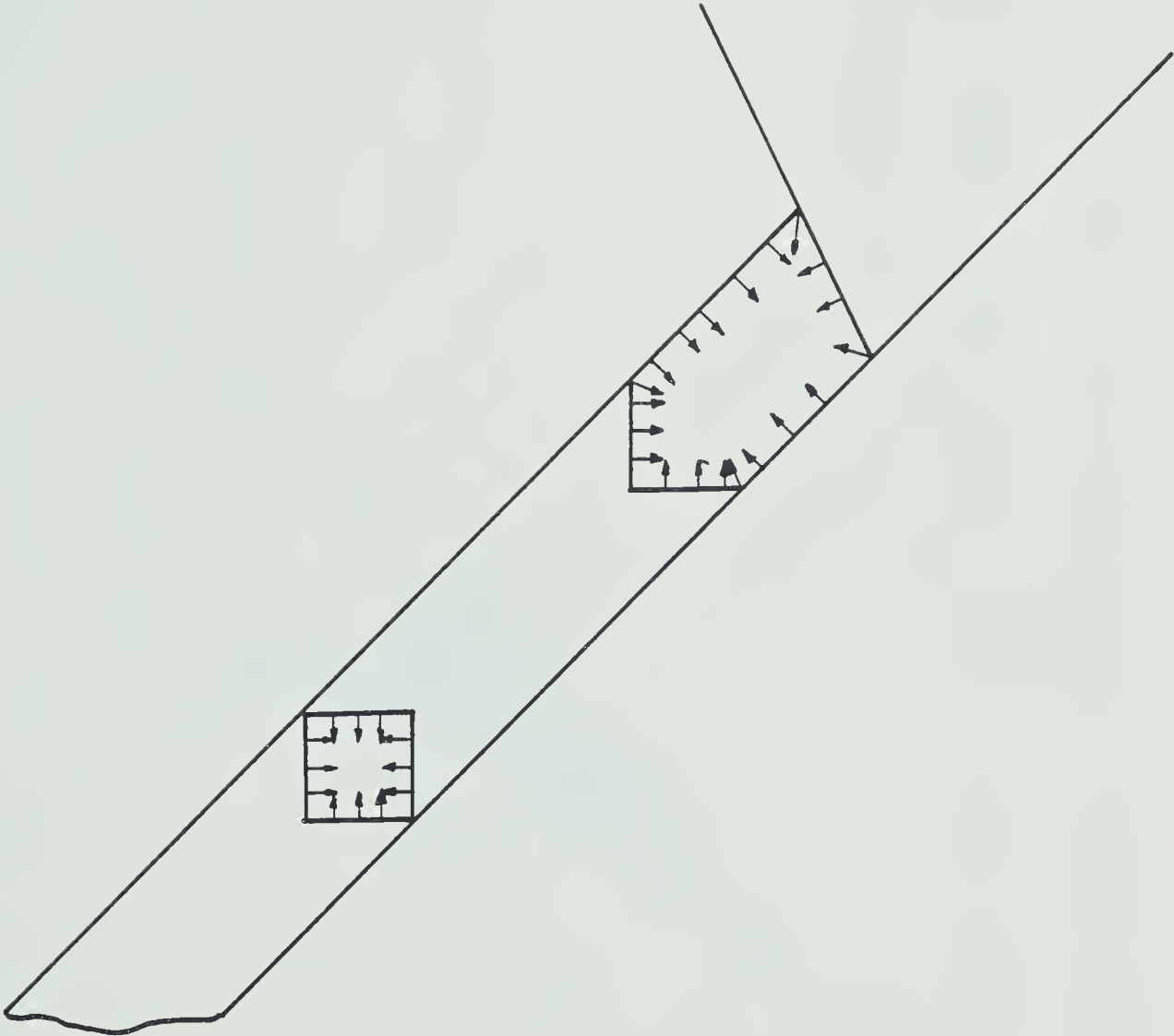


FIGURE 24      LOADING CONDITIONS FOR CONFIGURATION 2



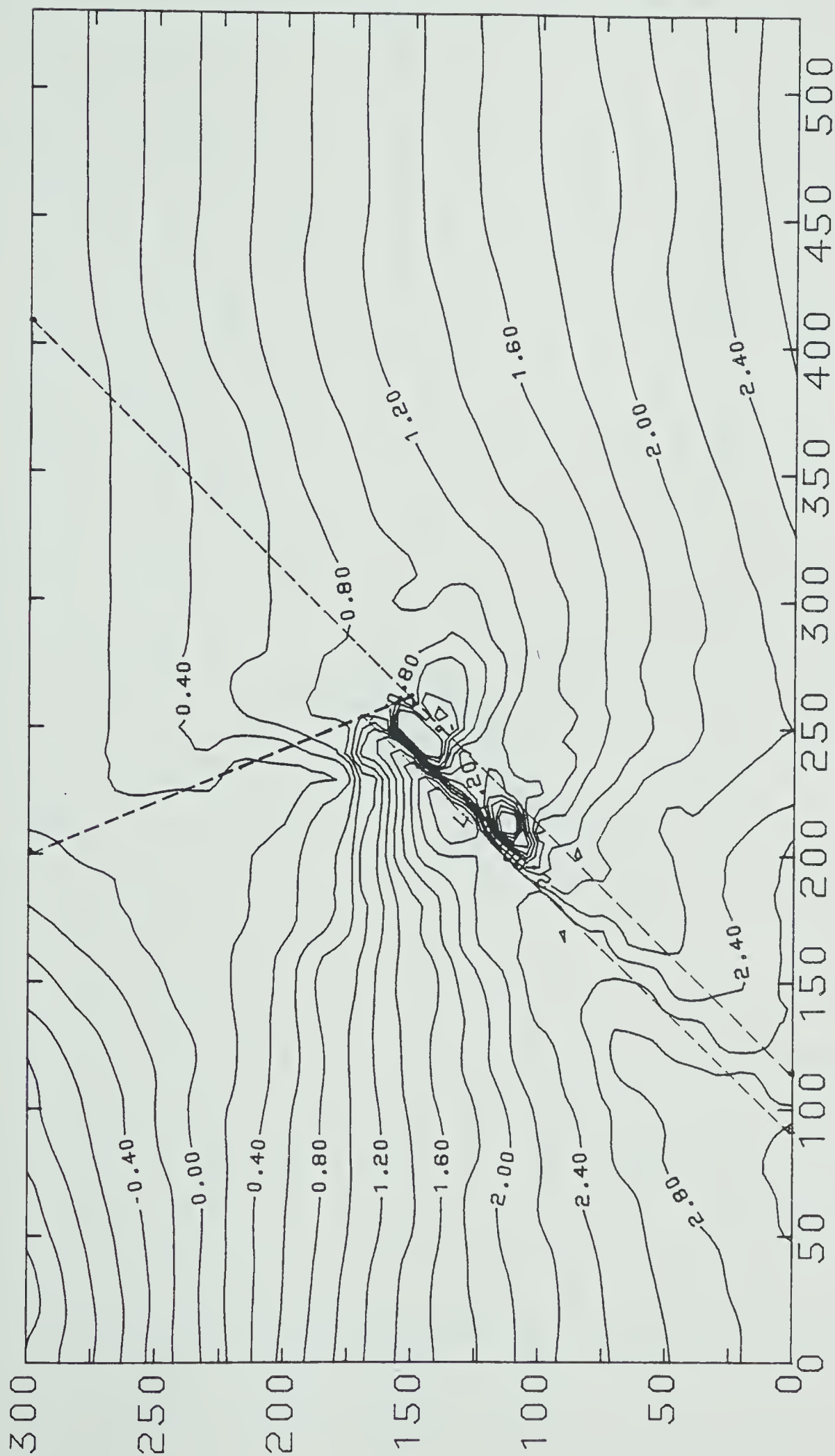


FIGURE 25  
HORIZONTAL STRESS DISTRIBUTION THROUGHOUT THE MESH



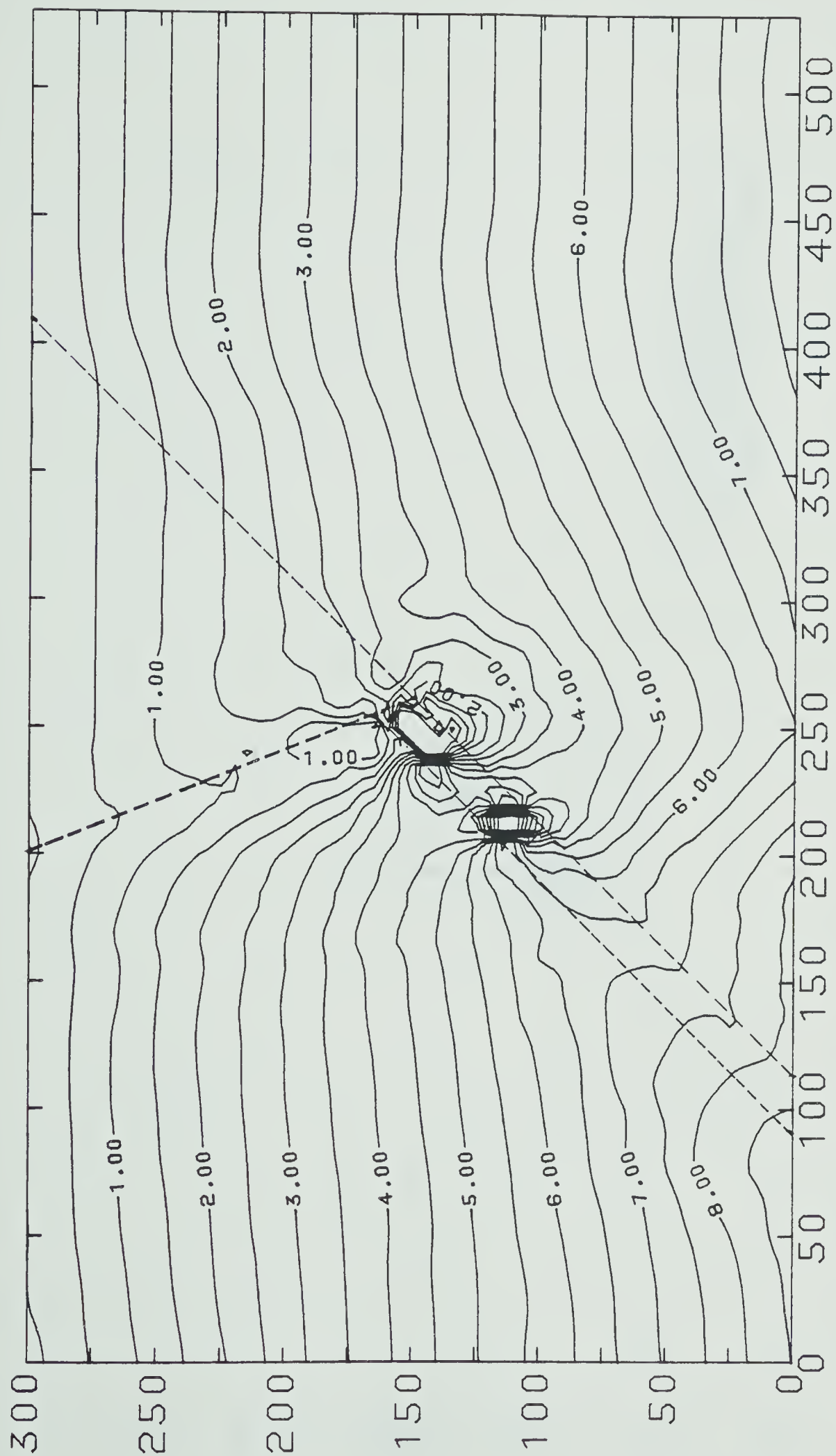


FIGURE 26

VERTICAL STRESS DISTRIBUTION THROUGHOUT THE MESH





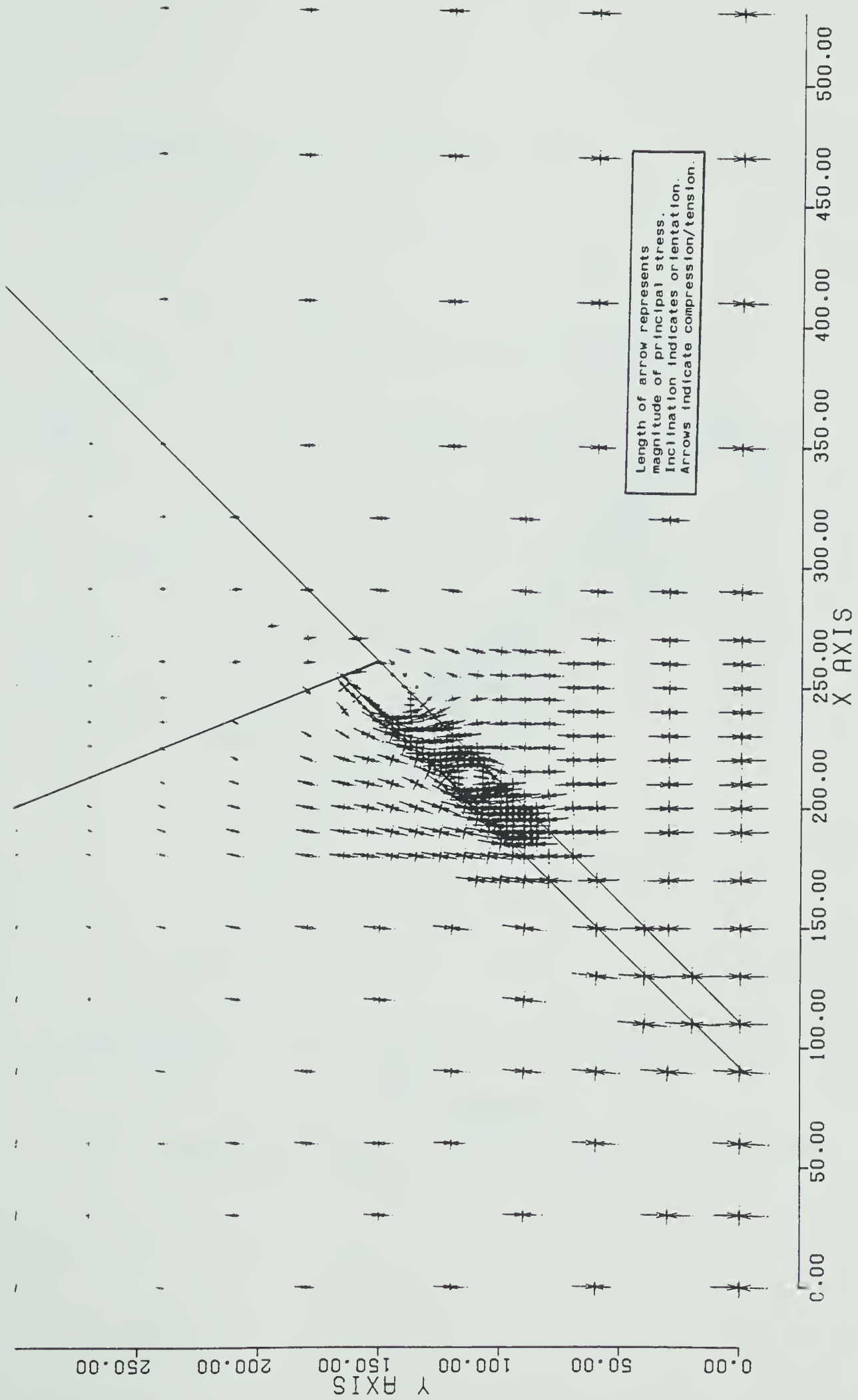


FIGURE 27 PRINCIPAL STRESSES THROUGHOUT THE MESH



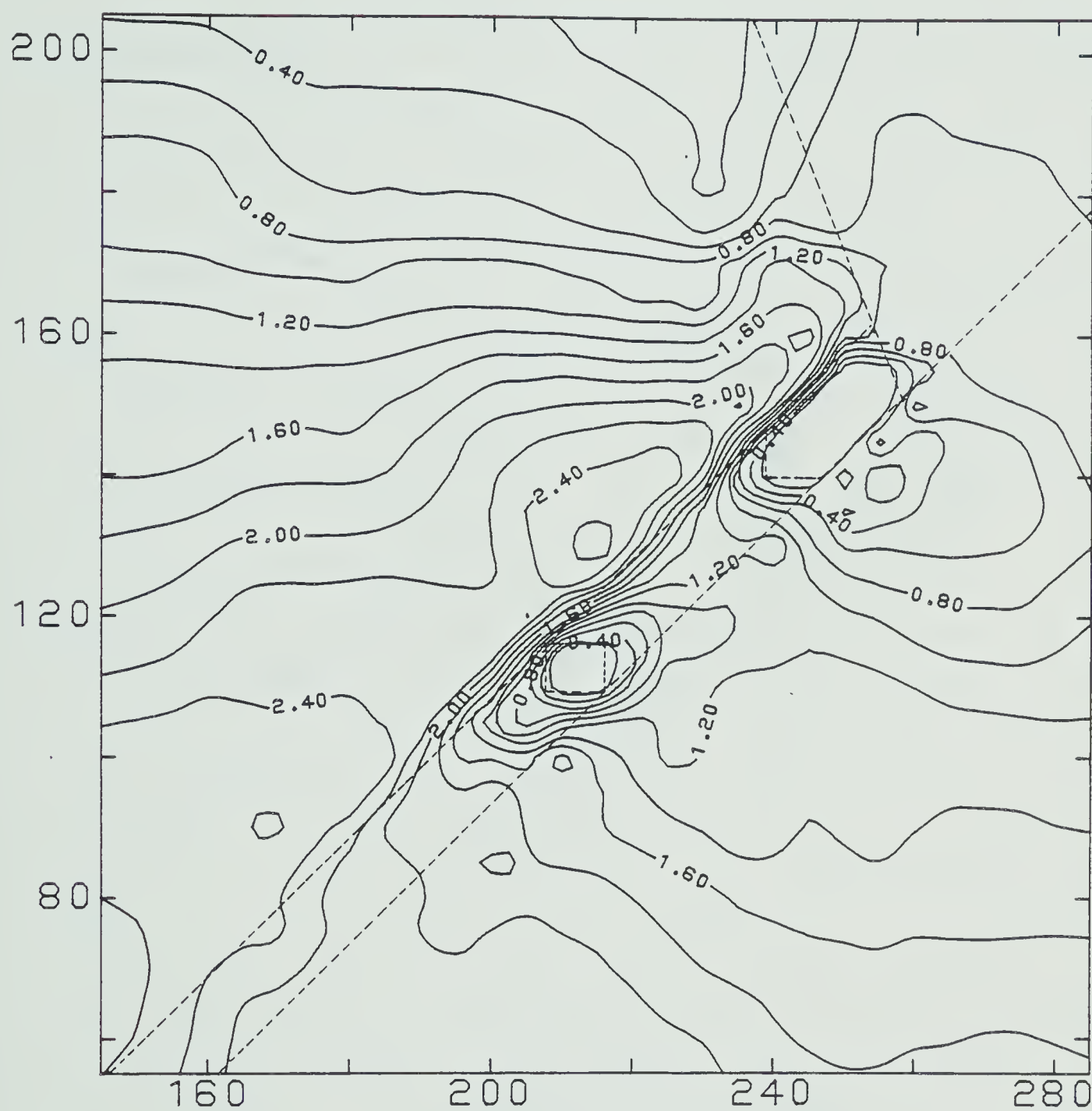


FIGURE 28

HORIZONTAL STRESS DISTRIBUTION AROUND THE EXCAVATIONS



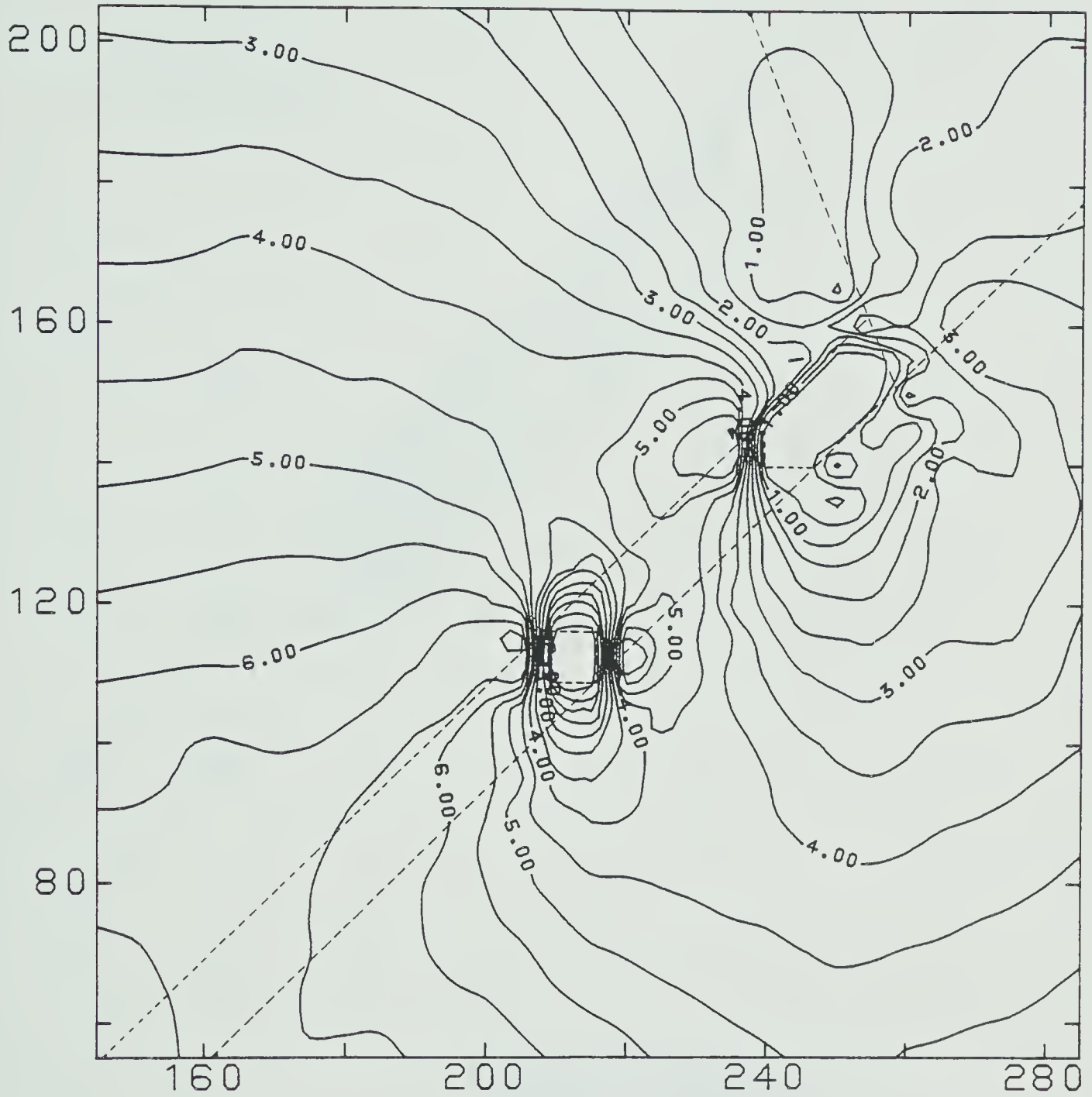
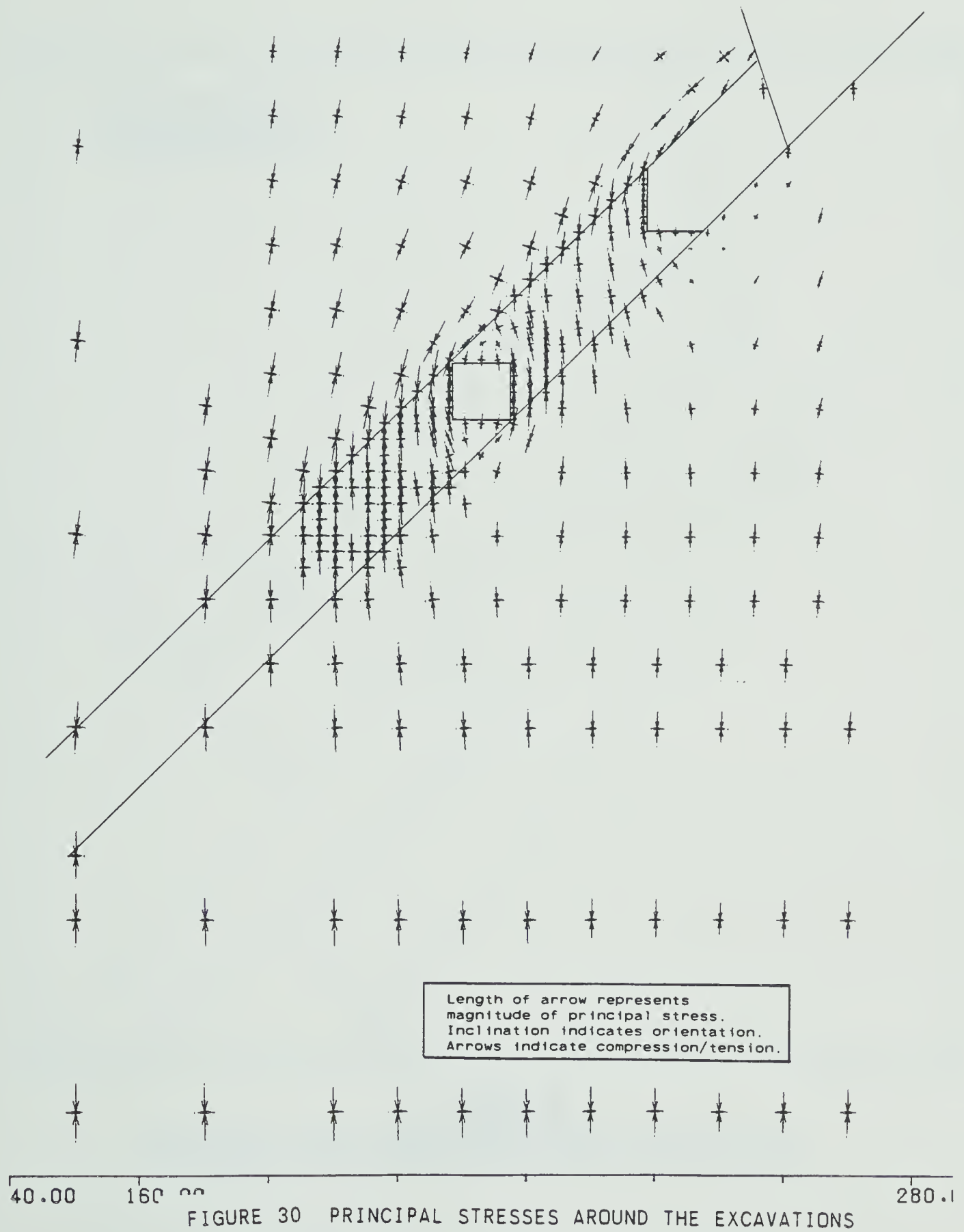


FIGURE 29

VERTICAL STRESS DISTRIBUTION AROUND THE EXCAVATIONS









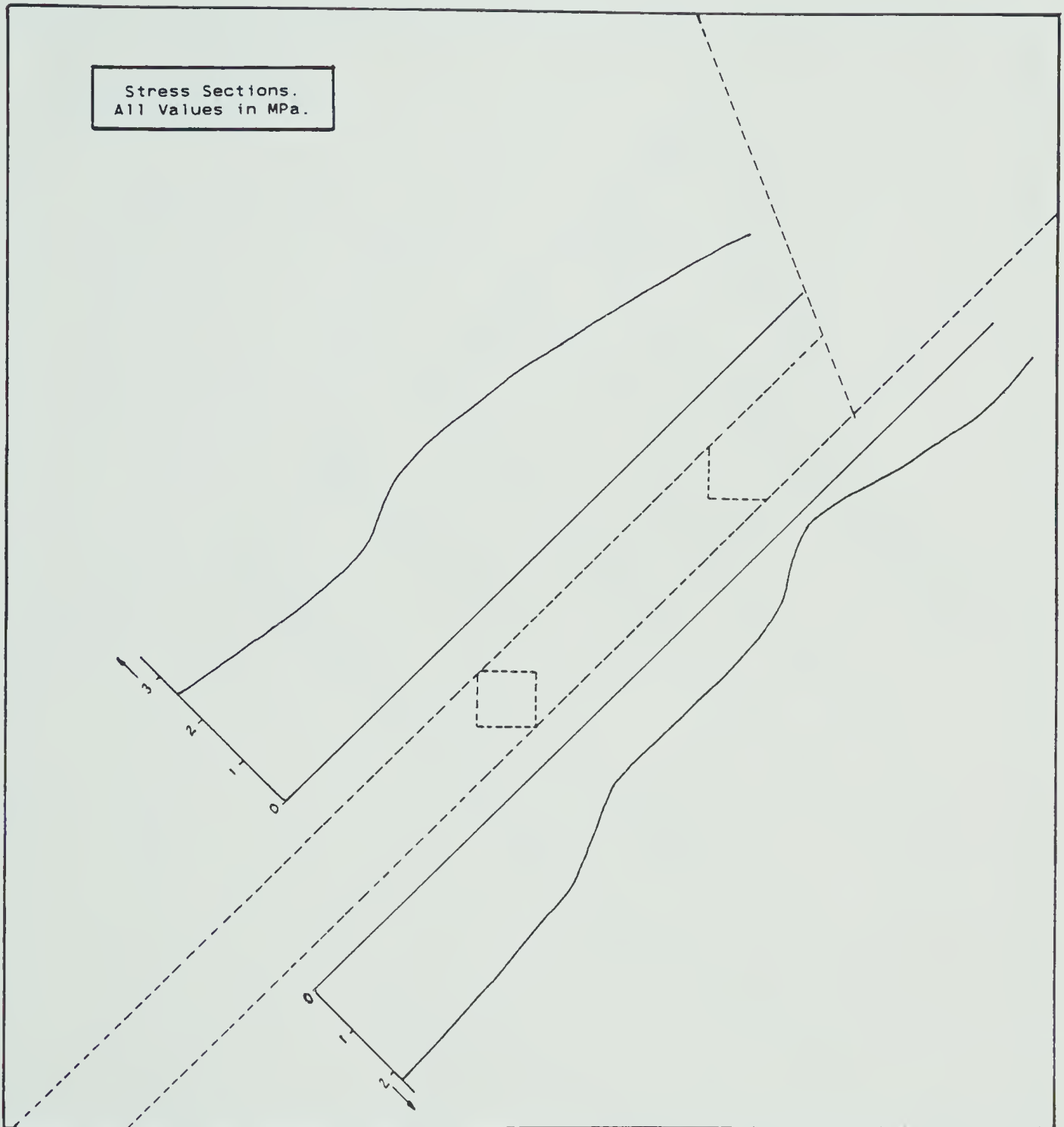


FIGURE 31  
CONFIGURATION 2  
HORIZONTAL STRESS VARIATION ALONG GIVEN SECTIONS



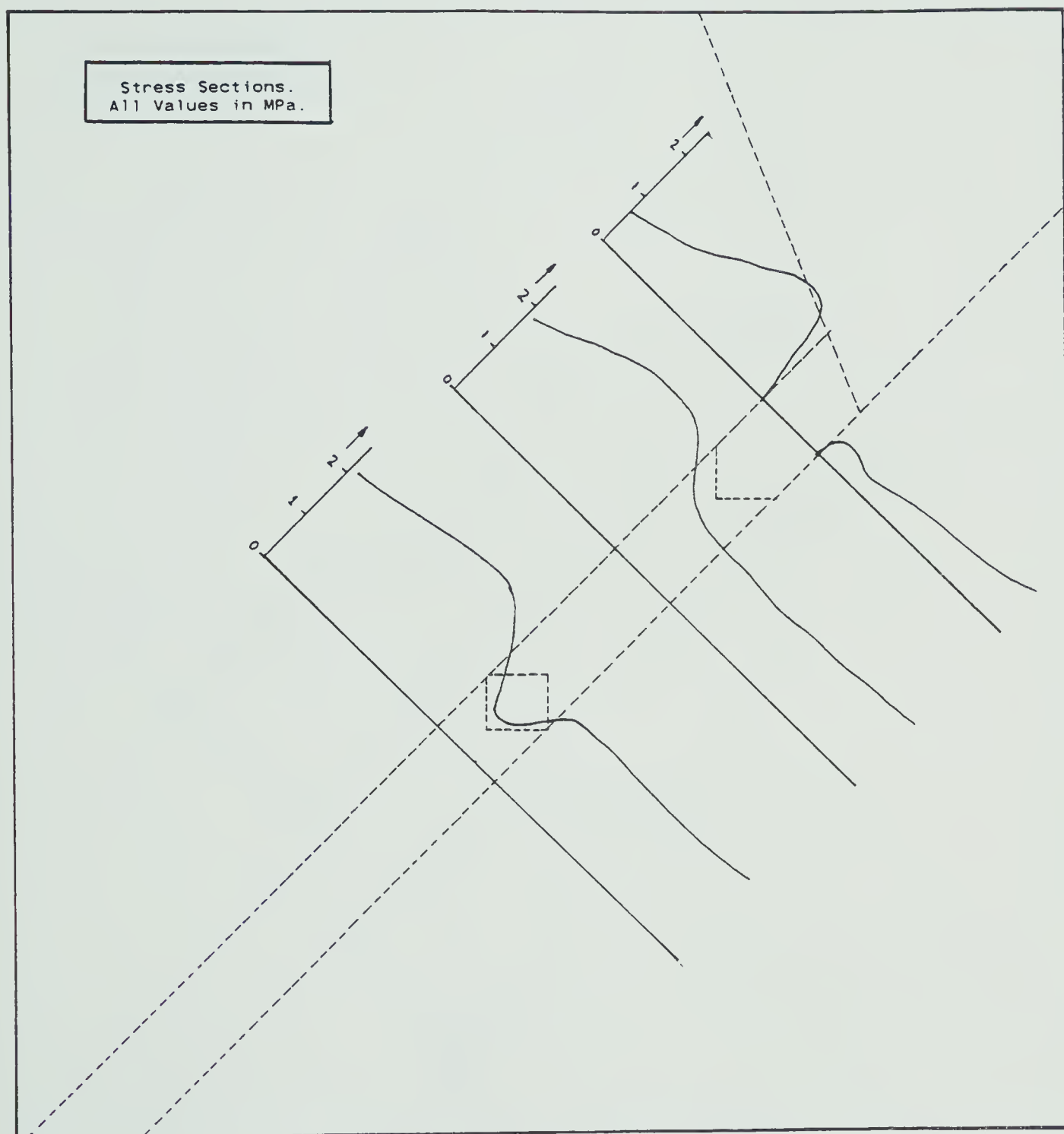


FIGURE 32  
CONFIGURATION 2  
HORIZONTAL STRESS VARIATION ALONG GIVEN SECTIONS



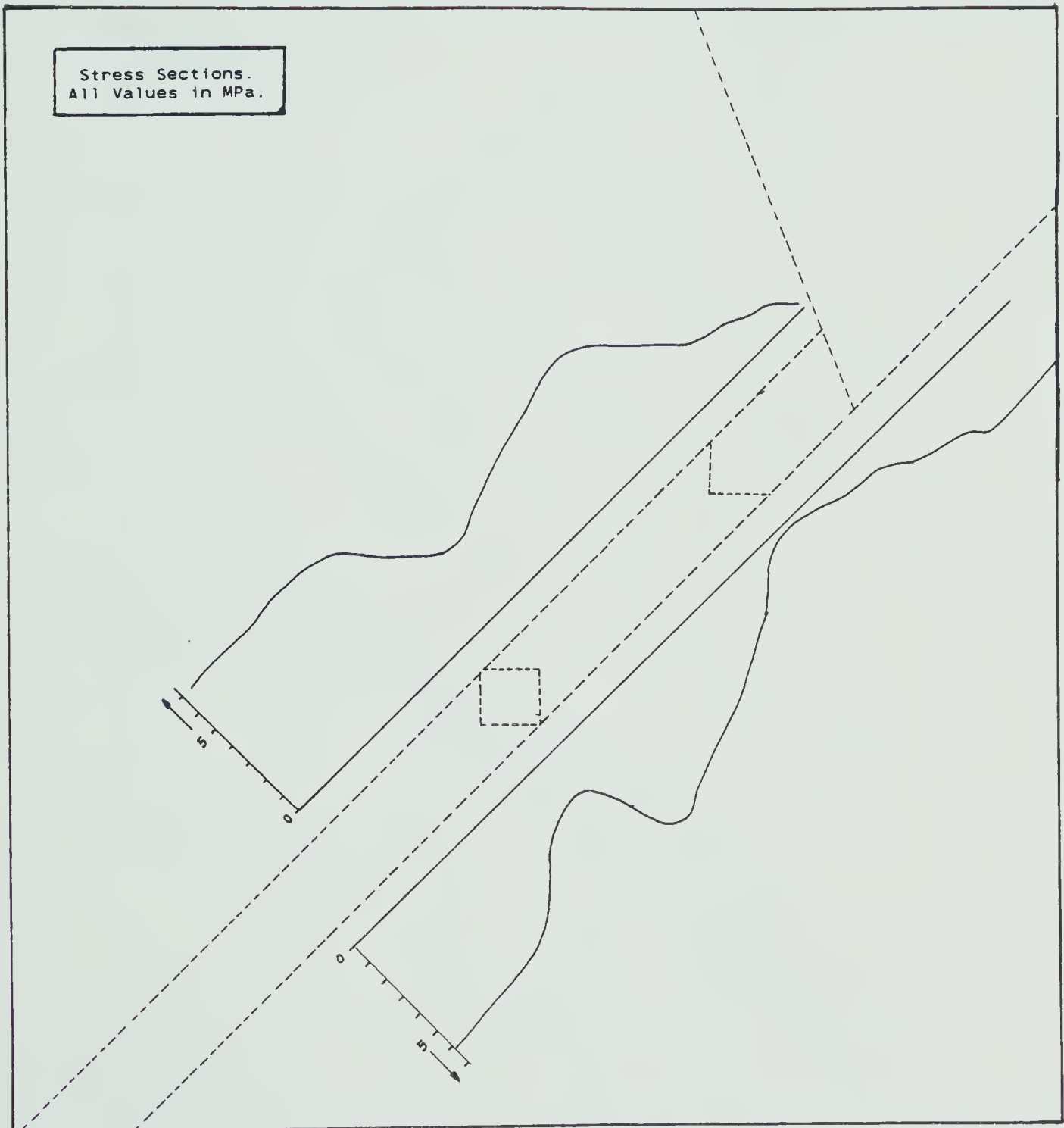


FIGURE 33  
CONFIGURATION 2  
VERTICAL STRESS VARIATION ALONG GIVEN SECTIONS





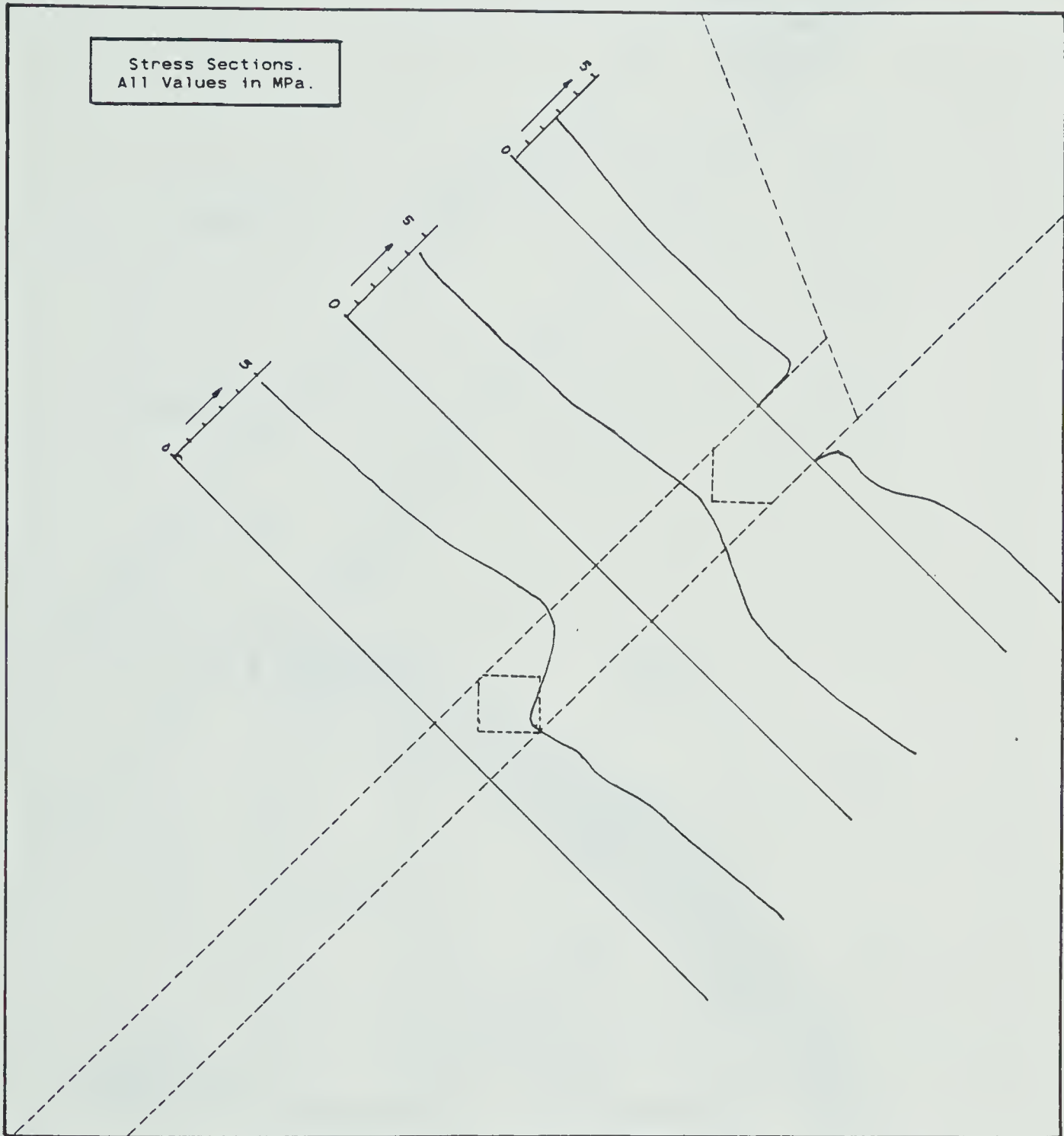


FIGURE 34

CONFIGURATION 2  
VERTICAL STRESS VARIATION ALONG GIVEN SECTIONS



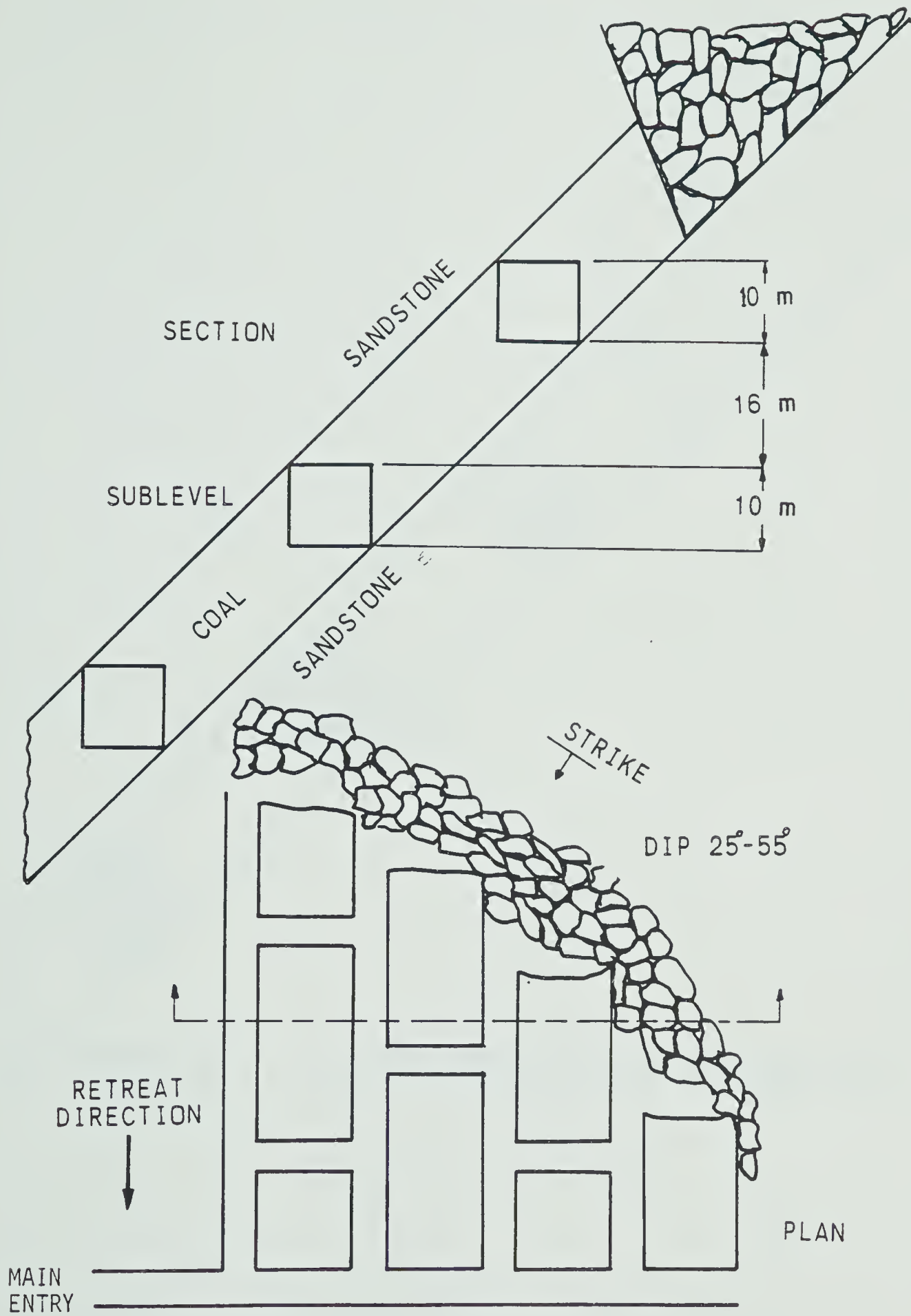


FIGURE 35

PLAN AND SECTION OF CONFIGURATION 3



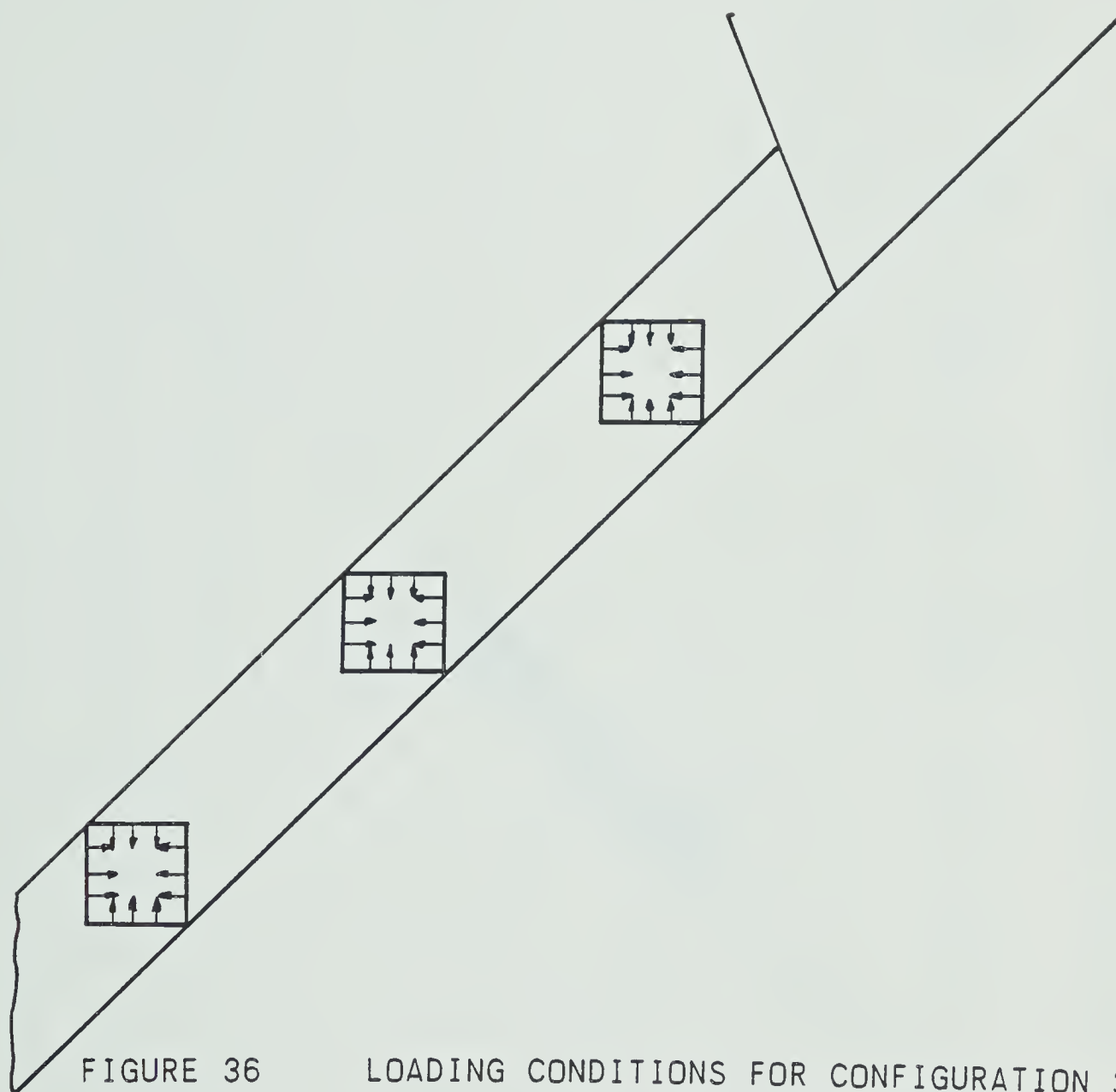


FIGURE 36

LOADING CONDITIONS FOR CONFIGURATION 3



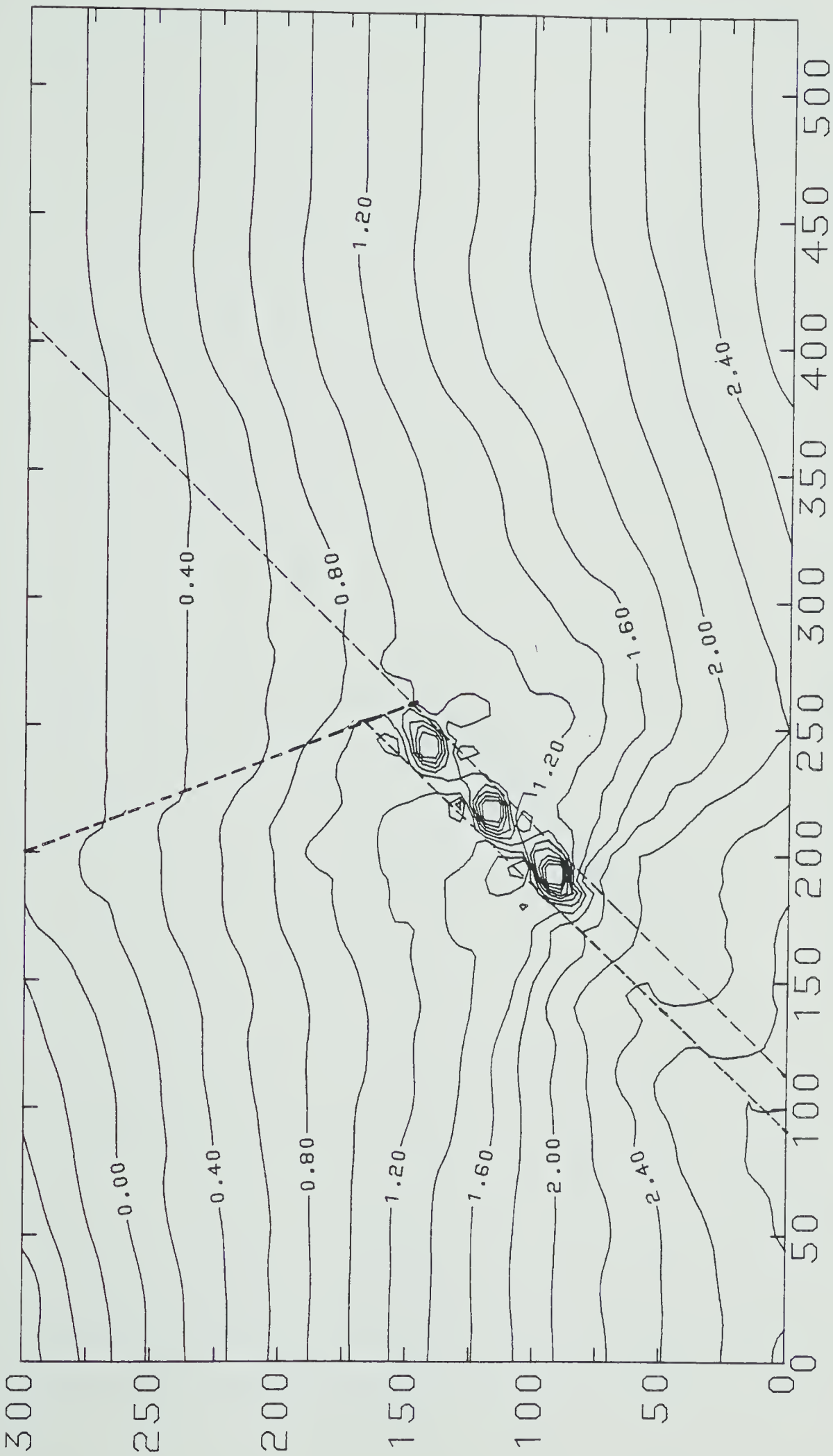


FIGURE 37

HORIZONTAL STRESS DISTRIBUTION THROUGHOUT THE MESH





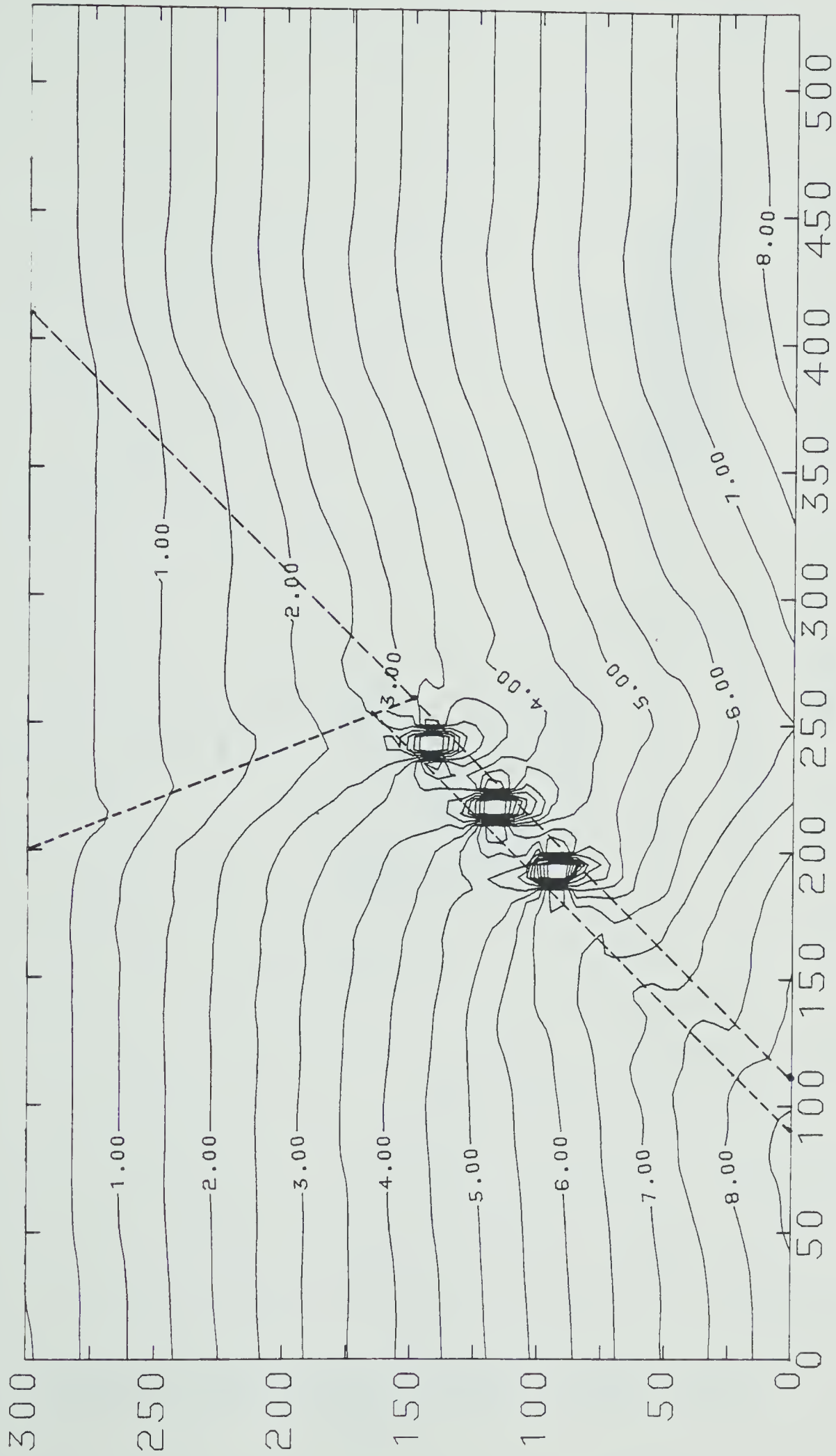


FIGURE 38

VERTICAL STRESS DISTRIBUTION THROUGHOUT THE MESH



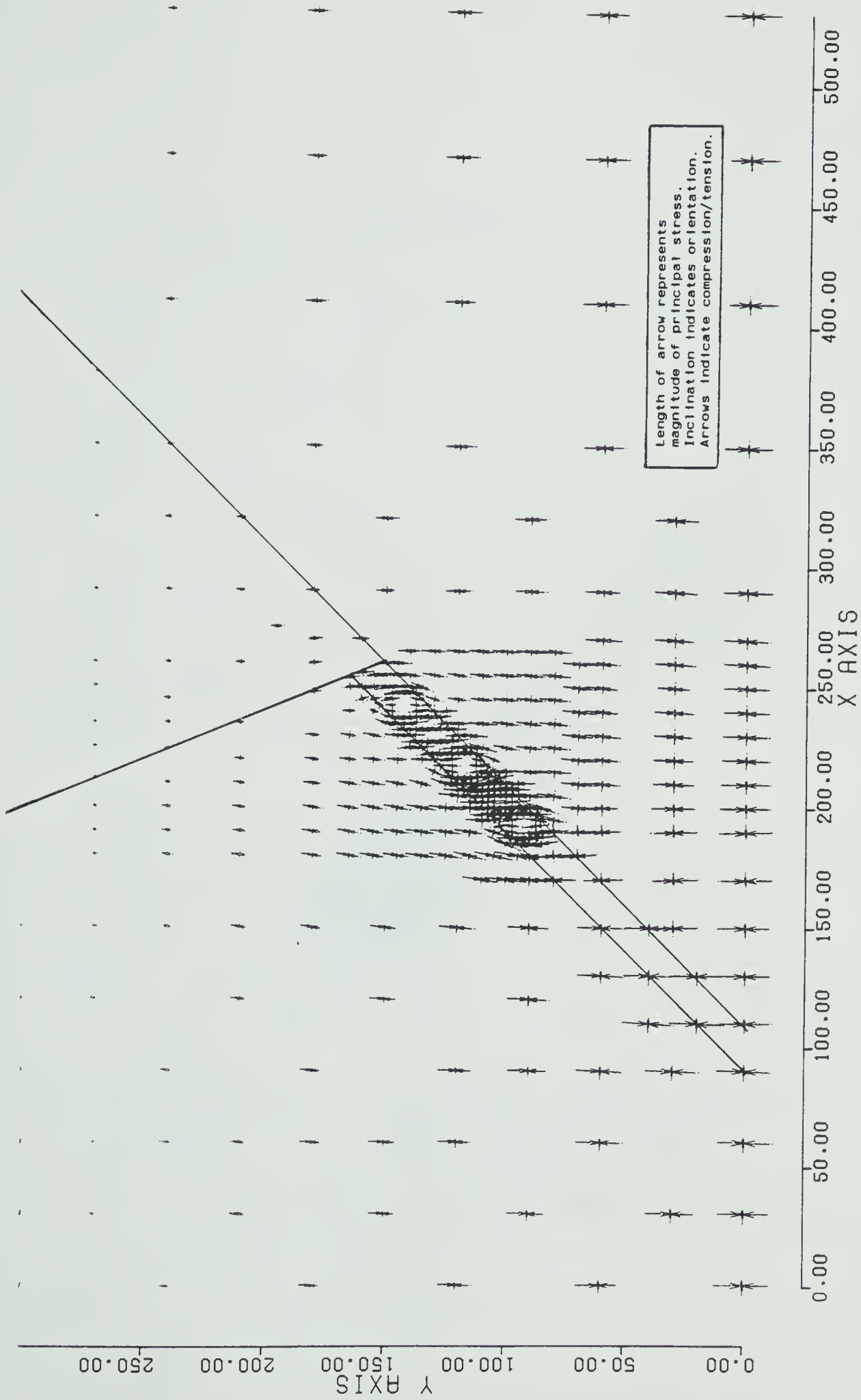
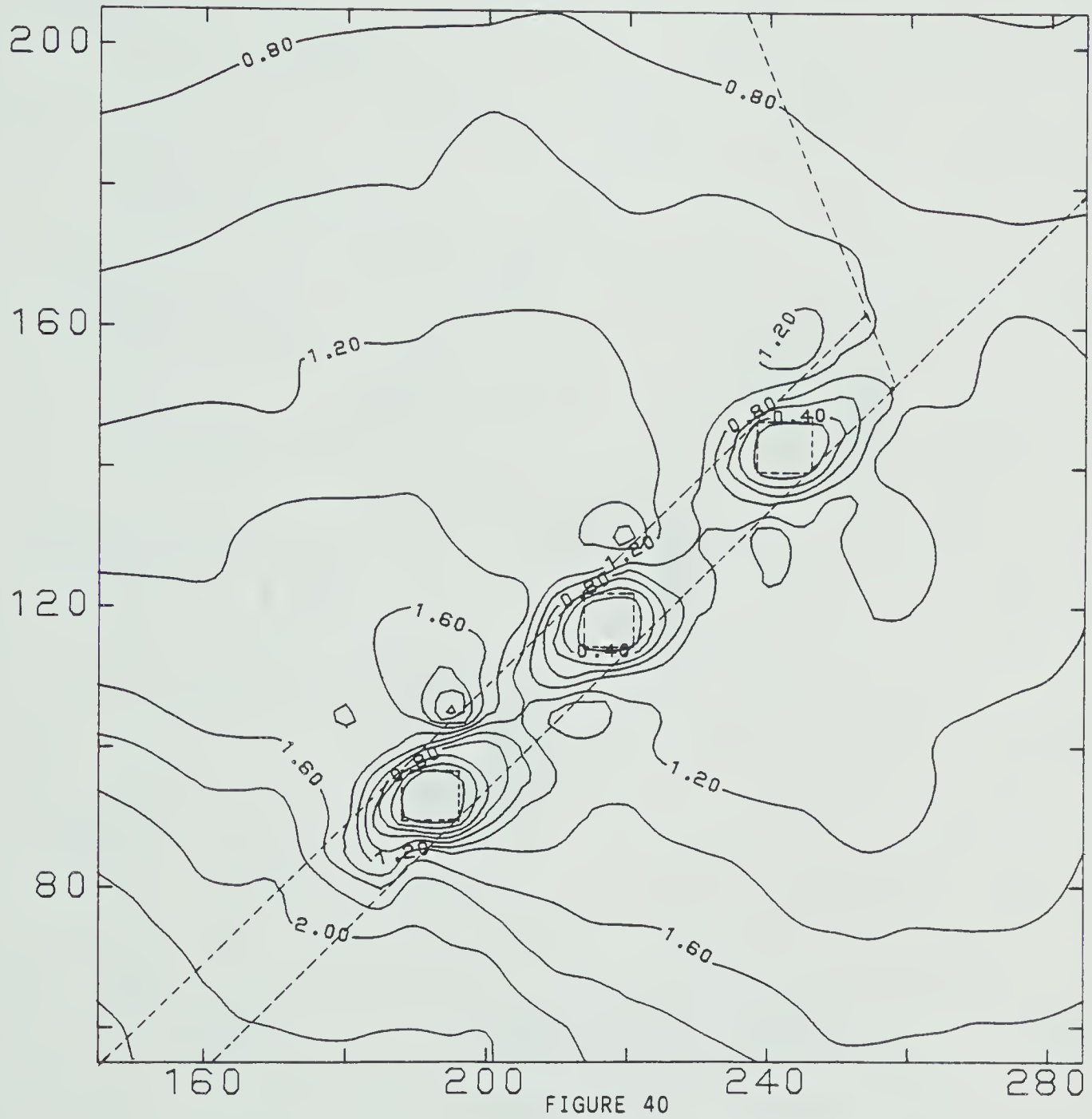


FIGURE 39 PRINCIPAL STRESSES THROUGHOUT THE MESH





HORIZONTAL STRESS DISTRIBUTION AROUND THE EXCAVATIONS



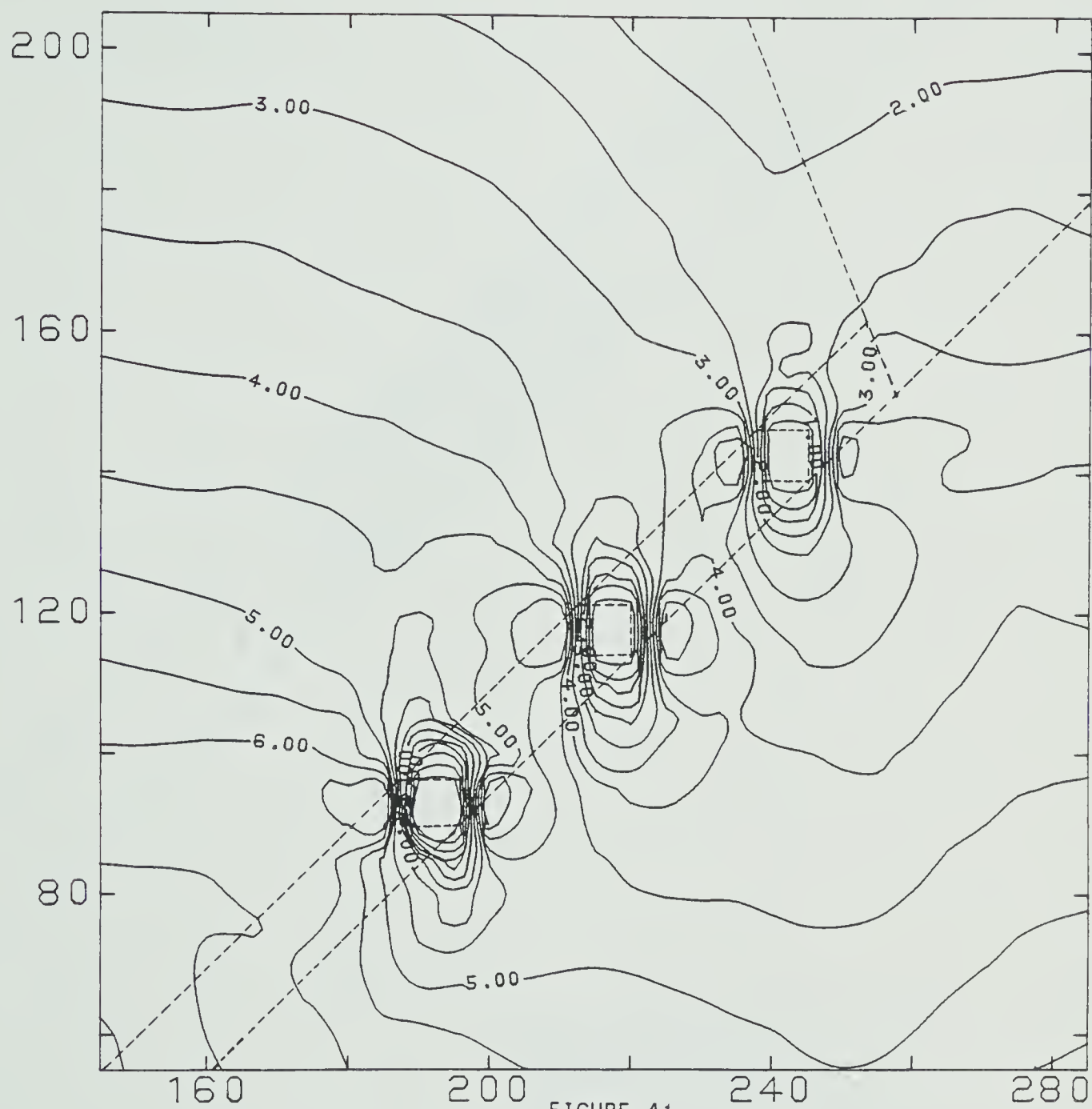


FIGURE 41

VERTICAL STRESS DISTRIBUTION AROUND THE EXCAVATIONS





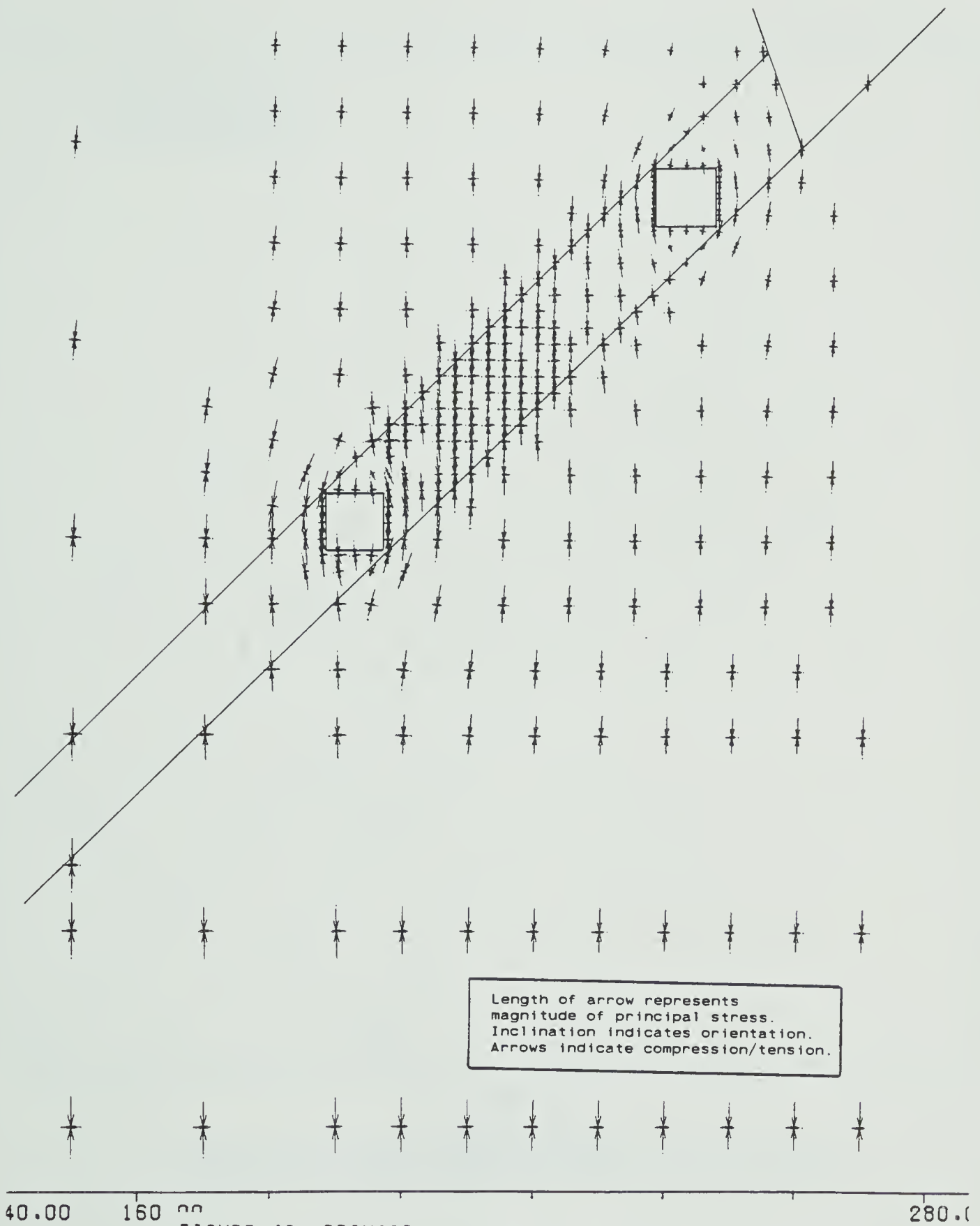


FIGURE 42 PRINCIPAL STRESSES AROUND THE EXCAVATIONS



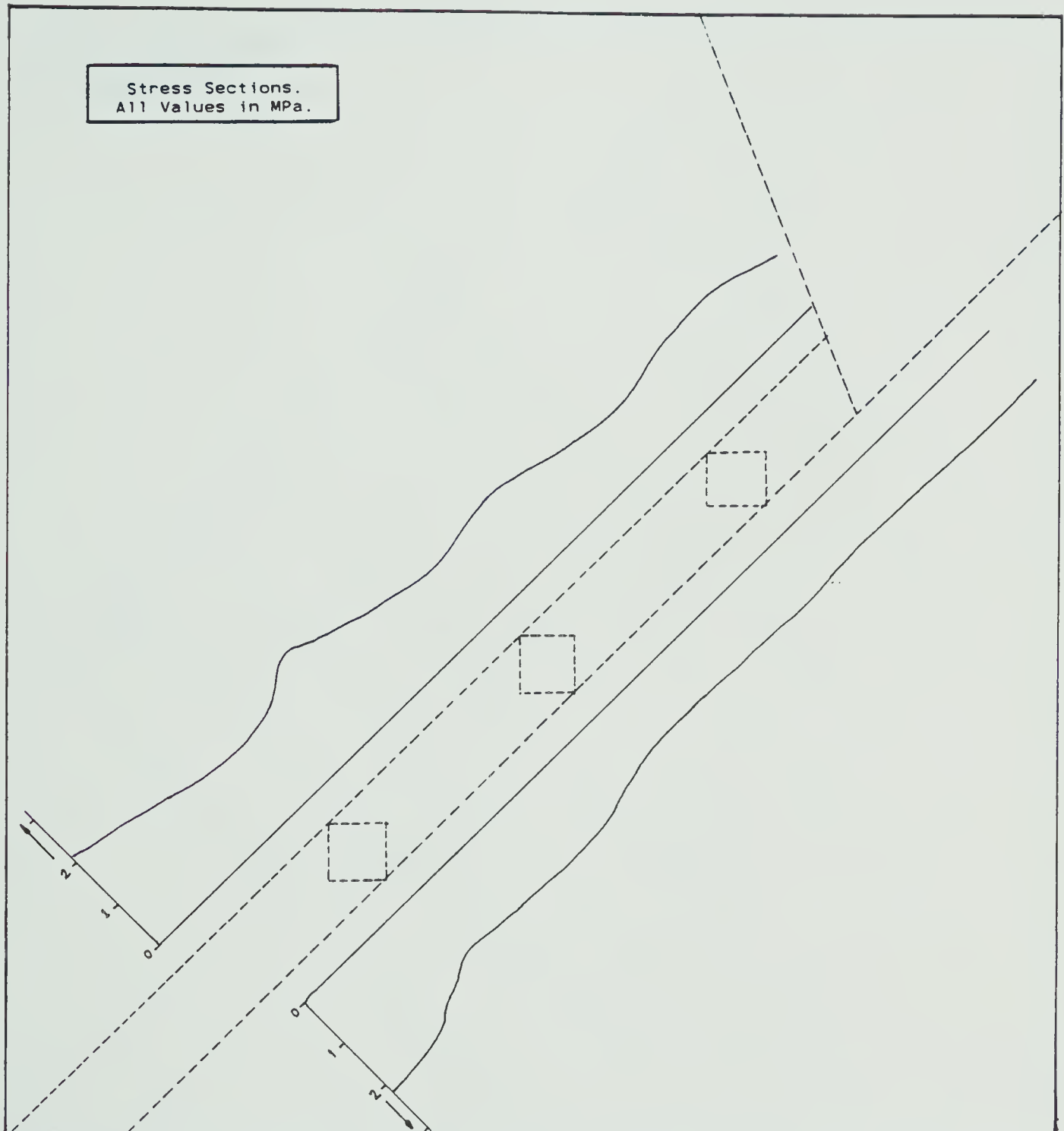


FIGURE 43  
CONFIGURATION 3  
HORIZONTAL STRESS VARIATION ALONG GIVEN SECTIONS



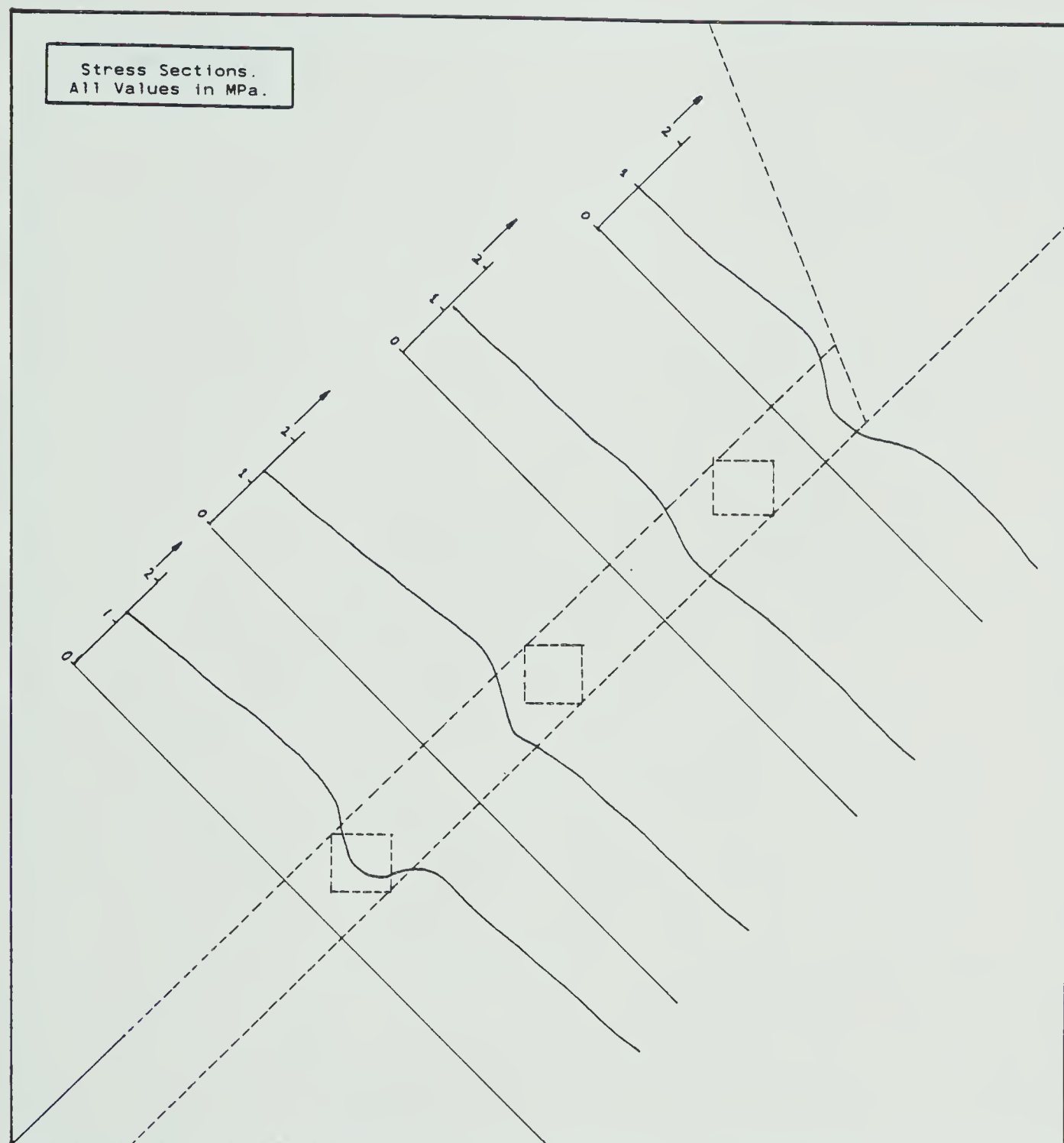


FIGURE 44  
CONFIGURATION 3  
HORIZONTAL STRESS VARIATION ALONG GIVEN SECTIONS



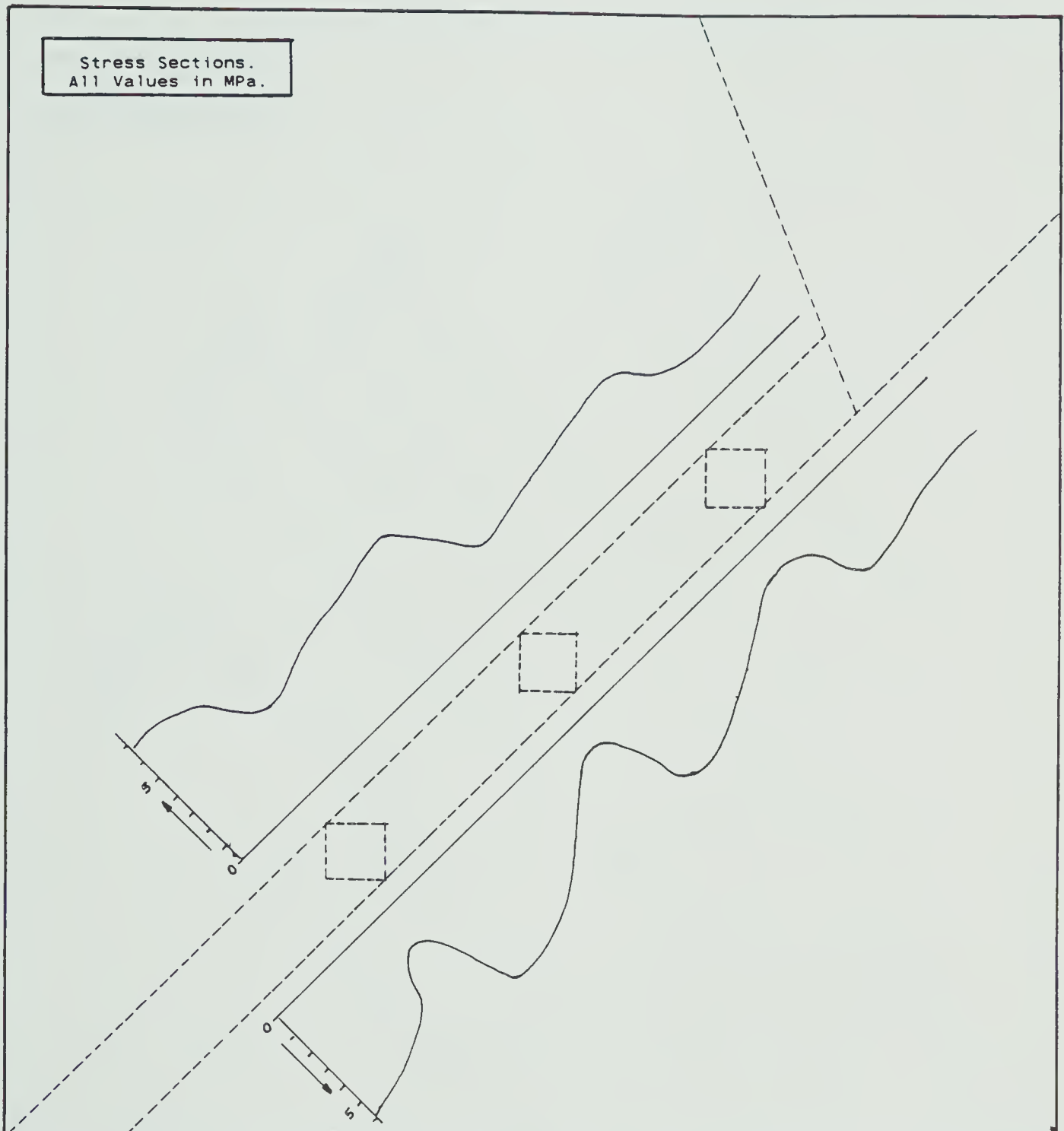


FIGURE 45

CONFIGURATION 3  
VERTICAL STRESS VARIATION ALONG GIVEN SECTIONS





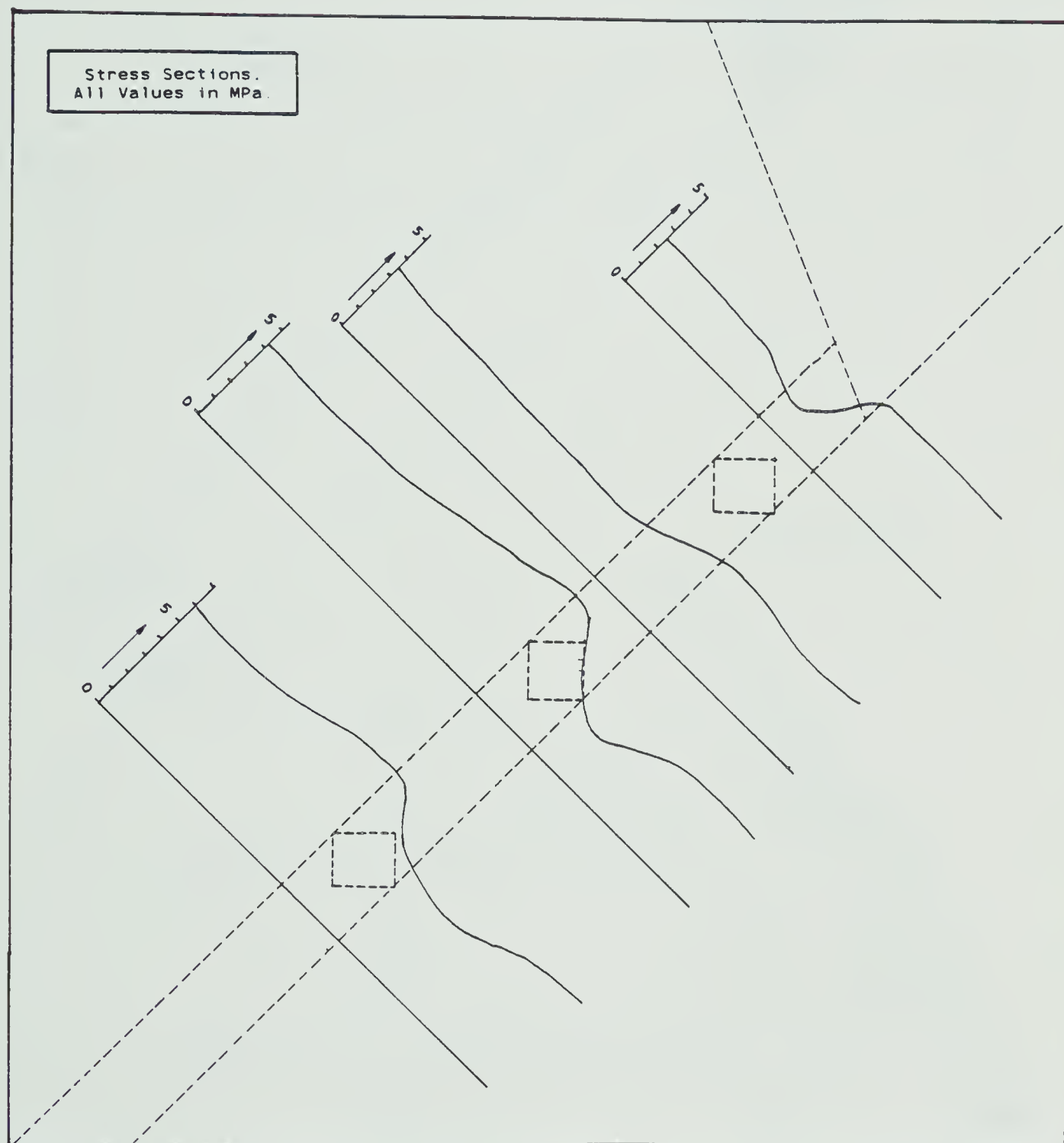


FIGURE 46  
CONFIGURATION 3  
VERTICAL STRESS VARIATION ALONG GIVEN SECTIONS



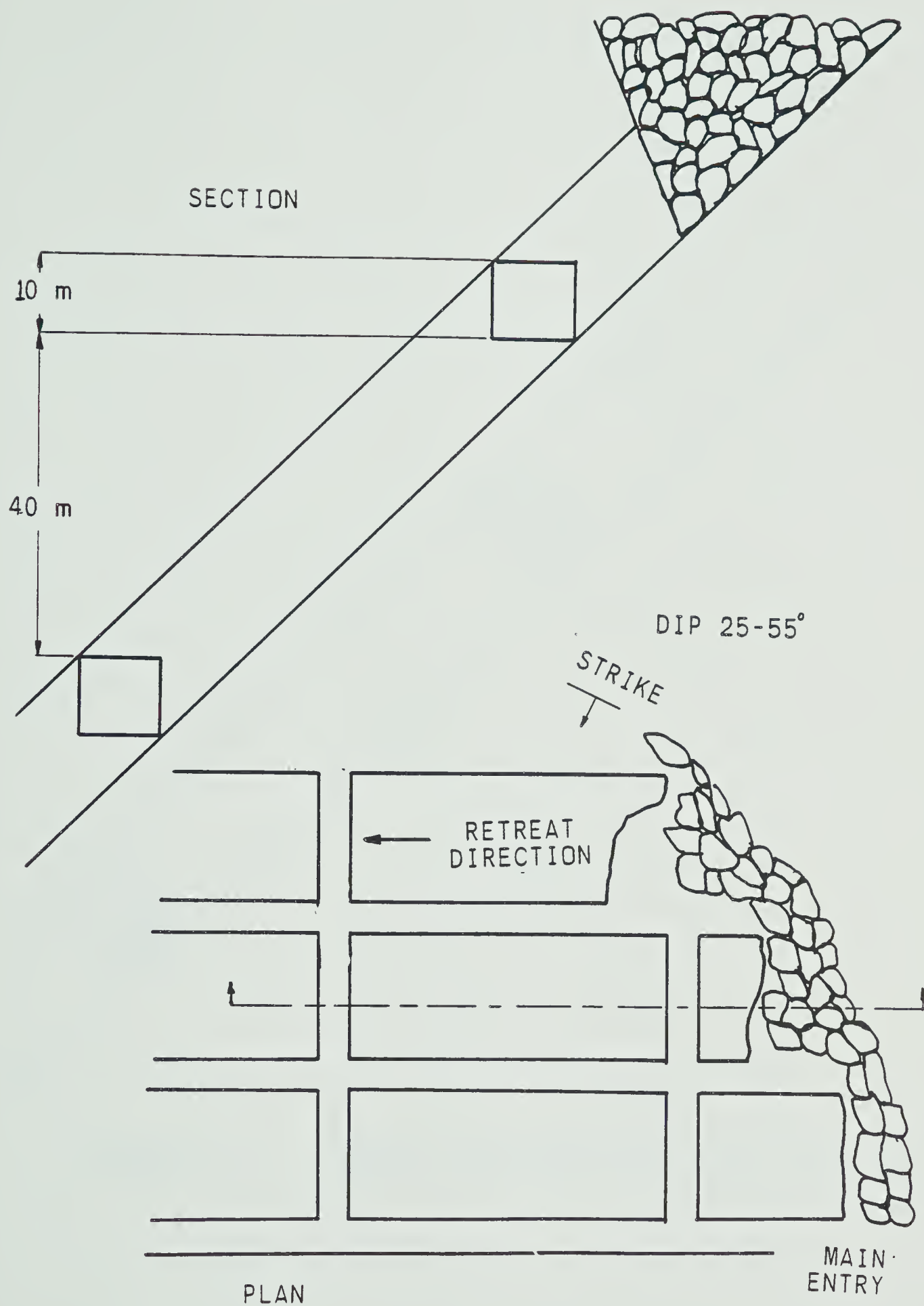


FIGURE 47

PLAN AND SECTION FOR CONFIGURATION 4



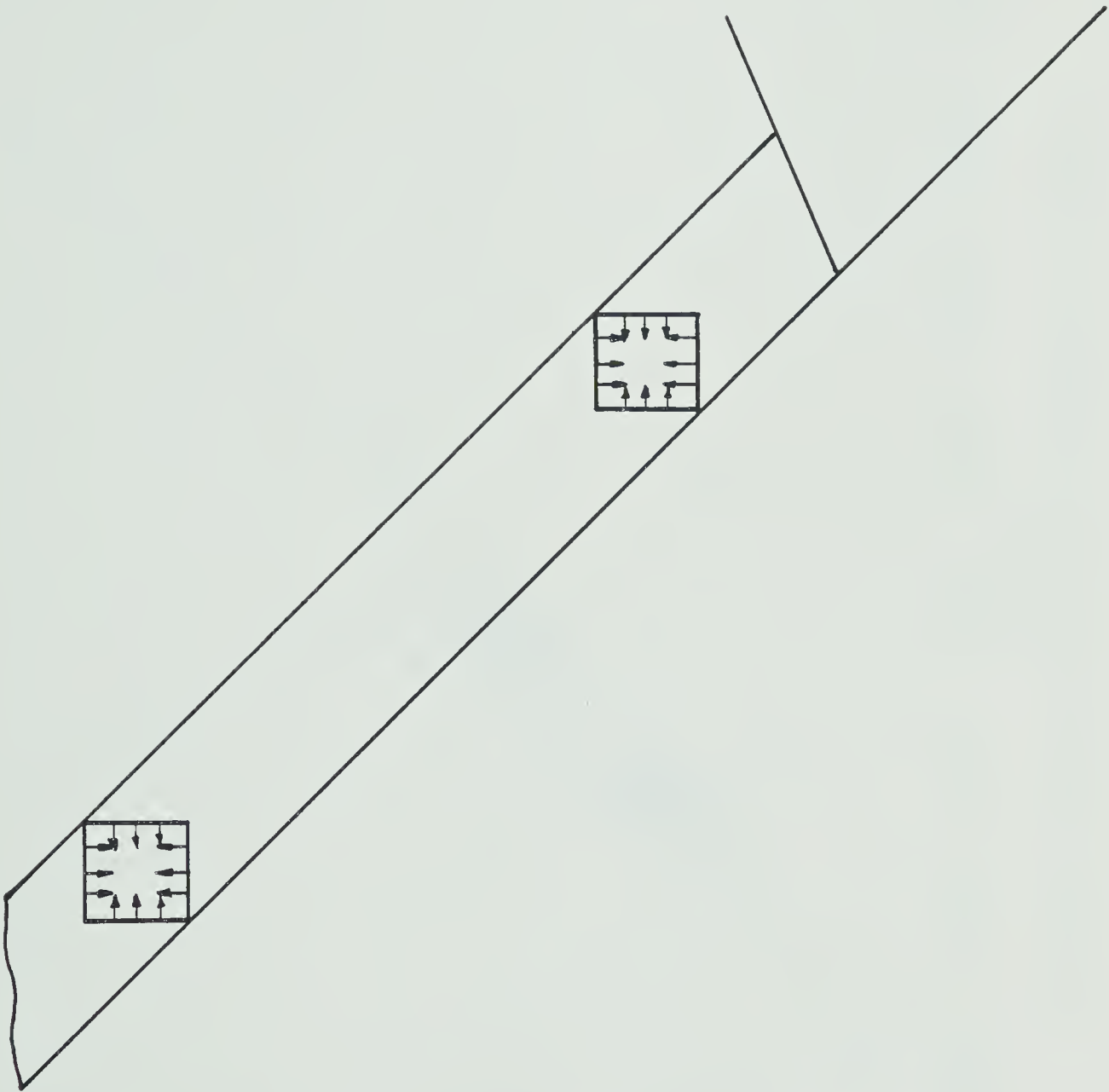


FIGURE 48

LOADING CONDITIONS FOR CONFIGURATION 4



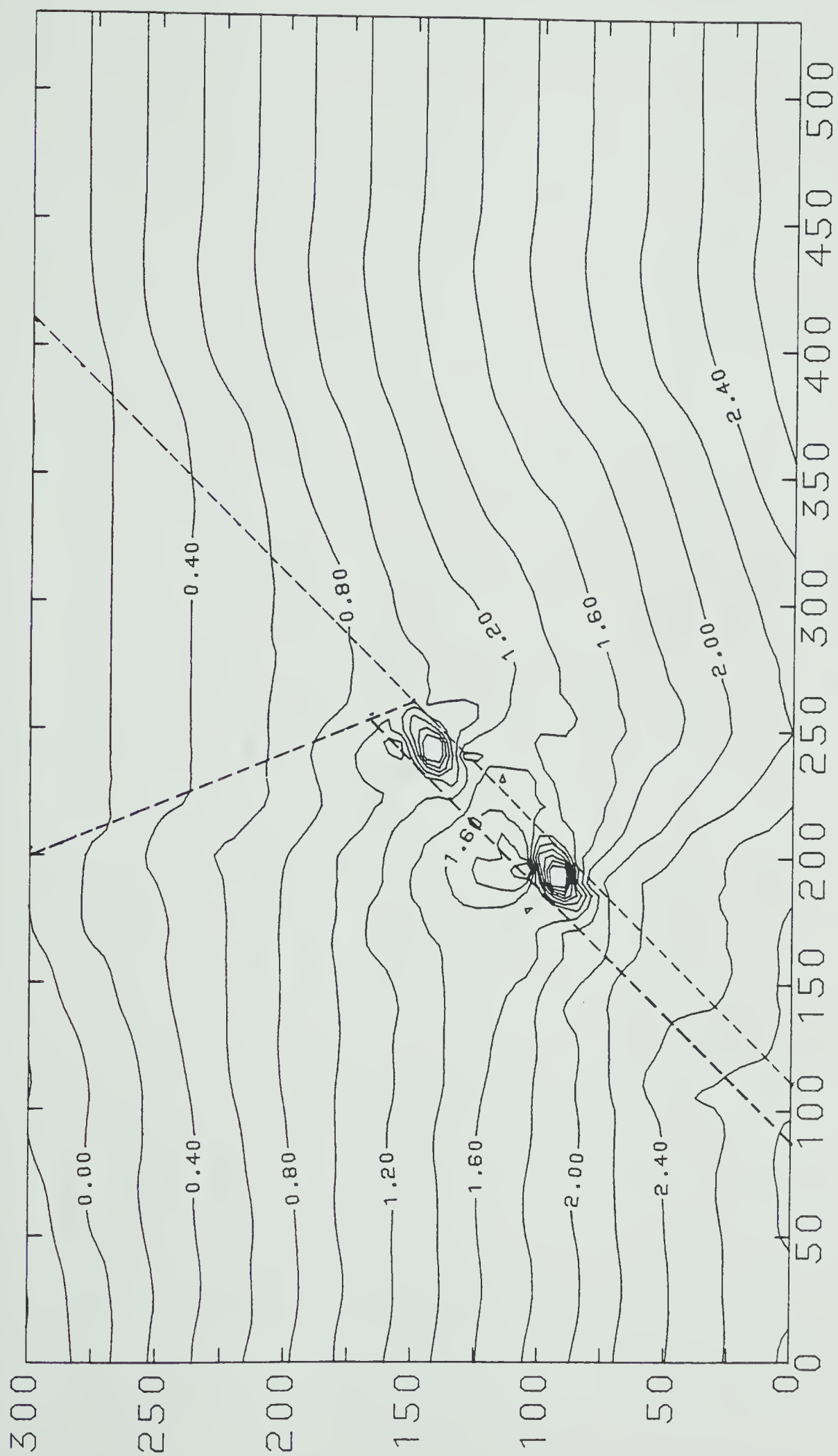


FIGURE 49

HORIZONTAL STRESS DISTRIBUTION THROUGHOUT THE MESH





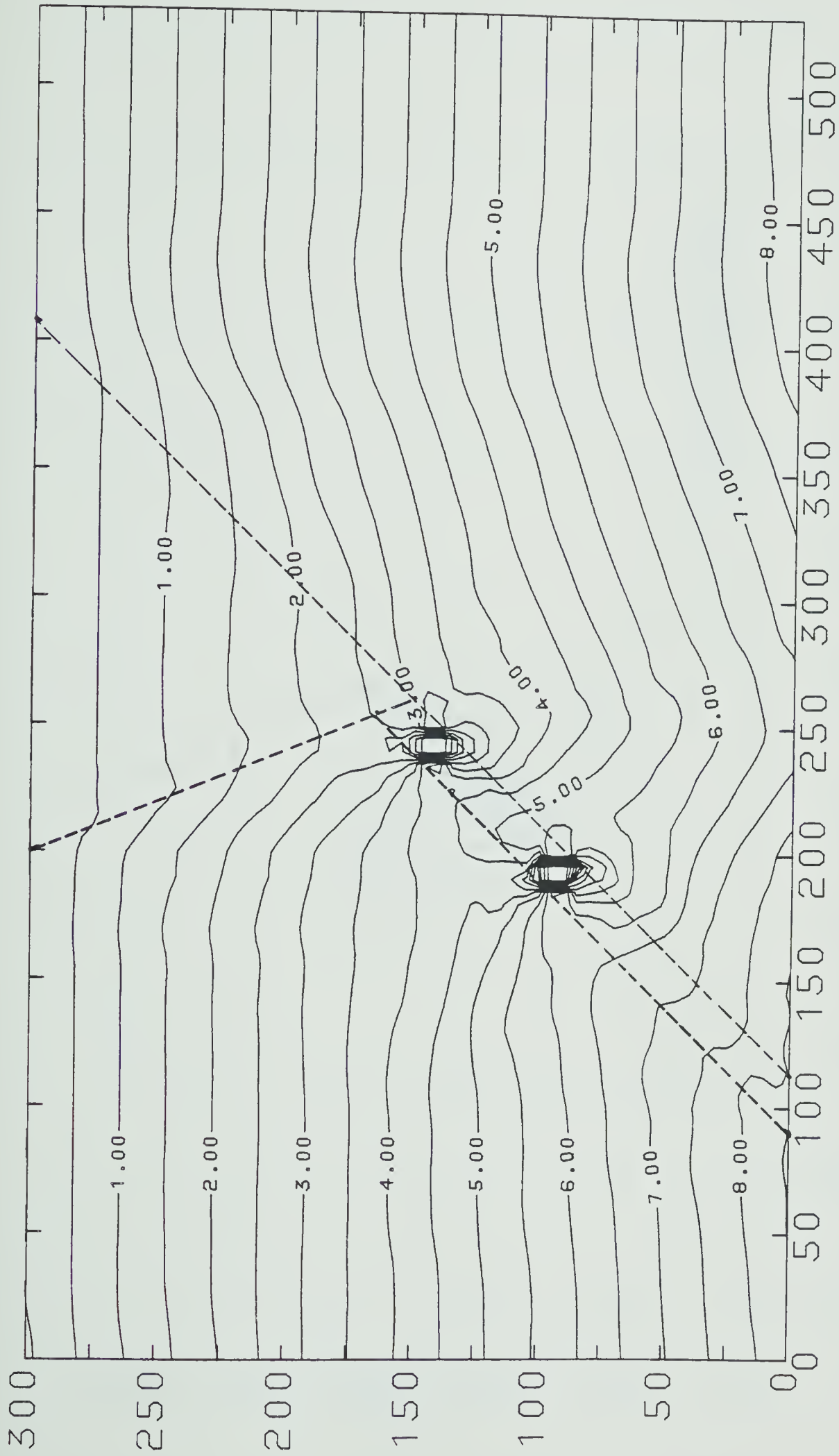


FIGURE 50

VERTICAL STRESS DISTRIBUTION THROUGHOUT THE MESH



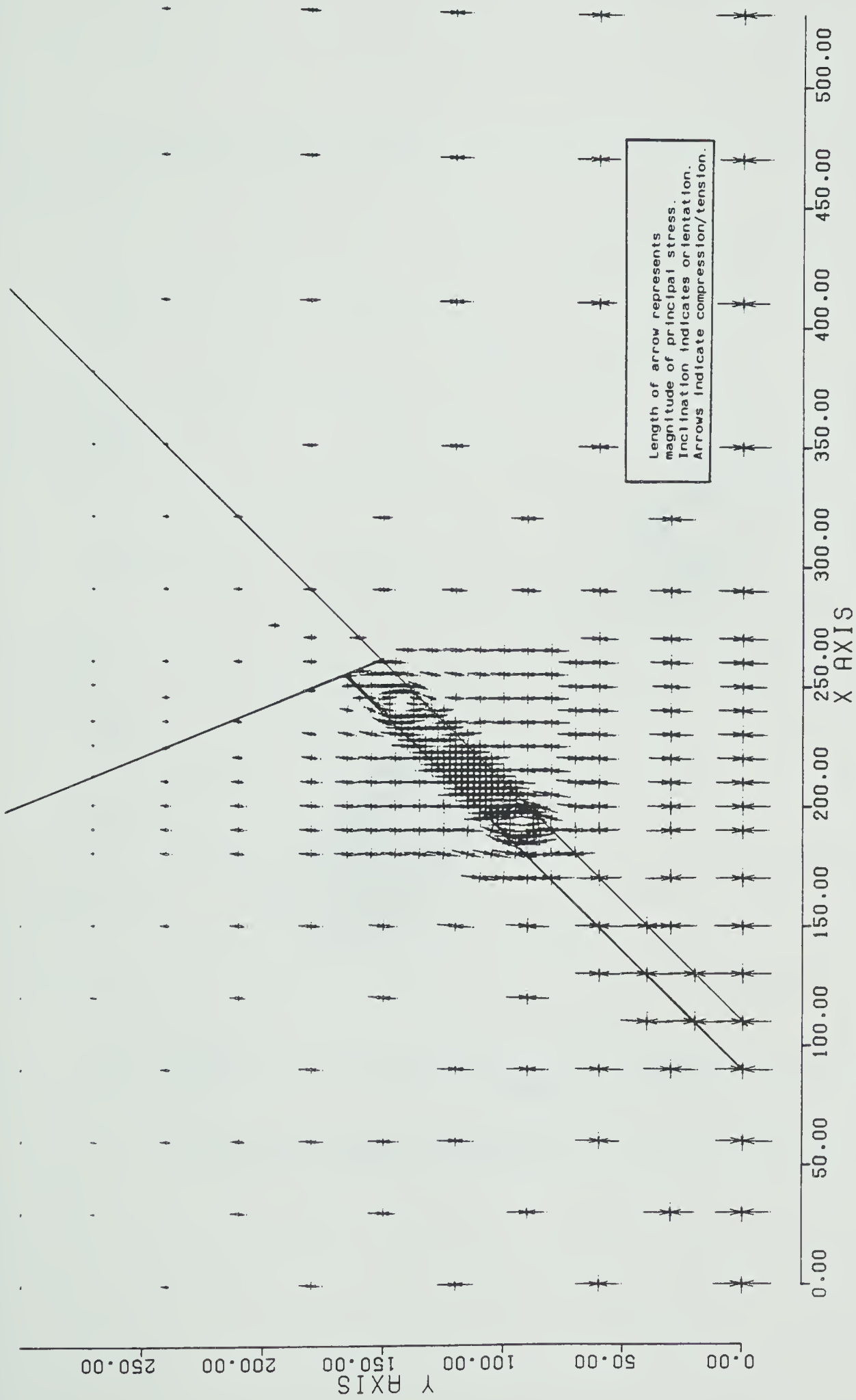
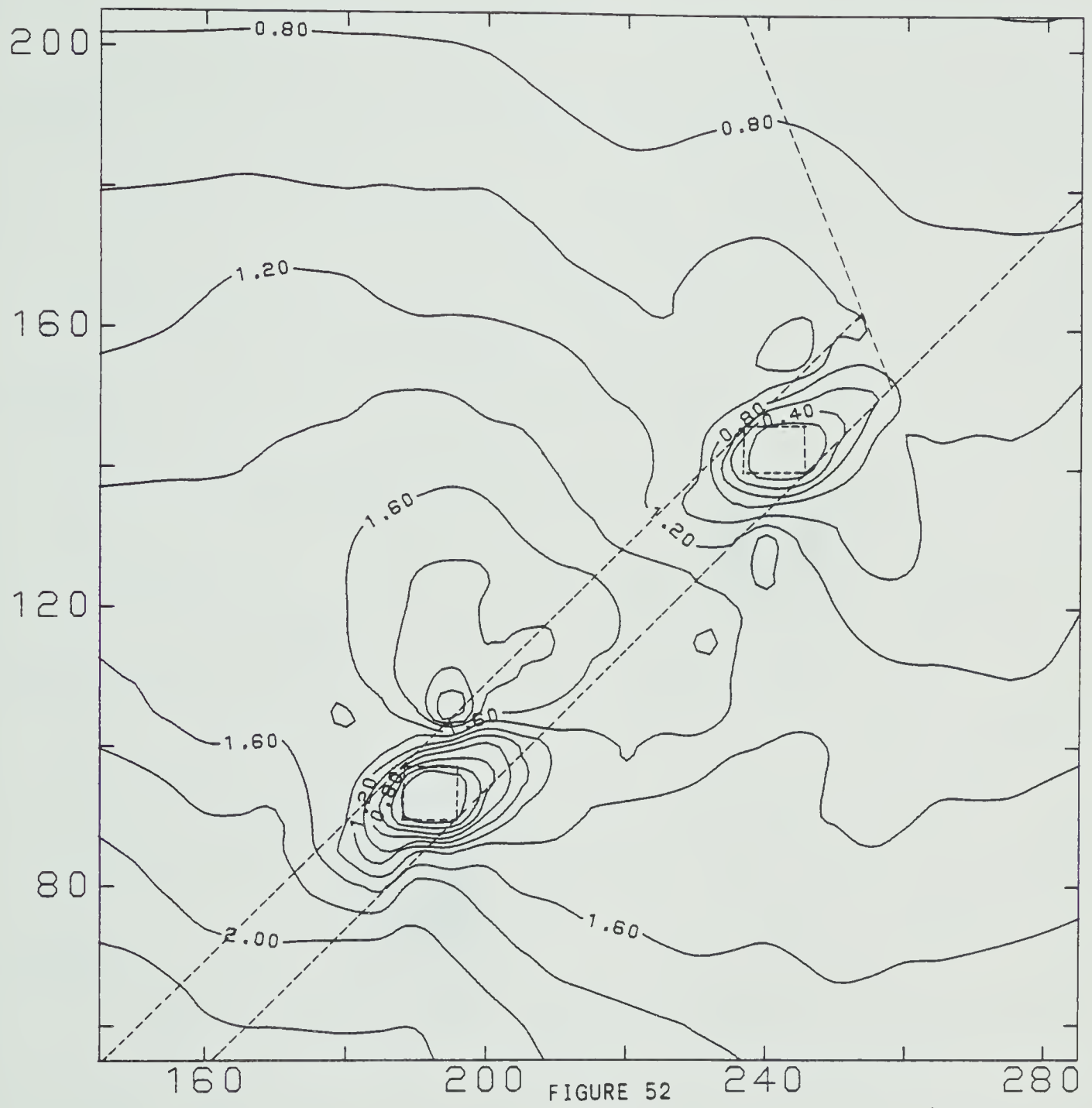


FIGURE 51  
PRINCIPAL STRESSES THROUGHOUT THE MESH





HORIZONTAL STRESS DISTRIBUTION AROUND THE EXCAVATIONS



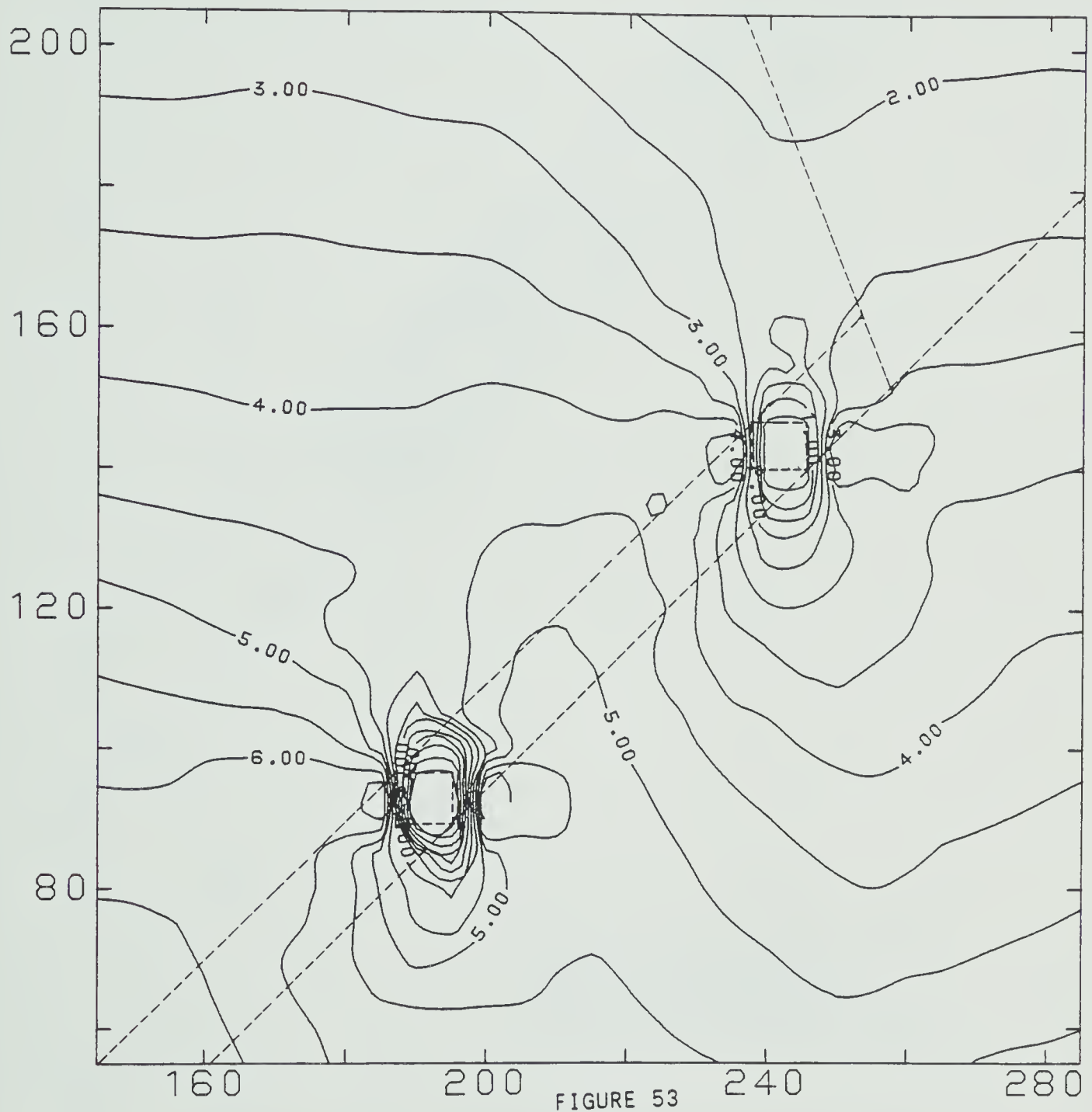
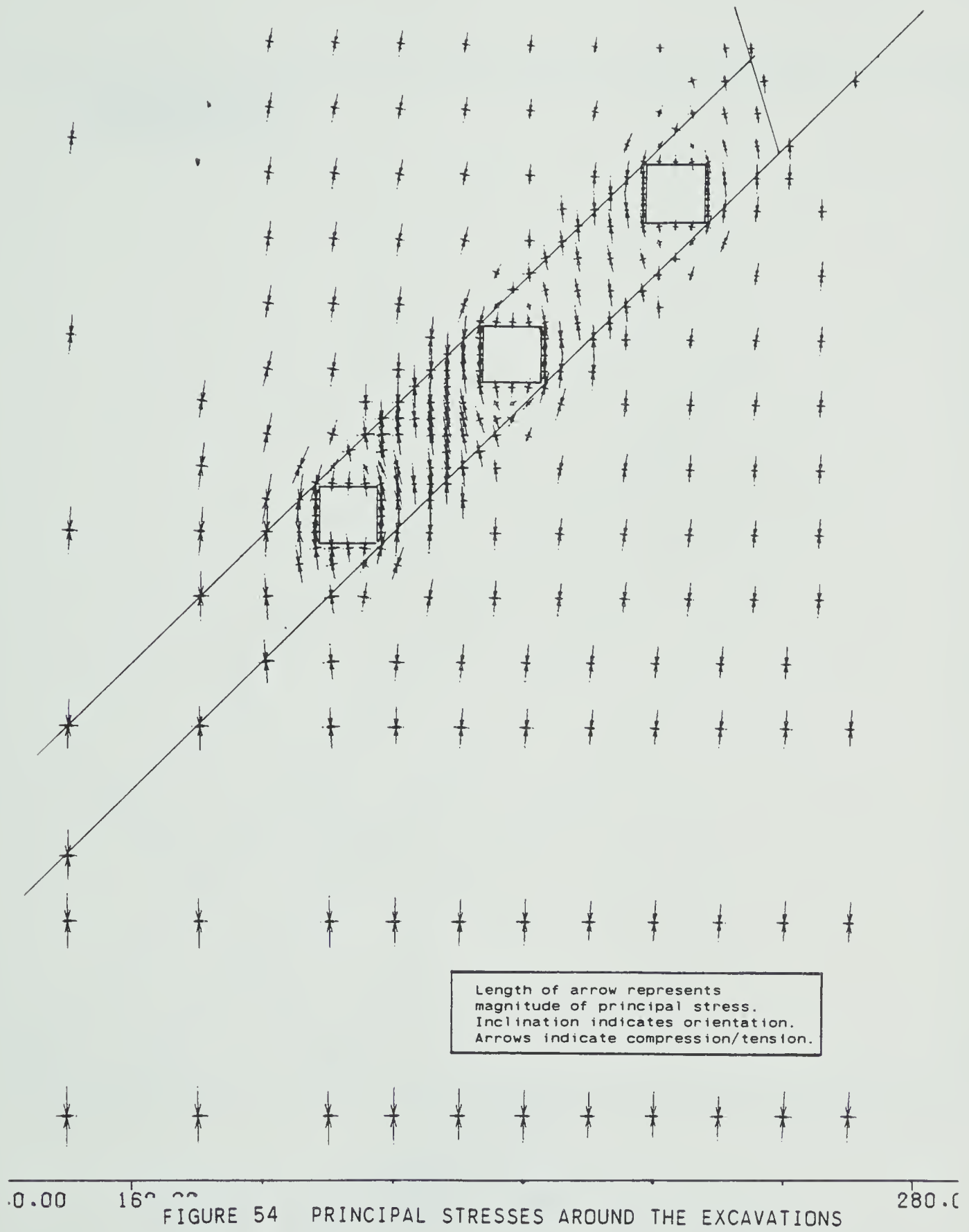


FIGURE 53  
VERTICAL STRESS DISTRIBUTION AROUND THE EXCAVATIONS









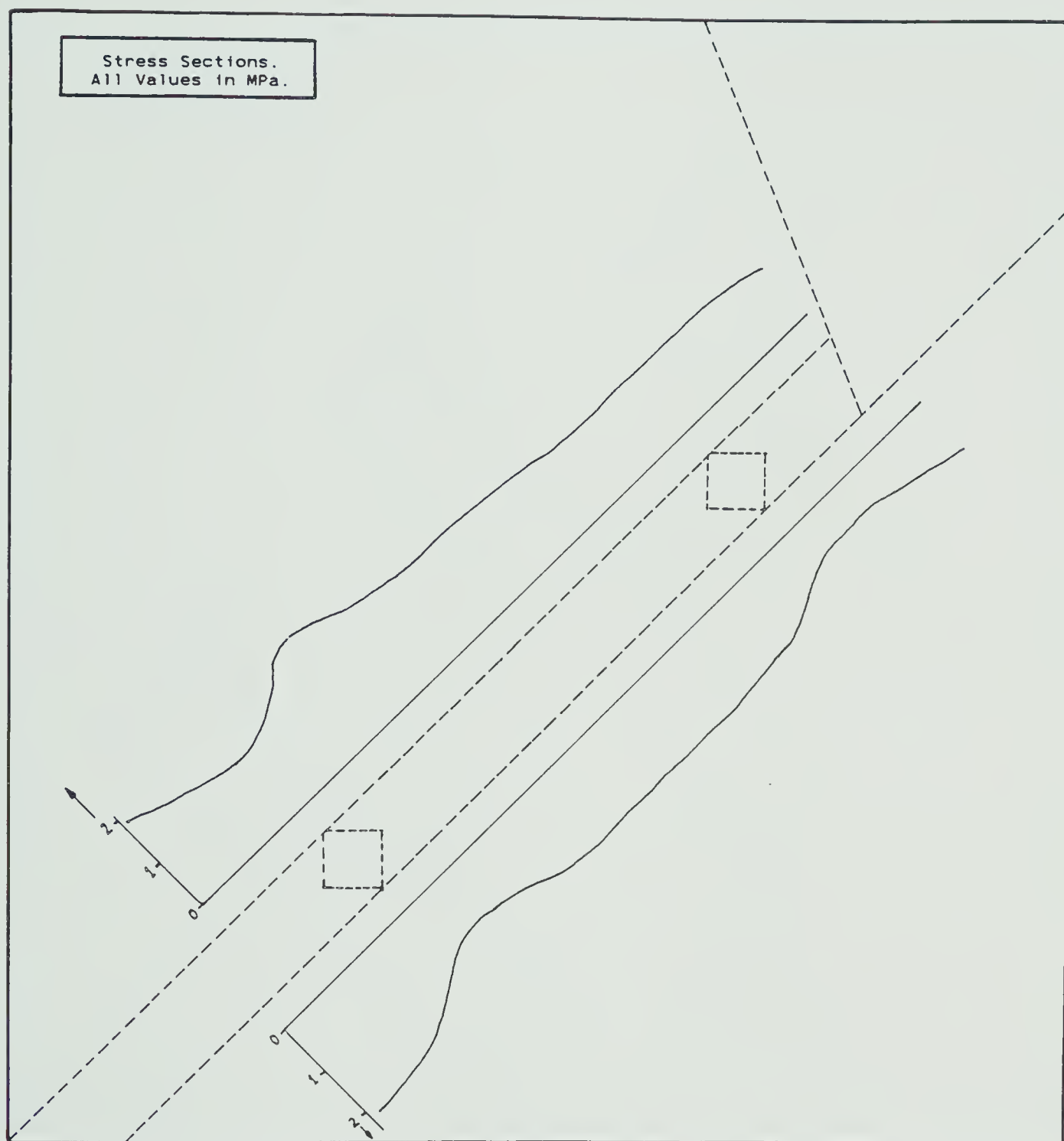


FIGURE 55

CONFIGURATION 4  
HORIZONTAL STRESS VARIATION ALONG GIVEN SECTIONS



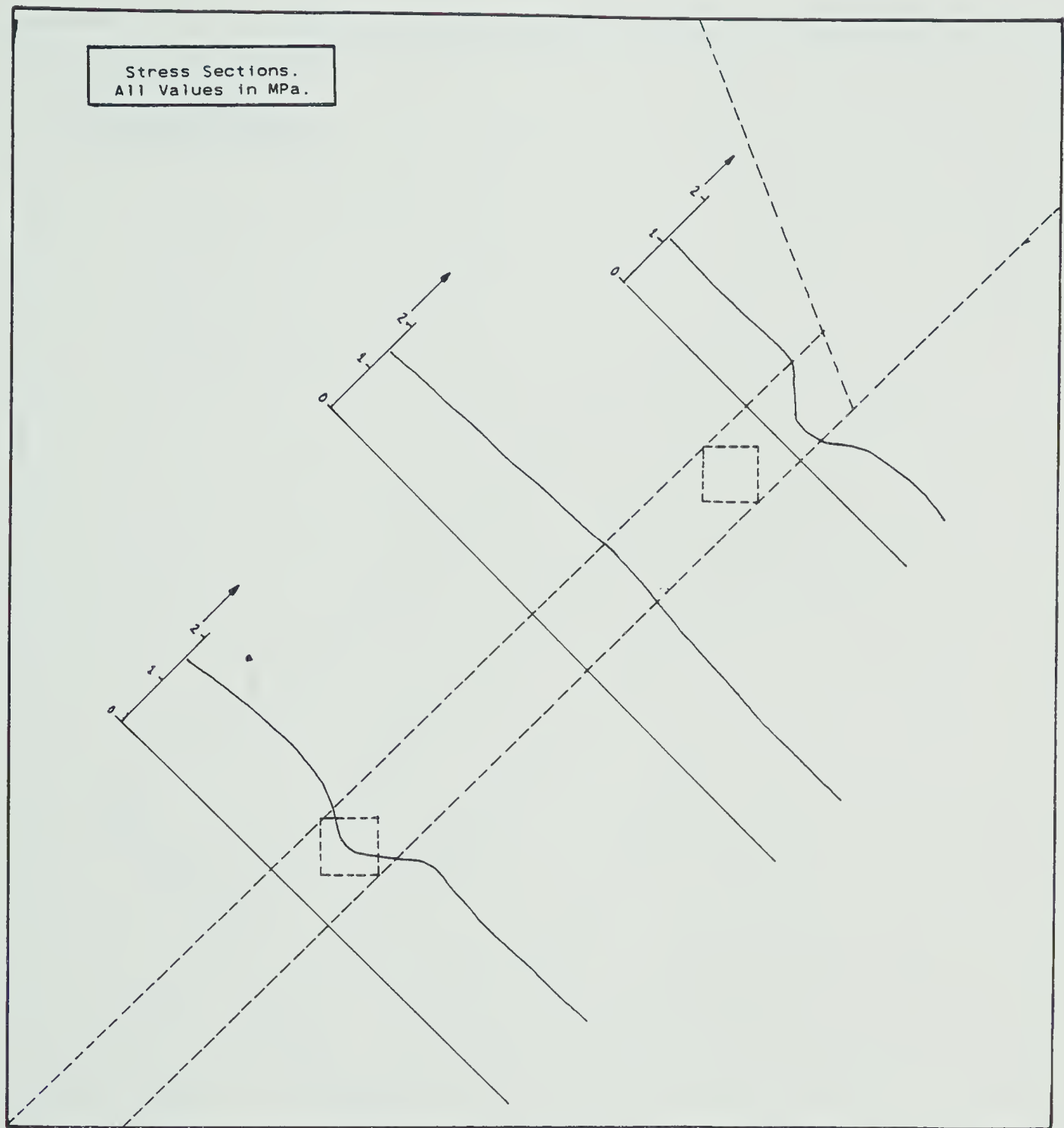


FIGURE 56

CONFIGURATION 4  
HORIZONTAL STRESS VARIATION ALONG GIVEN SECTIONS



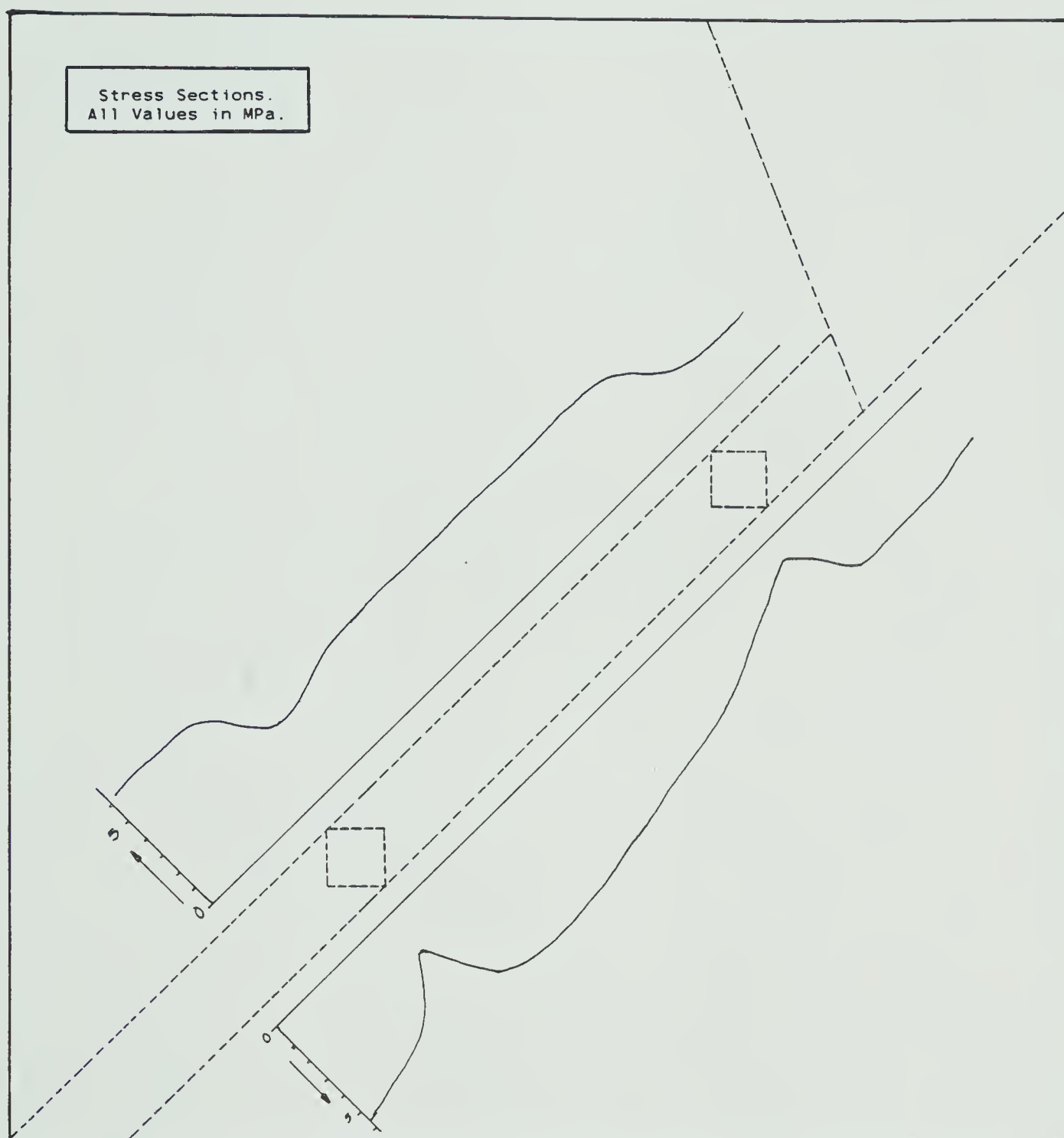


FIGURE 57  
CONFIGURATION 4  
VERTICAL STRESS VARIATION ALONG GIVEN SECTIONS





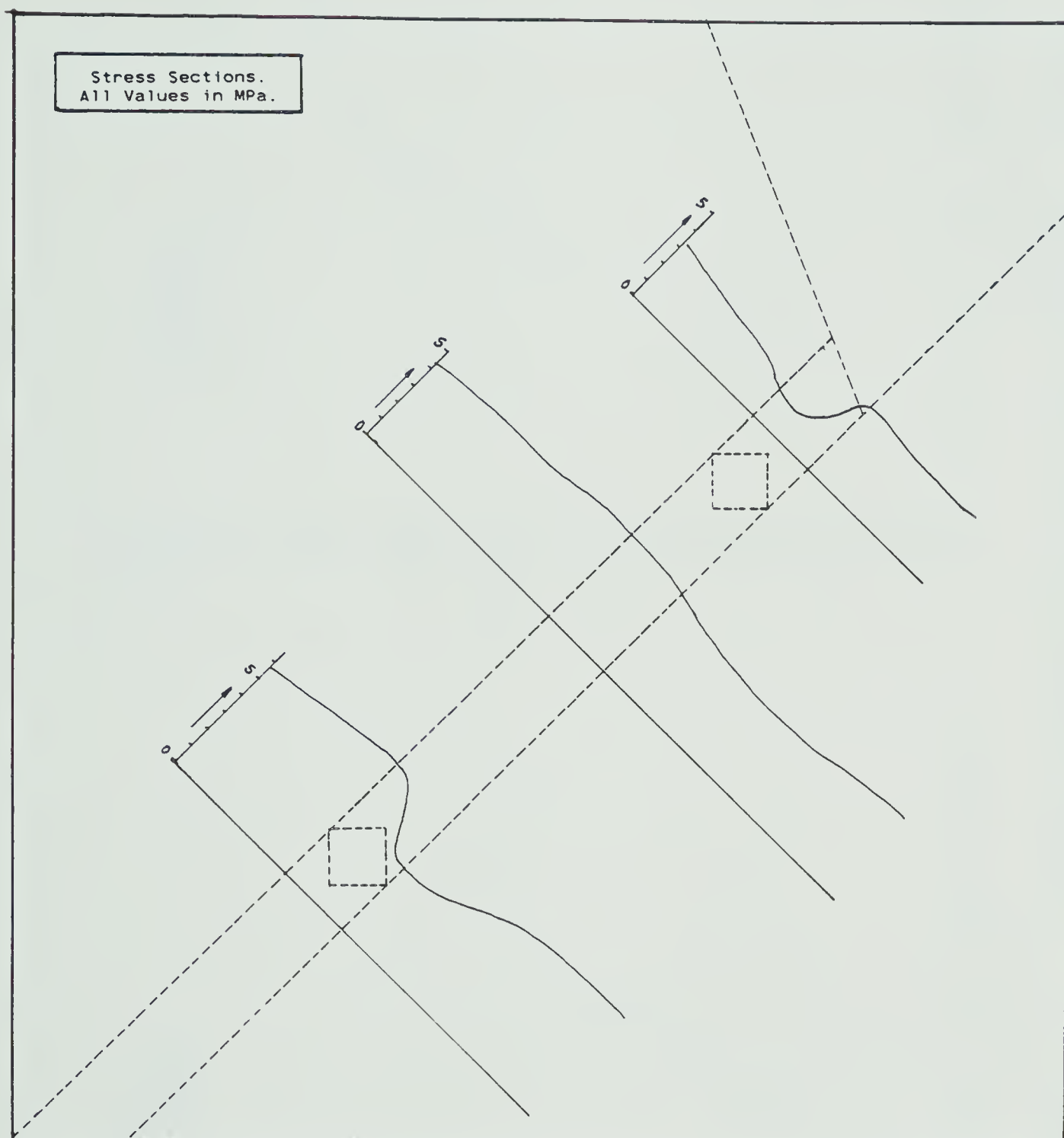


FIGURE 58

CONFIGURATION 4  
VERTICAL STRESS VARIATION ALONG GIVEN SECTIONS



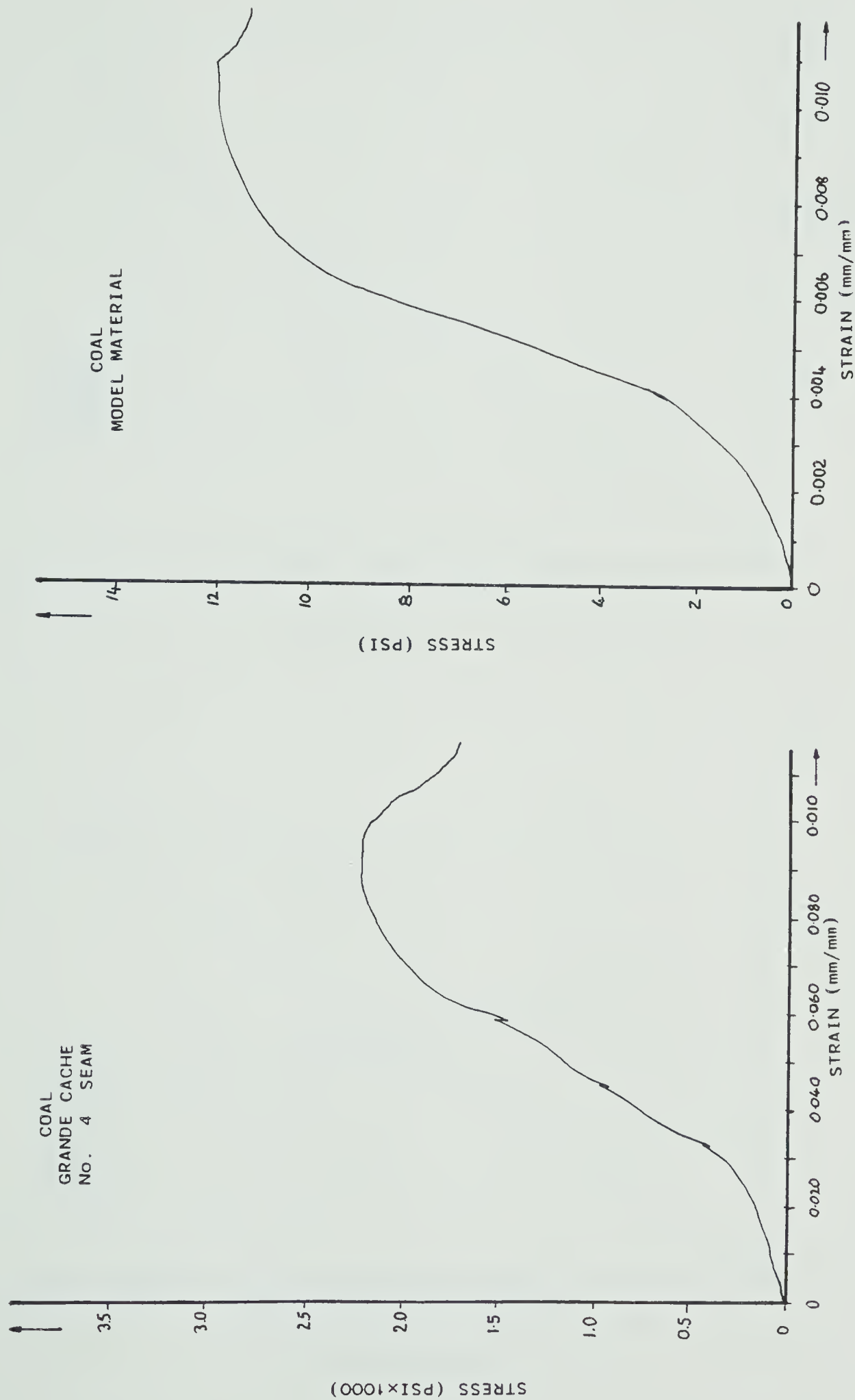


FIGURE 59 STRESS/STRAIN PROPERTIES OF COAL AND MODEL MATERIAL



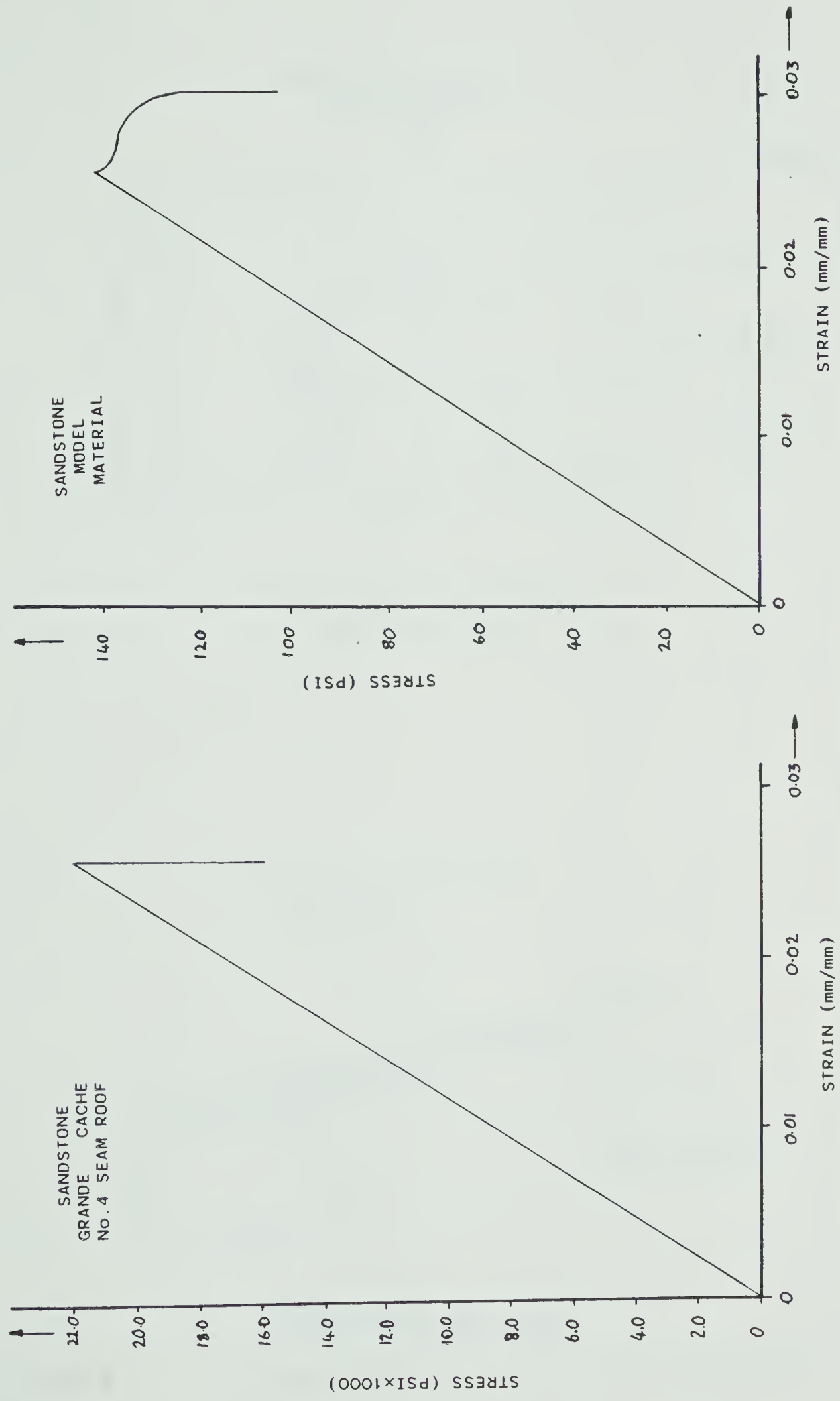


FIGURE 60 STRESS/STRAIN PROPERTIES OF SANDSTONE AND MODEL MATERIAL



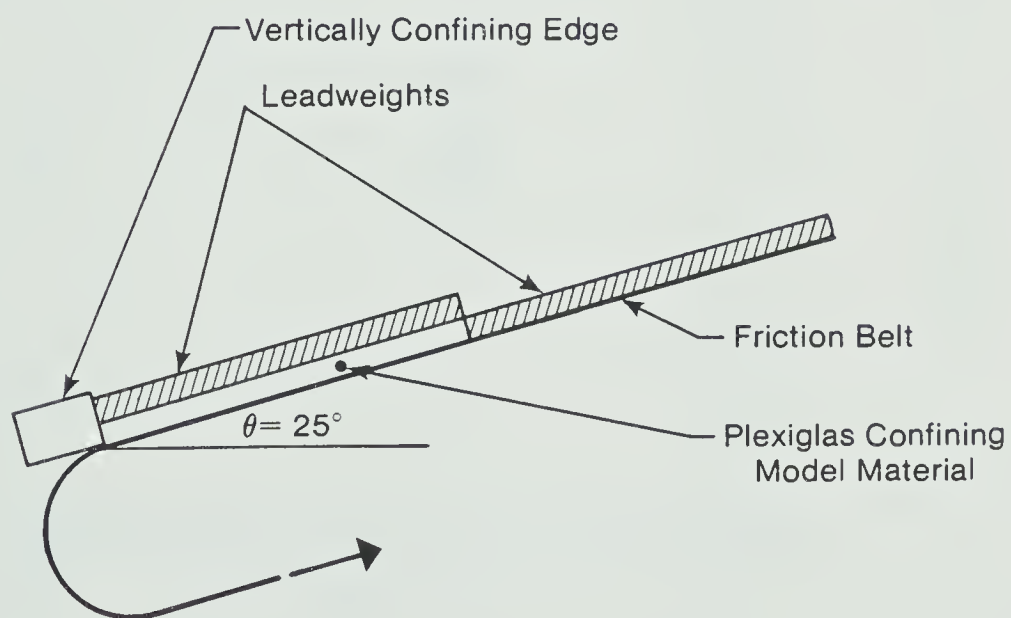
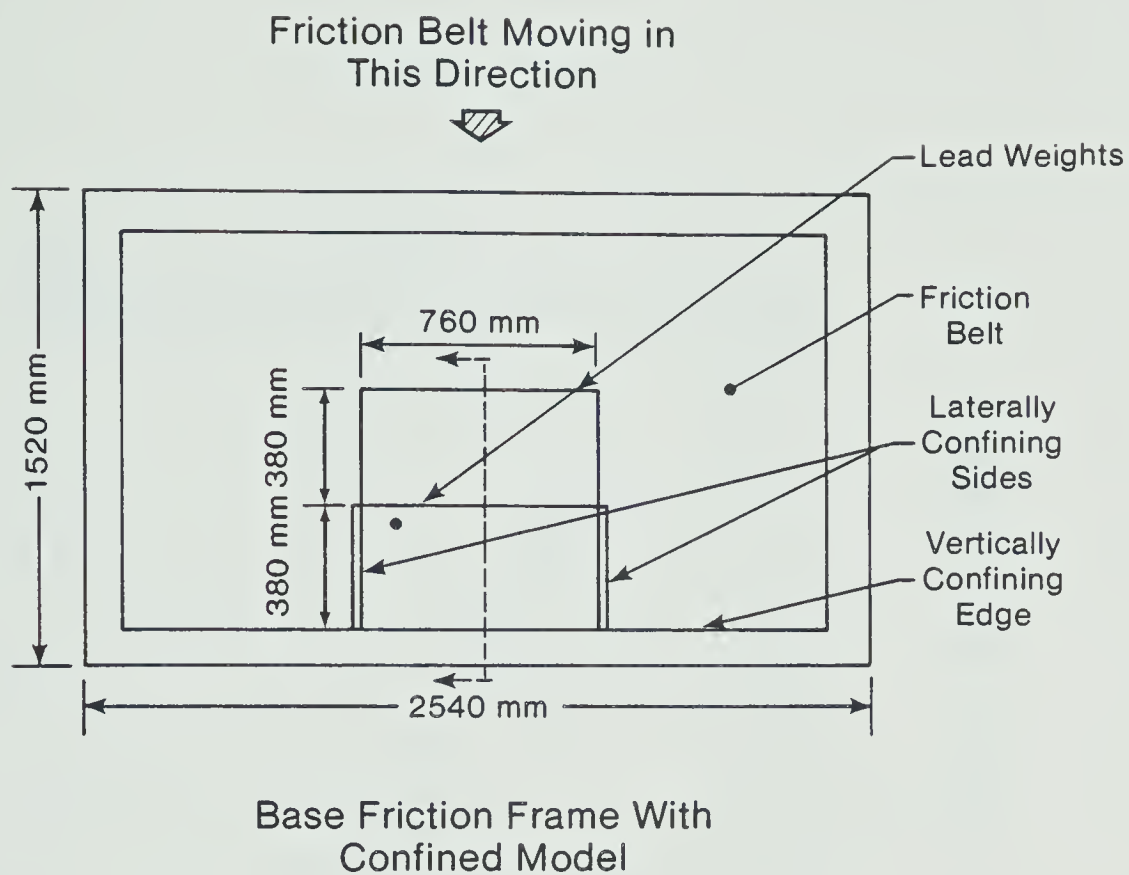


FIGURE 61 PLAN AND SECTION OF BASE FRICTION MODEL





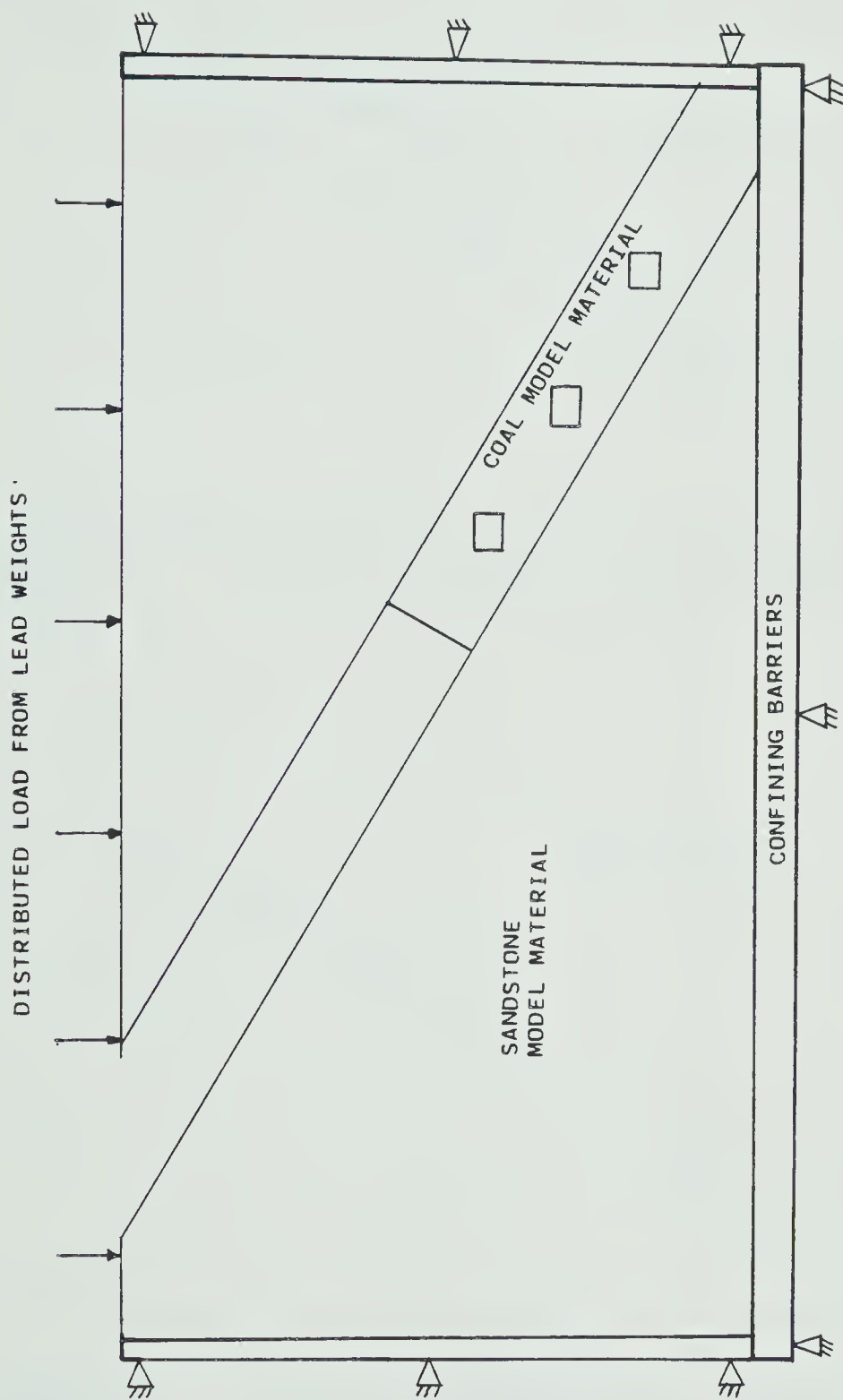


FIGURE 62 PHYSICAL MODEL LOADING CONDITIONS



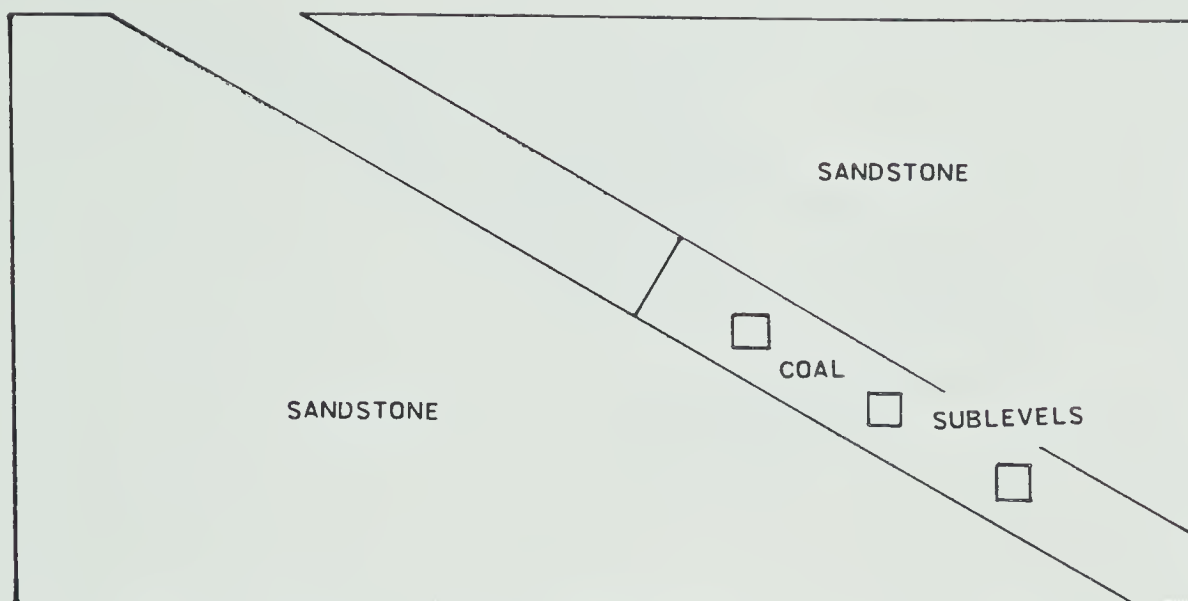


FIGURE 63 INITIAL CONFIGURATION OF MODEL

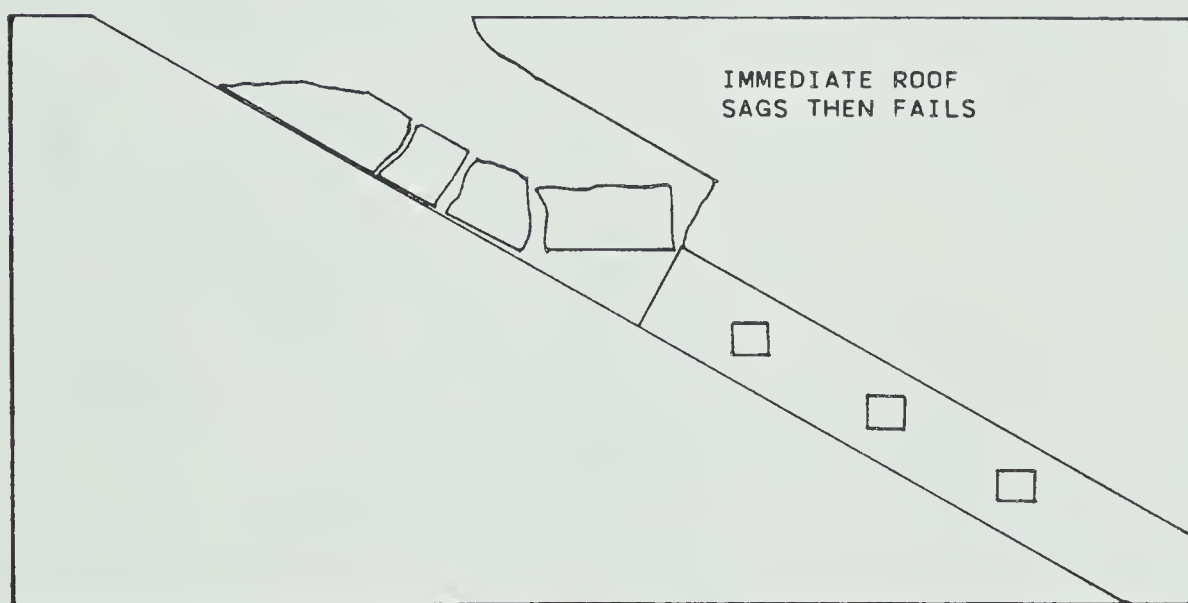


FIGURE 64 MODELLED HANGING WALL CAVING



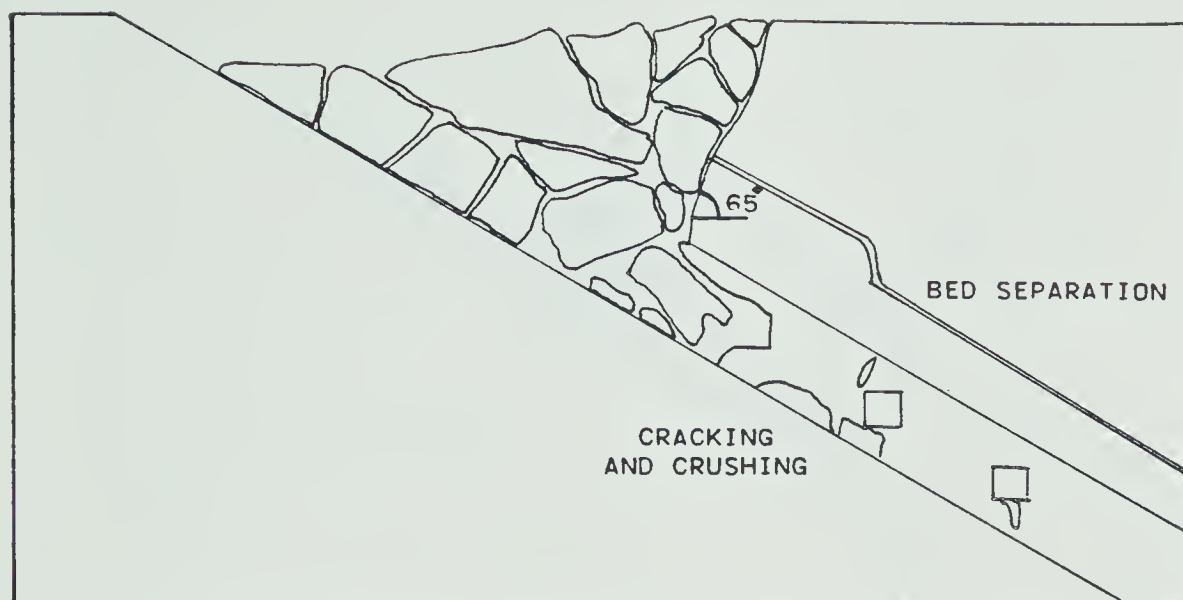


FIGURE 65 HANGING WALL FULLY CAVED

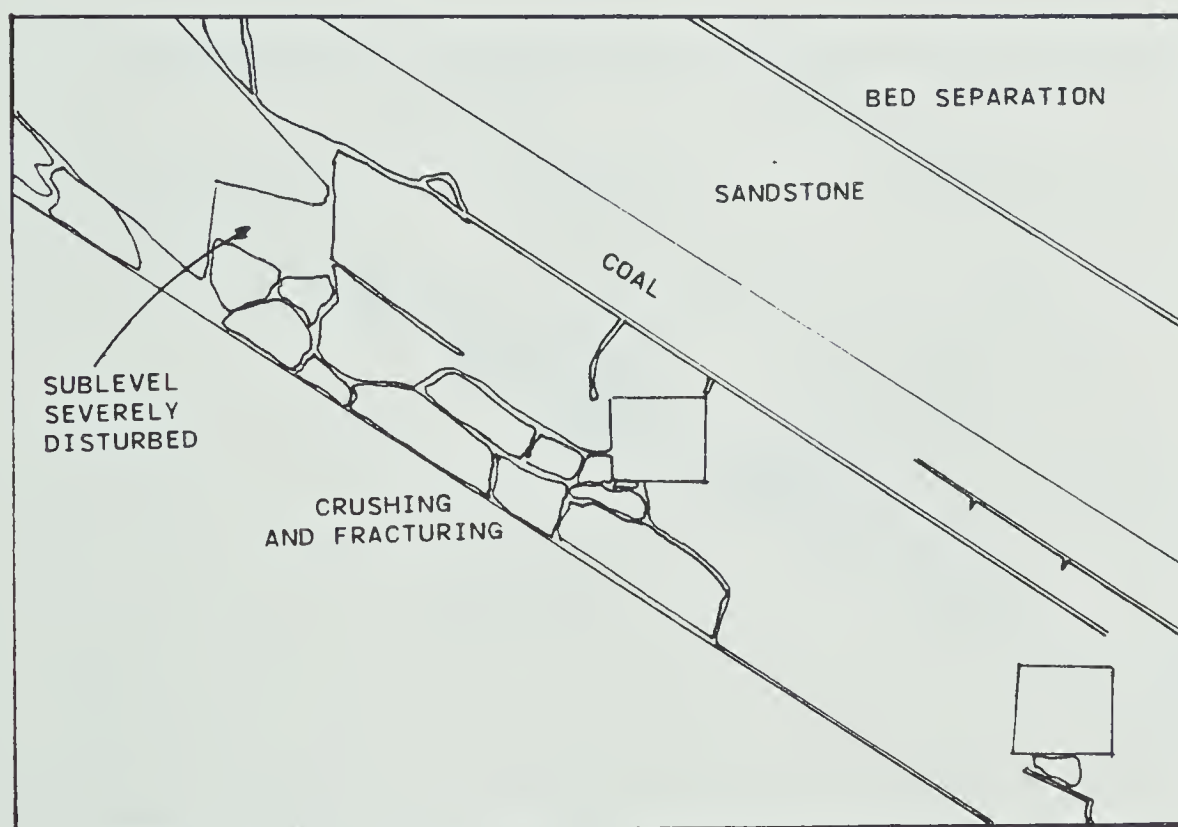


FIGURE 66 DEFORMATION AROUND SUBLEVELS (1)



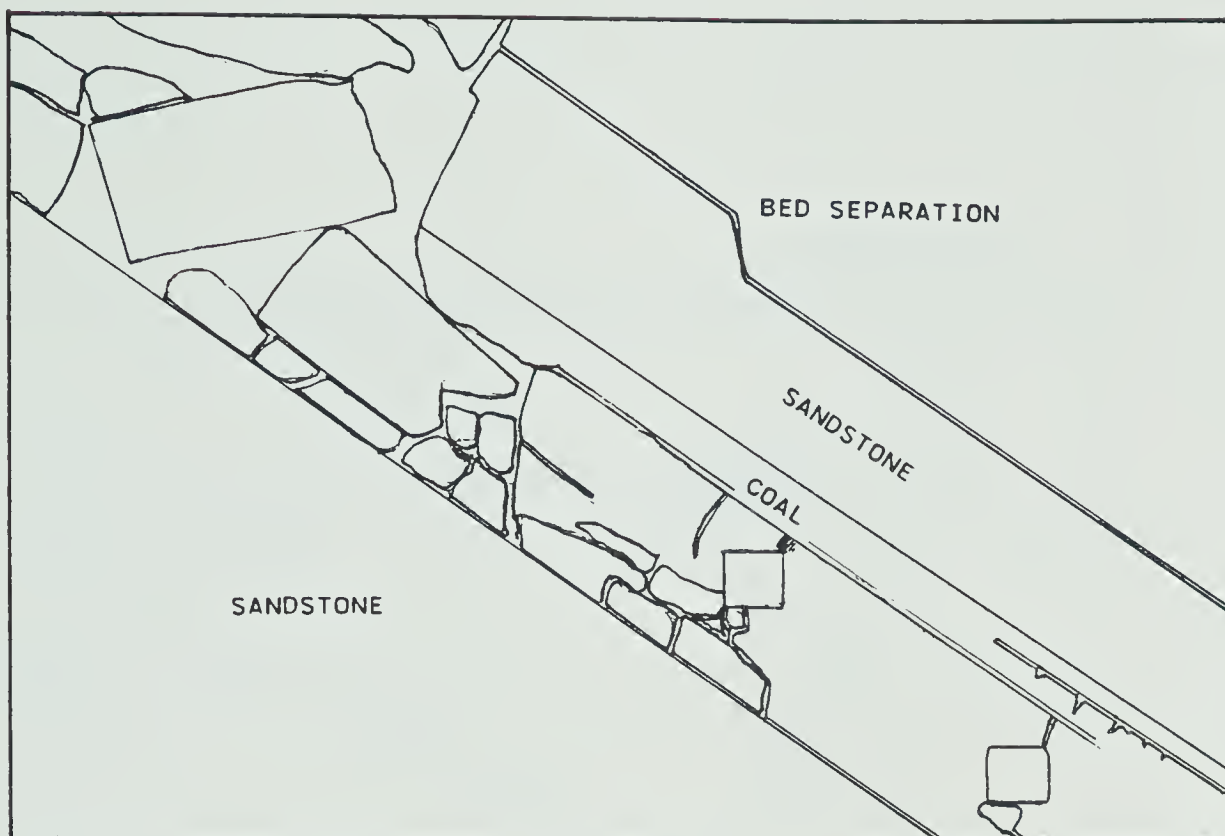


FIGURE 67      DEFORMATION AROUND SUBLEVELS (2)

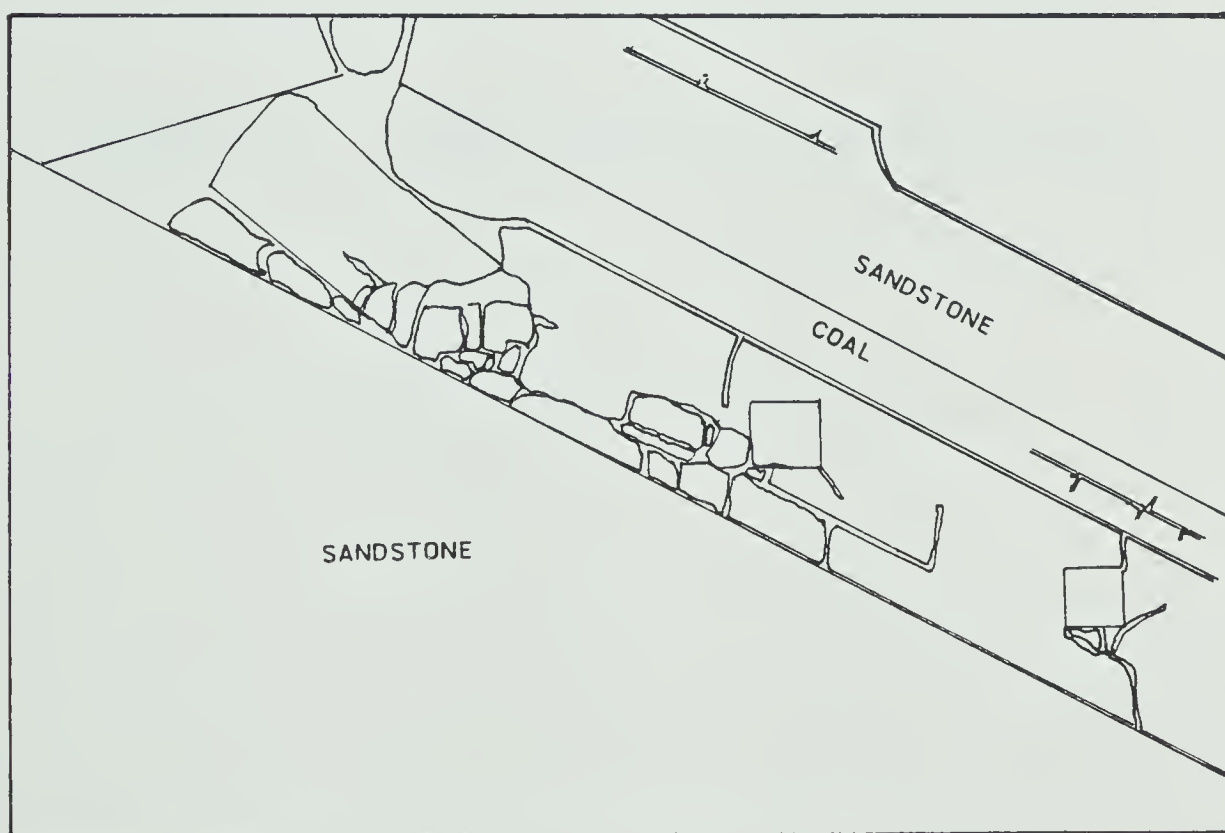


FIGURE 68      DEFORMATION AROUND SUBLEVELS (3)





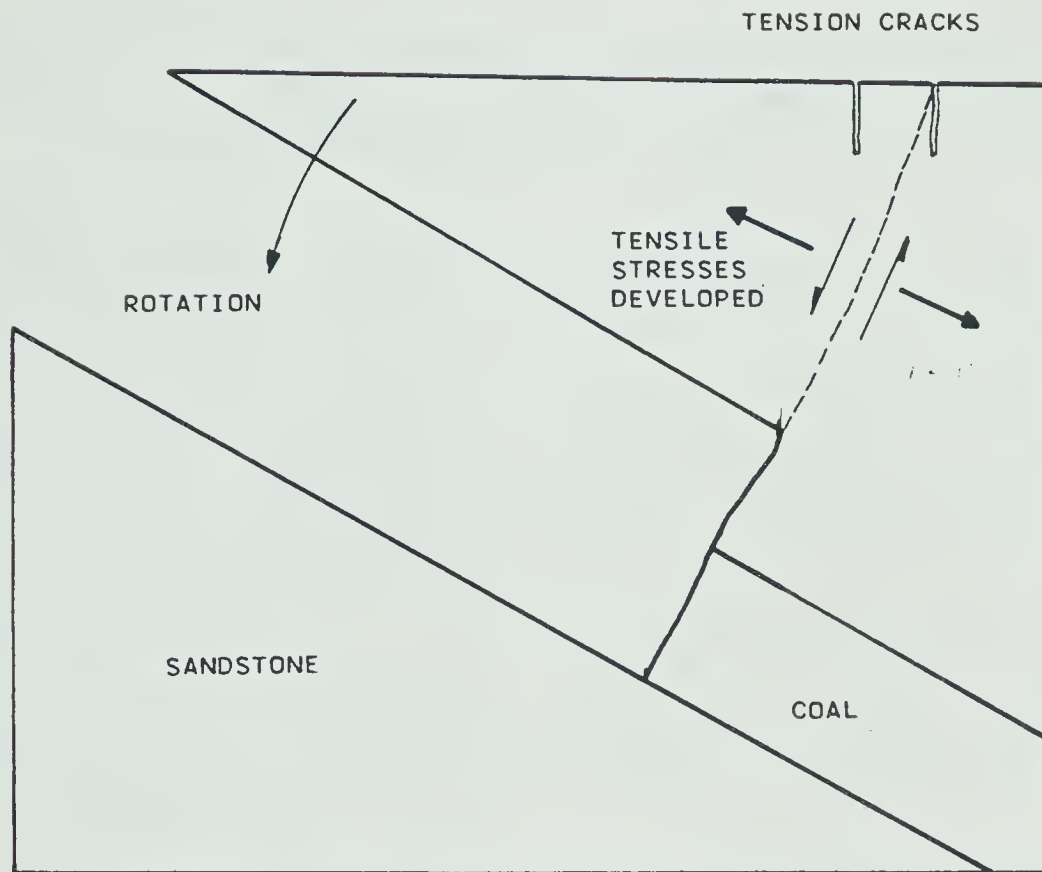


FIGURE 69 HANGING WALL FAILURE MECHANISM



PROVINCE	MEASURED	INDICATED	INFERRED	TOTAL
Low & Medium Volatile Bituminous				
Alberta				
Inner Foothills				
Luscar Formation.	542,000	7,426,500	3,535,400	11,503,900
Inner Foothills				
Kootenay Formation.	440,100	12,193,700	3,831,100	16,464,900
Alberta Total	982,100	19,620,200	7,366,500	27,968,800
British Columbia	6,943,000	10,775,000	40,480,100	58,198,100
RANK TOTAL	7,925,100	30,395,200	47,846,600	86,166,900
High Volatile Bituminous				
Alberta				
Outer Foothills		6,278,600	3,043,700	9,322,300
British Columbia	45,600	100,400	172,900	318,900
RANK TOTAL	45,600	6,379,000	3,216,600	9,641,200
Subbituminous				
Alberta	1,221,800	6,197,300	2,530,000	9,949,100
Lignitic				
British Columbia	340,000	300,000	300,000	940,000
Saskatchewan	291,500	7,024,000	4,698,400	12,013,900
RANK TOTAL	631,500	7,324,000	4,998,400	12,953,900
GRAND TOTAL	9,824,000	50,295,500	58,591,600	118,711,100

TABLE 1

COAL RESOURCES OF WESTERN CANADA BY RANK AND PROVINCE  
(Thousands of Short Tons)

(Dames and Moore; 1978)



PETROGRAPHIC DESCRIPTION	PROPORTIONAL THICKNESS	% SEAM
Soft flaky vitrain	6 ins	4.8
Durain, banded	6 ins	4.8
Clarain (vitrainous)	1 ft	9.5
Clarain (durainous)	1 ft	9.5
Interbanded vitrain, clarain, durain with dispersed fusain	1 ft 6 ins	14.3
Clarain (firm)	2 ft 6 ins	23.7
Clarain (vitrainous)	6 ins	4.8
Durain banded with clarain and fusain	1 ft 6 ins	14.3
Clarain (firm)	6 ins	4.8
Vitrain (soft)	6 ins	9.5

TABLE 2

PETROGRAPHIC DESCRIPTION OF A TYPICAL WESTERN CANADIAN SEAM



SAMPLE No.	ROCK TYPE	COMPRESSIVE STRENGTH (MPa)	YOUNG' S MODULUS (MPa)	POISSON' S RATIO
1	Banded Claystone	58.5	29200	0.41
2	Laminated Siltstone	46.3	23200	0.50
3	Sandstone Coarse gr.	196.4	34000	0.22
4	Sandstone Fine gr.	221.1	64000	0.166
5	Laminated Siltstone	135.5	36500	0.31

Table 3      Uniaxial Test Results Summary





SAMPLE No.	ROCK TYPE	CONFINING PRESSURE (MPa)	FAILURE LOAD (MPa)	INTERNAL FRICTION ANGLE	COHESION (MPa)
1	Silty Claystone	10.34	221.8		
2	Silty Claystone	20.68	250.3	28	20
3	Silty Claystone	31.02	260.9		
4	Claystone	6.89	180.24		
5	Claystone	6.89	77.80		
6	Claystone	13.78	209.13	32	30
7	Claystone	20.68	229.30		
8	Claystone	27.58	250.74		
9	Claystone	34.47	270.37		
10	Siltstone	6.89	112.10	42	15
11	Siltstone	13.78	153.70		
17	Coarse	13.78	323.50		
18	Grained	25.58	402.80	50	30
19	Sand-	20.68	325.10		
20	Stone	6.89	290.40		

Table 4      Triaxial Test Results Summary



SAMPLE No.	CONFINING PRESSURE (MPa)	FAILURE PRESSURE (MPa)	INTERNAL FRICTION ANGLE	COHESION (MPa)
1	6.89	48.05		
2	13.79	78.08		
3	20.69	56.40		
4	27.58	105.70	19	0
5	34.48	96.45		
6	41.38	111.72		

#### Coal Triaxial Data

#### Uniaxial Data

COMPRESSIVE STRENGTH (Average) (MPa)	YOUNG' S MODULUS (MPa)	POISSON' S RATIO
10.13	2034	0.35

Table 5 Coal Test Data





Plate 1 Initial Configuration of Model



Plate 2 Modelled Hanging Wall Caving





Plate 3 Hanging Wall Fully Caved



Plate 4 Deformation Around Sublevels (1)







Plate 5 Deformation Around Sublevels (2)



Plate 6 Deformation Around Sublevels (3)



APPENDIX I  
STRENGTH TEST DATA  
STRESS/STRAIN PLOTS  
MOHR CIRCLE DIAGRAMS



AXIAL LOAD MN	AXIAL STRESS MPa	AXIAL STRAIN mm/mm	LATERAL STRAIN mm/mm
0.00000	0.000	000	000
0.00266	0.925	137	- 46
0.00534	1.858	209	- 55
0.00854	2.971	274	- 59
0.01068	3.715	313	- 58
0.01601	5.569	398	- 51
0.02135	7.427	481	- 41
0.02669	9.284	562	- 23
0.03203	11.142	627	- 11
0.03737	12.999	702	10
0.04270	14.853	764	31
0.04804	16.711	836	52
0.05338	18.568	902	72
0.05872	20.426	960	92
0.06405	22.280	1018	113
0.07473	25.995	1146	160
0.08007	27.853	1208	185
0.08541	29.710	1268	209
0.09074	31.564	1332	236
0.09688	33.700	1390	260
0.10142	35.279	1456	295
0.10676	37.137	1523	328
0.11209	38.991	1577	357
0.11743	40.849	1640	394
0.12277	42.706	1705	434
0.12811	44.564	1771	470
0.13345	46.421	1835	520
0.13878	48.275	1902	565
0.14412	50.133	1966	620
0.14946	51.991	2028	683
0.15479	53.845	2091	760
0.16014	55.706	2161	876
0.16547	57.560	2225	1013

TEST RESULTS UNIAXIAL SAMPLE 1



AXIAL LOAD MN	AXIAL STRESS MPa	AXIAL STRAIN mm/mm	LATERAL STRAIN mm/mm
0.00000	0.000	000	000
0.00534	1.851	278	- 30
0.01068	3.703	482	- 29
0.02135	7.402	735	8
0.02802	9.715	854	40
0.03203	11.102	936	63
0.03737	12.957	1023	90
0.04324	14.992	1110	129
0.04857	16.839	1195	170
0.05365	18.601	1281	212
0.05872	20.358	1350	269
0.06405	22.207	1435	326
0.06939	24.058	1504	380
0.07553	26.187	1580	452
0.08007	27.761	1654	505
0.08487	29.425	1720	574
0.09074	31.460	1791	662
0.09608	33.312	1874	753
0.10142	35.163	1919	828
0.10676	37.015	1988	934
0.11209	38.863	2051	1043
0.11796	40.898	2097	1161
0.12277	42.566	2158	1334
0.12811	44.417	2215	1400
0.13345	46.269	2225	810

TEST RESULTS UNIAXIAL SAMPLE 2





AXIAL LOAD MN	AXIAL STRESS MPa	AXIAL STRAIN mm/mm	LATERAL STRAIN mm/mm
0.00000	0.000	000	000
0.00534	1.851	48	5
0.02135	7.403	207	17
0.04270	14.805	431	38
0.06405	22.208	690	61
0.08541	29.611	926	81
0.10676	37.014	1176	109
0.12811	44.416	1431	136
0.14946	51.819	1657	165
0.17081	59.222	1885	195
0.19216	66.624	2120	232
0.21351	74.027	2336	268
0.23487	81.430	2444	304
0.25622	88.833	2780	342
0.27577	96.236	2989	385
0.29892	103.638	3199	426
0.32027	111.041	----	471
0.34162	118.444	3619	520
0.36297	125.846	3832	567
0.38433	133.249	4040	622
0.40568	140.652	4254	682
0.42703	148.055	4465	743
0.44838	155.457	4690	808
0.46973	162.860	4912	875
0.49108	170.263	5146	959
0.51243	177.666	5355	1035
0.53379	185.068	----	1145
0.54980	190.620	5812	1228
0.56048	194.322	5926	1280

TEST RESULTS UNIAXIAL SAMPLE 3



AXIAL LOAD MN	AXIAL STRESS MPa	AXIAL STRAIN mm/mm	LATERAL STRAIN mm/mm
0.00000	0.000	000	000
0.01068	3.761	58	13
0.02135	7.521	116	23
0.03203	11.282	176	33
0.04270	15.043	236	44
0.05765	20.308	320	57
0.06405	22.564	354	63
0.07473	26.325	417	73
0.08541	30.086	477	85
0.09608	33.846	547	95
0.10676	37.607	596	104
0.13345	47.009	750	131
0.16014	56.411	898	157
0.18683	65.812	1042	186
0.21351	75.214	1200	215
0.24020	84.616	1338	239
0.26689	94.018	1483	270
0.29358	103.419	1629	299
0.32561	114.702	1804	317
0.34696	122.223	1973	320
0.37365	131.625	2116	342
0.40194	141.951	2280	369
0.42703	150.428	2425	385
0.45479	160.206	2576	425
0.48041	169.232	2728	453
0.50710	178.634	2884	485

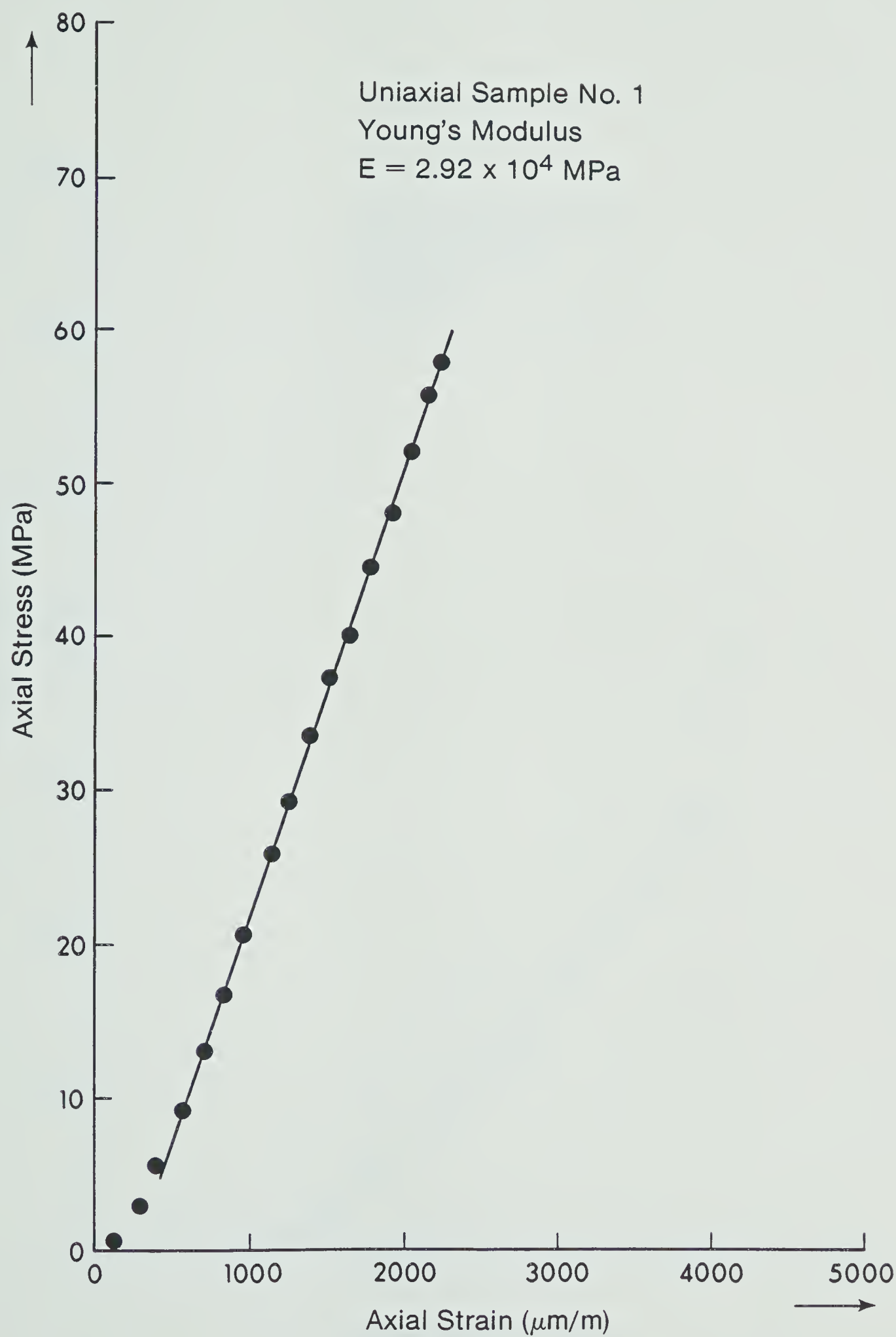
TEST RESULTS UNIAXIAL SAMPLE 4



AXIAL LOAD MN	AXIAL STRESS MPa	AXIAL STRAIN mm/mm	LATERAL STRAIN mm/mm
0.00000	0.000	000	000
0.02669	9.284	164	64
0.04270	14.854	276	109
0.05338	18.568	355	139
0.06405	22.282	440	163
0.07473	25.995	535	191
0.08541	29.709	648	216
0.09608	33.423	755	243
0.10676	37.136	860	269
0.11743	40.850	965	296
0.12811	44.563	1066	322
0.13878	48.277	1172	348
0.16014	55.704	1385	404
0.17348	60.346	1522	440
0.18683	64.988	1631	476
0.20017	69.630	1776	514
0.21351	74.272	1905	557
0.22419	77.986	2010	590
0.23487	81.699	2100	619
0.24554	85.413	2216	660
0.25622	89.127	2311	694
0.26689	92.840	2419	733
0.27757	96.554	2515	772
0.28824	100.268	2619	810
0.29892	103.981	2728	869
0.30960	107.695	2807	909
0.32027	111.408	2925	958
0.33095	115.122	3037	1007
0.34162	118.836	3155	1072
0.35230	122.549	3265	1120
0.36297	126.263	3372	1178
0.37365	129.976	3465	1231
0.38433	133.690	3550	1335

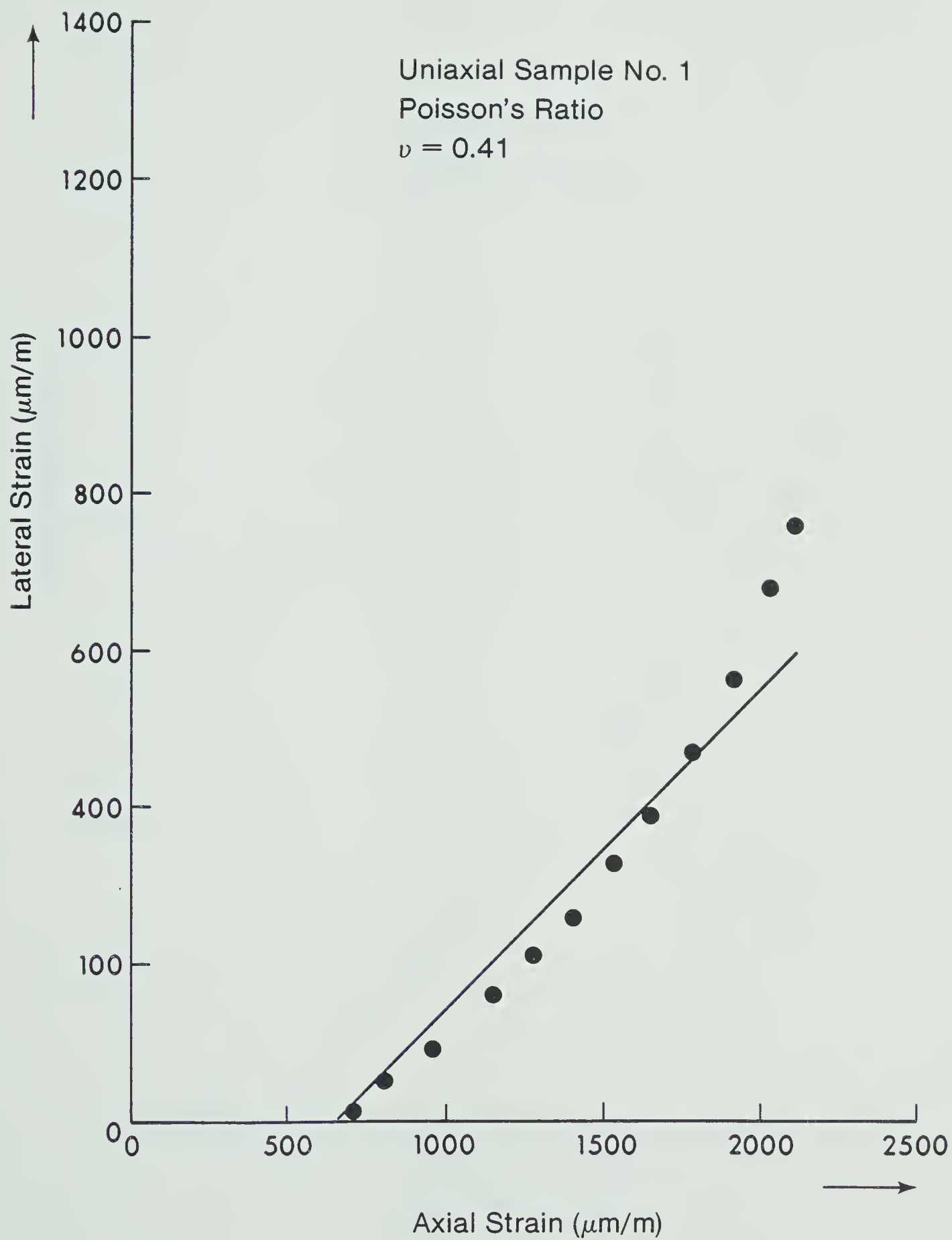
TEST RESULTS UNIAXIAL SAMPLE 5



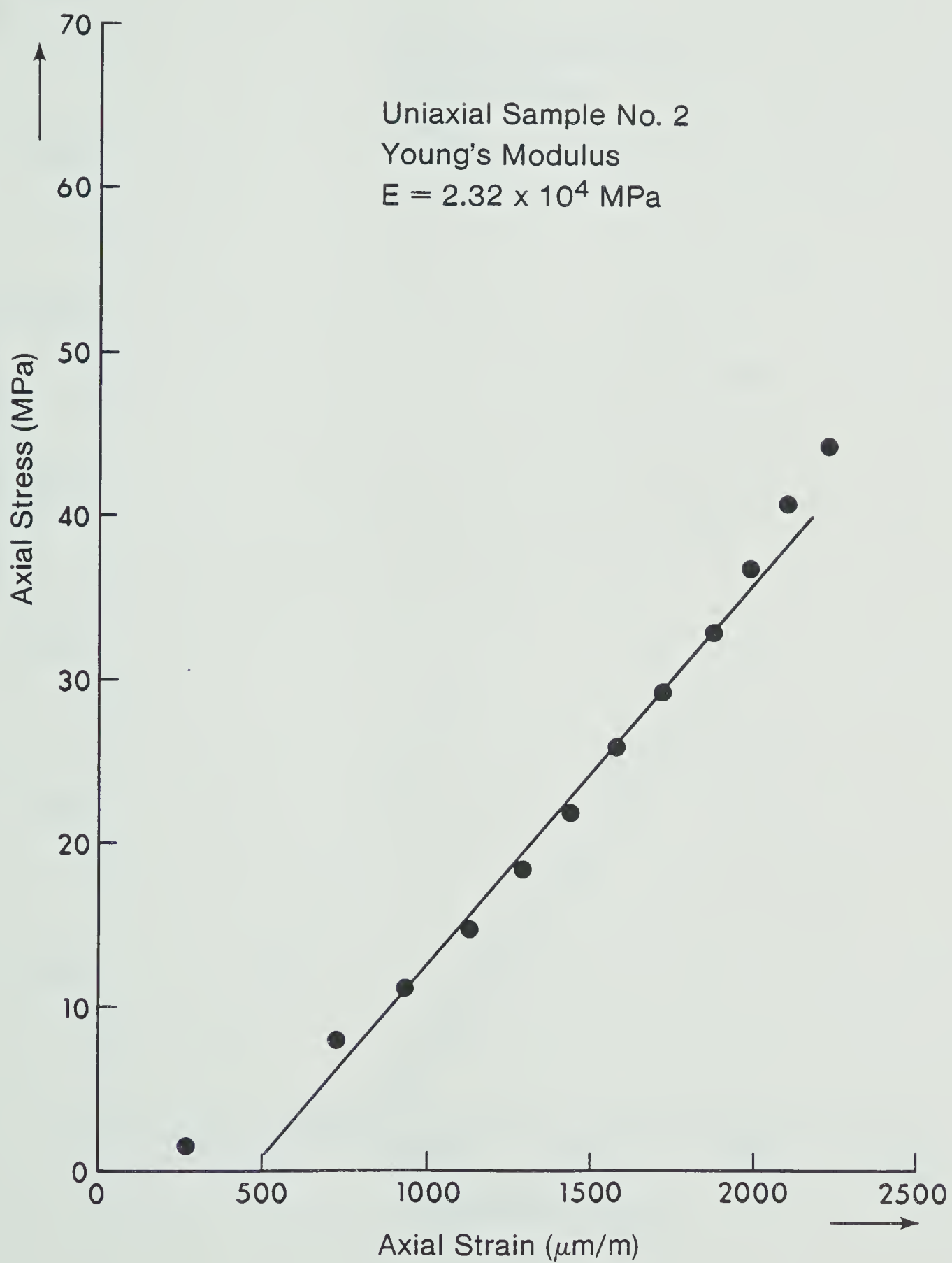




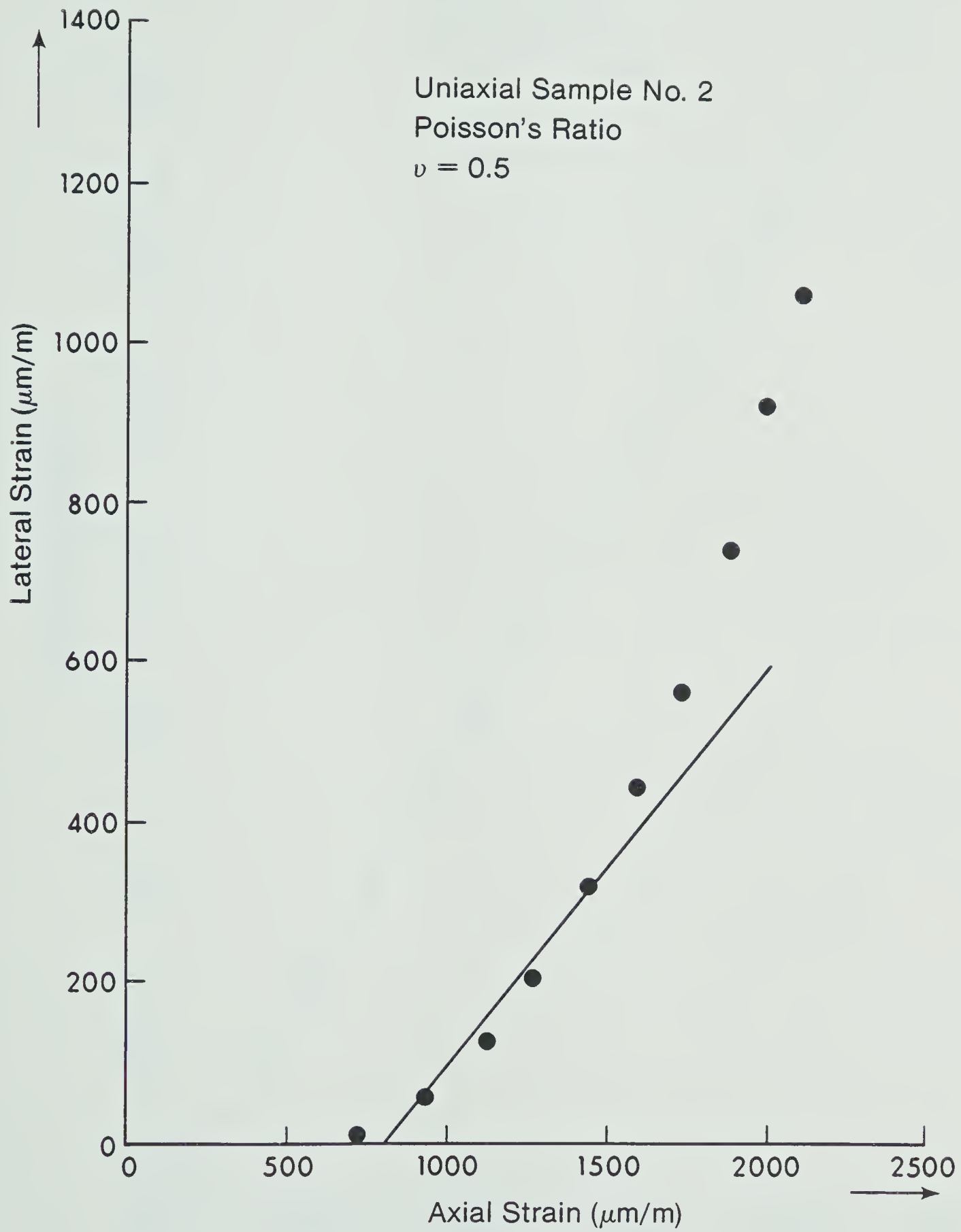




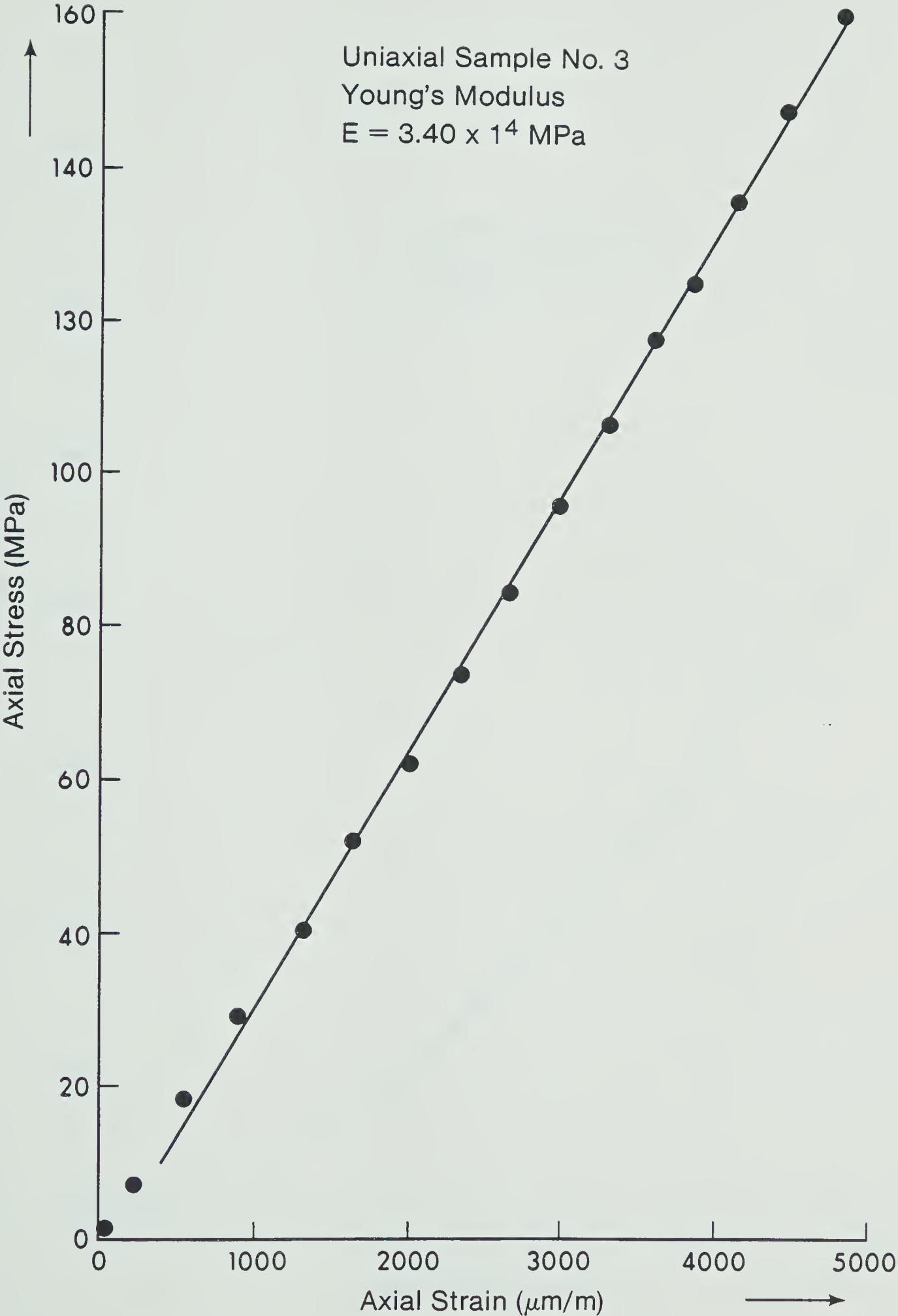






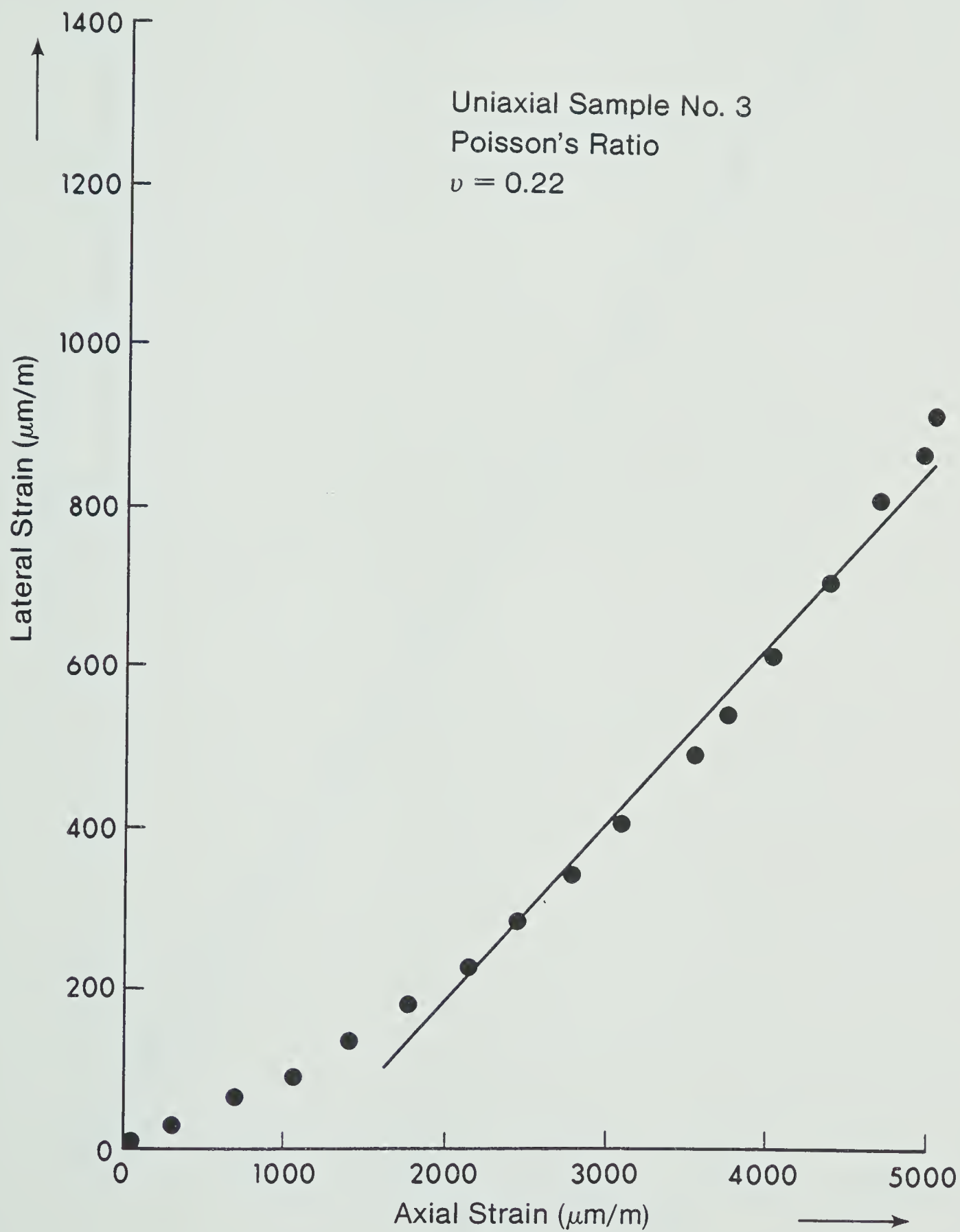




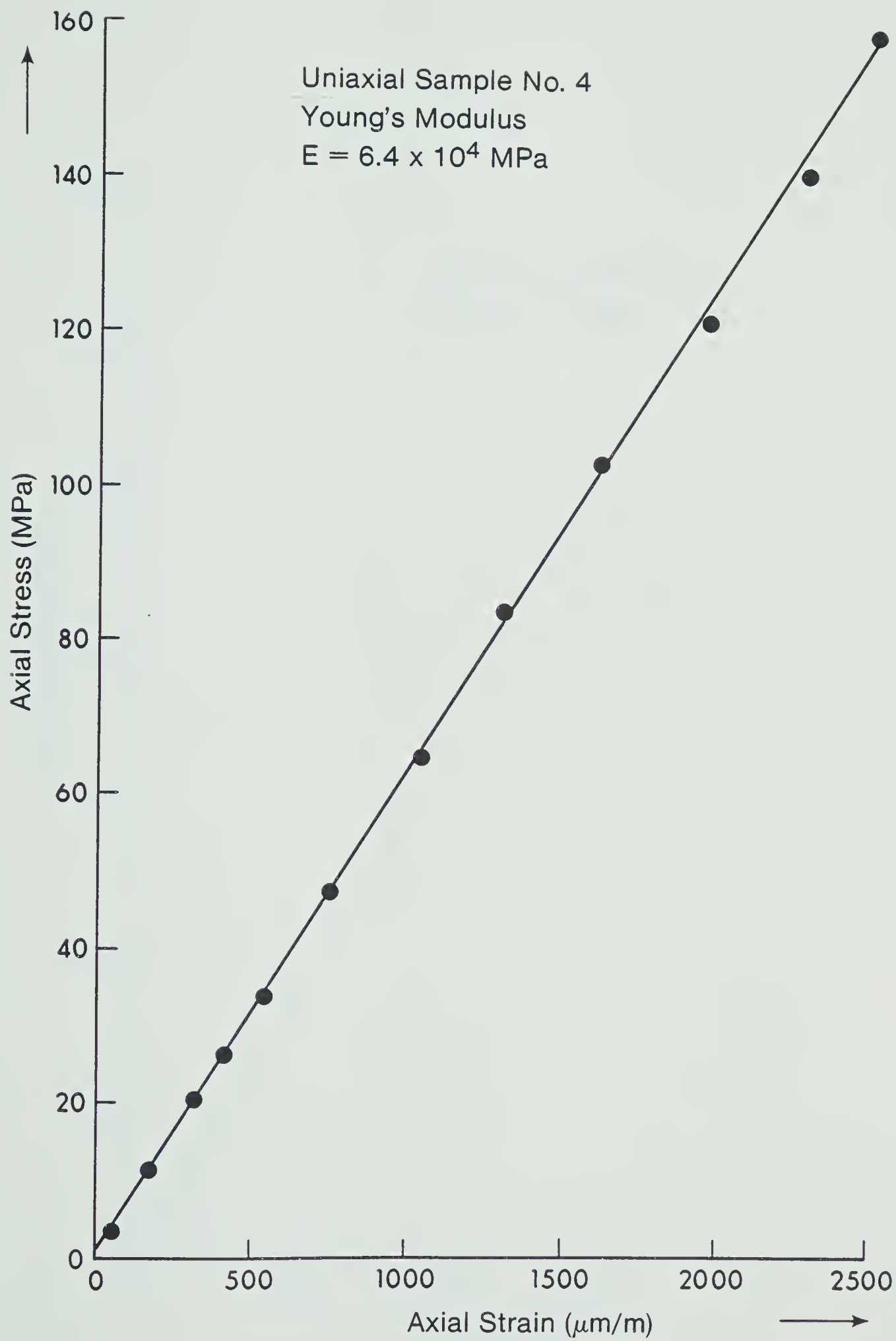




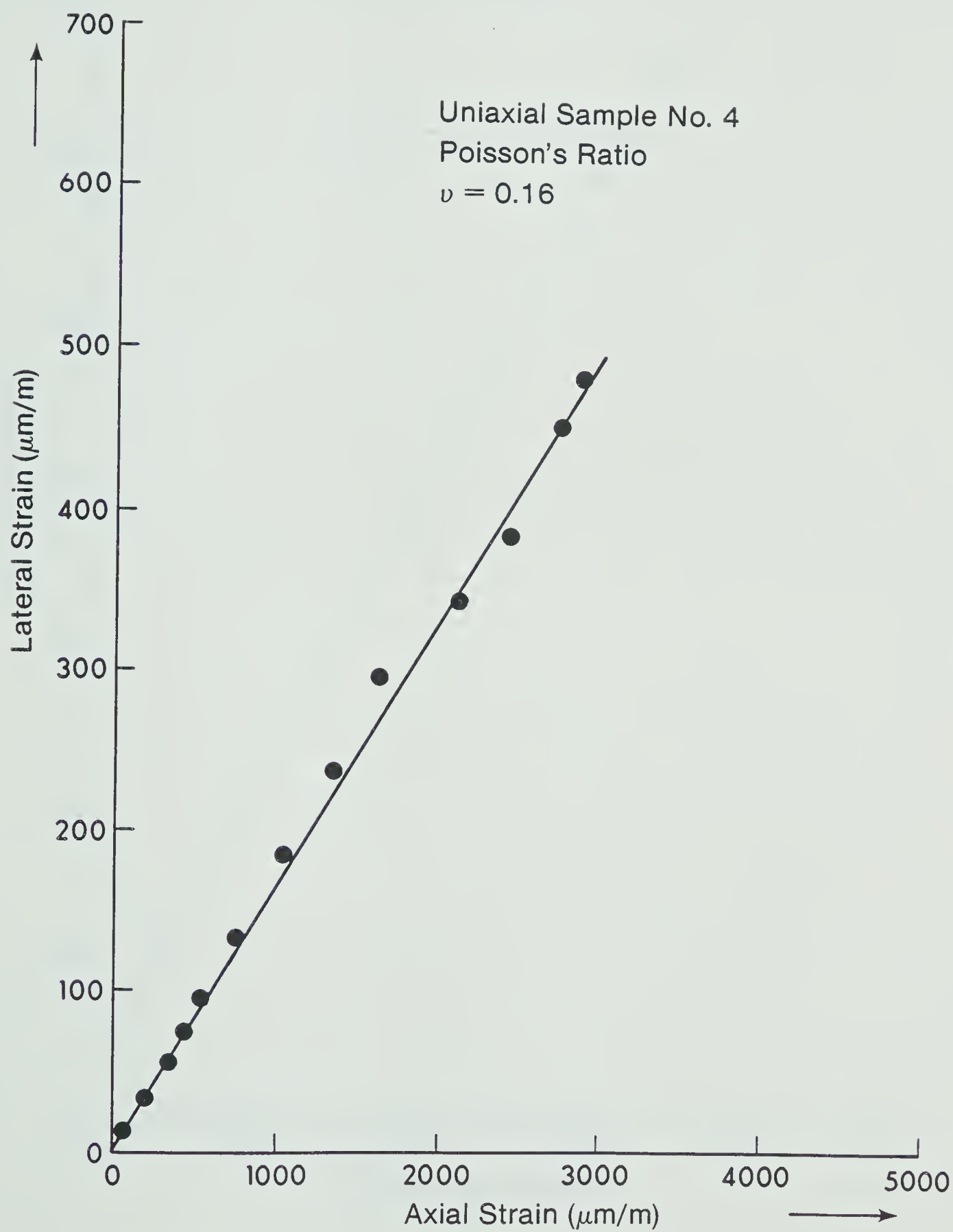




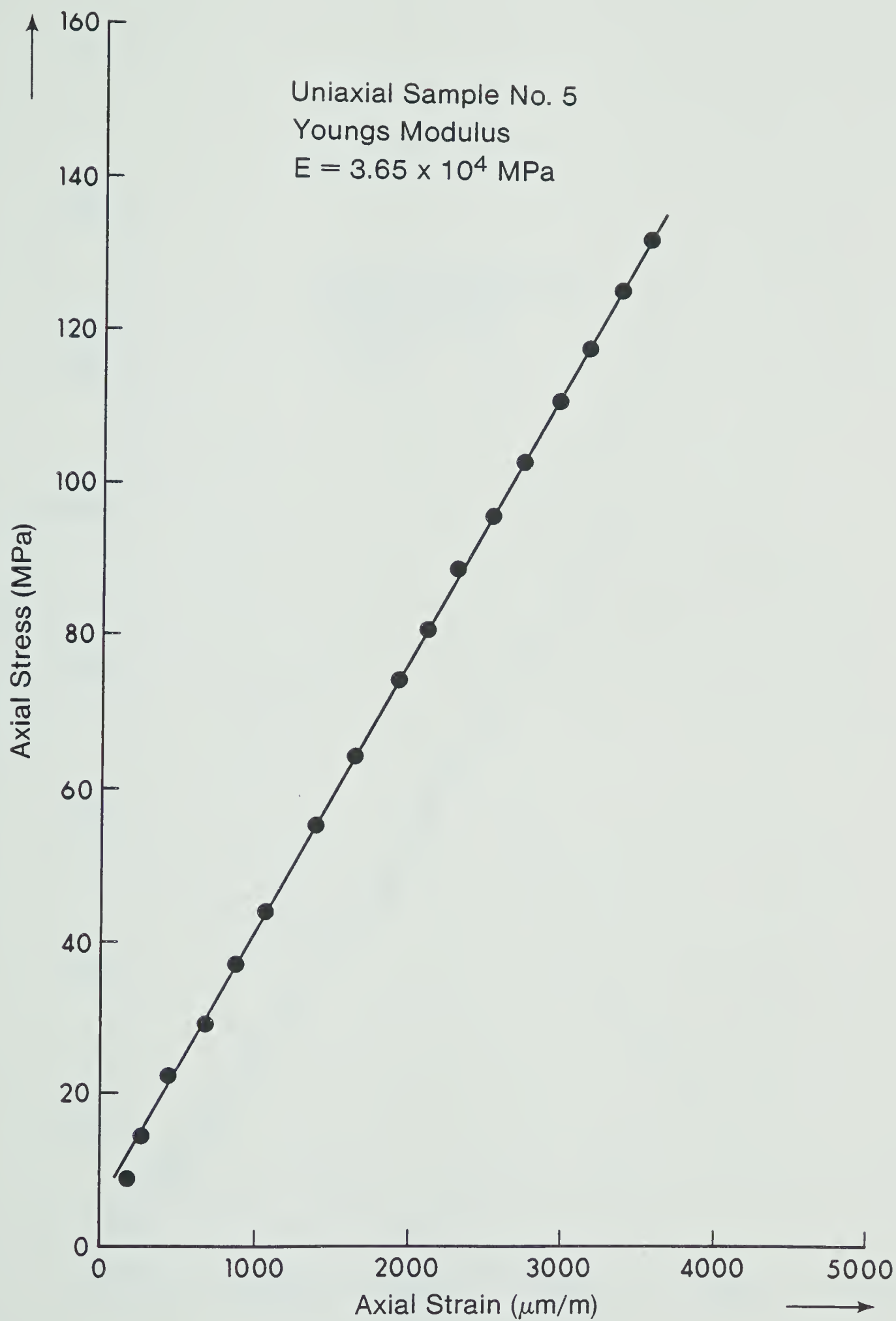






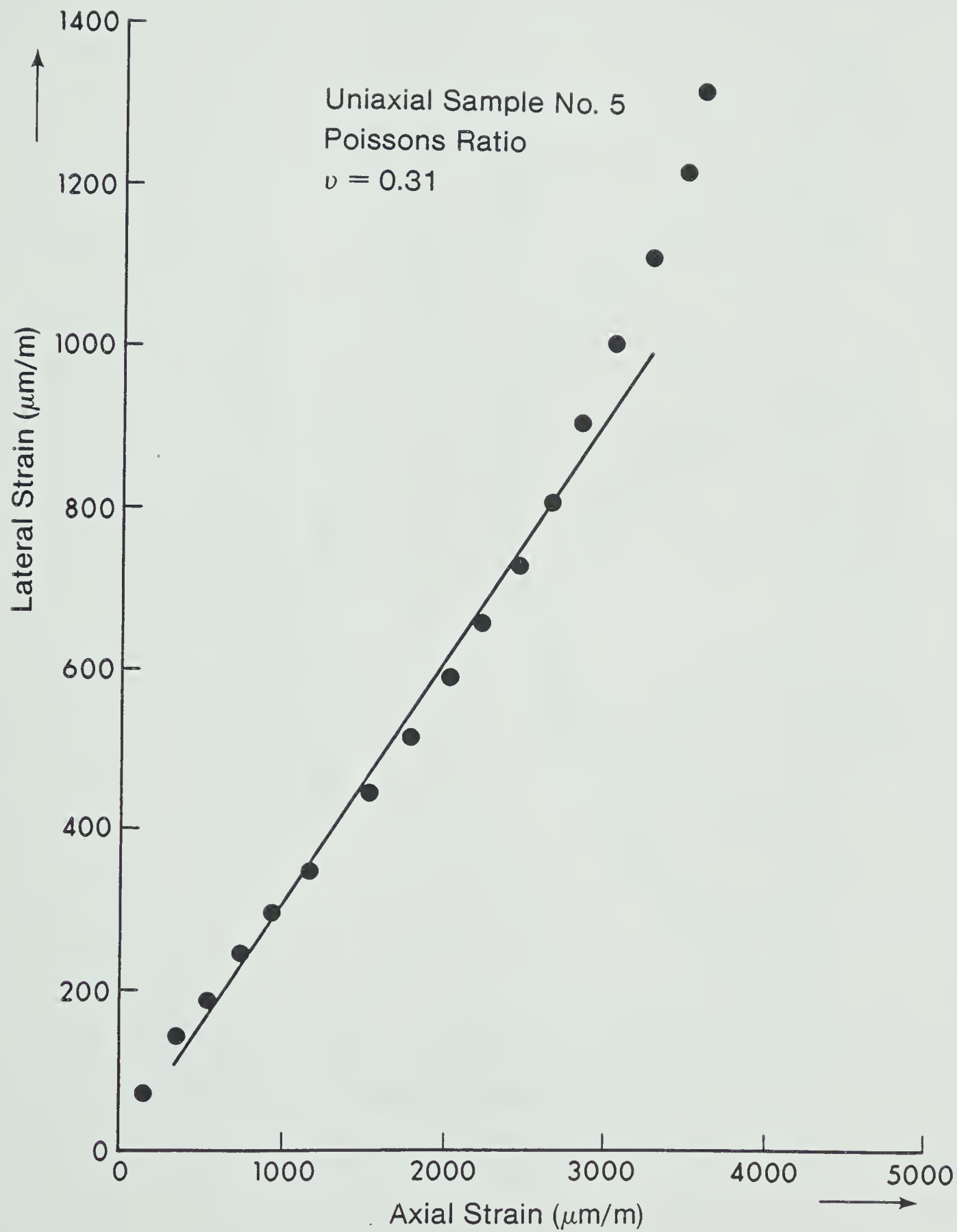




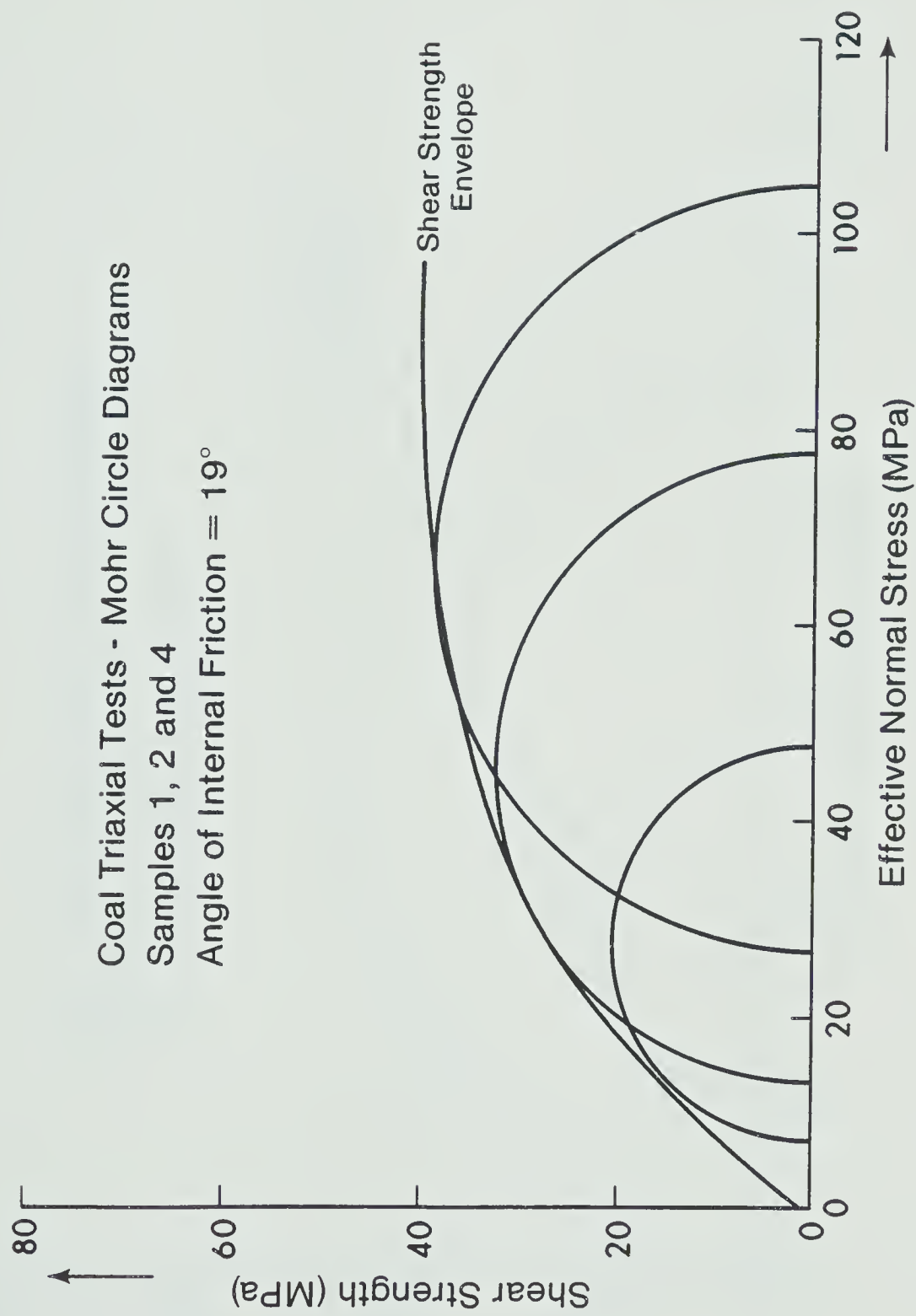




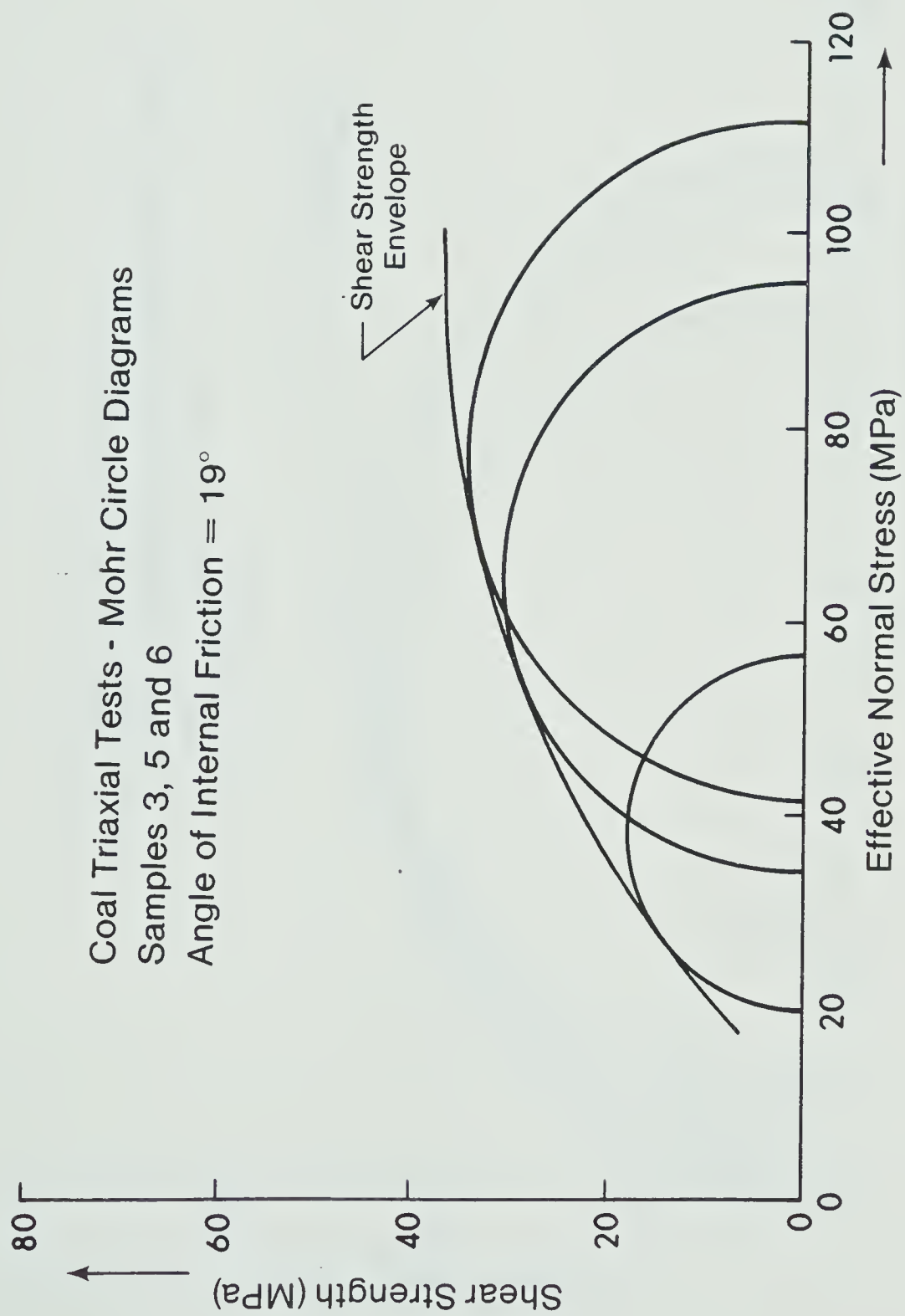




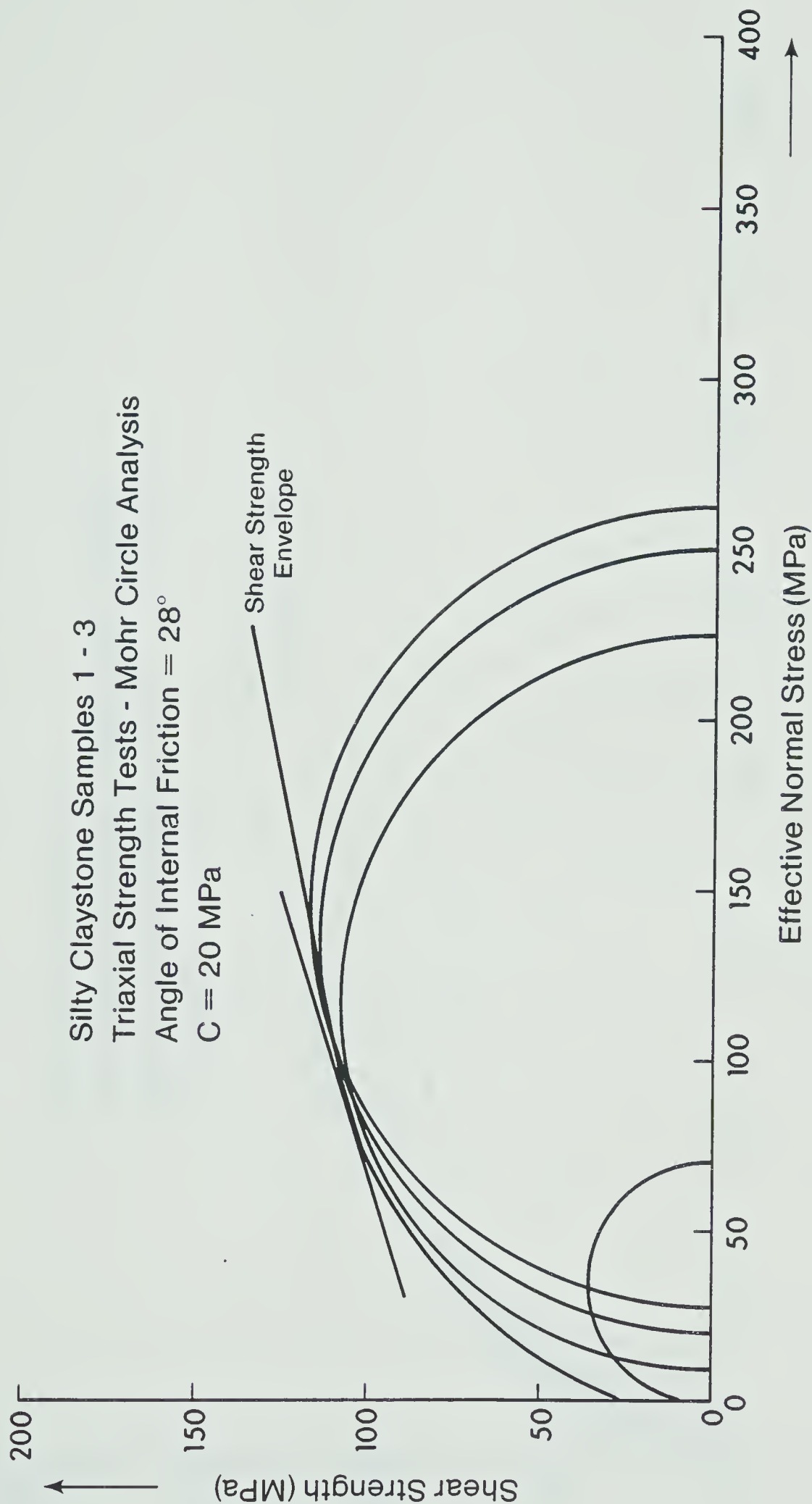






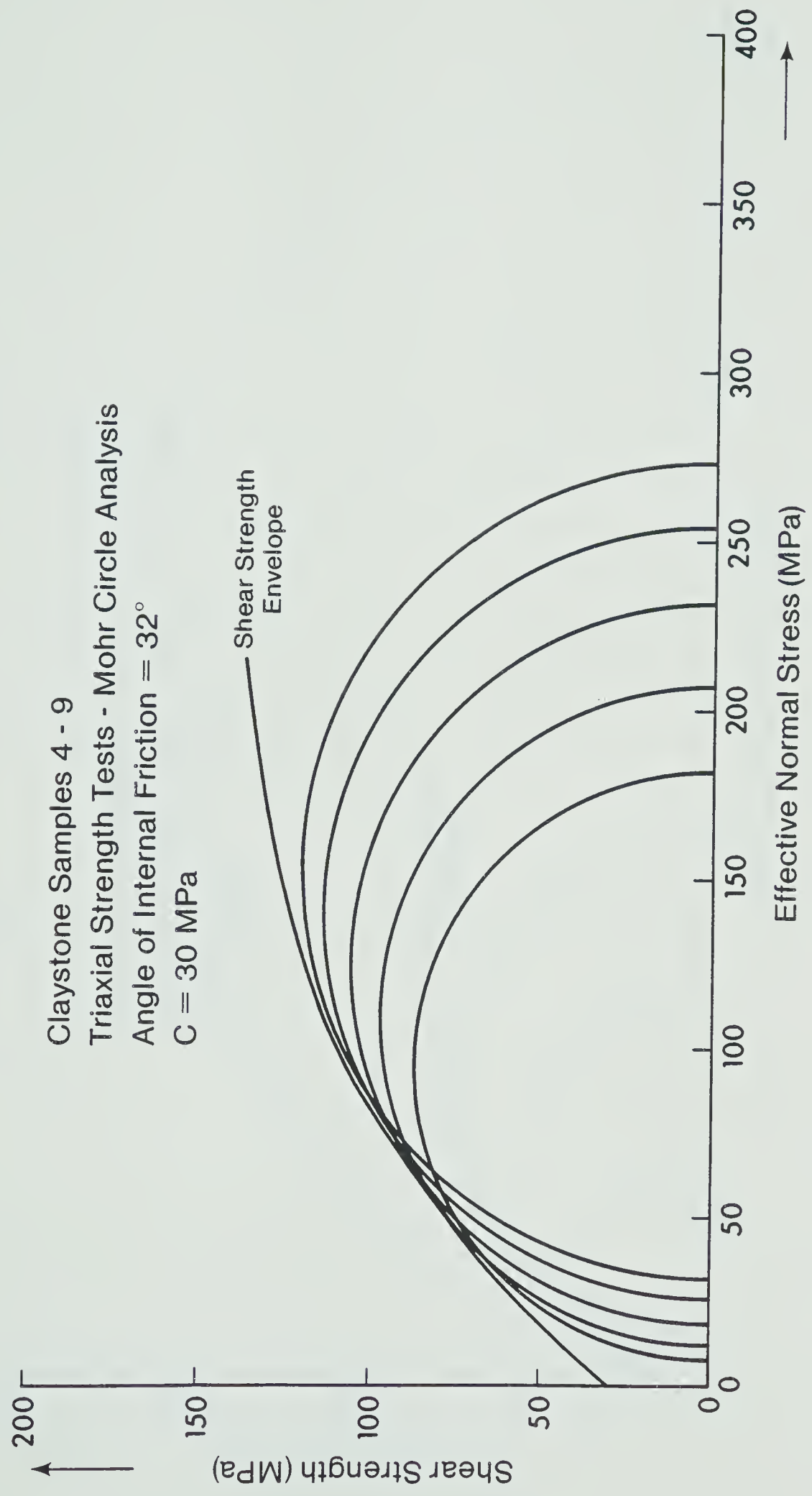




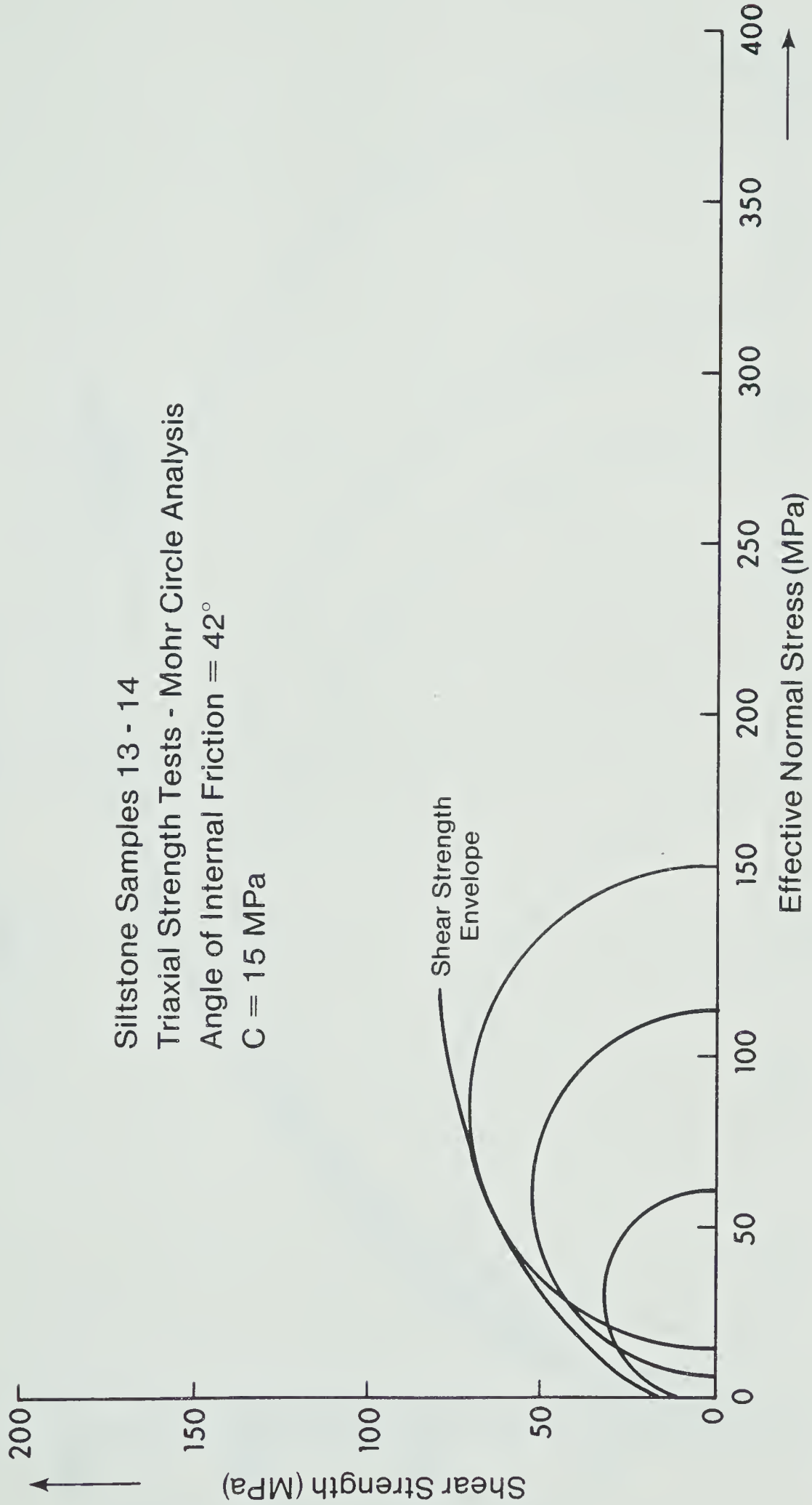






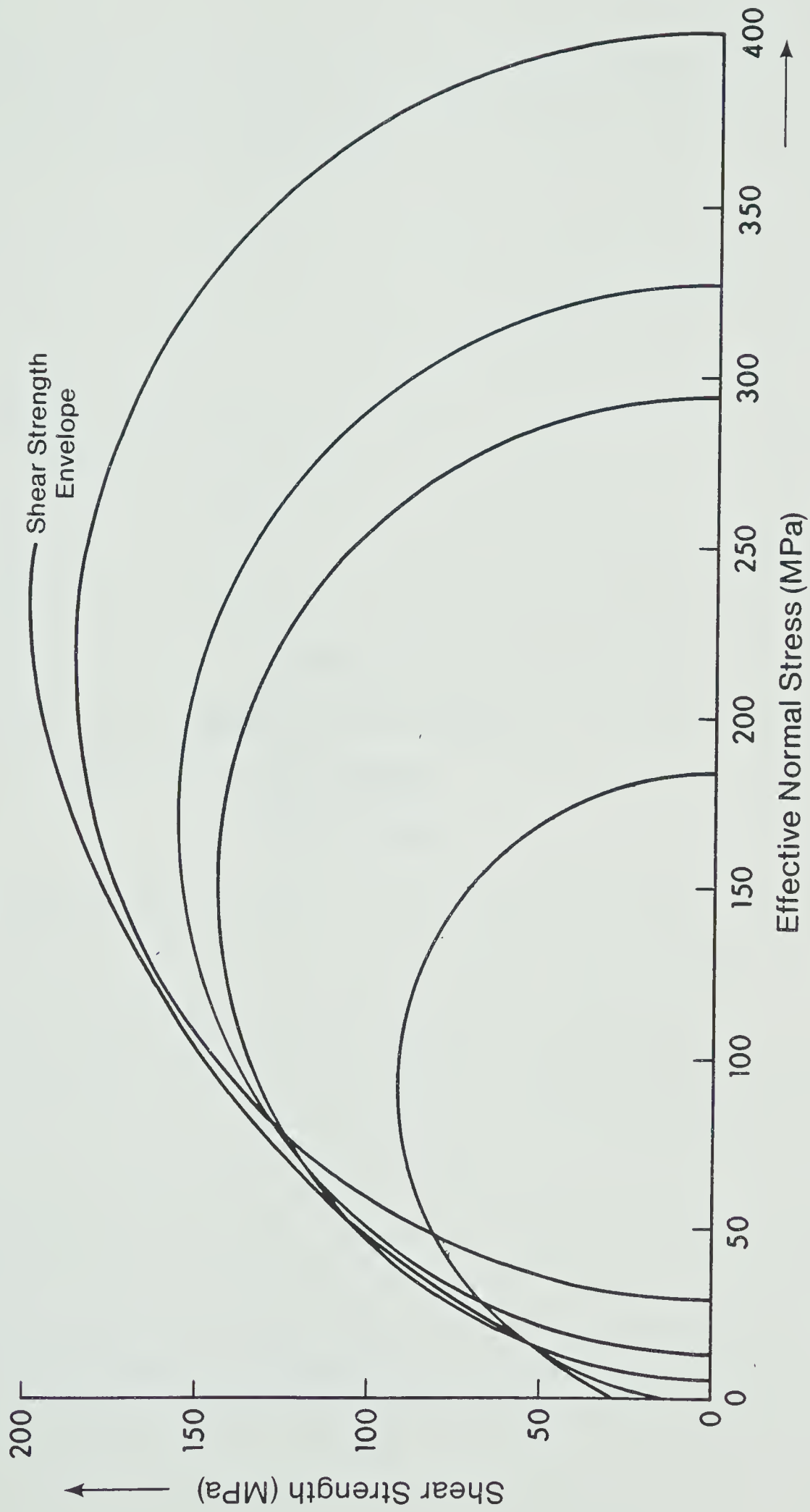








Sandstone Samples 17 - 20  
Triaxial Strength Tests - Mohr Circle Analysis  
Angle of Internal Friction =  $50^\circ$   
 $C = 30 \text{ MPa}$



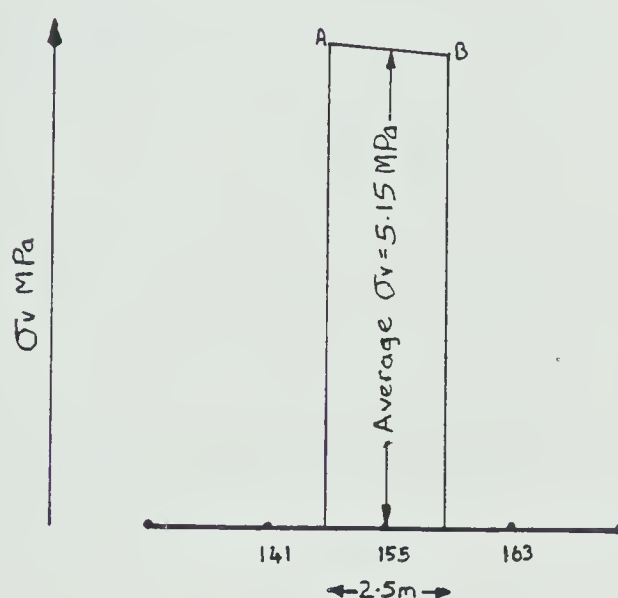


APPENDIX II  
SAMPLE CALCULATION  
OF LOADING  
CONDITIONS





The load to be applied at each nodal point on the boundary of an excavation was calculated by the following graphical method.



The magnitude of the vertical stress at each node is obtained from the initial stress distribution and is represented by the line AB. The area of loading for each node extends either side of the node to the midpoints between the adjacent nodes. The average stress along the area under consideration is multiplied by the area to give the load on that node.

e.g. node 155

$$\text{Area} = 2.5 \times 1 = 2.5 \text{ m}^2$$

$$\text{Average Stress} = 5.15 \text{ MPa}$$

$$\text{Load} = 5.15 \times 2.5 = 12.875 \text{ MN}$$

This process is repeated for all the nodes and the horizontal loads on the other faces are calculated in a similar manner.



## APPENDIX III



# CONFIGURATION 1



STRESS DATA : CONFIGURATION 1

XCOORD	YCOORD	SIGX	SIGY	SIGXY	SIG1	SIG3	TAU	THETA
0.0	0.0	2.942	8.510	0.100	8.512	2.940	2.786	88.971
0.0	60.000	2.594	6.748	0.100	6.750	2.592	2.079	88.622
0.0	120.000	1.845	5.086	0.100	5.089	1.842	1.624	88.234
0.0	180.000	0.897	3.224	0.100	3.228	0.893	1.168	87.544
0.0	240.000	-0.252	1.462	0.200	1.485	-0.275	0.880	83.432
0.0	300.000	-1.500	-0.300	0.200	-1.532	-0.268	0.632	170.782
30.000	0.0	2.842	8.610	0.100	8.612	2.840	2.886	89.007
30.000	30.000	2.768	7.679	0.100	7.681	2.766	2.458	88.834
30.000	90.000	2.220	5.917	0.100	5.920	2.217	1.851	88.452
30.000	150.000	1.371	4.255	0.100	4.258	1.368	1.445	88.017
30.000	210.000	0.323	2.393	0.100	2.398	0.318	1.040	87.241
30.000	270.000	-0.926	0.731	0.200	-0.950	0.755	0.852	173.214
30.000	300.000	-1.600	0.0	0.200	-1.625	0.025	0.825	172.982
60.000	0.0	3.042	8.810	0.200	8.817	3.035	2.891	88.016
60.000	60.000	2.594	7.048	0.200	7.057	2.585	2.236	87.434
60.000	120.000	1.845	5.186	0.200	5.198	1.833	1.682	86.586
60.000	150.000	1.371	4.255	0.200	4.269	1.357	1.456	86.052
60.000	180.000	0.797	3.424	0.200	3.439	0.782	1.329	85.671
60.000	210.000	0.323	2.593	0.200	2.610	0.306	1.152	85.003
60.000	240.000	-0.252	1.662	0.200	1.683	-0.273	0.978	84.098
60.000	270.000	-0.826	0.831	0.100	0.837	-0.832	0.835	86.559
60.000	300.000	-1.300	0.0	0.100	-1.308	0.008	0.658	175.627
90.000	0.0	3.142	9.010	0.300	9.025	3.127	2.949	87.081
90.000	30.000	2.968	8.279	0.500	8.326	2.921	2.702	84.668
90.000	60.000	2.694	7.248	0.400	7.283	2.659	2.312	85.018
90.000	90.000	2.320	6.217	0.300	6.240	2.297	1.971	85.624
90.000	120.000	1.845	5.286	0.200	5.298	1.833	1.732	86.685
90.000	150.000	0.797	3.524	0.200	3.539	0.782	1.378	85.828
90.000	180.000	-0.252	1.762	0.200	1.782	-0.272	1.027	84.383
90.000	240.000	-1.100	0.0	0.200	-1.135	0.035	0.585	170.008
110.000	0.0	2.648	8.124	-0.0	8.124	2.648	2.738	90.000
110.000	20.000	2.859	8.254	0.300	8.271	2.842	2.714	86.827
110.000	40.000	2.977	7.902	0.600	7.974	2.905	2.535	83.153
120.000	90.000	2.420	6.417	0.400	6.457	2.380	2.038	84.341
120.000	150.000	1.371	4.455	0.300	4.484	1.342	1.571	84.495
120.000	210.000	0.223	2.693	0.300	2.729	0.187	1.271	83.173
120.000	270.000	-0.526	0.931	0.200	0.958	-0.553	0.755	82.324
120.000	300.000	-1.000	0.0	0.100	-1.010	0.010	0.510	174.345
130.000	0.0	2.647	8.123	-0.100	8.125	2.645	2.740	-88.954
130.000	20.000	2.465	7.569	-0.0	7.569	2.465	2.552	90.000
130.000	40.000	2.676	7.699	0.300	7.717	2.658	2.529	86.594
130.000	60.000	2.794	7.348	0.500	7.402	2.740	2.331	83.807
150.000	0.0	2.647	8.121	-0.100	8.123	2.645	2.739	-88.954





## STRESS DATA : CONFIGURATION 1 cont.

XCOORD	YCOORD	SIGX	SIGY	SIGXY	SIG1	SIG3	TAU	THETA
150.000	30.000	2.373	7.290	-0.100	7.292	2.371	2.461	-88.835
150.000	40.000	2.281	7.113	-0.0	7.113	2.281	2.416	90.000
150.000	60.000	2.592	7.243	0.300	7.262	2.573	2.345	86.325
150.000	90.000	2.520	6.717	0.500	6.776	2.461	2.157	83.299
150.000	120.000	2.045	5.586	0.500	5.655	1.976	1.840	82.115
150.000	150.000	1.371	4.455	0.300	4.484	1.342	1.571	84.495
150.000	180.000	0.797	3.624	0.300	3.655	0.766	1.445	84.009
150.000	210.000	0.223	2.693	0.400	2.756	0.160	1.298	81.027
150.000	240.000	-0.152	1.762	0.400	1.842	-0.232	1.037	78.658
150.000	270.000	-0.326	0.831	0.300	0.904	-0.399	0.652	76.295
150.000	300.000	-0.600	0.0	0.200	-0.661	0.061	0.361	163.155
170.000	0.0	2.646	8.019	-0.100	8.021	2.644	2.688	-88.934
170.000	30.000	2.372	7.188	-0.100	7.190	2.370	2.410	-88.811
170.000	60.000	2.098	6.557	-0.100	6.559	2.096	2.232	-88.716
170.000	80.000	2.409	6.787	0.200	6.796	2.400	2.198	87.390
170.000	90.000	2.620	6.917	0.600	6.999	2.538	2.231	82.198
170.000	100.000	2.428	6.540	0.700	6.656	2.312	2.172	80.599
170.000	110.000	2.237	6.163	0.600	6.253	2.147	2.053	81.502
180.000	70.000	2.106	6.179	-0.200	6.189	2.096	2.046	-87.195
180.000	80.000	2.062	6.444	-0.100	6.446	2.060	2.193	-88.693
180.000	90.000	2.117	6.709	0.300	6.729	2.097	2.316	86.278
180.000	95.000	2.374	7.078	0.800	7.210	2.242	2.484	80.607
180.000	105.000	2.482	6.501	0.900	6.693	2.290	2.202	77.937
180.000	115.000	2.191	6.024	0.900	6.225	1.990	2.117	77.422
180.000	125.000	2.100	5.447	0.800	5.628	1.919	1.855	77.225
180.000	135.000	1.908	4.970	0.700	5.122	1.756	1.683	77.715
180.000	145.000	1.717	4.593	0.500	4.677	1.633	1.522	80.414
180.000	155.000	1.525	4.316	0.400	4.372	1.469	1.452	82.003
180.000	165.000	1.034	4.139	0.300	4.168	1.005	1.581	84.532
180.000	180.000	0.497	3.524	0.400	3.576	0.445	1.565	82.598
180.000	210.000	0.123	2.593	0.500	2.690	0.026	1.332	78.979
180.000	240.000	-0.052	1.662	0.500	1.797	-0.187	0.992	74.870
180.000	270.000	-0.126	0.831	0.300	0.917	-0.212	0.565	73.957
180.000	300.000	-0.300	0.0	0.200	-0.400	0.100	0.250	153.435
185.000	85.000	1.916	6.205	-0.200	6.214	1.907	2.154	-87.336
185.000	90.000	1.593	6.238	-0.200	6.247	1.584	2.331	-87.539
185.000	95.000	1.771	6.670	0.300	6.688	1.753	2.468	86.509
185.000	100.000	2.428	7.140	1.100	7.384	2.184	2.600	77.486
187.500	87.500	1.793	6.136	-0.300	6.157	1.772	2.192	-86.067
187.500	90.000	1.682	6.202	-0.300	6.222	1.662	2.280	-86.219
187.500	92.500	1.271	6.168	-0.300	6.186	1.253	2.467	-86.507
187.500	95.000	1.059	6.335	-0.200	6.343	1.051	2.646	-87.832
187.500	97.500	1.448	6.701	0.400	6.731	1.418	2.657	85.670



STRESS DATA : CONFIGURATION 1 cont.

XCOORD	YCOORD	SIGX	SIGY	SIGXY	SIG1	SIG3	TAU	THETA
190.000	0.0	2.546	7.817	-0.100	7.819	2.544	2.637	-88.914
190.000	30.000	2.371	6.986	-0.200	6.995	2.362	2.316	-87.523
190.000	60.000	2.097	6.055	-0.300	6.078	2.074	2.002	-85.690
190.000	70.000	2.006	5.478	-0.400	5.523	1.961	1.781	-83.512
190.000	80.000	1.914	5.701	-0.300	5.725	1.890	1.917	-85.499
190.000	85.000	1.892	5.934	-0.300	5.956	1.870	2.043	-85.778
190.000	87.500	1.781	6.000	-0.400	6.038	1.743	2.147	-84.631
190.000	90.000	1.570	5.966	-0.400	6.002	1.534	2.234	-84.843
190.000	95.000	1.048	5.999	-0.400	6.031	1.016	2.508	-85.411
190.000	97.500	0.936	6.465	-0.100	6.467	0.934	2.766	-88.964
190.000	100.000	1.625	7.031	0.400	7.060	1.596	2.732	85.791
190.000	105.000	2.482	7.201	1.300	7.535	2.148	2.694	75.573
190.000	115.000	2.191	5.924	1.400	6.391	1.724	2.333	71.564
190.000	125.000	2.300	5.047	1.200	5.497	1.850	1.824	69.428
190.000	135.000	2.308	4.770	0.900	5.064	2.014	1.525	71.914
190.000	145.000	2.017	4.593	0.600	4.726	1.884	1.421	77.511
190.000	155.000	1.625	4.416	0.500	4.503	1.538	1.482	80.144
190.000	165.000	1.034	4.039	0.300	4.069	1.004	1.532	84.354
190.000	180.000	0.497	3.524	0.500	3.604	0.417	1.594	80.859
190.000	210.000	0.123	2.393	0.600	2.542	-0.026	1.284	76.069
190.000	240.000	-0.052	1.462	0.500	1.612	-0.202	0.907	73.278
190.000	270.000	-0.026	0.731	0.300	0.835	-0.130	0.483	70.800
190.000	300.000	-0.200	0.0	0.200	-0.324	0.124	0.224	148.282
192.500	87.500	1.769	5.464	-0.500	5.530	1.703	1.914	-82.428
192.500	97.500	0.925	6.329	-0.300	6.346	0.908	2.719	-86.832
192.500	102.500	1.502	7.462	0.500	7.504	1.460	3.022	85.238
195.000	80.000	1.914	4.701	-0.500	4.788	1.827	1.480	-80.131
195.000	85.000	1.969	4.962	-0.400	5.015	1.916	1.549	-82.518
195.000	87.500	2.157	5.029	-0.300	5.060	2.126	1.467	-84.100
195.000	90.000	1.646	4.995	-0.600	5.099	1.542	1.779	-80.143
195.000	95.000	0.724	4.927	-1.100	5.197	0.454	2.372	-76.185
195.000	97.500	0.613	5.994	-1.100	6.210	0.397	2.907	-78.881
195.000	100.000	0.702	7.260	-0.600	7.314	0.648	3.333	-84.815
195.000	105.000	1.479	7.592	1.200	7.819	1.252	3.284	79.282
195.000	110.000	2.537	5.863	2.400	7.120	1.280	2.920	62.359
197.500	87.500	2.046	4.293	-0.400	4.362	1.977	1.193	-80.201
197.500	90.000	2.235	4.159	-0.400	4.239	2.155	1.042	-78.711
197.500	92.500	1.523	3.825	-0.800	4.076	1.272	1.402	-72.599
197.500	95.000	0.812	3.492	-1.200	3.951	0.353	1.799	-69.077
197.500	97.500	1.001	4.958	-1.100	5.243	0.716	2.264	-75.463
197.500	100.000	1.090	6.924	-0.400	6.951	1.063	2.944	-86.096
197.500	102.500	0.879	6.390	-0.100	6.392	0.877	2.757	-88.961
197.500	105.000	0.968	6.157	0.0	6.157	0.968	2.594	90.000



STRESS DATA : CONFIGURATION 1 cont.

XCOORD	YCOORD	SIGX	SIGY	SIGXY	SIG1	SIG3	TAU	THETA
197.500	107.500	1.857	5.123	1.300	5.577	1.403	2.087	70.739
200.000	0.0	2.545	7.716	-0.100	7.718	2.543	2.587	-88.892
200.000	30.000	2.371	6.785	-0.200	6.794	2.362	2.216	-87.411
200.000	60.000	2.197	5.754	-0.200	5.765	2.186	1.790	-86.792
200.000	70.000	2.106	5.077	-0.200	5.090	2.093	1.499	-86.166
200.000	85.000	1.768	3.662	-0.400	3.743	1.687	1.028	-78.551
200.000	90.000	1.923	3.123	-0.300	3.194	1.852	0.671	-76.717
200.000	95.000	1.100	2.056	-0.400	2.201	0.955	0.623	-70.038
200.000	97.500	1.189	3.322	-0.200	3.341	1.170	1.085	-84.689
200.000	100.000	0.0	0.0	0.0	0.0	0.0	0.0	45.000
200.000	105.000	0.0	0.0	0.0	0.0	0.0	0.0	45.000
200.000	107.500	1.445	2.887	0.300	2.947	1.385	0.781	78.704
200.000	110.000	1.834	2.053	1.100	3.049	0.838	1.105	47.842
200.000	115.000	2.591	4.024	1.300	4.792	1.823	1.484	59.431
200.000	125.000	2.600	4.647	0.900	4.986	2.261	1.363	69.337
200.000	135.000	2.508	4.770	0.700	4.969	2.309	1.330	74.123
200.000	145.000	2.117	4.593	0.500	4.690	2.020	1.335	79.004
200.000	155.000	1.625	4.316	0.400	4.374	1.567	1.404	81.722
200.000	165.000	1.034	4.039	0.400	4.091	0.982	1.555	82.546
200.000	180.000	0.497	3.324	0.600	3.446	0.375	1.536	78.500
200.000	210.000	0.123	2.293	0.700	2.499	-0.083	1.291	73.586
200.000	240.000	0.048	1.362	0.500	1.531	-0.121	0.826	71.364
200.000	270.000	-0.026	0.631	0.300	0.747	-0.142	0.445	68.798
200.000	300.000	-0.100	-0.100	0.100	-0.200	0.0	0.100	135.000
202.500	97.500	1.160	2.935	0.300	2.984	1.111	0.937	80.662
202.500	107.500	1.116	2.900	0.100	2.906	1.110	0.898	86.802
202.500	112.500	2.194	2.632	0.400	2.869	1.957	0.456	59.350
205.000	80.000	1.780	4.296	-0.0	4.296	1.780	1.258	90.000
205.000	90.000	1.588	3.419	0.500	3.547	1.460	1.043	75.679
205.000	95.000	1.343	1.681	0.400	1.946	1.078	0.434	56.452
205.000	97.500	1.632	3.647	0.500	3.764	1.515	1.125	76.803
205.000	100.000	0.0	0.0	0.0	0.0	0.0	0.0	45.000
205.000	105.000	0.0	0.0	0.0	0.0	0.0	0.0	45.000
205.000	107.500	1.087	3.112	-0.200	3.132	1.067	1.032	-84.413
205.000	110.000	1.076	1.878	-0.300	1.978	0.976	0.501	-71.599
205.000	115.000	2.554	3.611	0.300	3.690	2.475	0.608	75.209
205.000	120.000	2.811	4.382	0.600	4.585	2.608	0.988	71.313
207.500	97.500	1.503	4.559	0.500	4.639	1.423	1.608	80.940
207.500	100.000	0.991	6.026	0.0	6.026	0.991	2.517	90.000
207.500	102.500	0.880	6.092	-0.100	6.094	0.878	2.608	-88.901
207.500	105.000	1.069	6.658	-0.400	6.686	1.041	2.823	-85.927
207.500	107.500	0.958	4.824	-1.000	5.067	0.715	2.176	-76.323
207.500	110.000	1.047	3.491	-1.100	3.913	0.625	1.644	-69.004





## STRESS DATA : CONFIGURATION 1 cont.

XCOORD	YCOORD	SIGX	SIGY	SIGXY	SIG1	SIG3	TAU	THETA
207.500	112.500	1.636	3.357	-0.600	3.546	1.447	1.049	-72.557
207.500	115.000	1.925	3.523	-0.400	3.618	1.830	0.894	-76.703
207.500	117.500	2.414	4.189	-0.0	4.189	2.414	0.888	90.000
210.000	0.0	2.477	7.408	-0.100	7.410	2.475	2.468	-88.839
210.000	30.000	2.302	6.477	-0.100	6.479	2.300	2.090	-88.629
210.000	60.000	2.128	5.446	-0.100	5.449	2.125	1.662	-88.275
210.000	70.000	1.937	4.969	0.0	4.969	1.937	1.516	90.000
210.000	95.000	1.408	4.477	0.700	4.629	1.256	1.687	77.739
210.000	100.000	0.763	6.738	0.0	6.738	0.763	2.987	90.000
210.000	105.000	0.640	6.971	-0.600	7.027	0.584	3.222	-84.634
210.000	107.500	0.429	5.837	-1.100	6.052	0.214	2.919	-78.932
210.000	110.000	0.718	4.703	-1.100	4.986	0.435	2.276	-75.549
210.000	115.000	1.596	4.436	-0.700	4.599	1.433	1.583	-76.879
210.000	117.500	2.085	4.602	-0.400	4.664	2.023	1.321	-81.184
210.000	120.000	2.373	4.868	0.0	4.868	2.373	1.247	90.000
210.000	125.000	2.631	5.040	0.500	5.140	2.531	1.304	78.728
210.000	135.000	2.440	4.963	0.600	5.098	2.305	1.397	77.281
210.000	145.000	2.148	4.786	0.600	4.916	2.018	1.449	77.770
210.000	155.000	1.657	4.409	0.400	4.466	1.600	1.433	81.895
210.000	165.000	0.966	3.732	0.500	3.820	0.878	1.471	80.062
210.000	180.000	0.328	2.916	0.700	3.093	0.151	1.471	75.794
210.000	210.000	0.054	1.785	0.700	2.033	-0.194	1.113	70.517
210.000	240.000	-0.020	0.954	0.600	1.240	-0.306	0.773	64.532
212.000	270.000	-0.008	0.382	0.200	0.466	-0.092	0.279	67.137
212.500	102.500	0.923	6.517	-0.100	6.519	0.921	2.799	-88.976
212.500	107.500	0.700	5.849	-0.500	5.897	0.652	2.623	-84.505
212.500	112.500	1.078	5.082	-0.700	5.201	0.959	2.121	-80.364
212.500	115.000	1.367	4.948	-0.700	5.080	1.235	1.922	-79.323
212.500	117.500	1.756	4.914	-0.500	4.991	1.679	1.656	-81.215
212.500	120.000	2.045	4.981	-0.300	5.011	2.015	1.498	-84.225
212.500	122.500	2.233	5.247	-0.0	5.247	2.233	1.507	90.000
215.000	80.000	1.511	4.588	0.300	4.617	1.482	1.567	84.483
215.000	90.000	1.320	4.911	0.300	4.936	1.295	1.820	85.257
215.000	100.000	1.128	5.834	0.0	5.834	1.128	2.353	90.000
215.000	105.000	0.882	5.895	-0.200	5.903	0.874	2.514	-87.719
215.000	107.500	0.771	5.862	-0.300	5.880	0.753	2.563	-86.639
215.000	110.000	0.860	5.628	-0.400	5.661	0.827	2.417	-85.238
215.000	112.500	1.049	5.494	-0.600	5.574	0.969	2.302	-82.446
215.000	115.000	1.338	5.260	-0.600	5.350	1.248	2.051	-81.494
215.000	117.500	1.627	5.127	-0.500	5.197	1.557	1.820	-82.027
215.000	120.000	1.816	5.093	-0.400	5.141	1.768	1.687	-83.140
215.000	122.500	2.005	5.259	-0.300	5.286	1.978	1.654	-84.776
215.000	125.000	2.193	5.425	0.0	5.425	2.193	1.616	90.000





## STRESS DATA : CONFIGURATION 1 cont.

XCOORD	YCOORD	SIGX	SIGY	SIGXY	SIG1	SIG3	TAU	THETA
215.000	130.000	2.451	5.598	0.500	5.676	2.373	1.651	81.186
217.500	107.500	0.842	5.574	-0.200	5.582	0.834	2.374	-87.584
217.500	110.000	0.931	5.640	-0.200	5.648	0.923	2.363	-87.572
217.500	112.500	1.120	5.507	-0.400	5.543	1.084	2.230	-84.833
217.500	115.000	1.309	5.373	-0.500	5.434	1.248	2.093	-83.088
217.500	117.500	1.498	5.239	-0.500	5.305	1.432	1.936	-82.517
217.500	122.500	1.776	5.172	-0.400	5.218	1.730	1.744	-83.372
217.500	127.500	2.053	5.604	0.0	5.604	2.053	1.775	90.000
220.000	0.0	2.408	7.100	-0.100	7.102	2.406	2.348	-88.779
220.000	30.000	2.234	6.169	-0.100	6.172	2.231	1.970	-88.545
220.000	60.000	1.959	5.238	0.0	5.238	1.959	1.639	90.000
220.000	70.000	1.768	4.961	0.100	4.964	1.765	1.600	88.208
220.000	105.000	0.948	5.191	-0.400	5.228	0.911	2.159	-84.661
220.000	110.000	1.002	5.353	-0.400	5.389	0.966	2.212	-84.791
220.000	112.500	1.291	5.519	-0.300	5.540	1.270	2.135	-85.962
220.000	115.000	1.380	5.385	-0.400	5.425	1.340	2.042	-84.352
220.000	120.000	1.658	5.218	-0.400	5.262	1.614	1.824	-83.667
220.000	122.500	1.747	5.284	-0.400	5.329	1.702	1.813	-83.628
220.000	125.000	1.736	5.250	-0.300	5.275	1.711	1.782	-85.155
220.000	130.000	1.913	5.783	0.300	5.806	1.890	1.958	85.594
220.000	135.000	2.271	5.755	0.800	5.930	2.096	1.917	77.667
220.000	145.000	2.380	5.178	0.900	5.442	2.116	1.663	73.623
220.000	155.000	1.688	4.601	0.800	4.806	1.483	1.662	75.611
220.000	165.000	0.897	3.324	0.800	3.564	0.657	1.453	73.303
220.000	180.000	0.160	2.309	0.900	2.636	-0.167	1.402	70.025
220.000	210.000	-0.114	1.178	0.900	1.640	-0.576	1.108	62.835
220.000	300.000	0.0	0.0	-0.0	0.0	0.0	0.0	45.000
222.500	112.500	1.162	5.231	-0.400	5.270	1.123	2.073	-84.438
222.500	115.000	1.451	5.398	-0.300	5.421	1.428	1.996	-85.678
222.500	117.500	1.540	5.364	-0.400	5.405	1.499	1.953	-84.092
222.500	120.000	1.629	5.330	-0.400	5.373	1.586	1.893	-83.901
222.500	122.500	1.718	5.296	-0.400	5.340	1.674	1.833	-83.698
222.500	127.500	1.596	5.229	-0.400	5.273	1.552	1.860	-83.791
222.500	132.500	1.473	5.561	0.100	5.563	1.471	2.046	88.600
225.000	80.000	1.442	4.680	0.0	4.680	1.442	1.619	90.000
225.000	90.000	1.351	4.703	-0.200	4.715	1.339	1.688	-86.598
225.000	100.000	1.359	4.426	-0.400	4.477	1.308	1.585	-82.690
225.000	110.000	1.068	4.349	-0.700	4.492	0.925	1.784	-78.446
225.000	115.000	1.222	4.910	-0.600	5.005	1.127	1.939	-80.988
225.000	120.000	1.600	5.243	-0.400	5.286	1.557	1.865	-83.807
225.000	135.000	1.533	6.040	0.600	6.119	1.454	2.332	82.545
225.000	140.000	2.391	6.413	1.200	6.744	2.060	2.342	74.587
224.000	240.000	0.084	0.764	0.300	0.877	-0.029	0.453	69.288



STRESS DATA : CONFIGURATION 1 cont.

XC00RD	YC00RD	SIGX	SIGY	SIGXY	SIG1	SIG3	TAU	THETA
225.000	270.000	0.192	0.582	-0.0	0.582	0.192	0.195	90.000
227.500	122.500	1.660	5.021	-0.400	5.068	1.613	1.727	-83.306
227.500	127.500	1.438	4.854	-0.600	4.956	1.336	1.810	-80.322
227.500	132.500	0.815	4.986	-0.500	5.045	0.756	2.145	-83.259
227.500	137.500	1.093	5.819	0.200	5.827	1.085	2.371	87.581
230.000	0.0	2.339	6.791	-0.0	6.791	2.339	2.226	90.000
230.000	30.000	2.165	5.860	-0.0	5.860	2.165	1.847	90.000
230.000	60.000	1.891	5.029	0.0	5.029	1.891	1.569	90.000
230.000	70.000	1.699	4.652	0.0	4.652	1.699	1.476	90.000
230.000	115.000	0.988	3.506	-1.100	3.919	0.575	1.672	-69.428
230.000	120.000	1.242	4.067	-0.800	4.278	1.031	1.623	-75.237
230.000	140.000	2.053	7.197	0.900	7.350	1.900	2.725	80.357
230.000	145.000	2.611	6.671	2.100	7.562	1.720	2.921	67.014
230.000	155.000	1.720	4.394	1.800	5.299	0.815	2.242	63.302
230.000	165.000	0.929	2.117	1.500	3.136	-0.090	1.613	55.802
230.000	180.000	-0.009	1.401	1.300	2.175	-0.783	1.479	59.236
232.500	122.500	1.402	3.746	-0.800	3.993	1.155	1.419	-72.841
232.500	127.500	1.480	4.279	-0.600	4.402	1.357	1.523	-78.397
232.500	132.500	0.558	3.411	-1.100	3.786	0.183	1.801	-71.182
232.500	137.500	0.335	5.144	-1.300	5.473	0.006	2.733	-75.801
232.500	142.500	1.913	6.676	0.500	6.728	1.861	2.433	84.071
235.000	80.000	1.473	4.371	-0.100	4.374	1.470	1.452	-88.026
235.000	90.000	1.482	3.994	-0.300	4.029	1.447	1.291	-83.283
235.000	100.000	1.391	3.617	-0.400	3.687	1.321	1.183	-80.116
235.000	110.000	1.299	2.940	-0.700	3.198	1.041	1.079	-69.766
235.000	120.000	1.108	2.163	-1.100	2.855	0.416	1.220	-57.810
235.000	125.000	1.262	2.425	-1.100	3.088	0.599	1.244	-58.931
235.000	140.000	0.695	3.822	-0.900	4.063	0.454	1.804	-75.037
235.000	145.000	2.173	5.455	1.800	6.250	1.378	2.436	66.177
235.000	150.000	2.331	4.129	3.100	6.458	0.002	3.228	53.086
235.000	210.000	0.083	0.967	0.700	1.353	-0.303	0.828	61.135
235.000	240.000	0.384	1.164	-0.0	1.164	0.384	0.390	90.000
235.000	270.000	0.192	0.582	-0.0	0.582	0.192	0.195	90.000
235.000	300.000	0.0	0.0	-0.0	0.0	0.0	0.0	45.000
237.500	127.500	1.322	1.803	-0.900	2.494	0.631	0.932	-52.481
237.500	132.500	0.700	0.936	-0.500	1.332	0.304	0.514	-51.639
237.500	137.500	0.578	2.668	-0.700	2.881	0.365	1.258	-73.092
237.500	140.000	0.0	0.0	0.0	0.0	0.0	0.0	45.000
237.500	142.500	0.0	0.0	0.0	0.0	0.0	0.0	45.000
237.500	145.000	0.0	0.0	0.0	0.0	0.0	0.0	45.000
237.500	147.500	1.733	3.733	1.200	4.295	1.171	1.562	64.903
240.000	0.0	2.170	6.583	0.0	6.583	2.170	2.207	90.000
240.000	30.000	1.996	5.652	0.0	5.652	1.996	1.828	90.000



## STRESS DATA : CONFIGURATION 1 cont.

XCOORD	YCOORD	SIGX	SIGY	SIGXY	SIG1	SIG3	TAU	THETA
240.000	60.000	1.822	4.721	0.0	4.721	1.822	1.450	90.000
240.000	70.000	1.631	4.444	0.0	4.444	1.631	1.406	90.000
240.000	125.000	1.128	0.121	-1.100	1.834	-0.585	1.210	-32.703
240.000	130.000	1.182	-0.818	-0.500	1.300	-0.936	1.118	-13.283
240.000	135.000	0.760	2.215	-0.100	2.222	0.753	0.734	-86.087
240.000	137.500	0.0	0.0	0.0	0.0	0.0	0.0	45.000
240.000	140.000	0.0	0.0	0.0	0.0	0.0	0.0	45.000
240.000	145.000	0.0	0.0	-0.0	0.0	0.0	0.0	45.000
240.000	147.500	0.0	0.0	-0.0	0.0	0.0	0.0	45.000
240.000	150.000	1.793	2.912	1.400	3.860	0.845	1.508	55.892
240.000	155.000	2.252	2.486	2.800	5.171	-0.433	2.802	46.196
240.000	165.000	1.660	0.609	2.500	3.689	-1.420	2.555	39.065
242.500	132.500	0.642	-0.439	0.100	0.651	-0.448	0.550	5.241
242.500	137.500	0.0	0.0	0.0	0.0	0.0	0.0	45.000
242.500	147.500	0.0	0.0	-0.0	0.0	0.0	0.0	45.000
242.500	152.500	1.953	2.591	1.500	3.806	0.738	1.534	51.003
245.000	80.000	1.605	3.963	-0.0	3.963	1.605	1.179	90.000
245.000	90.000	1.513	3.486	-0.100	3.491	1.508	0.992	-87.106
245.000	100.000	1.522	3.009	-0.200	3.035	1.496	0.770	-82.472
245.000	110.000	1.431	2.132	-0.200	2.185	1.378	0.404	-75.145
245.000	120.000	1.139	0.955	-0.200	1.267	0.827	0.220	-32.649
245.000	130.000	0.648	-0.722	0.200	-0.751	0.677	0.714	98.138
245.000	135.000	0.902	1.839	0.300	1.927	0.814	0.556	73.683
245.000	137.500	0.0	0.0	-0.0	0.0	0.0	0.0	45.000
245.000	140.000	0.0	0.0	0.0	0.0	0.0	0.0	45.000
245.000	145.000	0.0	0.0	0.0	0.0	0.0	0.0	45.000
245.000	147.500	0.0	0.0	0.0	0.0	0.0	0.0	45.000
245.000	150.000	0.0	0.0	-0.0	0.0	0.0	0.0	45.000
245.000	155.000	1.613	2.669	1.300	3.544	0.738	1.403	56.052
245.000	160.000	2.172	1.744	3.400	5.365	-1.449	3.407	43.199
247.500	137.500	0.862	2.018	0.200	2.052	0.828	0.612	80.457
247.500	140.000	1.051	3.184	-0.0	3.184	1.051	1.066	90.000
247.500	142.500	1.040	3.150	0.0	3.150	1.040	1.055	90.000
247.500	145.000	1.029	3.117	0.0	3.117	1.029	1.044	90.000
247.500	147.500	0.0	0.0	0.0	0.0	0.0	0.0	45.000
248.000	180.000	0.468	0.428	1.800	2.248	-1.352	1.800	44.682
245.000	240.000	0.384	1.164	-0.0	1.164	0.384	0.390	90.000
250.000	0.0	2.102	6.275	0.0	6.275	2.102	2.086	90.000
250.000	50.000	1.745	4.890	0.100	4.893	1.742	1.576	88.181
250.000	60.000	1.753	4.513	0.100	4.517	1.749	1.384	87.928
250.000	70.000	1.662	4.136	0.100	4.140	1.658	1.241	87.689
250.000	135.000	0.368	-0.065	0.600	0.789	-0.486	0.638	35.079
250.000	140.000	0.722	1.697	0.300	1.782	0.637	0.572	74.196
250.000	145.000	0.0	0.0	-0.0	0.0	0.0	0.0	45.000





## STRESS DATA : CONFIGURATION 1 cont.

XCOORD	YCOORD	SIGX	SIGY	SIGXY	SIG1	SIG3	TAU	THEIA
250.000	150.000	0.0	0.0	0.0	0.0	0.0	0.0	45.000
250.000	155.000	0.0	0.0	0.0	0.0	0.0	0.0	45.000
250.000	160.000	1.133	2.427	1.000	2.971	0.589	1.191	61.451
250.000	165.000	1.392	0.402	3.400	4.333	-2.539	3.436	40.858
250.000	270.000	0.192	0.582	-0.0	0.582	0.192	0.195	90.000
250.000	300.000	0.0	0.0	-0.0	0.0	0.0	0.0	45.000
255.000	80.000	1.552	3.704	0.100	3.709	1.547	1.081	87.345
255.000	90.000	1.461	3.327	0.100	3.332	1.456	0.938	86.941
255.000	100.000	1.470	2.850	0.200	2.878	1.442	0.718	81.918
255.000	110.000	1.278	2.173	0.300	2.264	1.187	0.539	73.081
255.000	120.000	0.887	1.396	0.700	1.886	0.397	0.745	54.990
255.000	130.000	0.395	1.019	0.900	1.660	-0.246	0.953	54.560
255.000	140.000	0.204	0.242	1.100	1.323	-0.877	1.100	45.495
255.000	145.000	0.658	1.204	0.600	1.590	0.272	0.659	57.233
255.000	150.000	0.0	0.0	0.0	0.0	0.0	0.0	45.000
255.000	155.000	0.0	0.0	0.0	0.0	0.0	0.0	45.000
256.000	160.000	0.896	2.616	-0.100	2.622	0.890	0.866	-86.684
254.000	165.000	0.864	1.719	1.200	2.565	0.018	1.274	54.804
260.000	0.0	2.131	6.365	0.100	6.367	2.129	2.119	88.648
260.000	30.000	1.957	5.534	0.100	5.537	1.954	1.791	88.400
260.000	60.000	1.783	4.603	0.100	4.607	1.779	1.414	87.972
260.000	70.000	1.692	4.226	0.100	4.230	1.688	1.271	87.744
260.000	145.000	0.206	-0.552	1.300	-1.527	1.181	1.354	126.873
260.000	150.000	0.760	2.110	0.300	2.174	0.696	0.739	78.019
260.000	180.000	0.768	2.328	-0.0	2.328	0.768	0.780	90.000
260.000	210.000	0.576	1.746	-0.0	1.746	0.576	0.585	90.000
260.000	240.000	0.384	1.164	-0.0	1.164	0.384	0.390	90.000
260.000	270.000	0.192	0.582	-0.0	0.582	0.192	0.195	90.000
260.000	300.000	0.0	0.0	-0.0	0.0	0.0	0.0	45.000
265.000	80.000	1.514	3.990	0.200	4.006	1.498	1.254	85.411
265.000	90.000	1.422	3.513	0.300	3.555	1.380	1.088	81.995
265.000	100.000	1.331	3.336	0.400	3.413	1.254	1.079	79.124
265.000	110.000	1.040	2.859	0.600	3.039	0.860	1.090	73.293
265.000	120.000	0.748	2.482	0.900	2.865	0.365	1.250	66.965
265.000	130.000	0.657	2.505	0.900	2.871	0.291	1.290	67.877
265.000	140.000	0.565	2.228	0.700	2.483	0.310	1.087	69.954
270.000	0.0	2.259	6.548	0.100	6.550	2.257	2.147	88.665
270.000	30.000	1.985	5.617	0.100	5.620	1.982	1.819	88.424
270.000	60.000	1.710	4.786	0.200	4.799	1.697	1.551	86.295
270.000	160.000	0.796	3.016	0.0	3.016	0.796	1.110	90.000
270.000	180.000	0.768	2.128	-0.100	2.135	0.761	0.687	-85.817
275.000	195.000	0.672	2.037	-0.0	2.037	0.672	0.682	90.000
290.000	0.0	2.214	6.814	0.100	6.816	2.212	2.302	88.755
290.000	30.000	2.039	5.883	0.200	5.893	2.029	1.932	87.030





STRESS DATA : CONFIGURATION 1 cont.

XCOORD	YCOORD	SIGX	SIGY	SIGXY	SIG1	SIG3	TAU	THETA
290.000	60.000	1.765	5.152	0.200	5.164	1.753	1.705	86.632
290.000	90.000	1.391	4.121	0.300	4.154	1.358	1.398	83.802
290.000	120.000	0.917	3.390	0.400	3.453	0.854	1.300	81.037
290.000	150.000	0.942	3.259	0.300	3.297	0.904	1.197	82.741
290.000	180.000	0.768	2.428	0.100	2.434	0.762	0.836	86.565
290.000	210.000	0.576	1.746	-0.0	1.746	0.576	0.585	90.000
290.000	240.000	0.384	1.164	-0.0	1.164	0.384	0.390	90.000
290.000	270.000	0.192	0.582	-0.0	0.582	0.192	0.195	90.000
290.000	300.000	0.0	0.0	-0.0	0.0	0.0	0.0	45.000
320.000	30.000	2.122	6.332	0.200	6.341	2.113	2.114	87.286
320.000	90.000	1.473	4.770	0.200	4.782	1.461	1.661	86.541
320.000	150.000	1.025	3.408	0.100	3.412	1.021	1.196	87.601
320.000	210.000	0.576	1.746	0.0	1.746	0.576	0.585	90.000
320.000	240.000	0.384	1.164	-0.0	1.164	0.384	0.390	90.000
320.000	270.000	0.192	0.582	-0.0	0.582	0.192	0.195	90.000
320.000	300.000	0.0	0.0	-0.0	0.0	0.0	0.0	45.000
350.000	0.0	2.478	7.512	0.100	7.514	2.476	2.519	88.862
350.000	60.000	1.829	5.950	0.100	5.952	1.827	2.063	88.611
350.000	120.000	1.281	4.388	0.100	4.391	1.278	1.557	88.158
350.000	180.000	0.933	2.826	0.100	2.831	0.928	0.952	86.984
350.000	240.000	0.384	1.164	0.0	1.164	0.384	0.390	90.000
350.000	270.000	0.192	0.582	-0.0	0.582	0.192	0.195	90.000
350.000	300.000	0.0	0.0	-0.0	0.0	0.0	0.0	45.000
380.000	270.000	0.192	0.582	0.0	0.582	0.192	0.195	90.000
380.000	300.000	0.0	0.0	0.0	0.0	0.0	0.0	45.000
410.000	0.0	2.642	8.210	0.100	8.212	2.640	2.786	88.971
410.000	60.000	2.094	6.548	0.100	6.550	2.092	2.229	88.714
410.000	120.000	1.545	4.986	0.0	4.986	1.545	1.720	90.000
410.000	180.000	1.097	3.324	0.0	3.324	1.097	1.113	90.000
410.000	240.000	0.648	1.662	0.0	1.662	0.648	0.507	90.000
410.000	300.000	0.0	0.0	0.0	0.0	0.0	0.0	45.000
470.000	0.0	2.742	8.310	0.0	8.310	2.742	2.784	90.000
470.000	60.000	2.094	6.648	0.0	6.648	2.094	2.277	90.000
470.000	120.000	1.545	4.986	-0.0	4.986	1.545	1.720	90.000
470.000	180.000	1.097	3.324	-0.0	3.324	1.097	1.113	90.000
470.000	240.000	0.548	1.662	0.0	1.662	0.548	0.557	90.000
470.000	300.000	0.100	0.0	0.0	0.100	0.0	0.050	0.0
530.000	0.0	2.742	8.310	0.0	8.310	2.742	2.784	90.000
530.000	60.000	2.094	6.648	0.0	6.648	2.094	2.277	90.000
530.000	120.000	1.645	4.986	-0.0	4.986	1.645	1.670	90.000
530.000	180.000	1.097	3.324	0.0	3.324	1.097	1.113	90.000
530.000	240.000	0.648	1.662	0.0	1.662	0.648	0.507	90.000
530.000	300.000	0.100	0.0	0.0	0.100	0.0	0.050	0.0



## CONFIGURATION 2



STRESS DATA : CONFIGURATION 2

XCOORD	YCOORD	SIGX	SIGY	SIGXY	SIG1	SIG3	TAU	THETA
0.0	0.0	2.842	8.410	0.0	8.410	2.842	2.784	90.000
0.0	60.000	2.294	6.648	0.0	6.648	2.294	2.177	90.000
0.0	120.000	1.645	4.986	0.0	4.986	1.645	1.670	90.000
0.0	180.000	0.997	3.324	0.100	3.328	0.993	1.168	87.544
0.0	240.000	0.248	1.562	0.100	1.570	0.240	0.665	85.673
0.0	300.000	-0.500	-0.100	0.100	-0.524	-0.076	0.224	166.717
30.000	0.0	2.742	8.410	0.0	8.410	2.742	2.834	90.000
30.000	30.000	2.568	7.579	0.0	7.579	2.568	2.505	90.000
30.000	90.000	2.020	5.817	0.0	5.817	2.020	1.898	90.000
30.000	150.000	1.371	4.155	0.100	4.159	1.367	1.396	87.946
30.000	210.000	0.623	2.493	0.100	2.498	0.618	0.940	86.948
30.000	270.000	-0.126	0.831	0.100	0.841	-0.136	0.489	84.098
30.000	300.000	-0.500	0.0	0.100	-0.519	0.019	0.269	169.099
60.000	0.0	2.842	8.510	0.100	8.512	2.840	2.836	88.990
60.000	60.000	2.294	6.748	0.100	6.750	2.292	2.229	88.714
60.000	120.000	1.645	5.086	0.100	5.089	1.642	1.723	88.337
60.000	150.000	1.371	4.255	0.100	4.258	1.368	1.445	88.017
60.000	180.000	0.997	3.324	0.100	3.328	0.993	1.168	87.544
60.000	210.000	0.623	2.493	0.100	2.498	0.618	0.940	86.948
60.000	240.000	0.348	1.662	0.100	1.670	0.340	0.665	85.673
60.000	270.000	-0.026	0.831	0.100	0.843	-0.038	0.440	83.432
60.000	300.000	-0.400	0.0	0.100	-0.424	0.024	0.224	166.717
90.000	0.0	2.842	8.510	0.100	8.512	2.840	2.836	88.990
90.000	30.000	2.668	7.679	0.100	7.681	2.666	2.507	88.857
90.000	60.000	2.294	6.848	0.100	6.850	2.292	2.279	88.743
90.000	90.000	2.020	5.917	0.100	5.920	2.017	1.951	88.531
90.000	120.000	1.645	5.086	0.100	5.089	1.642	1.723	88.337
90.000	180.000	0.997	3.424	0.100	3.428	0.993	1.218	87.645
90.000	240.000	0.348	1.662	0.100	1.670	0.340	0.665	85.673
90.000	300.000	-0.300	0.0	0.100	-0.330	0.030	0.180	163.155
110.000	0.0	2.648	8.024	-0.0	8.024	2.648	2.688	90.000
110.000	20.000	2.659	7.954	0.100	7.956	2.657	2.649	88.919
110.000	40.000	2.577	7.402	0.200	7.410	2.569	2.421	87.630
120.000	90.000	2.020	6.017	0.100	6.019	2.018	2.001	88.568
120.000	150.000	1.271	4.255	0.100	4.258	1.268	1.495	88.083
120.000	210.000	0.623	2.493	0.100	2.498	0.618	0.940	86.948
120.000	270.000	0.074	0.831	0.100	0.844	0.061	0.391	82.600
120.000	300.000	-0.200	0.0	0.100	-0.241	0.041	0.141	157.500
130.000	0.0	2.647	8.023	-0.0	8.023	2.647	2.688	90.000
130.000	20.000	2.465	7.469	-0.0	7.469	2.465	2.502	90.000
130.000	40.000	2.476	7.399	0.100	7.401	2.474	2.464	88.837
130.000	60.000	2.394	6.848	0.200	6.857	2.385	2.236	87.434
150.000	0.0	2.647	8.021	-0.0	8.021	2.647	2.687	90.000



STRESS DATA : CONFIGURATION 2 cont.

XCOORD	YCOORD	SIGX	SIGY	SIGXY	SIG1	SIG3	TAU	THETA
150.000	30.000	2.373	7.190	-0.0	7.190	2.373	2.408	90.000
150.000	40.000	2.281	7.013	-0.0	7.013	2.281	2.366	90.000
150.000	60.000	2.292	6.843	0.100	6.845	2.290	2.278	88.742
150.000	90.000	2.120	6.117	0.100	6.119	2.118	2.001	88.568
150.000	120.000	1.645	5.186	0.100	5.189	1.642	1.773	88.384
150.000	150.000	1.271	4.255	0.200	4.268	1.258	1.505	86.183
150.000	180.000	0.997	3.324	0.200	3.341	0.980	1.181	85.123
150.000	210.000	0.723	2.493	0.200	2.515	0.701	0.907	83.633
150.000	240.000	0.448	1.662	0.100	1.670	0.440	0.615	85.322
150.000	270.000	0.174	0.831	0.100	0.846	0.159	0.343	81.534
150.000	300.000	-0.100	0.0	0.100	-0.162	0.062	0.112	148.282
170.000	0.0	2.646	8.019	-0.0	8.019	2.646	2.686	90.000
170.000	30.000	2.372	7.188	-0.0	7.188	2.372	2.408	90.000
170.000	60.000	2.098	6.457	-0.100	6.459	2.096	2.182	-88.686
170.000	80.000	2.109	6.387	0.100	6.389	2.107	2.141	88.662
170.000	90.000	2.120	6.217	0.100	6.219	2.118	2.051	88.603
170.000	100.000	1.928	5.940	0.100	5.942	1.926	2.008	88.573
170.000	110.000	1.737	5.563	0.100	5.566	1.734	1.916	88.504
180.000	70.000	2.106	6.179	-0.100	6.181	2.104	2.039	-88.595
180.000	80.000	2.062	6.144	-0.0	6.144	2.062	2.041	90.000
180.000	90.000	2.017	6.109	0.100	6.111	2.015	2.048	88.601
180.000	95.000	2.074	6.078	0.200	6.088	2.064	2.012	87.147
180.000	105.000	1.782	5.801	0.200	5.811	1.772	2.019	87.158
180.000	115.000	1.691	5.424	0.200	5.435	1.680	1.877	86.942
180.000	125.000	1.500	5.147	0.200	5.158	1.489	1.834	86.870
180.000	135.000	1.308	4.770	0.300	4.796	1.282	1.757	85.084
180.000	145.000	1.217	4.393	0.300	4.421	1.189	1.616	84.651
180.000	155.000	1.225	4.016	0.300	4.048	1.193	1.427	83.934
180.000	165.000	1.134	3.739	0.300	3.773	1.100	1.337	83.515
180.000	180.000	0.997	3.324	0.200	3.341	0.980	1.181	85.123
180.000	210.000	0.723	2.493	0.200	2.515	0.701	0.907	83.633
180.000	240.000	0.448	1.662	0.100	1.670	0.440	0.615	85.322
180.000	270.000	0.174	0.831	0.100	0.846	0.159	0.343	81.534
180.000	300.000	0.0	0.0	0.0	0.0	0.0	0.0	45.000
185.000	85.000	2.016	6.005	-0.100	6.008	2.013	1.997	-88.565
185.000	90.000	1.993	5.938	-0.100	5.941	1.990	1.975	-88.549
185.000	95.000	1.971	6.070	0.0	6.070	1.971	2.049	90.000
185.000	100.000	1.928	6.040	0.200	6.050	1.918	2.066	87.222
187.500	87.500	1.993	5.936	-0.100	5.939	1.990	1.974	-88.548
187.500	90.000	1.982	5.902	-0.100	5.905	1.979	1.963	-88.540
187.500	92.500	1.871	5.868	-0.100	5.870	1.869	2.001	-88.568
187.500	95.000	1.859	5.935	-0.100	5.937	1.857	2.040	-88.595
187.500	97.500	1.848	6.001	0.0	6.001	1.848	2.076	90.000





STRESS DATA : CONFIGURATION 2 cont.

XC00RD	YC00RD	SIGX	SIGY	SIGXY	SIG1	SIGXY	SIG3	TAU	THEIA
190.000	0.0	2.646	7.917	-0.0	7.917	-0.0	2.646	2.635	90.000
190.000	30.000	2.371	7.086	-0.100	7.088	-0.100	2.369	2.360	-88.785
190.000	60.000	2.097	6.255	-0.100	6.257	-0.100	2.095	2.081	-88.623
190.000	70.000	2.006	5.878	-0.200	5.888	-0.200	1.996	1.946	-87.051
190.000	80.000	2.014	5.901	-0.100	5.904	-0.100	2.011	1.946	-88.527
190.000	85.000	1.992	5.934	-0.100	5.937	-0.100	1.989	1.974	-88.548
190.000	87.500	1.981	5.900	-0.100	5.903	-0.100	1.978	1.962	-88.539
190.000	90.000	1.970	5.866	-0.100	5.869	-0.100	1.967	1.951	-88.531
190.000	95.000	1.848	5.799	-0.100	5.802	-0.100	1.845	1.978	-88.551
190.000	97.500	1.736	5.865	-0.100	5.867	-0.100	1.734	2.067	-88.613
190.000	100.000	1.725	5.931	0.0	5.931	0.0	1.725	2.103	90.000
190.000	105.000	1.682	5.901	0.200	5.910	0.200	1.673	2.119	87.292
190.000	115.000	1.591	5.524	0.400	5.564	0.400	1.551	2.007	84.251
190.000	125.000	1.400	5.147	0.400	5.189	0.400	1.358	1.916	83.974
190.000	135.000	1.208	4.570	0.500	4.643	0.500	1.135	1.754	81.718
190.000	145.000	1.217	4.193	0.400	4.246	0.400	1.164	1.541	82.477
190.000	155.000	1.225	3.916	0.400	3.974	0.400	1.167	1.404	81.722
190.000	165.000	1.134	3.639	0.300	3.674	0.300	1.099	1.288	83.265
190.000	180.000	0.997	3.224	0.200	3.242	0.200	0.979	1.131	84.909
190.000	210.000	0.723	2.393	0.200	2.417	0.200	0.699	0.859	83.265
190.000	240.000	0.448	1.562	0.100	1.571	0.100	0.439	0.566	84.911
190.000	270.000	0.274	0.831	0.100	0.848	0.100	0.257	0.296	80.124
190.000	300.000	0.0	0.0	0.0	0.0	0.0	0.0	0.0	45.000
192.500	87.500	1.969	5.764	-0.100	5.767	-0.100	1.966	1.900	-88.492
192.500	97.500	1.725	5.729	-0.100	5.731	-0.100	1.723	2.004	-88.570
192.500	102.500	1.502	5.962	0.0	5.962	0.0	1.502	2.230	90.000
195.000	80.000	1.914	5.501	-0.300	5.526	-0.300	1.889	1.818	-85.252
195.000	85.000	1.869	5.662	-0.200	5.673	-0.200	1.858	1.907	-86.990
195.000	87.500	1.957	5.729	-0.100	5.732	-0.100	1.954	1.889	-88.482
195.000	90.000	1.946	5.695	-0.100	5.698	-0.100	1.943	1.877	-88.473
195.000	95.000	1.824	5.627	-0.200	5.637	-0.200	1.814	1.912	-86.998
195.000	97.500	1.713	5.694	-0.200	5.704	-0.200	1.703	2.001	-87.131
195.000	100.000	1.602	5.760	-0.200	5.770	-0.200	1.592	2.089	-87.252
195.000	105.000	1.379	5.992	0.100	5.994	0.100	1.377	2.309	88.759
195.000	110.000	1.637	5.963	0.400	6.000	0.400	1.600	2.200	84.761
197.500	87.500	1.946	5.593	-0.200	5.604	-0.200	1.935	1.834	-86.870
197.500	90.000	2.035	5.659	-0.100	5.662	-0.100	2.032	1.815	-88.421
197.500	92.500	1.923	5.525	-0.200	5.536	-0.200	1.912	1.812	-86.832
197.500	95.000	1.812	5.592	-0.200	5.603	-0.200	1.801	1.901	-86.980
197.500	97.500	1.701	5.558	-0.300	5.581	-0.300	1.678	1.952	-85.579
197.500	100.000	1.590	5.624	-0.300	5.646	-0.300	1.568	2.039	-85.770
197.500	102.500	1.279	5.590	-0.200	5.599	-0.200	1.270	2.165	-87.349
197.500	105.000	0.968	5.657	-0.100	5.659	-0.100	0.966	2.347	-88.779



## STRESS DATA : CONFIGURATION 2 cont.

XCOORD	YCOORD	SIGX	SIGY	SIGXY	SIG1	SIG3	TAU	THETA
197.500	107.500	1.157	5.923	0.200	5.931	1.149	2.391	87.601
200.000	0.0	2.645	7.816	-0.0	7.816	2.645	2.585	90.000
200.000	30.000	2.371	6.985	-0.100	6.987	2.369	2.309	-88.759
200.000	60.000	2.197	6.054	-0.100	6.057	2.194	1.931	-88.516
200.000	70.000	2.106	5.677	-0.200	5.688	2.095	1.797	-86.804
200.000	85.000	1.768	5.162	-0.400	5.209	1.721	1.744	-83.368
200.000	90.000	1.923	5.323	-0.300	5.349	1.897	1.726	-84.996
200.000	95.000	1.900	5.356	-0.200	5.368	1.888	1.740	-86.699
200.000	97.500	1.689	5.522	-0.300	5.545	1.666	1.940	-85.552
200.000	100.000	1.478	5.388	-0.400	5.429	1.437	1.996	-84.218
200.000	105.000	0.956	5.421	-0.300	5.441	0.936	2.253	-86.173
200.000	107.500	0.845	5.787	-0.100	5.789	0.843	2.473	-88.841
200.000	110.000	1.234	6.053	0.200	6.061	1.226	2.418	87.627
200.000	115.000	1.591	6.024	0.700	6.132	1.483	2.324	81.237
200.000	125.000	1.300	4.947	0.800	5.115	1.132	1.991	78.156
200.000	135.000	1.308	4.170	0.700	4.332	1.146	1.593	76.967
200.000	145.000	1.417	3.993	0.500	4.087	1.323	1.382	79.392
200.000	155.000	1.325	3.716	0.400	3.781	1.260	1.261	80.750
200.000	165.000	1.134	3.539	0.300	3.576	1.097	1.239	82.996
200.000	180.000	0.997	3.124	0.200	3.143	0.978	1.082	84.675
200.000	210.000	0.723	2.393	0.200	2.417	0.699	0.859	83.265
200.000	240.000	0.448	1.562	0.100	1.571	0.439	0.566	84.911
200.000	270.000	0.274	0.731	0.100	0.752	0.253	0.249	78.182
200.000	300.000	0.0	0.0	0.0	0.0	0.0	0.0	45.000
202.500	97.500	1.760	4.935	-0.400	4.985	1.710	1.637	-82.929
202.500	107.500	0.816	5.600	-0.300	5.619	0.797	2.411	-86.426
202.500	112.500	1.094	6.432	0.200	6.439	1.087	2.676	87.857
205.000	80.000	1.980	4.996	-0.200	5.009	1.967	1.521	-86.223
205.000	90.000	1.788	4.519	-0.300	4.552	1.755	1.398	-83.804
205.000	95.000	1.743	4.781	-0.300	4.810	1.714	1.548	-84.414
205.000	97.500	1.932	4.547	-0.300	4.581	1.898	1.341	-83.539
205.000	100.000	1.420	4.413	-0.500	4.494	1.339	1.578	-80.762
205.000	105.000	0.598	4.246	-0.900	4.456	0.388	2.034	-76.869
205.000	107.500	0.487	5.312	-1.000	5.511	0.288	2.612	-78.743
205.000	110.000	0.676	6.378	-0.500	6.422	0.632	2.895	-85.026
205.000	115.000	1.054	6.411	0.800	6.528	0.937	2.795	81.685
205.000	120.000	1.511	4.582	1.500	5.193	0.900	2.147	67.835
207.500	97.500	2.003	4.259	-0.100	4.263	1.999	1.132	-87.467
207.500	100.000	1.991	3.626	-0.300	3.679	1.938	0.871	-79.924
207.500	102.500	1.380	3.292	-0.700	3.521	1.151	1.185	-71.894
207.500	105.000	0.769	2.958	-1.100	3.415	0.312	1.552	-67.428
207.500	107.500	0.858	4.424	-1.000	4.685	0.597	2.044	-75.357
207.500	110.000	0.947	6.191	-0.300	6.208	0.930	2.639	-86.736



STRESS DATA : CONFIGURATION 2 cont.

XCOORD	YCOORD	SIGX	SIGY	SIGXY	SIG1	SIG3	TAU	THETA
207.500	112.500	0.836	5.657	-0.100	5.659	0.834	2.413	-88.812
207.500	115.000	0.925	5.523	0.0	5.523	0.925	2.299	90.000
207.500	117.500	1.414	4.289	0.900	4.547	1.156	1.696	73.975
210.000	0.0	2.577	7.608	-0.0	7.608	2.577	2.516	90.000
210.000	30.000	2.302	6.677	-0.0	6.677	2.302	2.188	90.000
210.000	60.000	2.128	5.746	-0.100	5.749	2.125	1.812	-88.418
210.000	70.000	2.037	5.169	-0.100	5.172	2.034	1.569	-88.173
210.000	95.000	1.808	3.577	-0.100	3.583	1.802	0.890	-86.775
210.000	100.000	1.863	2.738	0.0	2.738	1.863	0.438	90.000
210.000	105.000	1.040	1.771	-0.200	1.822	0.989	0.417	-75.656
210.000	107.500	1.029	2.937	-0.200	2.958	1.008	0.975	-84.080
210.000	110.000	0.0	0.0	0.0	0.0	0.0	0.0	45.000
210.000	115.000	0.0	0.0	0.0	0.0	0.0	0.0	45.000
210.000	117.500	1.185	2.502	0.300	2.567	1.120	0.724	77.753
210.000	120.000	1.273	1.368	0.900	2.222	0.419	0.901	46.511
210.000	125.000	1.531	2.940	0.700	3.229	1.242	0.993	67.592
210.000	135.000	1.440	3.463	0.400	3.539	1.364	1.088	79.212
210.000	145.000	1.348	3.586	0.300	3.626	1.308	1.159	82.496
210.000	155.000	1.257	3.409	0.300	3.450	1.216	1.117	82.210
210.000	165.000	1.166	3.232	0.200	3.251	1.147	1.052	84.521
210.000	180.000	1.028	2.916	0.200	2.937	1.007	0.965	84.019
210.000	210.000	0.654	2.085	0.200	2.112	0.627	0.743	82.191
210.000	240.000	0.380	1.354	0.100	1.364	0.370	0.497	84.198
212.000	270.000	0.192	0.582	0.0	0.582	0.192	0.195	90.000
212.500	102.500	1.723	1.917	0.400	2.232	1.408	0.412	51.816
212.500	107.500	1.000	2.649	0.200	2.673	0.976	0.848	83.182
212.500	112.500	0.0	0.0	0.0	0.0	0.0	0.0	45.000
212.500	115.000	0.0	0.0	0.0	0.0	0.0	0.0	45.000
212.500	117.500	1.056	2.514	0.100	2.521	1.049	0.736	86.095
212.500	120.000	1.045	0.681	0.300	1.214	0.512	0.351	29.378
212.500	122.500	1.433	1.547	0.300	1.795	1.185	0.305	50.379
215.000	80.000	1.911	4.588	0.0	4.588	1.911	1.339	90.000
215.000	90.000	1.620	3.811	0.100	3.816	1.615	1.100	87.392
215.000	100.000	1.528	2.834	0.500	3.003	1.359	0.822	71.279
215.000	105.000	1.282	1.395	0.700	2.041	0.636	0.702	47.307
215.000	107.500	1.371	2.662	0.300	2.728	1.305	0.712	77.536
215.000	110.000	0.0	0.0	0.0	0.0	0.0	0.0	45.000
215.000	112.500	0.0	0.0	0.0	0.0	0.0	0.0	45.000
215.000	115.000	0.0	0.0	0.0	0.0	0.0	0.0	45.000
215.000	117.500	0.927	2.827	-0.300	2.873	0.881	0.996	-81.237
215.000	120.000	0.816	1.393	-0.400	1.598	0.611	0.493	-62.900
215.000	122.500	1.505	1.859	-0.200	1.949	1.415	0.267	-65.754
215.000	125.000	1.693	2.525	-0.100	2.537	1.681	0.428	-83.242





STRESS DATA : CONFIGURATION 2 CONT.

XCOORD	YCOORD	SIGX	SIGY	SIGXY	SIG1	SIG3	TAU	THETA
215.000	130.000	1.551	2.898	-0.100	2.905	1.544	0.681	-85.777
217.500	107.500	1.342	4.074	0.800	4.291	1.125	1.583	74.822
217.500	110.000	0.831	5.240	0.0	5.240	0.831	2.204	90.000
217.500	112.500	0.820	5.207	-0.100	5.209	0.818	2.196	-88.695
217.500	115.000	0.909	5.573	-0.300	5.592	0.890	2.351	-86.335
217.500	117.500	0.798	4.039	-0.700	4.184	0.653	1.765	-78.319
217.500	122.500	1.176	2.872	-0.700	3.124	0.924	1.100	-70.231
217.500	127.500	1.653	3.404	-0.400	3.491	1.566	0.963	-77.723
220.000	0.0	2.408	7.300	-0.0	7.300	2.408	2.446	90.000
220.000	30.000	2.234	6.469	0.0	6.469	2.234	2.117	90.000
220.000	60.000	2.059	5.438	0.0	5.438	2.059	1.689	90.000
220.000	70.000	1.968	4.961	0.100	4.964	1.965	1.500	88.089
220.000	105.000	1.348	4.091	1.200	4.542	0.897	1.822	69.408
220.000	110.000	0.802	5.653	0.500	5.704	0.751	2.476	84.176
220.000	112.500	0.291	5.619	-0.200	5.626	0.284	2.671	-87.853
220.000	115.000	0.380	5.485	-0.500	5.534	0.331	2.601	-84.458
220.000	120.000	0.558	3.818	-0.800	4.004	0.372	1.816	-76.929
220.000	122.500	0.847	3.784	-0.700	3.942	0.689	1.627	-77.257
220.000	125.000	1.336	3.750	-0.500	3.849	1.237	1.306	-78.749
220.000	130.000	1.513	3.783	-0.200	3.800	1.496	1.152	-85.003
220.000	135.000	1.271	3.555	-0.100	3.559	1.267	1.146	-87.498
220.000	145.000	1.280	3.478	0.100	3.483	1.275	1.104	87.401
220.000	155.000	1.188	3.401	0.200	3.419	1.170	1.124	84.877
220.000	165.000	1.097	3.024	0.200	3.045	1.076	0.984	84.137
220.000	180.000	0.960	2.609	0.200	2.633	0.936	0.848	83.182
220.000	210.000	0.686	1.778	0.100	1.787	0.677	0.555	84.811
220.000	300.000	0.0	0.0	-0.0	0.0	0.0	0.0	45.000
222.500	112.500	0.862	5.431	0.100	5.433	0.860	2.287	88.747
222.500	115.000	0.651	5.098	-0.200	5.107	0.642	2.232	-87.430
222.500	117.500	0.540	4.764	-0.300	4.785	0.519	2.133	-85.958
222.500	120.000	0.529	4.430	-0.500	4.493	0.466	2.014	-82.811
222.500	122.500	0.818	4.096	-0.600	4.202	0.712	1.745	-79.947
222.500	127.500	1.296	4.029	-0.400	4.086	1.239	1.424	-81.842
222.500	132.500	1.173	3.961	-0.300	3.993	1.141	1.426	-83.927
225.000	80.000	1.742	4.580	0.300	4.611	1.711	1.450	84.031
225.000	90.000	1.451	4.203	0.400	4.260	1.394	1.433	81.895
225.000	100.000	1.159	4.326	0.500	4.403	1.082	1.661	81.238
225.000	110.000	1.268	4.849	0.400	4.893	1.224	1.835	83.703
225.000	115.000	0.922	4.810	0.0	4.810	0.922	1.944	90.000
225.000	120.000	0.800	4.543	-0.300	4.567	0.776	1.895	-85.446
225.000	135.000	1.133	4.040	-0.100	4.043	1.130	1.457	-88.032
225.000	140.000	1.091	3.913	-0.0	3.913	1.091	1.411	90.000
224.000	240.000	0.384	1.064	0.0	1.064	0.384	0.340	90.000





## STRESS DATA : CONFIGURATION 2 cont.

XCOORD	YCOORD	SIGX	SIGY	SIGXY	SIG1	SIG3	TAU	THETA
225.000	270.000	0.192	0.582	-0.0	0.582	0.192	0.195	90.000
227.500	122.500	1.060	4.321	-0.300	4.348	1.033	1.658	-84.787
227.500	127.500	1.138	4.054	-0.400	4.108	1.084	1.512	-82.329
227.500	132.500	1.115	4.186	-0.300	4.215	1.086	1.565	-84.472
227.500	137.500	0.993	4.219	-0.100	4.222	0.990	1.616	-88.226
230.000	0.0	2.339	7.091	0.0	7.091	2.339	2.376	90.000
230.000	30.000	2.165	6.160	0.0	6.160	2.165	1.997	90.000
230.000	60.000	1.891	5.229	0.100	5.232	1.888	1.672	88.286
230.000	70.000	1.799	4.952	0.200	4.965	1.786	1.589	86.385
230.000	115.000	1.088	4.306	0.0	4.306	1.088	1.609	90.000
230.000	120.000	0.942	4.267	-0.100	4.270	0.939	1.666	-88.279
230.000	140.000	1.053	4.297	0.0	4.297	1.053	1.622	90.000
230.000	145.000	1.111	4.071	0.200	4.084	1.098	1.493	86.152
230.000	155.000	1.020	3.194	0.400	3.265	0.949	1.158	79.899
230.000	165.000	1.029	2.617	0.300	2.672	0.974	0.849	79.651
230.000	180.000	0.891	2.301	0.200	2.329	0.863	0.733	82.081
232.500	122.500	1.002	3.946	-0.300	3.976	0.972	1.502	-84.240
232.500	127.500	1.180	3.979	-0.300	4.011	1.148	1.431	-83.951
232.500	132.500	0.858	3.611	-0.500	3.699	0.770	1.464	-80.018
232.500	137.500	0.735	4.344	-0.400	4.388	0.691	1.848	-83.751
232.500	142.500	0.713	4.476	-0.0	4.476	0.713	1.881	90.000
235.000	80.000	1.573	4.571	0.300	4.601	1.543	1.529	84.341
235.000	90.000	1.282	4.394	0.300	4.423	1.253	1.585	84.544
235.000	100.000	1.191	4.317	0.200	4.330	1.178	1.576	86.354
235.000	110.000	1.199	3.940	0.100	3.944	1.195	1.374	87.913
235.000	120.000	1.108	3.563	-0.100	3.567	1.104	1.232	-87.671
235.000	125.000	1.162	3.425	-0.200	3.443	1.144	1.149	-84.988
235.000	140.000	0.395	4.822	-0.500	4.878	0.339	2.269	-83.636
235.000	145.000	0.673	4.555	0.400	4.596	0.632	1.982	84.178
235.000	150.000	1.031	3.129	0.900	3.462	0.698	1.382	69.686
235.000	210.000	0.583	1.567	0.100	1.577	0.573	0.502	84.255
235.000	240.000	0.384	1.164	-0.0	1.164	0.384	0.390	90.000
235.000	270.000	0.192	0.582	-0.0	0.582	0.192	0.195	90.000
235.000	300.000	0.0	0.0	-0.0	0.0	0.0	0.0	45.000
237.500	127.500	1.222	3.003	-0.300	3.052	1.173	0.940	-80.691
237.500	132.500	1.000	2.336	-0.300	2.400	0.936	0.732	-77.907
237.500	137.500	0.778	3.468	-0.500	3.558	0.688	1.435	-79.804
237.500	140.000	0.666	4.335	-0.200	4.346	0.655	1.845	-86.889
237.500	142.500	0.555	4.101	-0.100	4.104	0.552	1.776	-88.386
237.500	145.000	0.644	3.967	0.0	3.967	0.644	1.661	90.000
237.500	147.500	0.933	3.133	0.600	3.286	0.780	1.253	75.695
240.000	0.0	2.270	6.883	0.0	6.883	2.270	2.306	90.000
240.000	30.000	2.096	5.952	0.100	5.955	2.093	1.931	88.516



STRESS DATA : CONFIGURATION 2 cont.

XCOORD	YCOORD	SIGX	SIGY	SIGXY	SIG1	SIG3	TAU	THETA
240.000	60.000	1.822	5.121	0.200	5.133	1.810	1.662	86.543
240.000	70.000	1.631	4.844	0.200	4.856	1.619	1.619	86.452
240.000	125.000	1.228	2.721	-0.100	2.728	1.221	0.753	-86.185
240.000	130.000	1.382	2.382	-0.0	2.382	1.382	0.500	90.000
240.000	135.000	0.760	1.215	-0.200	1.290	0.685	0.303	-69.340
240.000	137.500	0.749	2.181	-0.200	2.208	0.722	0.743	-82.197
240.000	140.000	0.0	0.0	0.0	0.0	0.0	0.0	45.000
240.000	145.000	0.0	0.0	0.0	0.0	0.0	0.0	45.000
240.000	147.500	0.804	1.846	0.200	1.883	0.767	0.558	79.500
240.000	150.000	0.793	1.112	0.500	1.477	0.428	0.525	53.846
240.000	155.000	1.252	2.086	0.400	2.247	1.091	0.578	68.096
240.000	165.000	1.060	2.209	0.100	2.218	1.051	0.583	85.063
242.500	132.500	1.042	1.561	0.0	1.561	1.042	0.260	90.000
242.500	137.500	0.720	1.893	0.100	1.901	0.712	0.595	85.162
242.500	147.500	0.575	1.758	0.0	1.758	0.575	0.591	90.000
242.500	152.500	1.253	1.591	0.200	1.684	1.160	0.262	65.099
245.000	80.000	1.405	4.463	0.200	4.476	1.392	1.542	86.274
245.000	90.000	1.313	4.286	0.200	4.299	1.300	1.500	86.168
245.000	100.000	1.222	4.009	0.200	4.023	1.208	1.408	85.916
245.000	110.000	1.231	3.632	0.100	3.636	1.227	1.205	87.619
245.000	120.000	1.139	3.055	0.200	3.076	1.118	0.979	84.104
245.000	130.000	1.048	2.278	0.400	2.397	0.929	0.734	73.480
245.000	135.000	0.902	1.139	0.500	1.534	0.507	0.514	51.667
245.000	137.500	0.891	1.806	0.200	1.848	0.849	0.499	78.193
245.000	140.000	0.0	0.0	0.0	0.0	0.0	0.0	45.000
245.000	145.000	0.0	0.0	0.0	0.0	0.0	0.0	45.000
245.000	147.500	0.746	1.971	-0.200	2.003	0.714	0.644	-80.958
245.000	150.000	0.635	1.137	-0.300	1.277	0.495	0.391	-64.959
245.000	155.000	1.213	1.969	-0.100	1.982	1.200	0.391	-82.591
245.000	160.000	1.272	1.944	-0.100	1.959	1.257	0.351	-81.713
247.500	137.500	0.962	2.918	0.600	3.087	0.793	1.147	74.235
247.500	140.000	0.551	3.584	0.0	3.584	0.551	1.516	90.000
247.500	142.500	0.540	3.550	-0.100	3.553	0.537	1.508	-88.099
247.500	145.000	0.629	3.917	-0.200	3.929	0.617	1.656	-86.532
247.500	147.500	0.717	2.883	-0.600	3.038	0.562	1.238	-75.506
248.000	180.000	0.868	2.128	-0.0	2.128	0.868	0.630	90.000
245.000	240.000	0.384	1.164	-0.0	1.164	0.384	0.390	90.000
250.000	0.0	2.202	6.675	0.100	6.677	2.200	2.239	88.720
250.000	50.000	1.845	5.290	0.100	5.293	1.842	1.725	88.339
250.000	60.000	1.753	4.913	0.200	4.926	1.740	1.593	86.393
250.000	70.000	1.562	4.736	0.200	4.749	1.549	1.600	86.409
250.000	135.000	0.968	3.135	1.000	3.526	0.577	1.474	68.647
250.000	140.000	0.622	3.997	0.400	4.044	0.575	1.734	83.332
250.000	145.000	0.300	3.929	-0.400	3.973	0.256	1.858	-83.784



## STRESS DATA : CONFIGURATION 2 cont.

XCOORD	YCOORD	SIGX	SIGY	SIGXY	SIG1	SIG3	TAU	THETA
250.000	150.000	0.577	2.662	-0.600	2.822	0.417	1.203	-75.039
250.000	155.000	0.855	2.794	-0.300	2.839	0.810	1.015	-81.403
250.000	160.000	1.033	2.627	-0.200	2.652	1.008	0.822	-82.956
250.000	165.000	0.992	2.302	-0.200	2.332	0.962	0.685	-81.510
250.000	270.000	0.192	0.582	-0.0	0.582	0.192	0.195	90.000
250.000	300.000	0.0	0.0	-0.0	0.0	0.0	0.0	45.000
255.000	80.000	1.352	4.404	0.200	4.417	1.339	1.539	86.267
255.000	90.000	1.261	4.127	0.200	4.141	1.247	1.447	86.027
255.000	100.000	1.270	3.850	0.200	3.865	1.255	1.305	85.594
255.000	110.000	1.178	3.573	0.200	3.590	1.161	1.214	85.259
255.000	120.000	0.987	3.296	0.300	3.334	0.949	1.193	82.717
255.000	130.000	0.795	3.319	0.400	3.381	0.733	1.324	81.207
255.000	140.000	0.904	3.642	0.400	3.699	0.847	1.426	81.856
255.000	145.000	0.758	3.704	0.100	3.707	0.755	1.476	88.058
255.000	150.000	0.636	3.036	-0.300	3.073	0.599	1.237	-82.982
255.000	155.000	0.814	2.969	-0.300	3.010	0.773	1.118	-82.221
256.000	160.000	0.996	2.916	-0.100	2.921	0.991	0.965	-87.027
254.000	165.000	0.964	2.619	-0.100	2.625	0.958	0.834	-86.555
260.000	0.0	2.231	6.765	0.100	6.767	2.229	2.269	88.737
260.000	30.000	1.957	5.934	0.100	5.937	1.954	1.991	88.560
260.000	60.000	1.683	5.103	0.200	5.115	1.671	1.722	86.665
260.000	70.000	1.592	4.826	0.200	4.838	1.580	1.629	86.475
260.000	145.000	1.006	3.748	0.200	3.763	0.991	1.386	85.850
260.000	150.000	0.860	3.210	-0.100	3.214	0.856	1.179	-87.568
260.000	180.000	0.768	2.328	-0.0	2.328	0.768	0.780	90.000
260.000	210.000	0.576	1.746	-0.0	1.746	0.576	0.585	90.000
260.000	240.000	0.384	1.164	-0.0	1.164	0.384	0.390	90.000
260.000	270.000	0.192	0.582	-0.0	0.582	0.192	0.195	90.000
260.000	300.000	0.0	0.0	-0.0	0.0	0.0	0.0	45.000
265.000	80.000	1.414	4.690	0.200	4.702	1.402	1.650	86.519
265.000	90.000	1.322	4.413	0.200	4.426	1.309	1.558	86.313
265.000	100.000	1.231	4.136	0.200	4.150	1.217	1.466	86.080
265.000	110.000	1.140	3.959	0.200	3.973	1.126	1.424	85.962
265.000	120.000	1.048	3.682	0.200	3.697	1.033	1.332	85.682
265.000	130.000	0.957	3.605	0.100	3.609	0.953	1.328	87.840
265.000	140.000	1.065	3.428	0.100	3.432	1.061	1.186	87.581
270.000	0.0	2.259	6.848	0.100	6.850	2.257	2.297	88.752
270.000	30.000	1.985	6.017	0.100	6.019	1.983	2.018	88.580
270.000	60.000	1.710	5.286	0.100	5.289	1.707	1.791	88.399
270.000	160.000	0.896	2.816	-0.0	2.816	0.896	0.960	90.000
270.000	180.000	0.768	2.328	-0.100	2.334	0.762	0.786	-86.347
275.000	195.000	0.672	2.037	-0.0	2.037	0.672	0.682	90.000
290.000	0.0	2.314	7.114	0.100	7.116	2.312	2.402	88.807
290.000	30.000	2.039	6.283	0.100	6.285	2.037	2.124	88.651





STRESS DATA : CONFIGURATION 2 cont.

XCOORD	YCOORD	SIGX	SIGY	SIGXY	SIG1	SIG3	TAU	THETA
290.000	60.000	1.765	5.552	0.100	5.555	1.762	1.896	88.488
290.000	90.000	1.491	4.721	0.100	4.724	1.488	1.618	88.228
290.000	120.000	1.217	3.990	0.100	3.994	1.213	1.390	87.937
290.000	150.000	1.042	3.259	0.0	3.259	1.042	1.108	90.000
290.000	180.000	0.768	2.328	0.0	2.328	0.768	0.780	90.000
290.000	210.000	0.576	1.746	-0.0	1.746	0.576	0.585	90.000
290.000	240.000	0.384	1.164	-0.0	1.164	0.384	0.390	90.000
290.000	270.000	0.192	0.582	-0.0	0.582	0.192	0.195	90.000
290.000	300.000	0.0	0.0	-0.0	0.0	0.0	0.0	45.000
320.000	30.000	2.122	6.632	0.100	6.634	2.120	2.257	88.730
320.000	90.000	1.573	5.070	0.0	5.070	1.573	1.748	90.000
320.000	150.000	1.125	3.408	0.0	3.408	1.125	1.141	90.000
320.000	210.000	0.576	1.746	0.0	1.746	0.576	0.585	90.000
320.000	240.000	0.384	1.164	-0.0	1.164	0.384	0.390	90.000
320.000	270.000	0.192	0.582	-0.0	0.582	0.192	0.195	90.000
320.000	300.000	0.0	0.0	-0.0	0.0	0.0	0.0	45.000
350.000	0.0	2.478	7.712	0.100	7.714	2.476	2.619	88.906
350.000	60.000	1.929	6.150	0.0	6.150	1.929	2.110	90.000
350.000	120.000	1.381	4.488	0.0	4.488	1.381	1.554	90.000
350.000	180.000	0.933	2.826	0.0	2.826	0.933	0.946	90.000
350.000	240.000	0.384	1.164	0.0	1.164	0.384	0.390	90.000
350.000	270.000	0.192	0.582	-0.0	0.582	0.192	0.195	90.000
350.000	300.000	0.0	0.0	0.0	0.0	0.0	0.0	45.000
380.000	270.000	0.192	0.582	0.0	0.582	0.192	0.195	90.000
380.000	300.000	0.0	0.0	0.0	0.0	0.0	0.0	45.000
410.000	0.0	2.742	8.310	0.0	8.310	2.742	2.784	90.000
410.000	60.000	2.194	6.648	0.0	6.648	2.194	2.227	90.000
410.000	120.000	1.645	4.986	-0.0	4.986	1.645	1.670	90.000
410.000	180.000	1.097	3.324	-0.0	3.324	1.097	1.113	90.000
410.000	240.000	0.548	1.662	0.0	1.662	0.548	0.557	90.000
410.000	300.000	0.0	0.0	0.0	0.0	0.0	0.0	45.000
470.000	0.0	2.742	8.310	0.0	8.310	2.742	2.784	90.000
470.000	60.000	2.194	6.648	0.0	6.648	2.194	2.227	90.000
470.000	120.000	1.645	4.986	-0.0	4.986	1.645	1.670	90.000
470.000	180.000	1.097	3.324	-0.0	3.324	1.097	1.113	90.000
470.000	240.000	0.548	1.662	-0.0	1.662	0.548	0.557	90.000
470.000	300.000	0.0	0.0	-0.0	0.0	0.0	0.0	45.000
530.000	0.0	2.742	8.310	0.0	8.310	2.742	2.784	90.000
530.000	60.000	2.194	6.648	-0.0	6.648	2.194	2.227	90.000
530.000	120.000	1.645	4.986	-0.0	4.986	1.645	1.670	90.000
530.000	180.000	1.097	3.324	-0.0	3.324	1.097	1.113	90.000
530.000	240.000	0.548	1.662	-0.0	1.662	0.548	0.557	90.000
530.000	300.000	0.0	0.0	-0.0	0.0	0.0	0.0	45.000





## CONFIGURATION 3



STRESS DATA : CONFIGURATION 3

XCOORD	YCOORD	SIGX	SIGY	SIGXY	SIG1	SIG3	TAU	THETA
0.0	0.0	2.842	8.410	0.0	8.410	2.842	2.784	90.000
0.0	60.000	2.294	6.748	0.0	6.748	2.294	2.227	90.000
0.0	120.000	1.645	4.986	0.100	4.989	1.642	1.673	88.287
0.0	180.000	0.897	3.324	0.100	3.328	0.893	1.218	87.645
0.0	240.000	0.148	1.562	0.100	1.569	0.141	0.714	85.975
0.0	300.000	-0.700	-0.100	0.200	-0.761	-0.039	0.361	163.155
30.000	0.0	2.742	8.410	0.0	8.410	2.742	2.834	90.000
30.000	30.000	2.568	7.579	0.100	7.581	2.566	2.507	88.857
30.000	90.000	2.020	5.917	0.100	5.920	2.017	1.951	88.531
30.000	150.000	1.271	4.155	0.100	4.158	1.268	1.445	88.017
30.000	210.000	0.523	2.493	0.100	2.498	0.518	0.990	87.101
30.000	270.000	-0.226	0.731	0.100	0.741	-0.236	0.489	84.098
30.000	300.000	-0.700	0.0	0.100	-0.714	0.014	0.364	172.027
60.000	0.0	2.842	8.610	0.100	8.612	2.840	2.886	89.007
60.000	60.000	2.294	6.848	0.100	6.850	2.292	2.279	88.743
60.000	120.000	1.645	5.086	0.100	5.089	1.642	1.723	88.337
60.000	180.000	0.897	3.324	0.100	3.340	0.881	1.495	88.083
60.000	210.000	0.523	2.493	0.200	2.513	0.503	1.230	85.320
60.000	240.000	0.248	1.662	0.200	1.690	0.220	0.735	84.261
60.000	270.000	-0.126	0.831	0.100	0.841	-0.136	0.489	82.102
60.000	300.000	-0.500	0.0	0.100	-0.519	0.019	0.269	84.098
90.000	0.0	2.942	8.710	0.200	8.717	2.935	2.891	169.099
90.000	30.000	2.668	7.879	0.200	7.887	2.660	2.891	88.016
90.000	60.000	2.394	6.948	0.200	6.957	2.385	2.613	87.805
90.000	90.000	2.020	6.017	0.100	6.019	2.018	2.286	87.490
90.000	120.000	1.545	5.186	0.100	5.189	1.542	2.001	88.568
90.000	180.000	0.897	3.424	0.200	3.440	0.881	1.823	88.428
90.000	240.000	0.248	1.662	0.200	1.690	0.220	1.279	85.503
90.000	300.000	-0.400	0.0	0.100	-0.424	0.024	0.735	82.102
110.000	0.0	2.648	8.124	-0.0	8.124	2.648	0.224	166.717
110.000	20.000	2.759	8.054	0.200	8.062	2.751	2.738	90.000
110.000	40.000	2.677	7.602	0.300	7.620	2.659	2.655	87.840
120.000	90.000	2.020	6.117	0.200	6.127	2.010	2.481	86.527
120.000	150.000	1.171	4.255	0.200	4.268	1.158	2.058	87.212
120.000	210.000	0.623	2.493	0.200	2.514	0.602	1.555	86.305
120.000	270.000	-0.026	0.831	0.100	0.843	-0.038	0.956	83.963
120.000	300.000	-0.300	0.0	0.100	-0.330	0.030	0.440	83.432
130.000	0.0	2.647	8.123	-0.0	8.123	2.647	0.180	163.155
130.000	20.000	2.465	7.569	-0.0	7.569	2.465	2.738	90.000
130.000	40.000	2.576	7.499	0.100	7.501	2.574	2.552	90.000
130.000	60.000	2.394	6.948	0.200	6.957	2.385	2.464	88.837
150.000	0.0	2.647	8.021	-0.0	8.021	2.647	2.286	87.490
							2.687	90.000



## STRESS DATA : CONFIGURATION 3 cont.

XCOORD	YCOORD	SIGX	SIGY	SIGXY	SIG1	SIG3	TAU	THETA
150.000	30.000	2.373	7.190	-0.100	7.192	2.371	2.411	-88.811
150.000	40.000	2.281	7.013	-0.0	7.013	2.281	2.366	90.000
150.000	60.000	2.392	6.943	0.100	6.945	2.390	2.278	88.742
150.000	90.000	2.020	6.317	0.200	6.326	2.011	2.158	87.341
150.000	120.000	1.445	5.186	0.300	5.210	1.421	1.894	85.444
150.000	150.000	1.171	4.155	0.300	4.185	1.141	1.522	84.315
150.000	180.000	0.897	3.324	0.300	3.361	0.860	1.250	83.057
150.000	210.000	0.623	2.493	0.300	2.540	0.576	0.982	81.105
150.000	240.000	0.348	1.662	0.200	1.692	0.318	0.687	81.534
150.000	270.000	0.074	0.831	0.100	0.844	0.061	0.391	82.600
150.000	300.000	-0.200	0.0	0.100	-0.241	0.041	0.141	157.500
170.000	0.0	2.646	7.919	-0.100	7.921	2.644	2.638	-88.914
170.000	30.000	2.372	7.088	-0.100	7.090	2.370	2.360	-88.786
170.000	60.000	2.198	6.257	-0.100	6.259	2.196	2.032	-88.590
170.000	80.000	2.009	6.487	0.0	6.487	2.009	2.239	90.000
170.000	90.000	1.920	6.417	0.300	6.437	1.900	2.268	86.200
170.000	100.000	1.628	6.140	0.500	6.195	1.573	2.311	83.752
170.000	110.000	1.437	5.363	0.600	5.453	1.347	2.053	81.502
180.000	70.000	2.106	5.679	-0.300	5.704	2.081	1.812	-85.234
180.000	80.000	1.762	5.944	-0.300	5.965	1.741	2.112	-85.918
180.000	90.000	1.517	6.509	0.200	6.517	1.509	2.504	87.709
180.000	95.000	1.574	6.578	0.900	6.735	1.417	2.659	80.108
180.000	105.000	1.382	5.501	0.900	5.689	1.194	2.248	78.197
180.000	115.000	1.491	4.624	0.800	4.816	1.299	1.759	76.473
180.000	125.000	1.500	4.647	0.500	4.725	1.422	1.651	81.186
180.000	135.000	1.408	4.470	0.400	4.521	1.357	1.582	82.679
180.000	145.000	1.217	4.093	0.400	4.148	1.162	1.493	82.228
180.000	155.000	1.225	3.816	0.400	3.876	1.165	1.356	81.421
180.000	165.000	1.134	3.539	0.400	3.604	1.069	1.267	80.800
180.000	180.000	0.997	3.224	0.300	3.264	0.957	1.153	82.461
180.000	210.000	0.723	2.393	0.200	2.417	0.699	0.859	83.265
180.000	240.000	0.448	1.562	0.200	1.597	0.413	0.592	80.124
180.000	270.000	0.174	0.831	0.100	0.846	0.159	0.343	81.534
180.000	300.000	0.0	0.0	0.0	0.0	0.0	0.0	45.000
185.000	85.000	1.016	4.905	-0.700	5.027	0.894	2.067	-80.101
185.000	90.000	0.593	6.738	-0.500	6.778	0.553	3.113	-85.378
185.000	95.000	0.971	6.770	0.700	6.853	0.888	2.983	83.214
185.000	100.000	1.528	5.040	1.800	5.799	0.769	2.515	67.145
187.500	87.500	1.493	5.736	-0.600	5.819	1.410	2.205	-82.104
187.500	90.000	1.182	6.602	-0.300	6.619	1.165	2.727	-86.841
187.500	92.500	0.971	6.168	-0.100	6.170	0.969	2.600	-88.898
187.500	95.000	1.059	6.135	0.0	6.135	1.059	2.538	90.000
187.500	97.500	1.448	4.801	1.100	5.130	1.119	2.005	73.365



## STRESS DATA : CONFIGURATION 3 comt.

XCOORD	YCOORD	SIGX	SIGY	SIGXY	SIG1	SIG3	TAU	THETA
190.000	0.0	2.546	7.717	-0.100	7.719	2.544	2.587	-88.892
190.000	30.000	2.371	6.786	-0.100	6.788	2.369	2.210	-88.703
190.000	60.000	2.197	5.655	-0.200	5.667	2.185	1.741	-86.701
190.000	70.000	2.106	4.678	-0.200	4.693	2.091	1.301	-85.580
190.000	80.000	1.914	4.301	-0.300	4.338	1.877	1.231	-82.945
190.000	85.000	1.492	3.634	-0.500	3.745	1.381	1.182	-77.487
190.000	87.500	1.981	5.500	-0.300	5.525	1.956	1.785	-85.162
190.000	90.000	0.0	0.0	0.0	0.0	0.0	0.0	45.000
190.000	95.000	0.0	0.0	0.0	0.0	0.0	0.0	45.000
190.000	97.500	1.236	3.165	0.200	3.186	1.215	0.985	84.142
190.000	100.000	1.225	1.831	0.800	2.383	0.673	0.855	55.372
190.000	105.000	1.682	3.601	0.600	3.773	1.510	1.132	73.991
190.000	115.000	1.691	4.424	0.400	4.481	1.634	1.424	81.842
190.000	125.000	1.500	4.547	0.400	4.599	1.448	1.575	82.644
190.000	135.000	1.408	4.370	0.400	4.423	1.355	1.534	82.443
190.000	145.000	1.317	3.993	0.400	4.052	1.258	1.397	81.678
190.000	155.000	1.225	3.716	0.500	3.813	1.128	1.342	79.064
190.000	165.000	1.134	3.439	0.400	3.506	1.067	1.220	80.430
190.000	180.000	0.997	3.124	0.300	3.166	0.955	1.105	82.123
190.000	210.000	0.723	2.393	0.200	2.417	0.699	0.859	83.265
190.000	240.000	0.448	1.562	0.100	1.571	0.439	0.566	84.911
190.000	270.000	0.274	0.831	0.100	0.848	0.257	0.296	80.124
190.000	300.000	0.0	0.0	0.0	0.0	0.0	0.0	45.000
192.500	87.500	1.369	3.864	-0.300	3.900	1.333	1.283	-83.239
192.500	97.500	1.025	3.029	0.100	3.034	1.020	1.007	87.150
192.500	102.500	1.702	2.762	-0.200	2.798	1.666	0.566	-79.663
195.000	80.000	1.814	3.701	0.300	3.748	1.767	0.990	81.181
195.000	85.000	1.369	1.962	0.400	2.163	1.168	0.498	63.274
195.000	87.500	1.457	3.129	0.200	3.153	1.433	0.860	83.273
195.000	90.000	0.0	0.0	0.0	0.0	0.0	0.0	45.000
195.000	95.000	0.0	0.0	0.0	0.0	0.0	0.0	45.000
195.000	97.500	1.213	3.294	-0.300	3.336	1.171	1.083	-81.958
195.000	100.000	0.802	1.660	-0.500	1.890	0.572	0.659	-65.315
195.000	105.000	2.279	4.592	-0.300	4.630	2.241	1.195	-82.729
195.000	110.000	1.837	4.663	-0.0	4.663	1.837	1.413	90.000
197.500	87.500	1.346	4.593	0.900	4.826	1.113	1.856	75.499
197.500	90.000	1.035	6.059	0.0	6.059	1.035	2.512	90.000
197.500	92.500	0.923	6.025	-0.100	6.027	0.921	2.553	-88.878
197.500	95.000	1.112	6.492	-0.400	6.522	1.082	2.720	-85.771
197.500	97.500	1.001	4.558	-1.000	4.820	0.739	2.040	-75.326
197.500	100.000	0.690	2.524	-1.100	3.039	0.175	1.432	-64.908
197.500	102.500	1.579	3.990	-0.600	4.131	1.438	1.347	-76.770
197.500	105.000	2.168	5.457	-0.400	5.505	2.120	1.692	-83.165





STRESS DATA : CONFIGURATION 3 cont.

XCOORD	YCOORD	SIGX	SIGY	SIGXY	SIG1	SIG3	TAU	THETA
197.500	107.500	1.857	5.123	-0.200	5.135	1.845	1.645	-86.509
200.000	0.0	2.545	7.516	-0.0	7.516	2.545	2.485	90.000
200.000	30.000	2.371	6.585	-0.0	6.585	2.371	2.107	90.000
200.000	60.000	2.197	5.454	0.0	5.454	2.197	1.628	90.000
200.000	70.000	2.006	4.877	0.200	4.891	1.992	1.449	86.034
200.000	85.000	1.468	4.562	1.200	4.973	1.057	1.958	71.100
200.000	90.000	0.823	6.223	0.400	6.252	0.794	2.729	85.786
200.000	95.000	0.600	6.456	-0.500	6.498	0.558	2.970	-85.155
200.000	97.500	0.489	5.422	-1.000	5.617	0.294	2.662	-78.965
200.000	100.000	0.678	4.288	-0.900	4.500	0.466	2.017	-76.749
200.000	105.000	1.456	5.121	-0.500	5.188	1.389	1.899	-82.369
200.000	107.500	1.545	5.087	-0.300	5.112	1.520	1.796	-85.193
200.000	110.000	1.534	5.253	-0.100	5.256	1.531	1.862	-88.461
200.000	115.000	1.591	5.024	0.100	5.027	1.588	1.719	88.333
200.000	125.000	1.400	4.847	0.400	4.893	1.354	1.769	83.467
200.000	135.000	1.308	4.270	0.500	4.352	1.226	1.563	80.672
200.000	145.000	1.317	3.793	0.500	3.890	1.220	1.335	79.004
200.000	155.000	1.325	3.616	0.400	3.684	1.257	1.213	80.376
200.000	165.000	1.134	3.339	0.300	3.379	1.094	1.143	82.389
200.000	180.000	1.097	3.024	0.300	3.070	1.051	1.009	81.253
200.000	210.000	0.723	2.293	0.200	2.318	0.698	0.810	82.853
200.000	240.000	0.448	1.562	0.100	1.571	0.439	0.566	84.911
200.000	270.000	0.274	0.731	0.100	0.752	0.253	0.249	78.182
200.000	300.000	0.0	0.0	0.0	0.0	0.0	0.0	45.000
202.500	97.500	0.660	5.435	-0.400	5.468	0.627	2.421	-85.244
202.500	107.500	1.316	5.100	-0.400	5.142	1.274	1.934	-84.031
202.500	112.500	1.294	5.532	-0.100	5.534	1.292	2.121	-88.649
205.000	80.000	1.580	4.796	0.500	4.872	1.504	1.684	81.364
205.000	90.000	1.288	5.319	0.200	5.329	1.278	2.025	87.167
205.000	95.000	0.943	5.681	-0.0	5.681	0.943	2.369	90.000
205.000	97.500	0.932	5.447	-0.200	5.456	0.923	2.266	-87.469
205.000	100.000	1.020	5.113	-0.500	5.173	0.960	2.107	-83.135
205.000	105.000	1.198	5.046	-0.600	5.137	1.107	2.015	-81.340
205.000	107.500	1.187	5.212	-0.600	5.300	1.099	2.100	-81.699
205.000	110.000	1.076	5.278	-0.400	5.316	1.038	2.139	-84.610
205.000	115.000	1.254	5.711	0.100	5.713	1.252	2.231	88.715
205.000	120.000	1.511	5.582	0.400	5.621	1.472	2.074	84.441
207.500	97.500	1.203	5.259	-0.100	5.261	1.201	2.030	-88.589
207.500	100.000	1.191	5.126	-0.300	5.149	1.168	1.990	-85.665
207.500	102.500	1.180	4.792	-0.600	4.889	1.083	1.903	-80.811
207.500	105.000	1.369	4.858	-0.700	4.993	1.234	1.880	-79.068
207.500	107.500	1.058	4.924	-0.800	5.083	0.899	2.092	-78.758
207.500	110.000	0.747	5.291	-0.700	5.396	0.642	2.377	-81.438



STRESS DATA : CONFIGURATION 3 cont.

XCOORD	YCOORD	SIGX	SIGY	SIGXY	SIG1	SIG3	TAU	THETA
207.500	112.500	0.836	5.457	-0.400	5.491	0.802	2.345	-85.089
207.500	115.000	0.825	5.523	-0.300	5.542	0.806	2.368	-86.361
207.500	117.500	1.014	5.889	0.100	5.891	1.012	2.440	88.825
210.000	0.0	2.477	7.308	0.0	7.308	2.477	2.415	90.000
210.000	30.000	2.302	6.377	0.100	6.379	2.300	2.040	88.595
210.000	60.000	2.028	5.246	0.200	5.258	2.016	1.621	86.457
210.000	70.000	1.737	4.969	0.300	4.997	1.709	1.644	84.741
210.000	95.000	1.208	4.777	-0.100	4.780	1.205	1.787	-88.396
210.000	100.000	1.363	4.638	-0.300	4.665	1.336	1.665	-84.809
210.000	105.000	1.440	4.571	-0.600	4.682	1.329	1.677	-79.515
210.000	107.500	1.129	4.537	-0.900	4.760	0.906	1.927	-76.079
210.000	110.000	0.818	4.503	-0.900	4.711	0.610	2.051	-76.983
210.000	115.000	0.496	5.936	-0.600	6.001	0.431	2.785	-83.780
210.000	117.500	0.385	5.902	-0.200	5.909	0.378	2.766	-87.926
210.000	120.000	0.773	5.868	0.500	5.917	0.724	2.596	84.448
210.000	125.000	1.331	4.240	1.100	4.609	0.962	1.824	71.450
210.000	135.000	1.340	3.563	0.600	3.715	1.188	1.263	75.820
210.000	145.000	1.348	3.386	0.400	3.462	1.272	1.095	79.284
210.000	155.000	1.257	3.309	0.300	3.352	1.214	1.069	81.851
210.000	165.000	1.166	3.132	0.300	3.177	1.121	1.028	81.514
210.000	180.000	1.028	2.816	0.200	2.838	1.006	0.916	83.695
210.000	210.000	0.754	2.085	0.200	2.114	0.725	0.695	81.637
210.000	240.000	0.480	1.254	0.100	1.267	0.467	0.400	82.756
212.000	270.000	0.192	0.482	0.0	0.482	0.192	0.145	90.000
212.500	102.500	1.723	3.917	-0.500	4.026	1.614	1.206	-77.749
212.500	107.500	1.300	3.349	-0.800	3.624	1.025	1.300	-71.007
212.500	112.500	0.978	4.382	-0.800	4.561	0.799	1.881	-77.412
212.500	115.000	0.967	5.848	-0.300	5.866	0.949	2.459	-86.496
212.500	117.500	0.856	5.314	-0.100	5.316	0.854	2.231	-88.716
212.500	120.000	0.845	5.281	0.0	5.281	0.845	2.218	90.000
212.500	122.500	1.233	4.047	0.800	4.259	1.021	1.619	75.189
215.000	80.000	1.511	4.688	0.200	4.701	1.498	1.601	86.412
215.000	90.000	1.420	4.311	0.100	4.314	1.417	1.449	88.021
215.000	100.000	1.328	3.334	-0.200	3.354	1.308	1.023	-84.361
215.000	105.000	1.582	2.795	-0.300	2.865	1.512	0.677	-76.840
215.000	107.500	1.571	2.262	-0.300	2.374	1.459	0.458	-69.516
215.000	110.000	0.960	1.628	-0.500	1.895	0.693	0.601	-61.871
215.000	112.500	0.949	2.894	-0.300	2.939	0.904	1.018	-81.428
215.000	115.000	0.0	0.0	0.0	0.0	0.0	0.0	45.000
215.000	117.500	0.0	0.0	0.0	0.0	0.0	0.0	45.000
215.000	120.000	0.0	0.0	0.0	0.0	0.0	0.0	45.000
215.000	122.500	1.105	2.559	0.200	2.586	1.078	0.754	82.309
215.000	125.000	1.193	1.425	0.600	1.920	0.698	0.611	50.471



## STRESS DATA : CONFIGURATION 3 cont.

XC00RD	YC00RD	SIGX	SIGY	SIGXY	SIG1	SIG3	TAU	THETA
215.000	130.000	1.451	2.398	0.500	2.613	1.236	0.689	66.720
217.500	107.500	1.442	1.674	0.200	1.789	1.327	0.231	60.057
217.500	110.000	1.131	0.740	0.300	1.294	0.577	0.358	28.455
217.500	112.500	1.020	2.507	0.100	2.514	1.013	0.750	86.170
217.500	115.000	0.0	0.0	0.0	0.0	0.0	0.0	45.000
217.500	117.500	0.0	0.0	0.0	0.0	0.0	0.0	45.000
217.500	122.500	0.876	2.472	0.100	2.478	0.870	0.804	86.429
217.500	127.500	1.453	2.004	-0.0	2.004	1.453	0.275	90.000
220.000	0.0	2.408	7.000	0.100	7.002	2.406	2.298	88.753
220.000	30.000	2.234	6.169	0.100	6.172	2.231	1.970	88.545
220.000	60.000	1.859	5.238	0.200	5.250	1.847	1.701	86.624
220.000	70.000	1.668	4.961	0.300	4.988	1.641	1.674	84.837
220.000	105.000	1.248	2.391	0.500	2.579	1.060	0.759	69.409
220.000	110.000	1.102	1.253	0.800	1.981	0.374	0.804	47.696
220.000	112.500	1.191	2.419	0.300	2.488	1.122	0.683	76.980
220.000	115.000	0.0	0.0	0.0	0.0	0.0	0.0	45.000
220.000	120.000	0.0	0.0	0.0	0.0	0.0	0.0	45.000
220.000	122.500	0.847	2.784	-0.300	2.829	0.802	1.014	-81.395
220.000	125.000	0.736	1.550	-0.300	1.649	0.637	0.506	-71.803
220.000	130.000	1.713	2.883	-0.100	2.891	1.705	0.593	-85.150
220.000	135.000	1.371	2.955	-0.0	2.955	1.371	0.792	90.000
220.000	145.000	1.280	3.178	0.100	3.183	1.275	0.954	86.992
220.000	155.000	1.188	3.201	0.200	3.221	1.168	1.026	84.381
220.000	165.000	1.097	2.924	0.200	2.946	1.075	0.935	83.825
220.000	180.000	0.960	2.509	0.200	2.534	0.935	0.800	82.760
220.000	210.000	0.686	1.778	0.100	1.787	0.677	0.555	84.811
220.000	300.000	0.0	0.0	-0.0	0.0	0.0	0.0	45.000
222.500	112.500	1.162	3.831	0.800	4.052	0.941	1.556	74.529
222.500	115.000	0.751	4.898	0.0	4.898	0.751	2.073	90.000
222.500	117.500	0.740	4.864	-0.0	4.864	0.740	2.062	90.000
222.500	120.000	0.929	5.230	-0.300	5.251	0.908	2.171	-86.029
222.500	122.500	1.018	4.196	-0.700	4.343	0.871	1.736	-78.113
222.500	127.500	1.096	3.129	-0.500	3.245	0.980	1.133	-76.904
222.500	132.500	1.173	3.261	-0.400	3.335	1.099	1.118	-79.518
225.000	80.000	1.542	4.480	0.300	4.510	1.512	1.499	84.229
225.000	90.000	1.351	4.103	0.300	4.135	1.319	1.408	83.850
225.000	100.000	1.159	3.726	0.500	3.820	1.065	1.377	79.358
225.000	110.000	1.168	4.049	0.900	4.307	0.910	1.699	74.002
225.000	115.000	0.722	5.310	0.400	5.345	0.687	2.329	85.054
225.000	120.000	0.600	5.543	-0.400	5.575	0.568	2.504	-85.403
225.000	135.000	1.133	3.540	-0.300	3.577	1.096	1.240	-83.001
225.000	140.000	1.191	3.513	-0.200	3.530	1.174	1.178	-85.113
224.000	240.000	0.384	1.064	0.0	1.064	0.384	0.340	90.000





## STRESS DATA : CONFIGURATION 3 cont.

XCOORD	YCOORD	SIGX	SIGY	SIGXY	SIG1	SIG3	TAU	THETA
225.000	270.000	0.192	0.582	-0.0	0.582	0.192	0.195	90.000
227.500	122.500	0.860	4.521	-0.600	4.617	0.764	1.926	-80.926
227.500	127.500	0.938	3.954	-0.600	4.069	0.823	1.623	-79.152
227.500	132.500	1.115	4.086	-0.400	4.139	1.062	1.538	-82.465
227.500	137.500	0.993	4.119	-0.200	4.132	0.980	1.576	-86.354
230.000	0.0	2.339	6.791	0.100	6.793	2.337	2.228	88.714
230.000	30.000	2.065	5.960	0.200	5.970	2.055	1.958	87.068
230.000	60.000	1.791	5.129	0.300	5.156	1.764	1.696	84.905
230.000	70.000	1.599	4.852	0.300	4.879	1.572	1.654	84.775
230.000	115.000	1.188	4.706	0.200	4.717	1.177	1.770	86.757
230.000	120.000	0.942	4.767	-0.100	4.770	0.939	1.915	-88.503
230.000	140.000	1.053	4.197	-0.100	4.200	1.050	1.575	-88.180
230.000	145.000	1.111	3.871	0.200	3.885	1.097	1.394	85.877
230.000	155.000	1.020	3.094	0.400	3.168	0.946	1.111	79.453
230.000	165.000	1.129	2.517	0.200	2.545	1.101	0.722	81.962
230.000	180.000	0.991	2.301	0.100	2.309	0.983	0.663	85.660
232.500	122.500	0.902	4.146	-0.200	4.158	0.890	1.634	-86.485
232.500	127.500	1.080	4.079	-0.400	4.131	1.028	1.552	-82.532
232.500	132.500	0.858	3.611	-0.600	3.736	0.733	1.502	-78.224
232.500	137.500	0.835	4.444	-0.400	4.488	0.791	1.848	-83.751
232.500	142.500	0.713	4.576	-0.100	4.579	0.710	1.934	-88.518
235.000	80.000	1.473	4.471	0.300	4.501	1.443	1.529	84.341
235.000	90.000	1.282	4.194	0.400	4.248	1.228	1.510	82.319
235.000	100.000	1.091	4.117	0.400	4.169	1.039	1.565	82.596
235.000	110.000	1.099	4.140	0.200	4.153	1.086	1.534	86.253
235.000	120.000	1.108	3.763	-0.0	3.763	1.108	1.327	90.000
235.000	125.000	1.062	3.625	-0.200	3.641	1.046	1.297	-85.565
235.000	140.000	0.495	4.922	-0.500	4.978	0.439	2.269	-83.636
235.000	145.000	0.673	4.555	0.400	4.596	0.632	1.982	84.178
235.000	150.000	1.031	3.029	0.900	3.375	0.685	1.345	68.992
235.000	210.000	0.583	1.567	0.0	1.567	0.583	0.492	90.000
235.000	240.000	0.384	1.164	-0.0	1.164	0.384	0.390	90.000
235.000	270.000	0.192	0.582	-0.0	0.582	0.192	0.195	90.000
235.000	300.000	0.0	0.0	-0.0	0.0	0.0	0.0	45.000
237.500	127.500	1.122	3.103	-0.300	3.147	1.078	1.035	-81.575
237.500	132.500	1.000	2.536	-0.400	2.634	0.902	0.866	-76.244
237.500	137.500	0.878	3.468	-0.600	3.600	0.746	1.427	-77.570
237.500	140.000	0.666	4.435	-0.200	4.446	0.655	1.895	-86.971
237.500	142.500	0.555	4.201	-0.100	4.204	0.552	1.826	-88.430
237.500	145.000	0.644	3.967	0.0	3.967	0.644	1.661	90.000
237.500	147.500	0.933	3.133	0.600	3.286	0.780	1.253	75.695
240.000	0.0	2.270	6.683	0.100	6.685	2.268	2.209	88.702
240.000	30.000	1.996	5.852	0.200	5.862	1.986	1.938	87.039





STRESS DATA : CONFIGURATION 3 cont.

XCOORD	YCOORD	SIGX	SIGY	SIGXY	SIG1	SIG3	TAU	THETA
240.000	60.000	1.722	5.021	0.300	5.048	1.695	1.677	84.846
240.000	70.000	1.531	4.744	0.300	4.772	1.503	1.634	84.711
240.000	125.000	1.228	2.921	-0.100	2.927	1.222	0.852	-86.631
240.000	130.000	1.382	2.482	-0.0	2.482	1.382	0.550	90.000
240.000	135.000	0.760	1.315	-0.200	1.380	0.695	0.342	-72.109
240.000	137.500	0.849	2.181	-0.200	2.210	0.820	0.695	-81.642
240.000	140.000	0.0	0.0	0.0	0.0	0.0	0.0	45.000
240.000	145.000	0.0	0.0	0.0	0.0	0.0	0.0	45.000
240.000	147.500	0.804	1.846	0.100	1.856	0.794	0.531	84.567
240.000	150.000	0.893	1.112	0.400	1.417	0.588	0.415	52.655
240.000	155.000	1.252	1.986	0.300	2.093	1.145	0.474	70.368
240.000	165.000	1.060	2.209	0.0	2.209	1.060	0.574	90.000
242.500	132.500	1.142	1.661	-0.0	1.661	1.142	0.260	90.000
242.500	137.500	0.720	1.893	0.100	1.901	0.712	0.595	85.162
242.500	147.500	0.675	1.758	0.0	1.758	0.675	0.542	90.000
242.500	152.500	1.253	1.591	0.100	1.618	1.226	0.196	74.693
245.000	80.000	1.305	4.363	0.300	4.392	1.276	1.558	84.450
245.000	90.000	1.213	4.186	0.300	4.216	1.183	1.516	84.295
245.000	100.000	1.122	4.009	0.200	4.023	1.108	1.457	86.056
245.000	110.000	1.131	3.632	0.200	3.648	1.115	1.266	85.457
245.000	120.000	1.139	3.155	0.200	3.175	1.119	1.028	84.389
245.000	130.000	1.048	2.378	0.400	2.489	0.937	0.776	74.486
245.000	135.000	0.902	1.139	0.500	1.534	0.507	0.514	51.667
245.000	137.500	0.891	1.806	0.200	1.848	0.849	0.499	78.193
245.000	140.000	0.0	0.0	0.0	0.0	0.0	0.0	45.000
245.000	145.000	0.0	0.0	0.0	0.0	0.0	0.0	45.000
245.000	147.500	0.746	2.071	-0.200	2.101	0.716	0.692	-81.601
245.000	150.000	0.735	1.237	-0.300	1.377	0.595	0.391	-64.959
245.000	155.000	1.213	2.069	-0.200	2.113	1.169	0.472	-77.477
245.000	160.000	1.272	1.944	-0.200	1.999	1.217	0.391	-74.619
247.500	137.500	0.962	2.918	0.600	3.087	0.793	1.147	74.235
247.500	140.000	0.551	3.684	-0.0	3.684	0.551	1.566	90.000
247.500	142.500	0.540	3.650	-0.100	3.653	0.537	1.558	-88.160
247.500	145.000	0.629	4.017	-0.200	4.029	0.617	1.706	-86.633
247.500	147.500	0.817	2.983	-0.600	3.138	0.662	1.238	-75.506
248.000	180.000	0.868	2.128	-0.100	2.136	0.860	0.638	-85.490
245.000	240.000	0.384	1.164	-0.0	1.164	0.384	0.390	90.000
250.000	0.0	2.202	6.475	0.100	6.477	2.200	2.139	88.660
250.000	50.000	1.745	5.090	0.200	5.102	1.733	1.684	86.590
250.000	60.000	1.553	4.913	0.300	4.940	1.526	1.707	84.938
250.000	70.000	1.462	4.636	0.300	4.664	1.434	1.615	84.648
250.000	135.000	1.068	3.135	1.000	3.540	0.663	1.438	67.972
250.000	140.000	0.622	4.097	0.400	4.142	0.577	1.783	83.518
250.000	145.000	0.300	4.129	-0.400	4.170	0.259	1.956	-84.099



## STRESS DATA : CONFIGURATION 3 cont.

XCOORD	YCOORD	SIGX	SIGY	SIGXY	SIG1	SIG3	TAU	THETA
250.000	150.000	0.577	2.762	-0.600	2.916	0.423	1.246	-75.612
250.000	155.000	0.955	2.894	-0.400	2.973	0.876	1.049	-78.790
250.000	160.000	1.133	2.627	-0.200	2.653	1.107	0.773	-82.506
250.000	165.000	1.092	2.302	-0.200	2.334	1.060	0.637	-80.854
250.000	270.000	0.192	0.582	-0.0	0.582	0.192	0.195	90.000
250.000	300.000	0.0	0.0	-0.0	0.0	0.0	0.0	45.000
255.000	80.000	1.252	4.404	0.300	4.432	1.224	1.604	84.611
255.000	90.000	1.161	4.127	0.300	4.157	1.131	1.513	84.282
255.000	100.000	1.070	3.950	0.200	3.964	1.056	1.454	86.046
255.000	110.000	1.078	3.673	0.300	3.707	1.044	1.332	83.491
255.000	120.000	0.987	3.396	0.400	3.461	0.922	1.269	80.815
255.000	130.000	0.795	3.419	0.400	3.479	0.735	1.372	81.522
255.000	140.000	1.004	3.742	0.300	3.774	0.972	1.401	83.820
255.000	145.000	0.858	3.804	0.0	3.804	0.858	1.473	90.000
255.000	150.000	0.636	3.136	-0.400	3.198	0.574	1.312	-81.128
255.000	155.000	0.914	3.069	-0.300	3.110	0.873	1.118	-82.221
256.000	160.000	0.996	3.016	-0.200	3.036	0.976	1.030	-84.400
254.000	165.000	0.964	2.619	-0.100	2.625	0.958	0.834	-86.555
260.000	0.0	2.231	6.665	0.200	6.674	2.222	2.226	87.423
260.000	30.000	1.957	5.834	0.200	5.844	1.947	1.949	87.055
260.000	60.000	1.583	5.003	0.200	5.015	1.571	1.722	86.665
260.000	70.000	1.492	4.826	0.200	4.838	1.480	1.679	86.579
260.000	145.000	1.106	3.848	0.100	3.852	1.102	1.375	87.914
260.000	150.000	0.960	3.310	-0.100	3.314	0.956	1.179	-87.568
260.000	180.000	0.768	2.328	-0.100	2.334	0.762	0.786	-86.347
260.000	210.000	0.576	1.746	-0.0	1.746	0.576	0.585	90.000
260.000	240.000	0.384	1.164	-0.0	1.164	0.384	0.390	90.000
260.000	270.000	0.192	0.582	-0.0	0.582	0.192	0.195	90.000
260.000	300.000	0.0	0.0	-0.0	0.0	0.0	0.0	45.000
265.000	80.000	1.314	4.690	0.200	4.702	1.302	1.700	86.621
265.000	90.000	1.222	4.413	0.200	4.425	1.210	1.608	86.427
265.000	100.000	1.231	4.236	0.200	4.249	1.218	1.516	86.209
265.000	110.000	1.140	3.959	0.200	3.973	1.126	1.424	85.962
265.000	120.000	1.048	3.782	0.200	3.797	1.033	1.382	85.838
265.000	130.000	1.057	3.705	0.100	3.709	1.053	1.328	87.840
265.000	140.000	1.165	3.428	0.0	3.428	1.165	1.132	90.000
270.000	0.0	2.259	6.848	0.200	6.857	2.250	2.303	87.509
270.000	30.000	1.985	6.017	0.200	6.027	1.975	2.026	87.167
270.000	60.000	1.610	5.286	0.200	5.297	1.599	1.849	86.895
270.000	160.000	0.996	2.816	-0.0	2.816	0.996	0.910	90.000
270.000	180.000	0.768	2.428	-0.100	2.434	0.762	0.836	-86.565
275.000	195.000	0.672	2.037	-0.0	2.037	0.672	0.682	90.000
290.000	0.0	2.314	7.114	0.100	7.116	2.312	2.402	88.807
290.000	30.000	2.039	6.183	0.200	6.193	2.029	2.082	87.243



## STRESS DATA : CONFIGURATION 3 cont.

XC00RD	YC00RD	SIGX	SIGY	SIGXY	SIGI	SIG3	TAU	THETA
290.000	60.000	1.665	5.552	0.100	5.555	1.662	1.946	88.527
290.000	90.000	1.391	4.721	0.100	4.724	1.388	1.668	88.281
290.000	120.000	1.217	3.990	0.0	3.990	1.217	1.386	90.000
290.000	150.000	1.042	3.259	0.0	3.259	1.042	1.108	90.000
290.000	180.000	0.768	2.328	-0.0	2.328	0.768	0.780	90.000
290.000	210.000	0.576	1.746	-0.0	1.746	0.576	0.585	90.000
290.000	240.000	0.384	1.164	-0.0	1.164	0.384	0.390	90.000
290.000	270.000	0.192	0.582	-0.0	0.582	0.192	0.195	90.000
290.000	300.000	0.0	0.0	-0.0	0.0	0.0	0.0	45.000
320.000	30.000	2.122	6.632	0.100	6.634	2.120	2.257	88.730
320.000	90.000	1.573	5.070	0.0	5.070	1.573	1.748	90.000
320.000	150.000	1.125	3.408	-0.0	3.408	1.125	1.141	90.000
320.000	210.000	0.576	1.746	0.0	1.746	0.576	0.585	90.000
320.000	240.000	0.384	1.164	-0.0	1.164	0.384	0.390	90.000
320.000	270.000	0.192	0.582	-0.0	0.582	0.192	0.195	90.000
320.000	300.000	0.0	0.0	-0.0	0.0	0.0	0.0	45.000
350.000	0.0	2.478	7.712	0.100	7.714	2.476	2.619	88.906
350.000	60.000	1.929	6.150	0.0	6.150	1.929	2.110	90.000
350.000	120.000	1.381	4.488	-0.0	4.488	1.381	1.554	90.000
350.000	180.000	0.933	2.826	-0.0	2.826	0.933	0.946	90.000
350.000	240.000	0.384	1.164	0.0	1.164	0.384	0.390	90.000
350.000	270.000	0.192	0.582	-0.0	0.582	0.192	0.195	90.000
350.000	300.000	0.0	0.0	0.0	0.0	0.0	0.0	45.000
380.000	270.000	0.192	0.582	0.0	0.582	0.192	0.195	90.000
380.000	300.000	0.0	0.0	0.0	0.0	0.0	0.0	45.000
410.000	0.0	2.742	8.310	0.0	8.310	2.742	2.784	90.000
410.000	60.000	2.094	6.648	0.0	6.648	2.094	2.277	90.000
410.000	120.000	1.645	4.986	-0.0	4.986	1.645	1.670	90.000
410.000	180.000	1.097	3.324	-0.0	3.324	1.097	1.113	90.000
410.000	240.000	0.548	1.662	0.0	1.662	0.548	0.557	90.000
410.000	300.000	0.0	0.0	0.0	0.0	0.0	0.0	45.000
470.000	0.0	2.742	8.310	0.0	8.310	2.742	2.784	90.000
470.000	60.000	2.194	6.648	0.0	6.648	2.194	2.227	90.000
470.000	120.000	1.645	4.986	-0.0	4.986	1.645	1.670	90.000
470.000	180.000	1.097	3.324	-0.0	3.324	1.097	1.113	90.000
470.000	240.000	0.548	1.662	-0.0	1.662	0.548	0.557	90.000
470.000	300.000	0.0	0.0	-0.0	0.0	0.0	0.0	45.000
530.000	0.0	2.742	8.310	0.0	8.310	2.742	2.784	90.000
530.000	60.000	2.194	6.648	-0.0	6.648	2.194	2.227	90.000
530.000	120.000	1.645	4.986	-0.0	4.986	1.645	1.670	90.000
530.000	180.000	1.097	3.324	-0.0	3.324	1.097	1.113	90.000
530.000	240.000	0.548	1.662	-0.0	1.662	0.548	0.557	90.000
530.000	300.000	0.0	0.0	-0.0	0.0	0.0	0.0	45.000



#### CONFIGURATION 4





STRESS DATA : CONFIGURATION 4

XCOORD	YCOORD	SIGX	SIGY	SIGXY	SIG1	SIG3	TAU	THETA
0.0	0.0	2.842	8.310	0.0	8.310	2.842	2.734	90.000
0.0	60.000	2.294	6.648	0.0	6.648	2.294	2.177	90.000
0.0	120.000	1.645	4.986	0.0	4.986	1.645	1.670	90.000
0.0	180.000	0.997	3.324	0.100	3.328	0.993	1.168	87.544
0.0	240.000	0.348	1.562	0.100	1.570	0.340	0.615	85.322
0.0	300.000	-0.400	-0.100	0.100	-0.430	-0.070	0.180	163.155
30.000	0.0	2.742	8.410	0.0	8.410	2.742	2.834	90.000
30.000	30.000	2.568	7.579	0.0	7.579	2.568	2.505	90.000
30.000	90.000	1.920	5.817	0.0	5.817	1.920	1.948	90.000
30.000	150.000	1.271	4.155	0.100	4.158	1.268	1.445	88.017
30.000	210.000	0.623	2.493	0.100	2.498	0.618	0.940	86.948
30.000	270.000	-0.026	0.831	0.100	0.843	-0.038	0.440	83.432
30.000	300.000	-0.400	0.0	0.100	-0.424	0.024	0.224	166.717
60.000	0.0	2.842	8.510	0.100	8.512	2.840	2.836	88.990
60.000	60.000	2.294	6.748	0.100	6.750	2.292	2.229	88.714
60.000	120.000	1.645	5.086	0.100	5.089	1.642	1.723	88.337
60.000	180.000	0.997	4.255	0.100	4.258	1.268	1.495	88.083
60.000	210.000	0.623	3.324	0.100	3.328	0.993	1.168	87.544
60.000	240.000	0.348	2.493	0.100	2.498	0.618	0.940	86.948
60.000	270.000	0.074	1.662	0.100	1.670	0.340	0.665	85.673
60.000	300.000	-0.300	0.831	0.100	0.844	0.061	0.391	82.600
90.000	0.0	2.842	8.510	0.100	-0.330	0.030	0.180	163.155
90.000	30.000	2.568	7.679	0.100	8.512	2.840	2.836	88.990
90.000	60.000	2.294	6.848	0.100	7.681	2.566	2.557	88.879
90.000	90.000	1.920	5.917	0.100	6.850	2.292	2.279	88.743
90.000	120.000	1.645	5.086	0.100	5.919	1.918	2.001	88.568
90.000	180.000	0.997	3.324	0.100	5.089	1.642	1.723	88.337
90.000	240.000	0.348	1.662	0.100	3.328	0.993	1.168	87.544
90.000	300.000	-0.200	0.0	0.100	1.670	0.340	0.665	85.673
110.000	0.0	2.648	8.024	-0.0	-0.241	0.041	0.141	157.500
110.000	20.000	2.659	7.954	0.100	8.024	2.648	2.688	90.000
110.000	40.000	2.577	7.402	0.200	7.956	2.657	2.649	88.919
120.000	90.000	1.920	6.017	0.100	7.410	2.569	2.421	87.630
120.000	150.000	1.271	4.255	0.200	6.019	1.918	2.051	88.603
120.000	210.000	0.723	2.493	0.100	4.268	1.258	1.505	86.183
120.000	270.000	0.074	0.831	0.100	2.499	0.717	0.891	86.777
120.000	300.000	-0.200	0.0	0.100	0.844	0.061	0.391	82.600
130.000	0.0	2.647	8.023	0.0	-0.200	0.0	0.100	180.000
130.000	20.000	2.465	7.469	-0.0	8.023	2.647	2.688	90.000
130.000	40.000	2.476	7.399	0.100	7.469	2.465	2.502	90.000
130.000	60.000	2.294	6.848	0.100	7.401	2.474	2.464	88.837
150.000	0.0	2.647	8.021	-0.0	6.850	2.292	2.279	88.743
					8.021	2.647	2.687	90.000



## STRESS DATA : CONFIGURATION 4 cont.

XCOORD	YCOORD	SIGX	SIGY	SIGXY	SIG1	SIG3	TAU	THETA
150.000	30.000	2.373	7.190	-0.0	7.190	2.373	2.408	90.000
150.000	40.000	2.281	6.913	-0.0	6.913	2.281	2.316	90.000
150.000	60.000	2.292	6.843	0.100	6.845	2.290	2.278	88.742
150.000	90.000	1.920	6.117	0.200	6.127	1.910	2.108	87.278
150.000	120.000	1.545	5.086	0.300	5.111	1.520	1.796	85.191
150.000	150.000	1.271	4.055	0.200	4.069	1.257	1.406	85.912
150.000	180.000	0.997	3.324	0.100	3.328	0.993	1.168	87.544
150.000	210.000	0.723	2.493	0.100	2.499	0.717	0.891	86.777
150.000	240.000	0.448	1.662	0.100	1.670	0.440	0.615	85.322
150.000	270.000	0.174	0.831	0.100	0.846	0.159	0.343	81.534
150.000	300.000	-0.100	0.0	0.0	-0.100	0.0	0.050	180.000
170.000	0.0	2.646	7.919	-0.0	7.919	2.646	2.636	90.000
170.000	30.000	2.372	7.088	-0.100	7.090	2.370	2.360	-88.786
170.000	60.000	2.198	6.257	-0.100	6.259	2.196	2.032	-88.590
170.000	80.000	1.909	6.387	0.0	6.387	1.909	2.239	90.000
170.000	90.000	1.820	6.217	0.200	6.226	1.811	2.208	87.401
170.000	100.000	1.628	5.940	0.400	5.977	1.591	2.193	84.745
170.000	110.000	1.437	5.163	0.500	5.229	1.371	1.929	82.488
180.000	70.000	2.106	5.579	-0.200	5.590	2.095	1.748	-86.715
180.000	80.000	1.662	5.744	-0.300	5.766	1.640	2.063	-85.819
180.000	90.000	1.417	6.309	0.100	6.311	1.415	2.448	88.830
180.000	95.000	1.574	6.378	0.800	6.508	1.444	2.532	80.790
180.000	105.000	1.382	5.301	0.800	5.458	1.225	2.117	78.896
180.000	115.000	1.591	4.424	0.700	4.588	1.427	1.580	76.851
180.000	125.000	1.600	4.547	0.400	4.600	1.547	1.527	82.406
180.000	135.000	1.508	4.370	0.300	4.401	1.477	1.462	84.080
180.000	145.000	1.417	4.093	0.200	4.108	1.402	1.353	85.749
180.000	155.000	1.325	3.816	0.100	3.820	1.321	1.250	87.705
180.000	165.000	1.234	3.639	0.100	3.643	1.230	1.207	87.623
180.000	180.000	0.997	3.324	0.100	3.328	0.993	1.168	87.544
180.000	210.000	0.723	2.493	0.100	2.499	0.717	0.891	86.777
180.000	240.000	0.448	1.662	0.100	1.670	0.440	0.615	85.322
180.000	270.000	0.274	0.831	0.0	0.831	0.274	0.278	90.000
180.000	300.000	0.0	0.0	0.0	0.0	0.0	0.0	45.000
185.000	85.000	1.016	4.805	-0.700	4.930	0.891	2.020	-79.861
185.000	90.000	0.593	6.538	-0.500	6.580	0.551	3.014	-85.226
185.000	95.000	0.971	6.570	0.700	6.656	0.885	2.886	82.981
185.000	100.000	1.528	4.740	1.600	5.401	0.867	2.267	67.554
187.500	87.500	1.393	5.536	-0.500	5.595	1.334	2.131	-83.215
187.500	90.000	1.182	6.502	-0.300	6.519	1.165	2.677	-86.783
187.500	92.500	0.971	6.068	-0.100	6.070	0.969	2.550	-88.877
187.500	95.000	1.059	6.035	0.0	6.035	1.059	2.488	90.000
187.500	97.500	1.448	4.701	1.000	4.984	1.165	1.909	74.208



STRESS DATA : CONFIGURATION 4 cont.

XC00RD	YC00RD	SIGX	SIGY	SIGXY	SIG1	SIG3	TAU	THETA
190.000	0.0	2.546	7.717	-0.0	7.717	2.546	2.585	90.000
190.000	30.000	2.371	6.886	-0.100	6.888	2.369	2.260	-88.732
190.000	60.000	2.197	5.755	-0.100	5.758	2.194	1.782	-88.391
190.000	70.000	2.106	4.878	-0.100	4.882	2.102	1.390	-87.937
190.000	80.000	1.914	4.301	-0.200	4.318	1.897	1.210	-85.244
190.000	85.000	1.392	3.534	-0.500	3.645	1.281	1.182	-77.487
190.000	87.500	1.981	5.400	-0.300	5.426	1.955	1.736	-85.023
190.000	90.000	0.0	0.0	0.0	0.0	0.0	0.0	45.000
190.000	95.000	0.0	0.0	0.0	0.0	0.0	0.0	45.000
190.000	97.500	1.336	3.165	0.200	3.187	1.314	0.936	83.832
190.000	100.000	1.225	1.731	0.700	2.222	0.734	0.744	54.936
190.000	105.000	1.782	3.301	0.500	3.451	1.632	0.909	73.321
190.000	115.000	1.891	4.224	0.200	4.241	1.874	1.184	85.135
190.000	125.000	1.800	4.347	0.100	4.351	1.796	1.277	87.755
190.000	135.000	1.608	4.270	0.100	4.274	1.604	1.335	87.852
190.000	145.000	1.517	4.093	0.100	4.097	1.513	1.292	87.780
190.000	155.000	1.325	3.816	0.100	3.820	1.321	1.250	87.705
190.000	165.000	1.134	3.639	0.100	3.643	1.130	1.256	87.718
190.000	180.000	0.997	3.224	0.100	3.228	0.993	1.118	87.434
190.000	210.000	0.723	2.393	0.100	2.399	0.717	0.841	86.585
190.000	240.000	0.448	1.562	0.100	1.571	0.439	0.566	84.911
190.000	270.000	0.274	0.831	0.0	0.831	0.274	0.278	90.000
190.000	300.000	0.0	0.0	0.0	0.0	0.0	0.0	45.000
192.500	87.500	1.369	3.864	-0.300	3.900	1.333	1.283	-83.239
192.500	97.500	1.025	3.029	0.100	3.034	1.020	1.007	87.150
192.500	102.500	1.802	2.562	-0.100	2.575	1.789	0.393	-82.628
195.000	80.000	1.814	3.901	0.500	4.015	1.700	1.157	77.199
195.000	85.000	1.369	1.962	0.500	2.247	1.084	0.581	60.334
195.000	87.500	1.457	3.129	0.200	3.153	1.433	0.860	83.273
195.000	90.000	0.0	0.0	0.0	0.0	0.0	0.0	45.000
195.000	95.000	0.0	0.0	0.0	0.0	0.0	0.0	45.000
195.000	97.500	1.213	3.294	-0.300	3.336	1.171	1.083	-81.958
195.000	100.000	0.902	1.560	-0.400	1.749	0.713	0.518	-64.719
195.000	105.000	2.479	4.292	-0.300	4.340	2.431	0.955	-80.844
195.000	110.000	2.037	4.263	-0.200	4.281	2.019	1.131	-84.906
197.500	87.500	1.446	4.693	0.900	4.926	1.213	1.856	75.499
197.500	90.000	1.035	6.059	0.0	6.059	1.035	2.512	90.000
197.500	92.500	0.923	5.925	-0.100	5.927	0.921	2.503	-88.855
197.500	95.000	1.112	6.392	-0.300	6.409	1.095	2.657	-86.758
197.500	97.500	0.901	4.458	-0.900	4.673	0.686	1.993	-76.579
197.500	100.000	0.790	2.324	-1.000	2.817	0.297	1.260	-63.744
197.500	102.500	1.679	3.790	-0.500	3.902	1.567	1.168	-77.326
197.500	105.000	2.368	5.257	-0.300	5.288	2.337	1.475	-84.134





# STRESS DATA : CONFIGURATION 4 cont.

XCOORD	YCOORD	SIGX	SIGY	SIGXY	SIG1	SIG3	TAU	THETA
197.500	107.500	2.057	4.823	-0.200	4.837	2.043	1.397	-85.886
200.000	0.0	2.545	7.716	0.0	7.716	2.545	2.585	90.000
200.000	30.000	2.371	6.785	0.0	6.785	2.371	2.207	90.000
200.000	60.000	2.097	5.654	0.100	5.657	2.094	1.781	88.391
200.000	70.000	1.906	5.177	0.400	5.225	1.858	1.684	83.128
200.000	85.000	1.568	4.862	1.400	5.377	1.053	2.162	69.817
200.000	90.000	0.823	6.323	0.600	6.388	0.758	2.815	83.846
200.000	95.000	0.500	6.356	-0.400	6.383	0.473	2.955	-86.110
200.000	97.500	0.389	5.322	-0.900	5.481	0.230	2.626	-79.977
200.000	100.000	0.678	4.188	-0.700	4.322	0.544	1.889	-79.127
200.000	105.000	1.656	4.921	-0.300	4.948	1.629	1.660	-84.793
200.000	107.500	1.945	4.787	-0.200	4.801	1.931	1.435	-85.994
200.000	110.000	1.934	4.853	-0.200	4.867	1.920	1.473	-86.099
200.000	115.000	1.791	4.624	-0.200	4.638	1.777	1.431	-85.982
200.000	125.000	1.800	4.547	-0.100	4.551	1.796	1.377	-87.918
200.000	135.000	1.608	4.470	0.0	4.470	1.608	1.431	90.000
200.000	145.000	1.417	4.193	0.0	4.193	1.417	1.388	90.000
200.000	155.000	1.325	3.916	0.100	3.920	1.321	1.299	87.793
200.000	165.000	1.134	3.639	0.100	3.643	1.130	1.256	87.718
200.000	180.000	0.997	3.224	0.100	3.228	0.993	1.118	87.434
200.000	210.000	0.723	2.393	0.100	2.399	0.717	0.841	86.585
200.000	240.000	0.548	1.562	0.100	1.572	0.538	0.517	84.421
200.000	270.000	0.274	0.831	0.0	0.831	0.274	0.278	90.000
200.000	300.000	0.0	0.0	0.0	0.0	0.0	0.0	45.000
202.500	97.500	0.660	5.535	-0.200	5.543	0.652	2.446	-87.655
202.500	107.500	1.716	4.900	-0.300	4.928	1.688	1.620	-84.664
202.500	112.500	1.894	5.032	-0.200	5.045	1.881	1.582	-86.368
205.000	80.000	1.580	5.296	0.600	5.390	1.486	1.952	81.052
205.000	90.000	1.288	5.719	0.400	5.755	1.252	2.251	84.883
205.000	95.000	0.943	5.781	0.200	5.789	0.935	2.427	87.637
205.000	97.500	0.832	5.547	-0.100	5.549	0.830	2.360	-88.785
205.000	100.000	1.020	5.313	-0.300	5.334	0.999	2.167	-86.022
205.000	105.000	1.598	5.146	-0.300	5.171	1.573	1.799	-85.201
205.000	107.500	1.687	5.212	-0.200	5.223	1.676	1.774	-86.763
205.000	110.000	1.776	5.078	-0.200	5.090	1.764	1.663	-86.546
205.000	115.000	1.854	5.011	-0.200	5.024	1.841	1.591	-86.389
205.000	120.000	1.711	4.782	-0.200	4.795	1.698	1.548	-86.289
207.500	97.500	1.103	5.559	0.0	5.559	1.103	2.228	90.000
207.500	100.000	0.891	5.426	-0.200	5.435	0.882	2.276	-87.480
207.500	102.500	1.180	5.292	-0.300	5.314	1.158	2.078	-85.849
207.500	105.000	1.669	5.158	-0.200	5.169	1.658	1.756	-86.730
207.500	107.500	1.658	5.224	-0.200	5.235	1.647	1.794	-86.800
207.500	110.000	1.747	5.091	-0.200	5.103	1.735	1.684	-86.589





## STRESS DATA : CONFIGURATION 4 cont.

XCOORD	YCOORD	SIGX	SIGY	SIGXY	SIG1	SIG3	TAU	THETA
207.500	112.500	1.836	5.057	-0.100	5.060	1.833	1.614	-88.223
207.500	115.000	1.825	5.023	-0.100	5.026	1.822	1.602	-88.211
207.500	117.500	1.814	4.989	-0.100	4.992	1.811	1.591	-88.198
210.000	0.0	2.477	7.508	0.0	7.508	2.477	2.516	90.000
210.000	30.000	2.302	6.577	0.100	6.579	2.300	2.140	88.661
210.000	60.000	1.928	5.646	0.300	5.670	1.904	1.883	85.416
210.000	70.000	1.737	5.469	0.400	5.511	1.695	1.908	83.950
210.000	95.000	1.308	5.577	0.200	5.586	1.299	2.144	87.324
210.000	100.000	1.263	5.338	-0.100	5.340	1.261	2.040	-88.595
210.000	105.000	1.540	5.271	-0.200	5.282	1.529	1.876	-86.940
210.000	107.500	1.629	5.137	-0.200	5.148	1.618	1.765	-86.747
210.000	110.000	1.718	5.103	-0.200	5.115	1.706	1.704	-86.630
210.000	115.000	1.796	5.036	-0.100	5.039	1.793	1.623	-88.234
210.000	117.500	1.785	5.002	-0.100	5.005	1.782	1.612	-88.221
210.000	120.000	1.773	4.968	-0.100	4.971	1.770	1.601	-88.209
210.000	125.000	1.631	4.640	-0.100	4.643	1.628	1.508	-88.099
210.000	135.000	1.440	4.363	-0.0	4.363	1.440	1.462	90.000
210.000	145.000	1.348	4.186	0.0	4.186	1.348	1.419	90.000
210.000	155.000	1.257	3.809	0.100	3.813	1.253	1.280	87.760
210.000	165.000	1.066	3.432	0.100	3.436	1.062	1.187	87.584
210.000	180.000	0.928	3.016	0.100	3.021	0.923	1.049	87.264
210.000	210.000	0.654	2.185	0.100	2.192	0.647	0.772	86.279
210.000	240.000	0.480	1.354	0.100	1.365	0.469	0.448	83.555
212.000	270.000	0.192	0.582	0.0	0.582	0.192	0.195	90.000
212.500	102.500	1.423	5.317	-0.100	5.320	1.420	1.950	-88.530
212.500	107.500	1.600	5.149	-0.200	5.160	1.589	1.786	-86.785
212.500	112.500	1.678	4.982	-0.100	4.985	1.675	1.655	-88.268
212.500	115.000	1.667	4.948	-0.100	4.951	1.664	1.644	-88.256
212.500	117.500	1.756	4.914	-0.100	4.917	1.753	1.582	-88.188
212.500	120.000	1.745	4.981	-0.100	4.984	1.742	1.621	-88.232
212.500	122.500	1.633	4.847	-0.100	4.850	1.630	1.610	-88.220
215.000	80.000	1.511	5.388	0.300	5.411	1.488	1.962	85.601
215.000	90.000	1.420	5.311	0.200	5.321	1.410	1.956	87.065
215.000	100.000	1.328	5.134	-0.100	5.137	1.325	1.906	-88.496
215.000	105.000	1.482	5.095	-0.100	5.098	1.479	1.809	-88.416
215.000	107.500	1.571	5.162	-0.100	5.165	1.568	1.798	-88.406
215.000	110.000	1.560	5.028	-0.100	5.031	1.557	1.737	-88.350
215.000	112.500	1.649	4.994	-0.100	4.997	1.646	1.675	-88.289
215.000	115.000	1.638	4.960	-0.100	4.963	1.635	1.664	-88.277
215.000	117.500	1.627	4.927	-0.100	4.930	1.624	1.653	-88.266
215.000	120.000	1.716	4.893	-0.100	4.896	1.713	1.592	-88.199
215.000	122.500	1.705	4.859	-0.100	4.862	1.702	1.580	-88.186
215.000	125.000	1.593	4.825	-0.100	4.828	1.590	1.619	-88.230



STRESS DATA : CONFIGURATION 4 cont.

XCOORD	YCOORD	SIGX	SIGY	SIGXY	SIG1	SIG3	TAU	THETA
215.000	130.000	1.451	4.598	-0.100	4.601	1.448	1.577	-88.182
217.500	107.500	1.542	4.974	-0.100	4.977	1.539	1.719	-88.333
217.500	110.000	1.631	4.940	-0.100	4.943	1.628	1.658	-88.270
217.500	112.500	1.620	4.907	-0.100	4.910	1.617	1.647	-88.259
217.500	115.000	1.609	4.873	-0.100	4.876	1.606	1.635	-88.247
217.500	117.500	1.598	4.839	-0.100	4.842	1.595	1.624	-88.234
217.500	122.500	1.576	4.772	-0.100	4.775	1.573	1.601	-88.210
217.500	127.500	1.453	4.704	-0.100	4.707	1.450	1.629	-88.240
220.000	0.0	2.408	7.300	0.100	7.302	2.406	2.448	88.830
220.000	30.000	2.134	6.369	0.100	6.371	2.132	2.120	88.648
220.000	60.000	1.859	5.538	0.200	5.549	1.848	1.850	86.897
220.000	70.000	1.668	5.461	0.200	5.472	1.657	1.907	86.990
220.000	105.000	1.448	4.891	-0.200	4.903	1.436	1.733	-86.687
220.000	110.000	1.502	4.853	-0.100	4.856	1.499	1.678	-88.292
220.000	112.500	1.591	4.819	-0.100	4.822	1.588	1.617	-88.227
220.000	115.000	1.580	4.785	-0.100	4.788	1.577	1.606	-88.215
220.000	120.000	1.558	4.718	-0.100	4.721	1.555	1.583	-88.189
220.000	122.500	1.547	4.684	-0.100	4.687	1.544	1.572	-88.176
220.000	125.000	1.536	4.650	-0.100	4.653	1.533	1.560	-88.163
220.000	130.000	1.313	4.583	-0.100	4.586	1.310	1.638	-88.250
220.000	135.000	1.271	4.455	0.0	4.455	1.271	1.592	90.000
220.000	145.000	1.280	4.078	0.100	4.082	1.276	1.403	87.956
220.000	155.000	1.088	3.701	0.200	3.716	1.073	1.322	85.648
220.000	165.000	0.997	3.224	0.200	3.242	0.979	1.131	84.909
220.000	180.000	0.860	2.709	0.200	2.730	0.839	0.946	83.896
220.000	210.000	0.586	1.878	0.100	1.886	0.578	0.654	85.600
220.000	300.000	0.0	0.0	-0.0	0.0	0.0	0.0	45.000
222.500	112.500	1.562	4.631	-0.100	4.634	1.559	1.538	-88.136
222.500	115.000	1.551	4.698	-0.100	4.701	1.548	1.577	-88.182
222.500	117.500	1.540	4.664	-0.100	4.667	1.537	1.565	-88.168
222.500	120.000	1.529	4.630	-0.100	4.633	1.526	1.554	-88.155
222.500	122.500	1.518	4.596	-0.100	4.599	1.515	1.542	-88.141
222.500	127.500	1.496	4.529	-0.100	4.532	1.493	1.520	-88.114
222.500	132.500	1.173	4.461	-0.100	4.464	1.170	1.647	-88.260
225.000	80.000	1.442	5.180	0.100	5.183	1.439	1.872	88.469
225.000	90.000	1.451	5.003	0.0	5.003	1.451	1.776	90.000
225.000	100.000	1.359	4.726	-0.100	4.729	1.356	1.686	-88.300
225.000	110.000	1.468	4.449	-0.200	4.462	1.455	1.504	-86.179
225.000	115.000	1.522	4.410	-0.200	4.424	1.508	1.458	-86.057
225.000	120.000	1.600	4.543	-0.100	4.546	1.597	1.475	-88.056
225.000	135.000	1.133	4.540	0.0	4.540	1.133	1.703	90.000
225.000	140.000	1.191	4.413	0.200	4.425	1.179	1.623	86.461
224.000	240.000	0.384	1.064	0.0	1.064	0.384	0.340	90.000



## STRESS DATA : CONFIGURATION 4 cont.

XCOORD	YCOORD	SIGX	SIGY	SIGXY	SIG1	SIG3	TAU	THETA
225.000	270.000	0.192	0.582	-0.0	0.582	0.192	0.195	90.000
227.500	122.500	1.460	4.321	-0.100	4.324	1.457	1.434	-88.001
227.500	127.500	1.338	4.254	-0.200	4.268	1.324	1.472	-86.095
227.500	132.500	1.015	4.186	-0.200	4.199	1.002	1.598	-86.405
227.500	137.500	0.993	4.419	0.0	4.419	0.993	1.713	90.000
230.000	0.0	2.339	7.091	0.100	7.093	2.337	2.378	88.795
230.000	30.000	2.065	6.260	0.100	6.262	2.063	2.100	88.635
230.000	60.000	1.791	5.429	0.200	5.440	1.780	1.830	86.863
230.000	70.000	1.599	5.252	0.100	5.255	1.596	1.829	88.433
230.000	115.000	1.388	4.006	-0.300	4.040	1.354	1.343	-83.546
230.000	120.000	1.442	3.967	-0.200	3.983	1.426	1.278	-85.499
230.000	140.000	1.053	4.397	0.200	4.409	1.041	1.684	86.589
230.000	145.000	1.111	4.271	0.400	4.321	1.061	1.630	82.897
230.000	155.000	1.020	3.394	0.500	3.495	0.919	1.288	78.579
230.000	165.000	1.029	2.717	0.300	2.769	0.977	0.896	80.216
230.000	180.000	0.891	2.501	0.200	2.525	0.867	0.829	83.024
232.500	122.500	1.402	3.746	-0.200	3.763	1.385	1.189	-85.158
232.500	127.500	1.380	3.879	-0.200	3.895	1.364	1.265	-85.453
232.500	132.500	0.858	3.511	-0.400	3.570	0.799	1.385	-81.610
232.500	137.500	0.635	4.244	-0.300	4.269	0.610	1.829	-85.280
232.500	142.500	0.713	4.476	0.100	4.479	0.710	1.884	88.479
235.000	80.000	1.473	4.871	0.100	4.874	1.470	1.702	88.316
235.000	90.000	1.482	4.694	-0.0	4.694	1.482	1.606	90.000
235.000	100.000	1.391	4.317	-0.100	4.320	1.388	1.466	-88.045
235.000	110.000	1.399	3.840	-0.200	3.856	1.383	1.237	-85.347
235.000	120.000	1.408	3.363	-0.200	3.383	1.388	0.998	-84.218
235.000	125.000	1.362	3.225	-0.200	3.246	1.341	0.953	-83.941
235.000	140.000	0.395	4.722	-0.400	4.759	0.358	2.200	-84.762
235.000	145.000	0.673	4.555	0.500	4.618	0.610	2.004	82.777
235.000	150.000	1.131	3.229	1.000	3.629	0.731	1.449	68.185
235.000	210.000	0.583	1.667	0.100	1.676	0.574	0.551	84.773
235.000	240.000	0.384	1.164	-0.0	1.164	0.384	0.390	90.000
235.000	270.000	0.192	0.582	-0.0	0.582	0.192	0.195	90.000
235.000	300.000	0.0	0.0	-0.0	0.0	0.0	0.0	45.000
237.500	127.500	1.322	2.903	-0.200	2.928	1.297	0.815	-82.901
237.500	132.500	1.000	2.236	-0.300	2.305	0.931	0.687	-77.053
237.500	137.500	0.778	3.368	-0.500	3.461	0.685	1.388	-79.444
237.500	140.000	0.666	4.235	-0.200	4.246	0.655	1.796	-86.803
237.500	142.500	0.555	4.101	-0.100	4.104	0.552	1.776	-88.386
237.500	145.000	0.644	3.967	0.0	3.967	0.644	1.661	90.000
237.500	147.500	0.933	3.133	0.600	3.286	0.780	1.253	75.695
240.000	0.0	2.270	6.883	0.100	6.885	2.268	2.309	88.759
240.000	30.000	1.996	6.052	0.100	6.054	1.994	2.030	88.589





STRESS DATA : CONFIGURATION 4 cont.

XC00RD	YC00RD	SIGX	SIGY	SIGXY	SIG1	SIG3	TAU	THETA
240.000	60.000	1.722	5.321	0.100	5.324	1.719	1.802	88.410
240.000	70.000	1.631	5.044	0.100	5.047	1.628	1.709	88.323
240.000	125.000	1.428	2.621	-0.100	2.629	1.420	0.605	-85.242
240.000	130.000	1.482	2.182	0.0	2.182	1.482	0.350	90.000
240.000	135.000	0.760	1.115	-0.200	1.205	0.670	0.267	-65.794
240.000	137.500	0.749	2.181	-0.100	2.188	0.742	0.723	-86.025
240.000	140.000	0.0	0.0	0.0	0.0	0.0	0.0	45.000
240.000	145.000	0.0	0.0	0.0	0.0	0.0	0.0	45.000
240.000	147.500	0.804	1.846	0.200	1.883	0.767	0.558	79.500
240.000	150.000	0.893	1.112	0.500	1.514	0.491	0.512	51.176
240.000	155.000	1.252	2.086	0.500	2.320	1.018	0.651	64.914
240.000	165.000	1.060	2.209	0.200	2.243	1.026	0.608	80.403
242.500	132.500	1.042	1.561	0.0	1.561	1.042	0.260	90.000
242.500	137.500	0.720	1.893	0.100	1.901	0.712	0.595	85.162
242.500	147.500	0.575	1.758	0.0	1.758	0.575	0.591	90.000
242.500	152.500	1.253	1.591	0.200	1.684	1.160	0.262	65.099
245.000	80.000	1.505	4.663	0.100	4.666	1.502	1.582	88.188
245.000	90.000	1.413	4.386	0.0	4.386	1.413	1.486	90.000
245.000	100.000	1.422	4.009	0.0	4.009	1.422	1.293	90.000
245.000	110.000	1.331	3.532	0.0	3.532	1.331	1.100	90.000
245.000	120.000	1.239	3.055	0.100	3.060	1.234	0.913	86.858
245.000	130.000	1.148	2.278	0.400	2.405	1.021	0.692	72.351
245.000	135.000	0.902	1.039	0.500	1.475	0.466	0.505	48.900
245.000	137.500	0.891	1.806	0.200	1.848	0.849	0.499	78.193
245.000	140.000	0.0	0.0	0.0	0.0	0.0	0.0	45.000
245.000	145.000	0.0	0.0	0.0	0.0	0.0	0.0	45.000
245.000	147.500	0.746	1.971	-0.200	2.003	0.714	0.644	-80.958
245.000	150.000	0.635	1.137	-0.200	1.207	0.565	0.321	-70.726
245.000	155.000	1.213	1.969	-0.0	1.969	1.213	0.378	90.000
245.000	160.000	1.272	1.944	0.0	1.944	1.272	0.336	90.000
247.500	137.500	0.962	2.818	0.600	2.995	0.785	1.105	73.558
247.500	140.000	0.551	3.584	0.0	3.584	0.551	1.516	90.000
247.500	142.500	0.540	3.550	-0.100	3.553	0.537	1.508	-88.099
247.500	145.000	0.629	3.817	-0.200	3.829	0.617	1.606	-86.424
247.500	147.500	0.717	2.883	-0.500	2.993	0.607	1.193	-77.609
248.000	180.000	0.868	2.128	0.0	2.128	0.868	0.630	90.000
245.000	240.000	0.384	1.164	-0.0	1.164	0.384	0.390	90.000
250.000	0.0	2.202	6.675	0.100	6.677	2.200	2.239	88.720
250.000	50.000	1.745	5.390	0.100	5.393	1.742	1.825	88.430
250.000	60.000	1.653	5.113	0.100	5.116	1.650	1.733	88.346
250.000	70.000	1.562	4.836	0.100	4.839	1.559	1.640	88.252
250.000	135.000	0.968	3.035	1.000	3.440	0.563	1.438	67.972
250.000	140.000	0.622	3.897	0.400	3.945	0.574	1.686	83.136
250.000	145.000	0.300	3.829	-0.400	3.874	0.255	1.809	-83.614





STRESS DATA : CONFIGURATION 4 cont.

XCOORD	YCOORD	SIGX	SIGY	SIGXY	SIG1	SIG3	TAU	THETA
250.000	150.000	0.477	2.562	-0.500	2.676	0.363	1.156	-77.188
250.000	155.000	0.855	2.694	-0.300	2.742	0.807	0.967	-80.965
250.000	160.000	1.033	2.527	-0.100	2.534	1.026	0.754	-86.188
250.000	165.000	0.992	2.302	-0.100	2.310	0.984	0.663	-85.660
250.000	270.000	0.192	0.582	-0.0	0.582	0.192	0.195	90.000
250.000	300.000	0.0	0.0	-0.0	0.0	0.0	0.0	45.000
255.000	80.000	1.452	4.504	0.100	4.507	1.449	1.529	88.125
255.000	90.000	1.361	4.227	0.100	4.230	1.358	1.436	88.004
255.000	100.000	1.370	3.850	0.100	3.854	1.366	1.244	87.695
255.000	110.000	1.278	3.573	0.200	3.590	1.261	1.165	85.057
255.000	120.000	1.087	3.296	0.300	3.336	1.047	1.145	82.402
255.000	130.000	0.895	3.319	0.400	3.383	0.831	1.276	80.868
255.000	140.000	0.904	3.542	0.400	3.601	0.845	1.378	81.565
255.000	145.000	0.758	3.604	0.100	3.608	0.754	1.427	87.990
255.000	150.000	0.536	2.936	-0.300	2.973	0.499	1.237	-82.982
255.000	155.000	0.814	2.869	-0.300	2.912	0.771	1.070	-81.862
256.000	160.000	0.996	2.816	-0.100	2.821	0.991	0.915	-86.864
254.000	165.000	0.964	2.619	-0.100	2.625	0.958	0.834	-86.555
260.000	0.0	2.231	6.865	0.100	6.867	2.229	2.319	88.764
260.000	30.000	1.957	6.034	0.100	6.036	1.955	2.041	88.596
260.000	60.000	1.683	5.203	0.100	5.206	1.680	1.763	88.374
260.000	70.000	1.592	4.926	0.100	4.929	1.589	1.670	88.283
260.000	145.000	1.006	3.648	0.200	3.663	0.991	1.336	85.695
260.000	150.000	0.860	3.210	-0.0	3.210	0.860	1.175	90.000
260.000	180.000	0.768	2.328	-0.0	2.328	0.768	0.780	90.000
260.000	210.000	0.576	1.746	-0.0	1.746	0.576	0.585	90.000
260.000	240.000	0.384	1.164	-0.0	1.164	0.384	0.390	90.000
260.000	270.000	0.192	0.582	-0.0	0.582	0.192	0.195	90.000
260.000	300.000	0.0	0.0	-0.0	0.0	0.0	0.0	45.000
265.000	80.000	1.514	4.690	0.100	4.693	1.511	1.591	88.198
265.000	90.000	1.422	4.413	0.100	4.416	1.419	1.499	88.087
265.000	100.000	1.331	4.136	0.100	4.140	1.327	1.406	87.961
265.000	110.000	1.240	3.859	0.200	3.874	1.225	1.325	85.658
265.000	120.000	1.048	3.682	0.200	3.697	1.033	1.332	85.682
265.000	130.000	1.057	3.605	0.100	3.609	1.053	1.278	87.756
265.000	140.000	1.065	3.328	0.100	3.332	1.061	1.136	87.475
270.000	0.0	2.259	6.948	0.100	6.950	2.257	2.347	88.779
270.000	30.000	1.985	6.117	0.100	6.119	1.983	2.068	88.614
270.000	60.000	1.710	5.386	0.100	5.389	1.707	1.841	88.443
270.000	160.000	0.896	2.816	-0.0	2.816	0.896	0.960	90.000
270.000	180.000	0.768	2.328	-0.0	2.328	0.768	0.780	90.000
275.000	195.000	0.672	2.037	-0.0	2.037	0.672	0.682	90.000
290.000	0.0	2.314	7.214	0.100	7.216	2.312	2.452	88.831
290.000	30.000	2.039	6.383	0.100	6.385	2.037	2.174	88.682



## STRESS DATA : CONFIGURATION \$ CONT.

XCOORD	YCOORD	SIGX	SIGY	SIGXY	SIG1	SIG3	TAU	THETA
290.000	60.000	1.765	5.552	0.100	5.555	1.762	1.896	88.488
290.000	90.000	1.491	4.721	0.100	4.724	1.488	1.618	88.228
290.000	120.000	1.217	3.990	0.100	3.994	1.213	1.390	87.937
290.000	150.000	1.042	3.259	0.0	3.259	1.042	1.108	90.000
290.000	180.000	0.768	2.328	-0.0	2.328	0.768	0.780	90.000
290.000	210.000	0.576	1.746	-0.0	1.746	0.576	0.585	90.000
290.000	240.000	0.384	1.164	-0.0	1.164	0.384	0.390	90.000
290.000	270.000	0.192	0.582	-0.0	0.582	0.192	0.195	90.000
290.000	300.000	0.0	0.0	-0.0	0.0	0.0	0.0	45.000
320.000	30.000	2.122	6.632	0.100	6.634	2.120	2.257	88.730
320.000	90.000	1.573	5.070	0.0	5.070	1.573	1.748	90.000
320.000	150.000	1.125	3.408	0.0	3.408	1.125	1.141	90.000
320.000	210.000	0.576	1.746	0.0	1.746	0.576	0.585	90.000
320.000	240.000	0.384	1.164	-0.0	1.164	0.384	0.390	90.000
320.000	270.000	0.192	0.582	-0.0	0.582	0.192	0.195	90.000
320.000	300.000	0.0	0.0	-0.0	0.0	0.0	0.0	45.000
350.000	0.0	2.578	7.712	0.0	7.712	2.578	2.567	90.000
350.000	60.000	1.929	6.150	0.0	6.150	1.929	2.110	90.000
350.000	120.000	1.481	4.488	0.0	4.488	1.481	1.503	90.000
350.000	180.000	0.933	2.826	0.0	2.826	0.933	0.946	90.000
350.000	240.000	0.384	1.164	0.0	1.164	0.384	0.390	90.000
350.000	270.000	0.192	0.582	-0.0	0.582	0.192	0.195	90.000
350.000	300.000	0.0	0.0	0.0	0.0	0.0	0.0	45.000
380.000	270.000	0.192	0.582	0.0	0.582	0.192	0.195	90.000
380.000	300.000	0.0	0.0	0.0	0.0	0.0	0.0	45.000
410.000	0.0	2.742	8.310	0.0	8.310	2.742	2.784	90.000
410.000	60.000	2.194	6.648	0.0	6.648	2.194	2.227	90.000
410.000	120.000	1.645	4.986	-0.0	4.986	1.645	1.670	90.000
410.000	180.000	1.097	3.324	-0.0	3.324	1.097	1.113	90.000
410.000	240.000	0.548	1.662	0.0	1.662	0.548	0.557	90.000
410.000	300.000	0.0	0.0	0.0	0.0	0.0	0.0	45.000
470.000	0.0	2.742	8.310	0.0	8.310	2.742	2.784	90.000
470.000	60.000	2.194	6.648	0.0	6.648	2.194	2.227	90.000
470.000	120.000	1.645	4.986	-0.0	4.986	1.645	1.670	90.000
470.000	180.000	1.097	3.324	-0.0	3.324	1.097	1.113	90.000
470.000	240.000	0.548	1.662	-0.0	1.662	0.548	0.557	90.000
470.000	300.000	0.0	0.0	-0.0	0.0	0.0	0.0	45.000
530.000	0.0	2.742	8.310	0.0	8.310	2.742	2.784	90.000
530.000	60.000	2.194	6.648	-0.0	6.648	2.194	2.227	90.000
530.000	120.000	1.645	4.986	-0.0	4.986	1.645	1.670	90.000
530.000	180.000	1.097	3.324	-0.0	3.324	1.097	1.113	90.000
530.000	240.000	0.548	1.662	-0.0	1.662	0.548	0.557	90.000
530.000	300.000	0.0	0.0	-0.0	0.0	0.0	0.0	45.000











**B30302**